AD_____

Award Number: W81XWH-06-1-0116

TITLE: Role of Caveolin-1 in Prostate Cancer Angiogenesis

PRINCIPAL INVESTIGATOR: Timothy C. Thompson, Ph.D.

CONTRACTING ORGANIZATION: The University of Texas
M. D. Anderson Cancer Center
Houston, TX 77030

REPORT DATE: December 2009

TYPE OF REPORT: **FINAL**

PREPARED FOR: U.S. Army Medical Research and Materiel Command
Fort Detrick, Maryland 21702-5012

DISTRIBUTION STATEMENT:

X Approved for public release; distribution unlimited

REPORT DOCUMENTATION PAGE

Form Approved
OMB No. 0704-0188

1. REPORT DATE *(DD-MM-YYYY)*	2. REPORT TYPE	3. DATES COVERED *(From - To)*
01-12-2009	FINAL	15 NOV 2005 - 14 NOV 2009

4. TITLE AND SUBTITLE
Role of Caveolin-1 in Prostate Cancer Angiogenesis

5a. CONTRACT NUMBER

5b. GRANT NUMBER
W81XWH-06-1-0116

5c. PROGRAM ELEMENT NUMBER

6. AUTHOR(S)
Timothy C. Thompson, Ph.D.

5d. PROJECT NUMBER

5e. TASK NUMBER

5f. WORK UNIT NUMBER

7. PERFORMING ORGANIZATION NAME(S) AND ADDRESS(ES)

The University of Texas
M. D. Anderson Cancer Center
Houston, Texas 77030

8. PERFORMING ORGANIZATION REPORT NUMBER

9. SPONSORING / MONITORING AGENCY NAME(S) AND ADDRESS(ES)
US Army Medical Research
and Material Command
Fort Detrick, Maryland 21702

10. SPONSOR/MONITOR'S ACRONYM(S)

11. SPONSOR/MONITOR'S REPORT NUMBER(S)

12. DISTRIBUTION / AVAILABILITY STATEMENT
Approved for public release, distribution unlimited

13. SUPPLEMENTARY NOTES

14. ABSTRACT
We have proposed that prostate cancer cells secrete cav-1 which induces specific changes in EC which potentiate angiogenesis and metastatic activities. We have reported that prostate cancer cell derived, secreted caveolin-1 is taken up by cancer cells and tumor associated endothelial cells (Tahir et al, Cancer Res 2008). This autocrine/paracrine activity of secreted caveolin-1 promotes malignant progression by stimulation of specific angiogenic activities. We have shown in cav-1 negative LP-LNCaP cells that adenoviral vector mediated expression of cav-1 stimulated VEGF mediated VEGFR2 autophosphorylation and activated downstream signaling, whereas cav-1 knockdown in PC-3 and HUVECs impaired the VEGF-stimulated angiogenesis signaling. This showed cav-1 is an important regulator of basal and VEGF-stimulated angiogenesis signaling in prostate cancer cells and HUVECs (Tahir et al, Cancer Biol Ther 2009). Furthermore, we sought to determine whether there was any potential correlation between cav-1 and the GFs such as VEGF, TGF-β1, and FGF2. Our work revealed that cav-1 enhances cancer cell motility in an Akt-dependent manner and it up-regulates VEGF, TGF-β1, and FGF2 through Akt-mediated maintenance of mRNA stability (Li et al. Mol Cancer Res 2009).

Using cav-1 knock out mice system, we have shown wet prostate tumor weight of RM-9 was significantly reduced in cav-1-/- mice compared with cav-1+/+ mice. Also, tumor wet weight was significantly reduced in cav-1–/– mice which received cav-1 Ab compared to the mice treated with control IgG or HBSS only. Treatment with cav-1 Ab produced reduced lung metastasis in cav-1-/- model and increased survival time compared to the cav-1-/- littermate treated with control IgG or HBSS only(Watanabe et al. Mol cancer Res. 2009).Thus, cav-1 Ab reduced local tumor growth and experimental metastasis most likely by reducing systemic cav-1 levels secreted by RM-9 prostate tumor cell. Furthermore, our work revealed a cav-1–GF positive regulatory loop through PI3-K-Akt–mediated mRNA stability of VEGF, TGF-β1, and FGF2 which exert malignant properties in prostate cancer cells and fuels its progression. Our results indicate that cav-1 may be a clinically useful biomarker of prostate cancer progression and a potential therapeutic target.

15. SUBJECT TERMS
Prostate cancer, angiogenesis, caveolin-1

16. SECURITY CLASSIFICATION OF:			17. LIMITATION OF ABSTRACT	18. NUMBER OF PAGES	19a. NAME OF RESPONSIBLE PERSON
a. REPORT	b. ABSTRACT	c. THIS PAGE			19b. TELEPHONE NUMBER *(include area code)*
U	U	U	UU	86	USAMRMC

TABLE OF CONTENTS

Introduction 4

Body 6

Key Accomplishments 13

Reportable Outcomes 14

Conclusion 15

References 16

Appendix 17
Appendix 1. Abstracts

INTRODUCTION

Background: Caveolin-1 (cav-1) is an important structural/regulatory molecule involved in many aspects of molecular transport and cell signaling. Cav-1 activities are dependent on protein level and cell context, yet an understanding of the biological consequences of inappropriate cav-1 expression in malignant cells has been elusive. We have shown previously that cav-1 up-regulation is associated with metastatic, androgen-insensitive prostate cancer. In studies funded by this grant we identified an underlying mechanism for the selection of cav-1 overexpression in prostate cancer cells during progression. We found that cav-1 binds to and inhibits the activities of PP1/PP2A serine / threonine phosphatases, preventing inactivation of Akt through dephosphorylation and thus sustaining levels of phospho-Akt and its oncogenic activities. Recently we have shown that cav-1 overexpression leads to increased levels of c-myc protein, and our preliminary data and the results of published studies lead us to speculate that the mechanisms for cav-1 mediated c-myc stabilization also involve PP1/PP2A inhibition and phospho-Akt stabilization. We have also shown that cav-1 overexpression leads to up-regulation and secretion of VEGF, FGF2 and TGF-β1, indicating that cav-1 stimulated molecular pathways can regulate these growth factors (GF) /angiogenic cytokines (AC). Importantly, we have also discovered that cav-1 itself is specifically secreted by prostate cancer cells and is taken up by prostate cancer cells and endothelial cells (EC).

Hypothesis: These results suggest that cells expressing cav-1 can function as "feeder cells" for local and potentially distant prostate cancer cells and tumor-associated EC through secretion of cav-1 and cav-1 stimulated GF/AC. In support of this concept we have shown that experimentally induced metastasis is potentiated in host transgenic mice that overexpress cav-1 in and secrete cav-1 from prostatic epithelium. In contrast experimental metastasis is suppressed in host *cav-1*$^{-/-}$ mice compared to *cav-1*$^{+/+}$ mice. We propose that prostate cancer cells secrete cav-1 which induces specific changes in EC that potentiate angiogenesis and metastatic activities.

Specific Aims: Using in vitro and in vivo models that involve novel genetically mutant mice we propose to resolve the molecular and cellular pathways that support these oncogenic activities through specific aims to: (1) to analyze the effects of cav-1 conditioned media on cav-1$^{-/-}$ endothelial cell gene expression and biological activity; (2) map the molecular pathways involved in EC angiogenesis stimulated by cav-1 protein alone or together with specific GF/AC; and (3) to correlate the effects of prostate cancer cell derived cav-1 uptake by TAEC with tumor growth activities.

Study Design: We have generated and characterized mice that have a deletion of the *cav-1* gene. These will be a source for isolation of EC that will be treated with conditioned media derived from prostate cancer cells with controlled levels of cav-1 protein (Aim 1) or with purified cav-1 protein (Aim 2). We will determine the molecular events that are induced by cav-1 in EC by analyzing expression of signaling molecules such as phosphorylated Akt, c-myc and relevant GF/AC (VEGF, FGF-2, and TGF-β1) at the transcription level by quantitative RT-PCR and at the protein level by western blotting. Additionally we will evaluate events further downstream of signaling such as nitric oxide (NO) production. Biological activities of the EC in response to cav-1 that we will examine will include proliferation, chemoattraction, motility and vasculogenesis. The validation of these activities will be accomplished by using specific molecular inhibitors of the signaling molecules. The final aim of the grant will focus on in vivo studies using a novel mouse metastatic prostate cancer cell line that overexpresses cav-1 and has a high level of metastasis to lung and to bone. We will inject this cell line orthotopically (prostate) into *cav-1*$^{-/-}$ mice and then analyze TAEC responses locally and at distant sites of metastasis by immunohistochemistry. Treatment of the mice with cav-1 specific antibody will directly

test the effects of blocking cav-1 uptake in vivo on the growth and progression of experimental prostate cancer in this model.

Relevance: These studies could lead to the use of cav-1 positive TAEC as a potential prognostic/ predictive biomarker for prostate cancer in man. They will further serve to test the therapeutic potential of cav-1 antibody approaches for the treatment of prostate cancer.

The following personnel are receiving pay from the research effort of this grant:

Table 1. Key Personnel

Principal Investigator	Timothy C. Thompson, Ph.D. 713-792-9955 timthomp@mdanderson.org
Co-Investigator	Likun Li, Ph.D. 713-563-9001 lli@mdanderson.org
Co-Investigator	Salahaldin Tahir, Ph.D. 713-563-9002 stahir@mdanderson.org
Co-Investigator	Alexei Goltsov, Ph.D. 713-563-9005 agoltsov@mdanderson.org

2009 FINAL REPORT - BODY

Task 1. *To analyze the effects of cav-1 conditioned media (CM) on cav1$^{-/-}$ endothelial cell gene expression and biological activity*

1. Prepare EC from aorta of 40 *cav-1*$^{-/-}$ and 20 *cav-1*$^{+/+}$ mice and CM from cav-1 (500ml) or pcDNA (500ml) transfected LP-LNCaP cells.
2. Perform western blotting and QRT-PCR on EC lysates treated with cav-1 CM.
3. Develop biological assays for the EC activity (Motility/invasion, migration, tubule formation, NO and PGI2 determination) and analyze the effect of soluble cav-1 on these activities.

We isolated EC cells from wild type (WT) *Cav1*$^{+/+}$ and *Cav1*$^{-/-}$ mice and demonstrated that cav-1^{+}CM(from cav-1 stimulated LP-LNCap cells) or recombinant cav-1 protein promote cell motility/invasion of cav-1 $^{-/-}$EC cells (**Fig. 1**) but has minimal effects on cav-1$^{+/+}$ EC cells (not shown). Similarly, endothelial tubule formation, motility and NO production was stimulated by cav-1 CM or protein in *Cav1*$^{-/-}$EC (**Fig. 1B**). However, mutagenesis experiments have identified the cav-1 scaffolding domain (CSD) residues 82-101 as the region of cav-1 responsible for mediating the interaction with a number of signaling proteins including eNOS, platelet activating factor (PDGF) receptors, epidermal growth factor (EGF), the kinases Src and Fyn, heterotrimeric G-protein and cholesterol binding. Therefore we constructed cav-1 plasmid with deleted CSD termed phΔcav-1-V5-His, and prepared CM from phΔcav-1-V5-His transfected LNCaP cells. The use of recombinant protein with deleted CSD (rΔcav-1) as well as CM was important to investigate the role of CSD in the secretion, uptake and angiogenic activities of ECs.

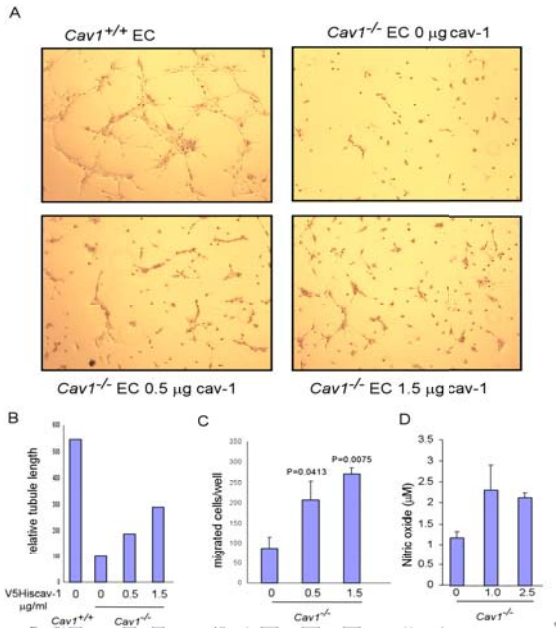

Fig. 1 - Micrographs of *Cav1*$^{+/+}$ or *Cav1*$^{-/-}$ aortic EC tubule formation on growth factor reduced matrigel 24h after addition of recombinant V5Hiscav-1 protein at indicated concentration (μg/ml). **B**. Relative tubule length with *Cav1*$^{-/-}$ EC at 0 cav-1 protein set at 100%. **C**. Migration of *Cav1*$^{-/-}$ EC in response to protein. **D**. NO production determined by colorimetric assay.

To test the effect of CSD on VEGF-stimulated angiogenesis signaling, we treated HUVECs with CSD peptide in serum free medium followed by treatment with VEGF. CSD treatment of HUVECs significantly reduced VEGF-stimulated phosphorylation of VEGFR2 (Y951), PLCγ1 (Y783) and Akt (S473 &T308) as compared to those treated with control sCSD. Modest reductions in basal phosphorylation levels of Akt were observed in CSD-treated compared to sCSD-treated HUVECs (**Fig. 2**). These data demonstrate that CSD inhibits VEGF-stimulated angiogenesis signaling through inhibition of endogenous cav-1 function. We found that VEGF treatment of HUVECs increased the tubule length and cell migration in NC transfected cells compared to their untreated counterparts, but this stimulatory effect of VEGF was significantly impaired when cav-1 was down-regulated (**Fig. 3A, B, C, D**).

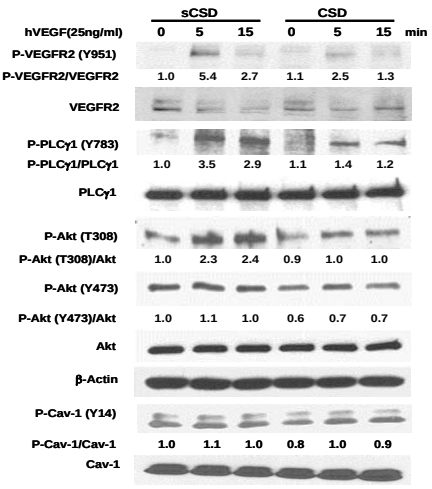

Fig. 2 - CSD Inhibited VEGF and cav-1 mediated angiogenesis signaling in HUVECs.

We further found that CSD treatment of unstimulated and VEGF-stimulated HUVECs reduced the tubule length in NC-transfected cells ($P < 0.05$, and $P < 0.01$, respectively; **Fig. 3B**), but not in cav-1 siRNA transfected cells (Fig. 3B) compared to treatment with sCSD. Additionally, CSD treatment of unstimulated and VEGF-stimulated HUVECs significantly reduced cell migration in NC-transfected cells ($P < 0.05$, and $P < 0.01$, respectively; **Fig. 3D**), and in cav-1 siRNA transfected cells ($P < 0.05$, and $P < 0.05$, respectively; **Fig. 3D**) compared to treatment with sCSD. These results show that down-regulation of cav-1 through cav-1 siRNA or CSD treatment alone led to significant reductions of angiogenic activities in HUVECs, and that combining the two treatments yields additive or synergistic effects. These data present a novel mechanism for potential therapeutic use of CSD to suppress angiogenic signaling in prostate cancer.

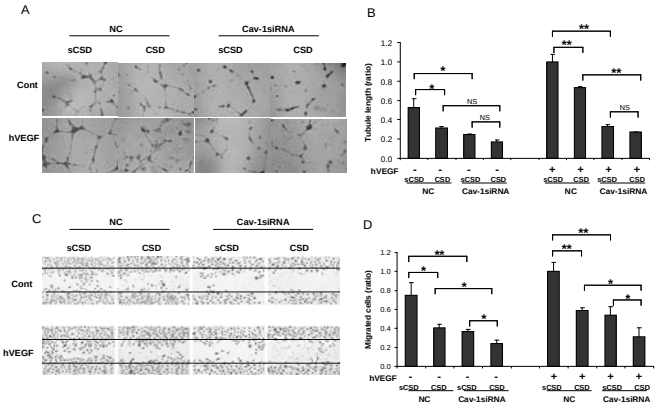

Fig. 3 - VEGF-stimulated tubule formation and cell migration is mediated by cav-1 and inhibited by CSD.

To investigate the role of cav-1 in VEGF-stimulated angiogenic activities in ECs, we introduced cav-1 into *cav-1*$^{-/-}$ ECs either by Adcav-1 infection to the MOI 200, or by rcav-1 treatment, followed by analysis of the phosphorylation status of VEGF/VEGFR2 signaling pathway associated proteins. We found that introduction of cav-1 into *cav-1*$^{-/-}$ ECs, followed by treatment with VEGF increased phosphorylation of VEGFR2 (Y951), (Y783), Akt (S473) and Akt (T308), and a further increase in the phosphorylation status of these proteins as well as PLCγ1 (Y783) was observed after VEGF treatment (**Fig. 4 & 5**). These results indicate that in the absence of cav-1, VEGF stimulation of VEGFR2 autophosphorylation and its downstream effects is minimal, and that cav-1 is required for optimal VEGF-stimulated signaling.

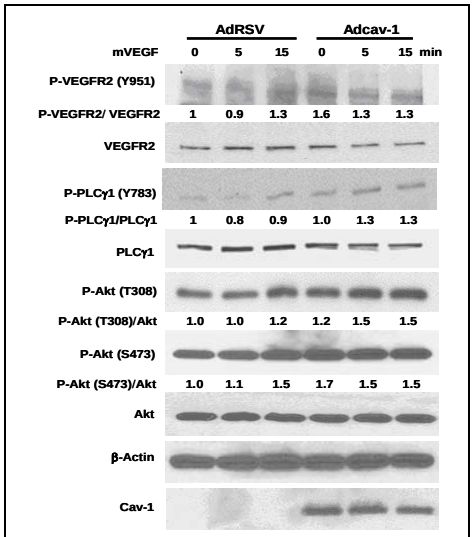

Fig. 4 - Adcav-1 stimulated the VEGF/VEGFR2 induced angiogenesis signaling pathway *cav-1*$^{-/-}$ ECs.

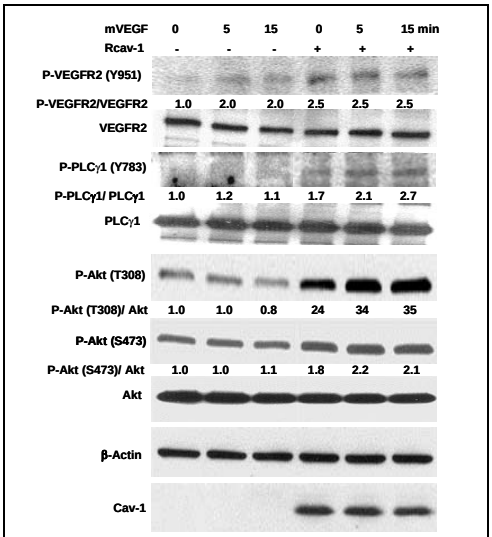

Fig. 5 - Rcav-1 stimulated the VEGF/VEGFR2 induced angiogenesis signaling pathway in *cav-1*$^{-/-}$ ECs

Thus, we have completed the analysis of the effects of cav-1 conditioned media (CM) on *cav-1*$^{-/-}$ endothelial cell gene expression and biological activities as proposed in the Task 1 and the results from our experiments were incorporated into publications listed in the reference section.

Task 2. ***Map the molecular pathways involved in EC angiogenesis stimulated by cav-1 protein alone or together with specific GF/AC.***

1. Preparation/purchase of reagents, including recombinant cav-1, VEGF, FGF-2, TGF-β1, siRNA for VEGFR2, PI3-K, Akt, ERK1/2 and eNOS, chemical inhibitors for VEGFR2, PI3-K, ERK1/2 and eNOS.
2. Optimize conditions for siRNA transfection and for chemical inhibitions.
3. Analysis of gene knock down, including QRT-PCR analysis for mRNA and western analysis for protein. Analysis range covers target genes and their downstream components.

We investigated cav-1 regulation of basal and VEGF-stimulated VEGFR2-mediated angiogenic signaling in PC-3 cells and human ECs. We found that cav-1 knockdown in PC-3 and HUVECs impaired the VEGF-stimulated angiogenesis signaling as shown in reduced phosphorylation of VEGFR2 (Y951), PLCγ1 (Y783) and Akt (S473 & T308) at two time points (5 and 15 min) as compared with that of the NC. Interestingly, rcav-1 treatment of these cells restored the basal phosphorylation status of these signaling molecules and partially restored the response to VEGF stimulation, i.e., P-VEGFR2, PLCγ1and P-Akt (**Fig. 6 & 7**). These results demonstrate that cav-1 is an important regulator of basal and VEGF-stimulated angiogenesis signaling in prostate cancer cells and HUVECs. Importantly, rcav-1 restored VEGF stimulated angiogenic signaling in cav-1 siRNA treated HUVECs, further demonstrating a potential role for secreted cav-1 in vivo.

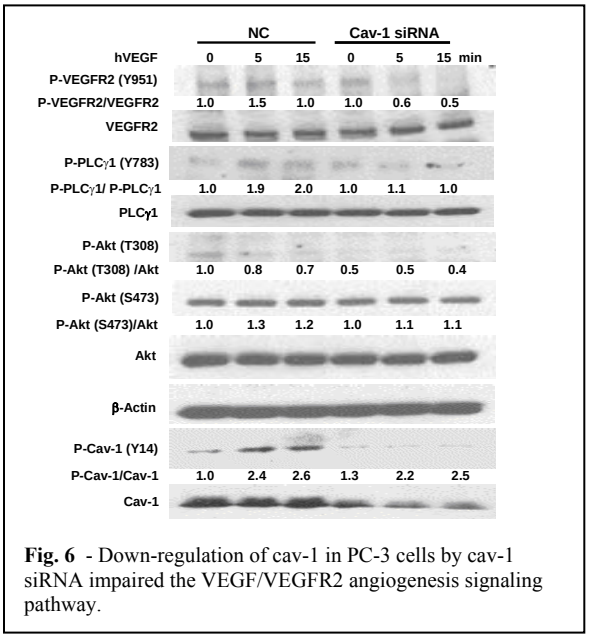

Fig. 6 - Down-regulation of cav-1 in PC-3 cells by cav-1 siRNA impaired the VEGF/VEGFR2 angiogenesis signaling pathway.

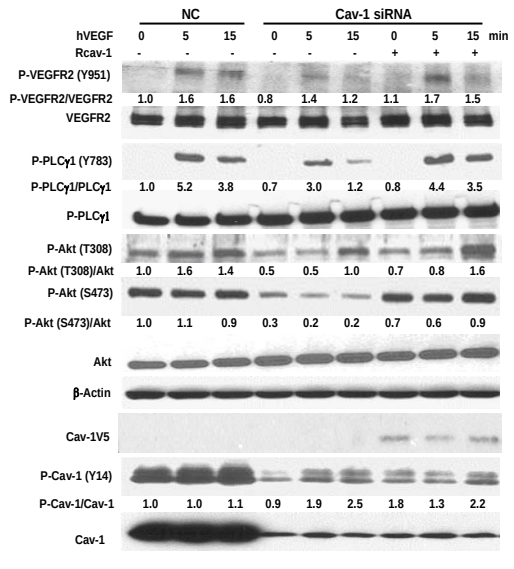

Fig. 7 - Down-regulation of cav-1 in HUVECs by cav-1 siRNA impaired the VEGF/VEGFR2 angiogenesis signaling pathway.

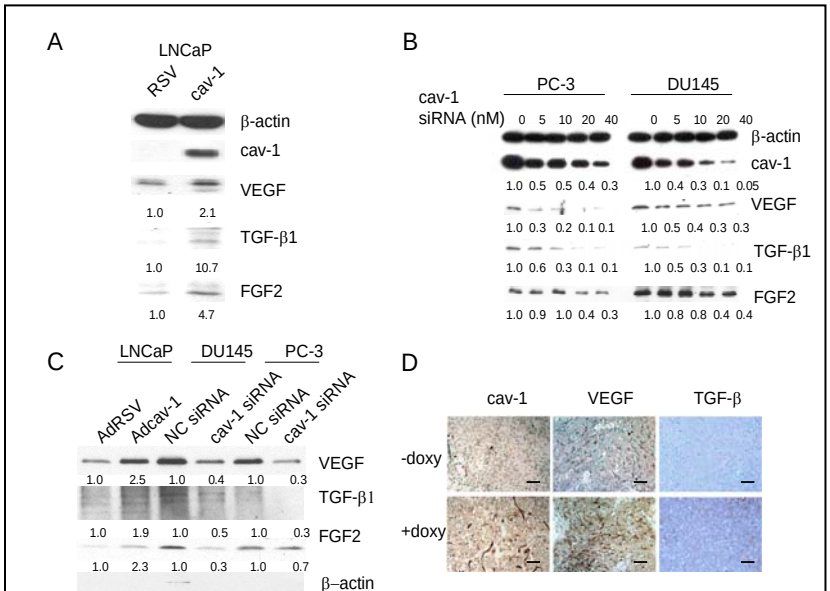

Fig. 8 - Cav-1 up-regulates protein levels of VEGF, TGF-b1 and FGF2.

Since overexpression of specific cancer-promoting GFs occurs in parallel with cav-1 overexpression in many types of malignancies, including prostate cancer, we sought to determine whether there was any potential correlation between cav-1 and these GFs. As shown in Figure 8, overexpression of cav-1 in cav-1–negative, low-passage LNCaP prostate cancer cells using adenoviral vector–mediated gene transduction led to significantly increased levels of VEGF, TGF-β1, and FGF2 mRNA (data not shown) and protein (**Fig. 8A**). In contrast, when endogenous cav-1 in high–cav-1 PC-3 and DU145 prostate cancer cell lines was knocked down by cav-1 siRNA, FGF2, TGF-β1, and VEGF mRNA (data not shown) and protein levels (**Fig. 8B**) were remarkably reduced. In addition to its stimulatory effect on the cellular levels of VEGF, TGF-β1, and FGF2, cav-1 promoted the secretion of these GFs into the medium (**Fig. 8C**), indicating that cav-1 and these cav-1–stimulated GFs can generate a positive autocrine loop.

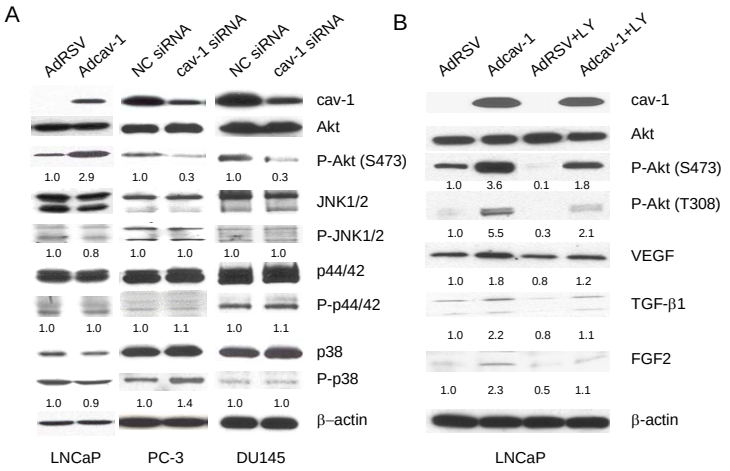

Fig. 9 - Akt is required for the cav-1-induced up-regulation of VEGF, TGF-b1 and FGF2

To confirm the relationship between cav-1 and the expression of these cancer-promoting GFs *in vivo*, we used an LNCaP tet-on stable clone (LNTB25cav) to establish LNTB25cav subcutaneous xenografts. Immunochemical analysis of tumor tissues from the doxycycline + sucrose– and sucrose only–treated mice showed that the induction of cav-1 in the LNTB25cav xenografts resulted in increased expression of VEGF and TGF-β1 (**Fig. 8D**). Thus, our *in vivo* data validated our *in vitro* results that show increased VEGF and TGF-β1 levels in cav-1–overexpressing cancer cells. We did not include FGF2 immunochemical analysis of tumor tissues owing to low FGF2 protein level in the LNTB25cav tumors.

We reported previously that overexpression of cav-1 in cav-1–negative LNCaP cells through adenoviral vector–mediated gene transduction led to significantly increased levels of phosphorylated Akt, which in turn led to enhanced cancer cell survival. We wondered whether cav-1–mediated Akt activities are also associated with the expression of cancer-promoting GFs in prostate cancer cells. As we reported previously, overexpression of cav-1 in cav-1–negative LNCaP cells resulted in significantly increased levels of phosphorylated Akt, whereas the phosphorylation status of the JNK, p44/p42, and p38 pathways remained relatively unchanged. In contrast, suppression of endogenous cav-1 using cav-1–specific siRNA in the high–cav-1 prostate cancer cell lines PC-3 and DU145 reduced the levels of phosphorylated Akt whereas the activities of JNK, p44/42, and p38 were still relatively unchanged (**Fig. 9A**). To address whether Akt is involved in cav-1–mediated up-regulation of VEGF, TGF-β1, and FGF2, we suppressed Akt activities in LNCaP cells using the PI3-K inhibitor LY 3 h after the cells were transduced with cav-1–expressing adenoviral vector. The results demonstrated that the treatment with LY effectively inhibited cav-1–mediated Akt activation and largely if not completely eliminated cav-1–mediated up-regulation of VEGF, TGF-β1, and FGF2 (**Fig. 9B**). Note that LY also suppressed activity of endogenous Akt, leading to lower levels of VEGF, TGF-β1, and FGF2 (**Fig. 9B** , compared AdRSV+LY to AdRSV).

Further studies revealed that cav-1 enhances cancer cell motility in an Akt-dependent manner and it up-regulates VEGF, TGF-β1, and FGF2 through Akt-mediated maintenance of mRNA stability. Overall,

our results demonstrate that the cav-1–induced PI3-K-Akt–mediated increased mRNA stability of VEGF, TGF-β1, and FGF2 is a novel and important molecular mechanism by which cav-1 promotes cancer progression. Our results further define a cav-1–GF positive regulatory loop that could sustain many malignant properties in prostate cancer cells (**Fig. 10**).

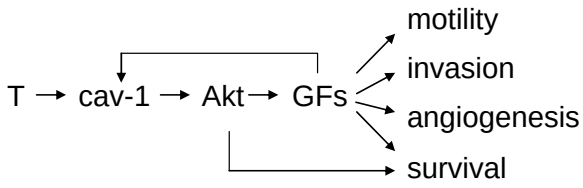

Fig. 10 - Diagram summarizes cav-1–GF autoregulatory loop. T = testosterone.

Thus, we have completed mapping the molecular pathways involved in EC angiogenesis stimulated by cav-1 protein alone or together with specific GF/AC as proposed in this task. The results from our experiments were incorporated into publications listed in the reference section.

Task 3. ***To correlate the effects of prostate cancer cell derived cav-1 uptake by TAEC with tumor growth activities.***

1. Inject 178-2 BMAK cells into dorsolateral prostate of twenty *cav-1*$^{-/-}$ mice and analyze tumor weight and metastasis at 21 day, fixed time point. Analyze tissues by immunohistochemistry.
2. Inject 178-2 BMAK cells into dorsolateral prostate of thirty nine *cav-1*$^{-/-}$ mice then treat with HBSS, rabbit IgG, or rabbit anti-cav-1 serum (thirteen per group) and analyze tumor weight and metastasis at 21 day, fixed time point. Analyze tissues by immunohistochemistry.
3. Inject 178-2 BMAK cells into dorsolateral prostate of thirty *cav-1*$^{-/-}$ mice then treat with HBSS, rabbit IgG, or rabbit anti-cav-1 serum (ten per group) and analyze tumor weight and metastasis at survival time point. Analyze tissues by immunohistochemistry.

As we explained in our previous report, due to minor histocompatibility problems and poor "take" of 178-2 BMAK cells in *cav1*$^{-/-}$mice we replaced 178-2 BMAK cells with RM-9 prostate cancer cells that were originally isolated from C57/BL6 mice. We have previously demonstrated that RM-9 cells secrete cav-1 into conditioned media in vitro and can be used in the orthotopic mouse prostate cancer model in vivo.

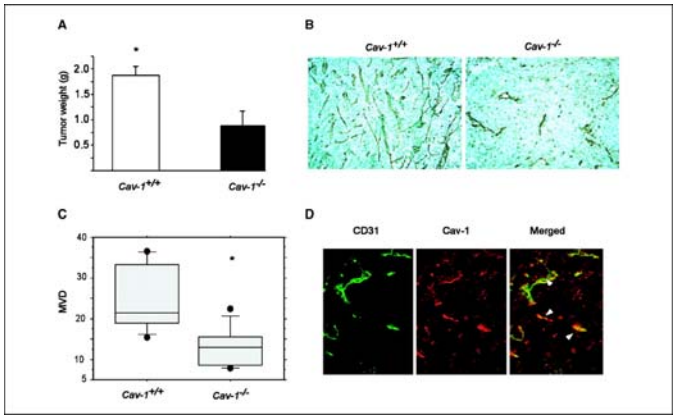

Fig. 11 - Secreted cav-1 promotes growth and angiogenesis in orthotopic RM-9 mouse prostate cancer model.

RM-9 prostate cancer cells were injected directly into the dorsolateral prostate of male *cav-1*$^{+/+}$ or *cav-1*$^{-/-}$ mice. In this model, the mean (1.85 ± 0.167g) tumor wet weight was significantly higher in *cav-1*$^{+/+}$ versus *cav-1*$^{-/-}$ mice (P = 0.045; **Fig. 11A**). Moreover, immunohistochemical analysis of tumor sections collected from sacrificed mice showed that RM-9 tumors had significantly higher microvessel densities in *cav-1*$^{+/+}$ compared with *cav-1*$^{-/-}$ hosts [median, 21.5 (range, 15.6–36.1) versus 13.3 (range, 8.2–22.8; P = 0.0078); **Fig. 11B and C**]. Interestingly, >70% of the CD31^{+} microvessels in the *cav-1*$^{-/-}$ mouse tumor sections were positive for cav-1 staining, indicating uptake of RM-9 cell–derived cav-1 by tumor-associated endothelial cells (**Fig. 11D**, *arrows*).

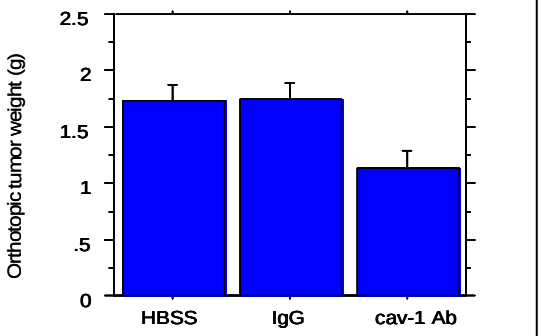

Fig. 12 - Anti-cav-1 antibody treatment significantly reduces the wet weight of orthotopic RM-9 tumors grown in cav-1$^{-/-}$ mice compared to control IgG or HBSS groups (* $P < 0.05$).

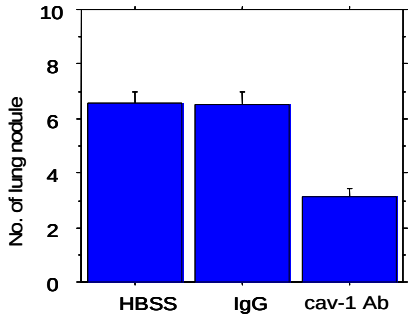

Fig. 13 - Anti-cav-1 antibody treatment significantly reduces the number of RM-9 experimental lung metastases tumors in cav-1$^{-/-}$mice compare to control IgG or HBSS groups (* $P < 0.05$).

To test for anti-metastatic potential and the therapeutic effects of cav-1 Ab in *cav-1*$^{-/-}$ mice, a mouse model of metastatic prostate cancer which involves simultaneous inoculation of RM-9 prostate cancer cells (pre-established metastasis model) via orthotopic prostate and tail vein was used. Wet prostate tumor weight was significantly reduced in *cav-1*$^{-/-}$ mice that received cav-1 Ab compared to the mice treated with control IgG or HBSS only (**Fig. 12**). Treatment with cav-1 Ab also had an anti-metastatic effect in *cav-1*$^{-/-}$ model and reduced number of lung metastasis compared to the control treatment groups (**Fig. 13**). Interestingly, in the same experimental setting the adult male *cav-1*$^{-/-}$ mice that received cav-1 Ab survived significantly longer then *cav-1*$^{-/-}$ littermate treated with control IgG or HBSS only (**Fig. 14**). Thus, cav-1 Ab can significantly reduce local tumor growth as well as experimental metastasis most likely by reducing systemic cav-1 levels secreted by RM-9 prostate tumor cell. It is possible that high metastatic activity of *cav-1*$^{-/-}$ mice in HBSS and IgG groups are partially due to cav-1 secreted from the prostate tumor in **Fig. 6**. The data supports our hypothesis that prostate cancer cells secrete cav-1 which potentiates angiogenesis and metastatic activities.

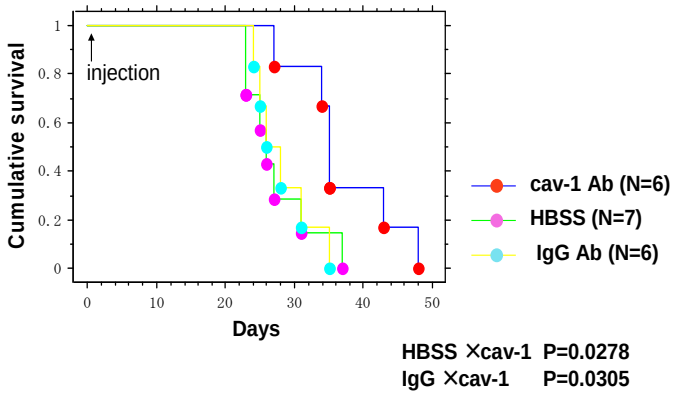

Fig. 14 - The cav-1$^{-/-}$ mice with orthotopic RM-9 tumor and lung metastases treated with anti-cav-1 antibody survive significantly longer compare to mice treated with control IgG or HBSS (Kaplan-Meier survival plot).

Our animal model is a good example of the effect of cav-1AB in serum cav-1 level in mice bearing prostate tumor and metastasis as it neutralizes the cav-1-GF positive regulatory loop described in **Fig. 10**. The data suggests that cav-1 Ab can potentially be a novel systemic therapeutic modality for the treatment of metastatic prostate cancer.

Thus we have correlated the effects of prostate cancer cell derived cav-1 uptake by TAEC with tumor growth activities as proposed in this task and the results were incorporated into the publications listed in the reference section.

Significance

Our mechanistic data are consistent with the concept that angiogenic activities of prostate cancer cell derived, secreted cav-1 promotes tumor progression and the progression could be reduced by lowering serum cav-1 level. Our novel concept of CSD and cav-1 AB will lead to novel approaches for prostate cancer diagnosis and therapy.

Plans

Our data thus far yielded important mechanistic insight into the angiogenic activities of prostate cancer cell derived, secreted cav-1. The results of our studies using cav-1 Ab treatment raise the possibility of developing this approach toward therapeutic applications as single or as combination therapy. In our view, the next important step is to apply this new knowledge to the clinical settings for prostate cancer diagnosis and therapy.

Publications

1. Tahir SA, Frolov A, Hayes TG, Mims MP, Miles BJ, Lerner SP, Wheeler TM, Ayala G, Thompson TC, and Kadmon D. Preoperative serum caveolin-1 as a prognostic marker for recurrence in a radical prostatectomy cohort. Clin Cancer Res 12(16): 4872-5, 2006.
2. Yang G, et al. Correlative evidence that prostate cancer cell-derived caveolin-1 mediates angiogenesis. Hum Pathol 38(11):1688-95, 2007.
3. Tahir SA, et al. Tumor cell-secreted caveolin-1 has proangiogenic activities in prostate cancer. Cancer Res 68(3):731-9, 2008.
4. Yang G, et al. Mice with cav-1 gene disruption have benign stromal lesions and compromised epithelial differentiation. Exp Mol Pathol 84(2):131-40, 2008.
5. Tahir SA, Park S, and Thompson TC. Caveolin-1 regulates VEGF-stimulated angiogenic activities in prostate cancer and endothelial cells. Cancer Biol Ther, 2009. 8(23). [Epub ahead of print]
6. Watanabe M, et al. Functional analysis of secreted caveolin-1 in mouse models of prostate cancer progression. Mol Cancer Res 7(9):1446-55, 2009.
7. Li L, et al. Caveolin-1 promotes autoregulatory, Akt-mediated induction of cancer-promoting growth factors in prostate cancer cells. Mol Cancer Res 7(11):1781-1791, 2009.
8. Thompson TC, et al. The role of caveolin-1 in prostate cancer: clinical implications. Prostate Cancer Prostatic Dis, 2009 Jul 7. [Epub ahead of print]

KEY RESEARCH ACCOMPLISHMENTS

1. Secreted cav-1 stimulates angiogenic activities in *cav-1*$^{-/-}$ mouse EC.

2. Akt (S473, T308) and eNOS (S1177) are significantly phosphorylated in rcav-1 treated *cav-1*$^{-/-}$ mouse EC.

3. Δrcav-1 (CSD delection mutant) did not stimulate the phosphorylation of eNOS on S1177 in *cav-1*$^{-/-}$ mouse EC.

4. Cav-1 is an important regulator of VEGF-stimulated angiogenesis signaling in prostate cancer cells and HUVEC.

5. CSD inhibited the effects of cav-1 in prostate cancer cells and HUVEC.

6. Overexpression of cav-1 in cav-1 negative cells led to significant increased level of VEGF, FGF2 and TGF-β1 mRNA and protein.

7. Cav-1 stimulated expression of VEGF, FGF2 and TGF-β1 mRNA and protein was mediated by Akt.

8. Cav-1 promoted the secretion of VEGF, FGF2 and TGF-β1 into the medium.

9. Cav-1 and cav-1 stimulated VEGF, FGF2 and TGF-β1 can form a positive-feedback autocrine loop.

10. Cav-1 enhances cancer cell motility in an Akt-dependent manner and up-regulates VEGF, TGF-β1, and FGF2 through Akt-mediated maintenance of mRNA stability.

11. Cav-1 Ab treatment reduced tumor size, number of lung metastasis and increased longevity of mice bearing prostate tumors that secrete cav-1.

REPORTABLE OUTCOMES

Presentations

1. Tahir SA, Yang G, Goltsov A, Watanabe M, Tabata K, and Thompson TC. Caveolin-1 uptake by endothelial cells promotes angiogenic activities and is associated with prostate cancer progression. American Association for Cancer Research, 97th Annual Meeting, Washington DC, April 1-5, 2006.
2. Tahir SA, Yang G, Goltsov A, Watanabe M, Tabata K and Thompson TC. Caveolin-1 uptake by endothelial cells promotes angiogenic activities and is associated with prostate cancer progression. 4th Annual Cancer Center Symposium, Houston, Texas, November 3, 2006.
3. Miles BJ, Yang G, Addai J, Wheeler TM, Frolov A, Kadmon D and Thompson TC. Correlative evidence that prostate cancer cell-derived caveolin-1 mediates angiogenesis. American Society of Clinical Oncology Annual Meeting, Chicago, Illinois , June 1 – 5, 2007.
4. Tahir SA, Park SH, and Thompson TC. Caveolin-1 regulates VEGF/VEGFR2 induced stimulation of angiogenesis. 100th AACR Annual Meeting, Denver, Colorado, 2009.

Manuscripts

1. Tahir SA, Frolov A, Hayes TG, Mims MP, Miles BJ, Lerner SP, Wheeler TM, Ayala G, Thompson TC, and Kadmon D. Preoperative serum caveolin-1 as a prognostic marker for recurrence in a radical prostatectomy cohort. Clin Cancer Res 12(16):4872-5, 2006.
2. Yang G, et al. Correlative evidence that prostate cancer cell-derived caveolin-1 mediates angiogenesis. Hum Pathol 38(11):1688-95, 2007.
3. Tahir SA, et al. Tumor cell-secreted caveolin-1 has proangiogenic activities in prostate cancer. Cancer Res 68(3):731-9, 2008.
4. Yang G, et al. Mice with cav-1 gene disruption have benign stromal lesions and compromised epithelial differentiation. Exp Mol Pathol 84(2):131-40, 2008.
5. Tahir SA., Park S, and Thompson TC. Caveolin-1 regulates VEGF-stimulated angiogenic activities in prostate cancer and endothelial cells. Cancer Biol Ther, 2009. 8(23). [Epub ahead of print]
6. Watanabe M, et al. Functional analysis of secreted caveolin-1 in mouse models of prostate cancer progression. Mol Cancer Res 7(9): 1446-55, 2009.
7. Li L, et al. Caveolin-1 promotes autoregulatory, Akt-mediated induction of cancer-promoting growth factors in prostate cancer cells. Mol Cancer Res 7(11):1781-1791, 2009.
8. Thompson TC, et al. The role of caveolin-1 in prostate cancer: clinical implications. Prostate Cancer Prostatic Dis, 2009 Jul 7. [Epub ahead of print]

CONCLUSION

Our experiments effectively addressed our proposed Tasks and yielded interesting and important results. Specifically, the results of our experiments yielded important mechanistic insight into the angiogenic activities of prostate cancer cell derived, secreted cav-1. During the last three years, we have published eight important papers defining the role of cav-1 in prostate cancer. We have reported that cav-1 potentiates VEGF-stimulated angiogenic signaling in HUVEC through increased tubule length and cell migration. Interestingly, CSD treatment reduced the stimulatory effect. We reported cav-1 stimulates the expression and secretion of VEGF, FGF2 and TGF-β1, generating a positive-feedback autocrine loop. We have shown in *cav-1*$^{-/-}$ mice model, cav-1 Ab treatment reduced the tumor size, metastasis number and increased longevity of mice bearing cav-1 secreting RM-9 tumor. Our work strongly supports use of serum and tissue cav-1 as a prognostic biomarker in prostate cancer. In addition our studies indicate that systemic cav-1 Ab treatment represents a novel and promising therapeutic approach for metastatic prostate cancer.

REFERENCES

None cited in text

APPENDICES

1. Tahir SA, Frolov A, Hayes TG, Mims MP, Miles BJ, Lerner SP, Wheeler TM, Ayala G, Thompson TC, and Kadmon D. Preoperative serum caveolin-1 as a prognostic marker for recurrence in a radical prostatectomy cohort. Clin Cancer Res 12(16):4872-5, 2006.
2. Yang G, et al. Correlative evidence that prostate cancer cell-derived caveolin-1 mediates angiogenesis. Hum Pathol 38(11):1688-95, 2007.
3. Tahir SA, et al. Tumor cell-secreted caveolin-1 has proangiogenic activities in prostate cancer. Cancer Res 68(3):731-9, 2008.
4. Yang G, et al. Mice with cav-1 gene disruption have benign stromal lesions and compromised epithelial differentiation. Exp Mol Pathol 84(2):131-40, 2008.
5. Tahir SA, Park S, and Thompson TC. Caveolin-1 regulates VEGF-stimulated angiogenic activities in prostate cancer and endothelial cells. Cancer Biol Ther, 2009. 8(23). [Epub ahead of print]
6. Watanabe M, et al. Functional analysis of secreted caveolin-1 in mouse models of prostate cancer progression. Mol Cancer Res 7(9):1446-55, 2009.
7. Li L, et al. Caveolin-1 promotes autoregulatory, Akt-mediated induction of cancer-promoting growth factors in prostate cancer cells. Mol Cancer Res 7(11):1781-1791, 2009.
8. Thompson TC, et al. The role of caveolin-1 in prostate cancer: clinical implications. Prostate Cancer Prostatic Dis, 2009 Jul 7. [Epub ahead of print]

Preoperative Serum Caveolin-1 as a Prognostic Marker for Recurrence in a Radical Prostatectomy Cohort

Salahaldin A. Tahir,[1] Anna Frolov,[1] Teresa G. Hayes,[4] Martha P. Mims,[4] Brian J. Miles,[1] Seth P. Lerner,[1] Thomas M. Wheeler,[2] Gustavo Ayala,[2] Timothy C. Thompson,[1,3,5] and Dov Kadmon[1]

Abstract

Purpose: Up-regulation of caveolin-1 (cav-1) is associated with virulent prostate cancer, and serum cav-1 levels are elevated in prostate cancer patients but not in benign prostatic hyperplasia. In this study, we evaluated the potential of high preoperative serum cav-1 levels to predict biochemical progression of prostate cancer. The value of the combined preoperative markers, prostate-specific antigen (PSA), biopsy Gleason score, and serum cav-1 for predicting biochemical recurrence was also investigated.

Experimental Design: Serum samples taken from 419 prostate cancer patients before radical prostatectomy were selected from our Specialized Programs of Research Excellence prostate cancer serum and tissue bank. Serum samples were obtained 0 to 180 days before surgery and all patients had complete data on age, sex, race, stage at enrollment, and follow-up for biochemical recurrence. Serum cav-1 levels were measured according to our previously reported ELISA protocol.

Results: Cav-1 levels were measured in the sera of 419 prostate cancer patients; the mean serum level was 4.52 ng/mL (median 1.01 ng/mL). Patients with high serum cav-1 levels had a 2.7-fold ($P = 0.0493$) greater risk of developing biochemical recurrence compared with those with low serum cav-1 levels. Importantly, patients with serum PSA $\geq$ 10 ng/mL and elevated levels of serum cav-1 had 2.44 times higher risk ($P = 0.0256$) of developing biochemical recurrence compared with patients with low levels of cav-1. In addition, high serum cav-1 levels combined with increasing biopsy Gleason score predicted much shorter recurrence-free survival in the group of patients with PSA $\geq$ 10 ng/mL ($P = 0.0353$). Cav-1 was also able to distinguish between high- and low- risk patients with biopsy Gleason score of seven, after adjusting, for patients PSA levels ($P = 0.0429$).

Conclusions: Overall, elevated preoperative levels of serum cav-1 predict decreased time to cancer recurrence. In the subset of patients with serum PSA of $\geq$10 ng/mL, the combination of serum cav-1 and biopsy Gleason score has the capacity to predict time to biochemical recurrence.

In 2005, ~90% of newly diagnosed prostate cancer patients had clinically localized disease (1). Consequently, the majority of patients are treated with curative intent by either radical prostatectomy or radiation therapy. It is well established, however, that 10% to 50% of patients who undergo radical prostatectomy will show biochemical evidence of disease recurrence [prostate-specific antigen (PSA) recurrence] within 5 years of surgery (2, 3). Various clinical variables have been used, singly and in combination (nomograms, tables, etc.), to predict, preoperatively, which patients are likely to fail definitive therapy (4). However, the predictive value of these variables has been thwarted by the vexing biological diversity of clinical prostate cancer. New markers are needed, preferably serum markers that have been mechanistically implicated in the progression of virulent disease. We believe that serum caveolin-1 (cav-1) may be such a marker.

Cav-1 is an important structural/regulatory molecule involved in many aspects of molecular transport and cell signaling (5, 6). Tissue cav-1 is overexpressed in metastatic and in hormone-resistant prostate cancer (7). Overexpression correlates with a shortened interval to disease recurrence following therapy for localized disease and tends to be associated with a high Gleason score pathologically (8–10). Interestingly, cav-1 is secreted by prostate cancer cells (11) and we have developed a sensitive ELISA immunoassay for the detection of cav-1 in the serum (12). In a preliminary study, we documented that prostate cancer patients have a higher serum cav-1 level when compared with age-matched controls with benign prostatic hyperplasia (12).

We report here the utility of a single preoperative measurement of serum cav-1 for predicting disease recurrence in a cohort of 419 prostate cancer patients undergoing radical prostatectomy at our institution.

Authors' Affiliations: [1]Scott Department of Urology and Departments of [2]Pathology, [3]Radiology, [4]Medicine, and [5]Molecular and Cellular Biology, Baylor College of Medicine, Houston, Texas

Received 2/21/06; revised 3/31/06; accepted 4/20/06.

Grant support: National Cancer Institute Specialized Programs of Research Excellence grants P50-58204 and RO1-68814.

The costs of publication of this article were defrayed in part by the payment of page charges. This article must therefore be hereby marked *advertisement* in accordance with 18 U.S.C. Section 1734 solely to indicate this fact.

Requests for reprints: Dov Kadmon, Scott Department of Urology, Baylor College of Medicine, 6560 Fannin, Suite 2100, Houston, TX 77030. E-mail: dkadmon@bcm.tmc.edu.

doi:10.1158/1078-0432.CCR-06-0417

Materials and Methods

Study population. The sera of 419 prostate cancer patients were obtained from the Specialized Programs of Research Excellence prostate cancer blood and tissue bank at Baylor College of Medicine. Entry into the study required availability of preoperative serum samples obtained within 6 months of surgery and complete data on age, race, stage at enrollment and follow-up, as well as availability of postoperative serum samples, as this is a part of a larger ongoing investigation. In addition, patients could have had no preoperative therapy. After completion of cav-1 measurements in the serum, it was discovered that seven patients were missing reliable data on their preoperative PSA and/or biopsy Gleason score and/or follow-up information. These patients were included in all analyses that did not require missing data. The preoperative serum collected from 355 patients was at a time period between prostate biopsy and surgery. No information was available in our database on the exact preoperative serum collection timing with respect to biopsy for 64 patients. The mean age of this patient group was 62.6 years (range 42.6-78.9 years); 91.4% were White males, with Hispanics, African-Americans, and Asians comprising 6.0%, 2.4%, and 0.2%, respectively. Mean follow-up time among this group of patients was 52 months, with a median follow-up time of 48 months. Biochemical recurrence is defined throughout this study as serum PSA level of $\geq$0.2 ng/mL on two consecutive measurements, using the first-generation postresection PSA assay (Hybritech, Beckman Coulter, Inc., Fullerton, CA). Patient data were gathered from the Informatics Core using the Specialized Programs of Research Excellence in Prostate Cancer Information System.

Determination of serum cav-1. Cav-1 was determined in the serum samples by the sandwich ELISA protocol developed in our laboratory (12). Briefly, Costar microplate wells were coated with 0.5 μg cav-1 polyclonal antibody (Transduction Laboratories, San Diego, CA) and blocked with TBS buffer containing 1.5% bovine serum albumin and 0.05% v/v Tween 20. Serum samples, calibrators, and controls (50 μL) were added to the well, and 50 μL TBS containing 0.5% v/v Tween 20 was added to each well. The plate was incubated at room temperature for 2 hours with shaking and after extensive washing, 100 μL horseradish peroxidase–conjugated cav-1 antibody (Santa Cruz Biotechnology, Santa Cruz, CA) diluted 1:200 in blocking buffer was added to each well. The microplate was incubated for 90 minutes at room temperature with shaking, the wells were then washed extensively, and 100 μL 3,3′,5,5′-tetramethylbenzidine substrate solution (Sigma-Aldrich, St. Louis, MO) was added and the blue color was allowed to develop for 20 minutes in the dark. The reaction was stopped by adding 50 μL of 2 N H_2SO_4, and the absorbance was read at 450 nm using a microplate reader (Sunrise Microplate Reader, Tecan US, Inc., Charlotte, NC).

Statistical analysis. Correlations of preoperative serum cav-1 levels with clinical and pathologic variables were evaluated using the Spearman correlation. The predictive value of cav-1 univariately and multivariately with other preoperative clinical and pathologic variables, such as preoperative PSA and biopsy Gleason score, as well as of the interactive terms, were analyzed using the Cox proportional hazards regression model. The minimum *P* value method was used to group patients into "low-level" and "high-level" cav-1 categories (13). The hazard ratio (HR) and 95% confidence intervals (95% CI) were computed for each marker. Kaplan-Meier survival curves were plotted for each risk category. $P < 0.05$ was considered statistically significant. All analyses were done using the SPSS 12.0 software package (SPSS, Inc., Chicago, IL)

Table 1. Preoperative serum cav-1 level correlation with clinical and pathologic variables

	n	Mean (range), %	r^2	*P*
Preoperative cav-1	419	4.5 (0.0-156.7)	—	—
Preoperative PSA (ng/mL)	415	8.6 (0.4-53.2)	0.01	0.9013
Age	419	62.6 (42.6-78.9)	0.02	0.6268
Biopsy Gleason score	412	6.1 (3-9)	−0.06	0.2051
Seminal vesicle invasion	419	7.6%	−0.01	0.8543
Lymph node involvement	419	3.8%	0.08	0.1024
Extraprostatic extension	419	32.7%	0.07	0.1378
Margin positive	419	11.9%	0.06	0.2425
Gleason score	419	6.5 (3-9)	−0.01	0.8342

Table 2. Preoperative serum cav-1 is a univariate and multivariate predictor of decreased biochemical recurrence-free survival

	HR (95% CI)	*P*
Univariate model		
Preoperative cav-1	2.78 (1.003-7.70)	0.0493
Multivariate model		
Preoperative cav-1	2.57 (0.92-7.12)	<0.0704
Ln(PSA)	2.31 (1.60-3.33)	<0.0001
Biopsy Gleason score	1.74 (1.32-2.30)	0.0001

Results

Serum cav-1 levels were measured in 419 prostate cancer patients. The mean cav-1 value was 4.52 ng/mL and the median level was 1.01 ng/mL (range 0.0-156.7 ng/mL). Serum cav-1 levels seemed to have a bimodal distribution, with positive values distributed log normally. The serum cav-1 levels were analyzed for correlation with other pathologic and clinical variables using the Spearman correlation. No statistically significant correlations with clinicopathologic variables were found (Table 1).

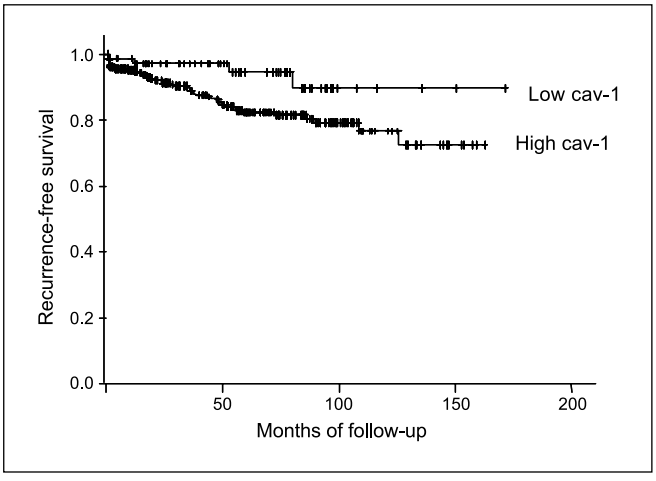

Fig. 1. High expression of cav-1 predicts decreased biochemical recurrence-free survival. This Kaplan-Meier plot illustrates the differences in recurrence-free survival between the low and high groups when separated by cav-1 cut point of 0.13 ng/mL. Patients with high level of cav-1 experienced significantly higher risk of recurrence than those with low levels ($P = 0.0493$).

There were 414 patients with complete follow-up information were included in the analysis of recurrence-free survival (mean follow-up 52.3 months, maximum 171.3 months); 54 patients had PSA recurrence during follow-up. Although it was clear that patients with no or very low levels of cav-1 had a better prognosis, the optimal cutoff was selected using the minimum *P* value method (13). This defined the low cav-1 group as patients with levels of <0.13 ng/mL and the high cav-1 group as those with >0.13 ng/mL. In univariate analysis, the risk of experiencing biochemical recurrence, estimated by HR, was 2.8 times higher ($P = 0.0493$) for the high cav-1 group compared with the low cav-1 group (Table 2). Kaplan-Meier plots illustrate the shorter time to biochemical recurrence following radical prostatectomy in the high cav-1 group compared with low cav-1 group. The 5- and 10-year recurrence-free survival rates were 94.4% and 90.5% for the low cav-1 group compared with 82.0% and 71.8% for the high cav-1 group. This corresponds to a consistent 12% to 21% increased progression-free survival for the low cav-1 group (Fig. 1). When the preoperative serum PSA level and the biopsy Gleason score were incorporated into the multivariate Cox proportional hazard model, the recurrence risk was 2.6 times higher for the high cav-1 group, but this effect was just below the level of significance ($P = 0.0704$; Table 2).

The effect of the serum cav-1 level on biochemical recurrence was further analyzed in patients with more advanced cancers, characterized by PSA of ≥10 ng/mL. The distribution shape remained the same and patients with low cav-1 levels continued to have a better prognosis. A new optimal cutoff of 2.86 ng/mL was identified for this subgroup of patients. Univariately, the estimated risk of recurrence was 2.44 times higher ($P = 0.0256$) in the high cav-1 group (serum cav-1 >2.86 ng/mL) than in its low cav-1 counterpart (serum cav-1 ≤ 2.86 ng/mL; Table 3). Kaplan-Meier plots illustrate that patients in the high cav-1 group had a much shorter time to recurrence than those in the low cav-1 group (Fig. 2). This figure also indicates a 10-year recurrence-free survival rate of 70.3% in the low cav-1 group compared with 47.4% in the high cav-1 group corresponding to a >20% decrease in progression-free survival in the low cav-1 group.

Incorporating the biopsy Gleason score into the Cox proportional hazard model (Table 3), we found that the interaction term between Gleason score and the cav-1 was the most predictive ($P = 0.0353$). This indicates that the biopsy Gleason score was an additional risk factor only in the high cav-1 group. The Kaplan-Meier plot (Fig. 3) illustrates this result by showing the highest recurrence risk in patients with high cav-1 and high biopsy Gleason score (7–9); and lower

Table 3. Preoperative serum cav-1 is a univariate and multivariate predictor of decreased biochemical recurrence-free survival among patients with preoperative PSA of ≥10

	HR (95% CI)	*P*
Univariate model		
Preoperative cav-1	2.44 (1.12-5.34)	0.0256
Multivariate model		
Preoperative Cav-1 × biopsy Gleason score	1.13 (1.01-1.27)	0.0353

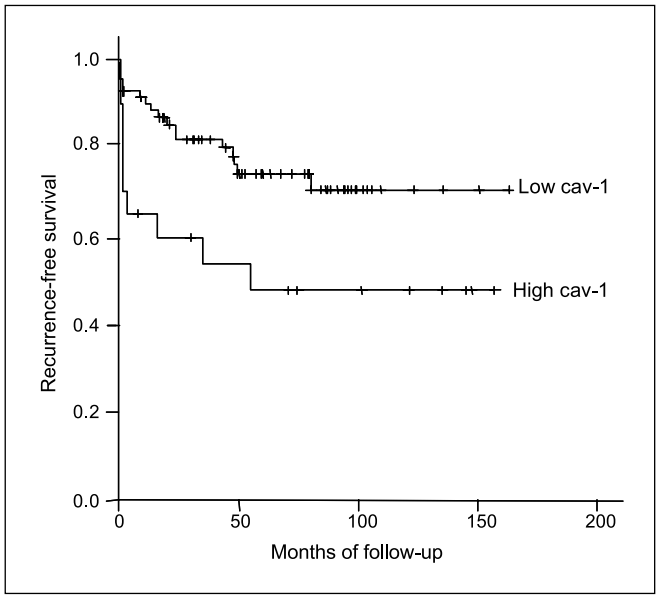

Fig. 2. For patients with PSA of ≥10, high expression of cav-1 is a strong predictor of decreased biochemical recurrence-free survival. For this high-risk patient subgroup, optimal cutoff was determined to be at 2.86 ng/mL. The Kaplan-Meier plot here shows the difference observed in the data.

recurrence risk in the high cav-1 and low biopsy Gleason score (<7) group, and those patients with low cav-1 regardless of the biopsy Gleason score. Recurrence-free survival curve for patients with low PSA (<10) was plotted for reference as well.

For biopsy Gleason 7 patients, the trend was the same: Higher cav-1 was observed in higher-risk patients. The difference in risk of recurrence, estimated by HR, between low and high cav-1 patients with cutoff defined at upper quartile of cav-1 (and confirmed by minimum *P* value method), was not statistically significant ($P = 0.0953$). However, after including preoperative PSA in the model, the

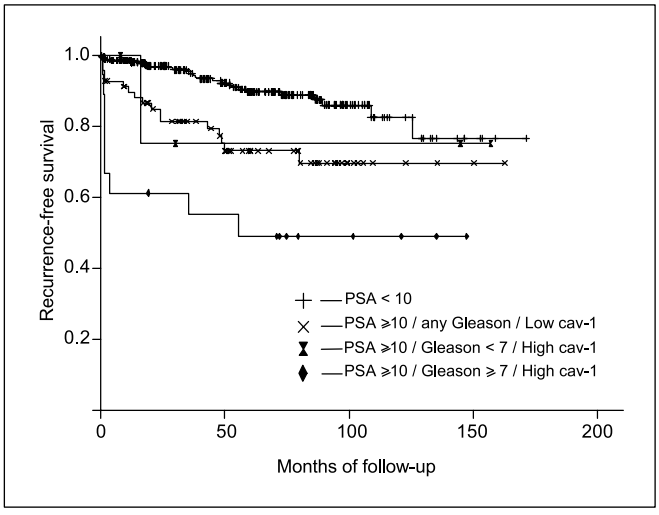

Fig. 3. Cav-1 works with biopsy Gleason score and preoperative PSA to predict biochemical recurrence-free survival. The interaction term between biopsy Gleason score and the cav-1, incorporated into the Cox proportional hazard, was the most predictive of recurrence-free survival among patients with PSA of ≥10 ($P = 0.0353$). This Kaplan-Meier plot illustrates how patients with both high cav-1 (>2.86 ng/mL) and biopsy Gleason score of ≥7 have the poorest prognosis. Curve for patients with PSA < 10 was plotted for reference.

difference became statistically significant (HR, 2.29; P = 0.0429). A patient with cav-1 in the upper quartile had over twice the risk of recurrence of one with cav-1 in the lower three quartiles if their preoperative PSA levels were the same.

Discussion

This study is part of our ongoing efforts to elucidate the biology and to define the clinical usefulness of serum cav-1 in prostate cancer. Although the factors modulating the serum levels of this biomarker remain largely unknown, the current study points out that a single preoperative serum cav-1 determination has prognostic value in a radical prostatectomy cohort. We observed the increase of the risk of biochemical recurrence with high levels of serum cav-1, and so we used the minimum P value method to segregate the patients into low-level and high-level groups. Remarkably, the risk of experiencing a PSA recurrence, estimated by HR, was 2.78 (95% CI, 1.003-7.70) times higher for the high-level cav-1 group (P = 0.0493), (see Fig. 1; Table 2). Incorporating the preoperative serum PSA level and the biopsy Gleason score into the model dropped the effect of cav-1 to just below the level of significance (HR, 2.57; P = 0.0704).

Interestingly, we found that the serum cav-1 levels are particularly important in predicting recurrence-free survival in patients with more advanced disease as defined by the preoperative serum PSA. When only patients with preoperative serum PSA levels of 10 ng/mL or higher were analyzed, cav-1 remained a significant predictor of recurrence-free survival (HR, 2.44; P = 0.0256). Additionally, the cav-1/biopsy Gleason score interaction term was a significant predictor (P = 0.0353). This implies that patients with both a high biopsy Gleason score and a high serum cav-1 level have a higher risk of biochemical recurrence than the remaining patients. Also, a subgroup of biopsy Gleason 7 prostate cancer patients, defined by the upper 25% of serum cav-1 levels, seems to harbor a biologically more aggressive prostate cancer after correction for individual PSA levels. All of these findings are consistent with our previous reports based on tissue up-regulation of cav-1 expression (8).

Notably, the distribution of the serum cav-1 values in the study population was not a normal distribution. About 10% of patients had undetectable serum levels by our sensitive ELISA essay. We can only speculate at this point as to the possible reason for this phenomenon. It is possible that the presence of any cav-1 in the serum is dictated by the genetic background of the individual and that, physiologically, there may be "secretors" and "nonsecretors." Within the secretor population, the specific makeup of the cancer may be contributing to the absolute serum level.

Surprisingly, we could not correlate the serum cav-1 levels with any of a large number of clinical and/or pathologic variables using the Spearman correlation (Table 1). We suggest that the reason is that cav-1 is an independent biomarker causally implicated in disease progression and not simply an epiphenomenon.

Many questions remain. For instance, we do not know the incidence of false-positive and/or false-negative elevated serum cav-1 values vis-à-vis the tumor tissue cav-1 expression. Only a correlative study of tissue and serum levels of cav-1 can answer this question. Likewise, the kinetics of the serum cav-1 has not been worked out, nor do we know what the stability of serum cav-1 is over extended periods of time. Clearly, we are at the beginning of the road leading to the establishment of serum cav-1 as a prognostic marker for prostate cancer. The data presented here suggest that this road is worth pursuing.

References

1. Cooperberg MR, Moul JW, Carroll PR. The changing face of prostate cancer. J Clin Oncol 2005;23:8146–51.
2. Shipley WU, Thames HD, Sandler HM, et al. Radiation therapy for clinically localized prostate cancer: a multi-institutional pooled analysis. JAMA 1999;281:1598–604.
3. Bracarda S, de Cobelli O, Greco C, et al. Cancer of the prostate. Crit Rev Oncol Hematol 2005;56:379–96.
4. Chin JL, Reiter RE. Molecular markers and prostate cancer prognosis. Clin Prostate Cancer 2004;3:157–64.
5. Shaul PW, Anderson RG. Role of plasmalemmal caveolae in signal transduction. Am J Physiol 1998;275:L843–51.
6. Ikonen E, Parton RG. Caveolins and cellular cholesterol balance. Traffic 2000;1:212–7.
7. Nasu Y, Timme TL, Yang G, et al. Suppression of caveolin expression induces androgen sensitivity in metastatic androgen-insensitive mouse prostate cancer cells. Nat Med 1998;4:1062–4.
8. Yang G, Truong LD, Wheeler TM, Thompson TC. Caveolin-1 expression in clinically confined human prostate cancer: a novel prognostic marker. Cancer Res 1999;59:5719–23.
9. Satoh T, Yang G, Egawa S, et al. Caveolin-1 expression is a predictor of recurrence-free survival in pT_2N_0 prostate carcinoma diagnosed in Japanese patients. Cancer 2003;97:1225–33.
10. Yang G, Addai J, Ittmann M, Wheeler TM, Thompson TC. Elevated caveolin-1 levels in African-American versus White-American prostate cancer. Clin Cancer Res 2000;6:3430–3.
11. Tahir SA, Yang G, Ebara S, et al. Secreted caveolin-1 stimulates cell survival/clonal growth and contributes to metastasis in androgen-insensitive prostate cancer. Cancer Res 2001;61:3882–5.
12. Tahir SA, Ren C, Timme TL, et al. Development of an immunoassay for serum caveolin-1: a novel biomarker for prostate cancer. Clin Cancer Res 2003;9:3653–9.
13. Mazumdar M, Glassman JR. Categorizing a prognostic variable: review of methods, code for easy implementation and applications to decision-making about cancer treatments. Stat Med 2000;19:113–32.

Human Pathology (2007) **38**, 1688–1695

ELSEVIER

Human PATHOLOGY

www.elsevier.com/locate/humpath

Original contribution

Correlative evidence that prostate cancer cell-derived caveolin-1 mediates angiogenesis☆

Guang Yang MD[a], Josephine Addai MS[a], Thomas M. Wheeler MD[b], Anna Frolov MS[a], Brian J. Miles MD[a], Dov Kadmon MD[a], Timothy C. Thompson PhD[a,c,d,*]

[a] *Department of Urology, Baylor College of Medicine, Houston, TX 77030, USA*
[b] *Department of Pathology, Baylor College of Medicine, Houston, TX 77030, USA*
[c] *Department of Molecular and Cellular Biology, Baylor College of Medicine, Houston, TX 77030, USA*
[d] *Department of Radiology, Baylor College of Medicine, Houston, TX 77030, USA*

Received 30 November 2006; revised 20 March 2007; accepted 23 March 2007

Keywords:
Prostate cancer;
Angiogenesis;
Caveolin-1

Summary Up-regulation of caveolin-1 (cav-1) has been implicated in human prostate cancer progression/metastasis and shown to promote cancer cell survival. It has also been shown that cav-1 is secreted by tumor cells and may regulate the growth, functional activities, and migration of vascular endothelial cells. However, the relationship of cav-1 expression in prostate cancer cells and tumor associated endothelial cells (TAEC) to tumor-associated angiogenesis remains to be investigated. Dual immunofluorescent labeling with antibodies to CD34 and cav-1 was performed on 56 prostate cancer specimens obtained by radical prostatectomy and stratified according to cav-1 positivity in cancer cells. The tumor microvessel densities (MVD) and cav-1 expression in TAEC within these specimens were measured and correlated with cav-1 expression in prostate cancer cells. The MVD values were significantly higher in cav-1-positive (n = 25) than in the cav-1-negative (n = 31) tumors (median of 44 versus 25 vessels/field, P = .0140). Additional studies showed that the cav-1 positivity in microvessels within tumor specimens was significantly less frequent than in the blood vessels of benign prostatic tissues (94.4% versus 98.6%, P = .0012). In contrast, the percentage of cav-1-positive TAEC in cav-1-positive tumors was significantly higher than in cav-1-negative tumors (95.8% versus 92.7%, P = .0024). This increased cav-1 positivity in TAEC was predominantly confined to regions with cav-1-positive tumor cells corresponding to the higher percentage of cav-1-positive microvessels within these regions in cav-1-positive, as opposed to cav-1-negative tumors (P = .0086). These positive correlations provide new evidence for the involvement of prostate cancer cell derived cav-1 in mediating angiogenesis during prostate cancer progression. They also establish a conceptual framework for further investigation of cav-1 proangiogenic activities.

1. Introduction

Caveolin-1 (cav-1) is an important structural/regulatory molecule involved in many aspects of molecular transport and normal cell signaling. The biologic consequences of inappropriate cav-1 expression in malignant cells depend

☆ This work was supported by NIH grants SPORE CA58204 and RO1 CA68814 and a grant from the Department of Defense.

* Corresponding author. Department of Urology, Baylor College of Medicine, Houston, TX 77030, USA.
E-mail address: timothyt@bcm.edu (T. C. Thompson).

0046-8177/$ – see front matter © 2007 Elsevier Inc. All rights reserved.
doi:10.1016/j.humpath.2007.03.024

on protein level and cell context (for review, see [1]). In contrast to studies that suggest a growth suppressor role for cav-1 in malignant cells [2-4], our research has documented overexpression of cav-1 in both mouse and human prostate cancer cells [5] and established its correlation with metastasis and androgen insensitivity of prostate cancer cells [6,7]. We have also shown that cav-1 overexpression is associated with an unfavorable clinical prognosis in men who have undergone radical prostatectomy [8]. A positive correlation between cav-1 overexpression and clinicopathologic markers of cancer progression has been reported for other malignancies, including colon cancer [9], renal cancer [10,11], bladder cancer [12,13], oral squamous cancer [14], esophageal squamous cancer [15,16], papillary carcinoma of the thyroid [17], lung cancer [18-20], pancreatic cancer [21,22], ovarian cancer [23], and some types of breast cancer [24].

The molecular mechanism(s) that underlie the role of increased cav-1 expression in promoting prostate cancer cell progression are unclear. However, we have recently shown that cav-1 protein binds to and inhibits the activities of PP1/PP2A serine/threonine phosphatases, preventing inactivation of Akt through dephosphorylation and thus sustaining levels of phospho-Akt and its activity in procancer cells survival [25,26]. We have also demonstrated that metastatic prostate cancer cells secrete biologically active cav-1 in a steroid-regulated fashion [27]. Using an in vivo mouse prostate cancer model, we showed that antibody to cav-1 protein may inhibit prostate cancer metastasis, whereas cav-1 derived from cancer cells may function as a paracrine/endocrine factor [27]. This clearly indicates that the function of cav-1 in prostate cancer progression/metastasis may involve a complex series of cell/cell interactions, some with cancer cells exclusively, some with stromal cells, and others with vascular endothelial cell (EC).

Accumulating evidence suggests that cav-1 can regulate the growth, differentiation, and functional activities of vascular EC [28-30]. In cultured human EC, cav-1 up-regulation enhances EC tubule formation [31] and stimulates the migration of cultured human EC [32]. In an experimental tumor model based on a melanoma cell line, B16-F10, angiogenesis is impaired in *cav-1*$^{-/-}$ compared to *cav-1*$^{+/+}$ mice, indicating a critical role for this regulatory protein in tumor angiogenesis [33].

We therefore analyzed the role of cav-1 expression in angiogenesis in human prostate cancer specimens with close attention to the potential interaction between cancer cells and tumor-associated EC (TAEC). Using a dual immunofluorescent technique that detects colocalization of cav-1 protein and CD34 antigen, an EC marker [34], in situ, we compared measurements of cav-1expression in prostate cancer cells with tumor microvessel densities (MVDs) or cav-1 positivity in TAEC. Results indicate an important role for prostate cancer cell-derived cav-1 in tumor angiogenesis and thus in the promotion of tumor progression/metastasis.

2. Materials and methods

2.1. Patients and tissue processing

For this study, prostate cancer specimens were obtained from Baylor College of Medicine Prostate Cancer Specialized Programs of Research Excellence Tissue Core, and collected from fresh radical prostatectomy specimens after informed consent was obtained under an institutional review board-approved protocol. Fifty-six specimens derived from a patient cohort (n = 189) that had been previously selected in a consecutive manner by an independent statistician and had been characterized for cav-1 expression using ABC immunostaining as described [8] were included in this study. All patients had undergone radical prostatectomy for moderate to poorly differentiated prostate adenocarcinoma (Gleason score, 5-9) that was clinically localized to the prostate (cT1/T2, NX, M0) as determined by physical examination and transrectal ultrasound imaging in each case. The dominant focus of tumor cells within the radical prostatectomy specimen was representative of the overall grade ascribed to that tumor using the method of Gleason. The 56 specimens, based on cav-1 immunostaining result, were categorized into the following 2 groups: those with (n = 25) or without (n = 31) cav-1-positive cancer cells. Eight benign prostate specimens from cystoprostatectomies were used as controls.

2.2. Immunohistochemistry

Double immunofluorecence staining was performed on formalin-fixed, paraffin-embedded, 5-μm sections derived from punch biopsies of archived blocks of prostate tumor specimens. The rabbit polyclonal anti-cav-1 antibody (Santa Cruz Biotechnology Inc, Santa Cruz, CA) and mouse monoclonal anti-CD34 antibody (QBEnd/10; Neo-Markers, Fremont, CA) were used to identify cav-1 protein accumulation in vascular EC. Briefly, after tissue sections were deparaffinized and rehydrated through graded alcohol, they were heated in 0.01 mol/L citrate buffer at pH 6.0 by microwave for 10 minutes to enhance antigen retrieval. After a 20-minute blocking step with 3% normal horse or goat serum, the sections were sequentially incubated with cav-1 antibody diluted 1:200 for 90 minutes, and then in biotinylated antirabbit IgG and in streptavidin-FITC for 30 minutes each. The sections were reblocked in 1.5% normal horse serum for 20 minutes and incubated in CD34 antibody diluted 1:80, followed by incubation in Cy-3 conjugated antimouse IgG. Positive and negative controls were included in each experiment. The specificity of immunoreactions was verified by replacing the primary antibodies with phosphate-buffered saline or with normal rabbit or mouse serum. In addition, double labeling with cav-1 and PCNA (DaKo, Glostrup, Denmark), or cav-1 and vascular endothelial growth factor

receptor 2 (VEGFR2) (Santa Cruz Biotechnology Inc) as well as VEGFR2 and factor VIII (Dako) antibodies were performed by using similar protocols on some specimens. The labeled specimens were evaluated with a Zeiss fluorescent microscope (Carl Zeiss Inc, Jena, Germany) equipped with a video camera that captured and digitized the images from each fluorophore (red for CD34 and green for cav-1). Each complete section was viewed systematically field-by-field over the entire cancer area, with each measured field corresponding to a real tissue area of 0.0625 mm^2. The densities of microvessels labeled by CD34 and the percentages of the cav-1-negative microvessels were measured on individually acquired images for each fluorophore and on superimposed images of both fluorophores with the aid of OPTIMAS (6.0) software. The percentage of cav-1-positive microvessels was calculated by the formula, 100 × (total number of CD34-positive vessels − cav-1-negative vessels) / total number of CD34-positive vessels. The percentage of VEGFR2-positive microvessels was also measured by using a similar procedure.

2.3. Statistical methods

Mann-Whitney rank analysis was used to compare MVD values, the percentages of cav-1-positive microvessels, and the percentages of VEGFR2-positive microvessels. Wilcoxon signed-rank test was used to analyze paired comparisons of cav-1 positivity in the TAEC of cav-1-positive versus cav-1-negative tumor regions. A *t* test for independent samples and Mann-Whitney rank test were used to compare covariates distributions between groups. Logistic regression analysis was used to verify the significance of the observed differences among covariates. *P* values of less than .05 were considered statistically significant. All analyses were performed with the SPSS 12.0 software package (SPSS Inc, Chicago, IL).

3. Results

Immunohistochemical analyses were conducted on the adjacent sections of a subset of prostate cancer specimens that had been analyzed for cav-1 expression and in which positive correlations between cancer cell cav-1 expression and adverse clinicopathologic features, as well as a poor clinical outcome, had been found [8]. The specimens were then stratified as cav-1-positive (n = 25) or cav-1-negative (n = 31) based on the detection of cav-1 expression in cancer cells by the ABC immunohistochemical analysis with confirmation by immunofluorescence staining (100% concurrence between the 2 procedures). The 2 groups of patients represented by the stratified specimens were comparable in age, pathologic and clinical staging, and Gleason score. CD34 antigen and cav-1 were expressed simultaneously in the vascular EC of these specimens; hence, specific expression of cav-1 in EC could be recognized on the superimposed images derived from dual labeling (Fig. 1). The specificity of each antibody reaction was confirmed by the loss of staining after the primary antibody was replaced with nonspecific IgG or phosphate-buffered saline (data not shown).

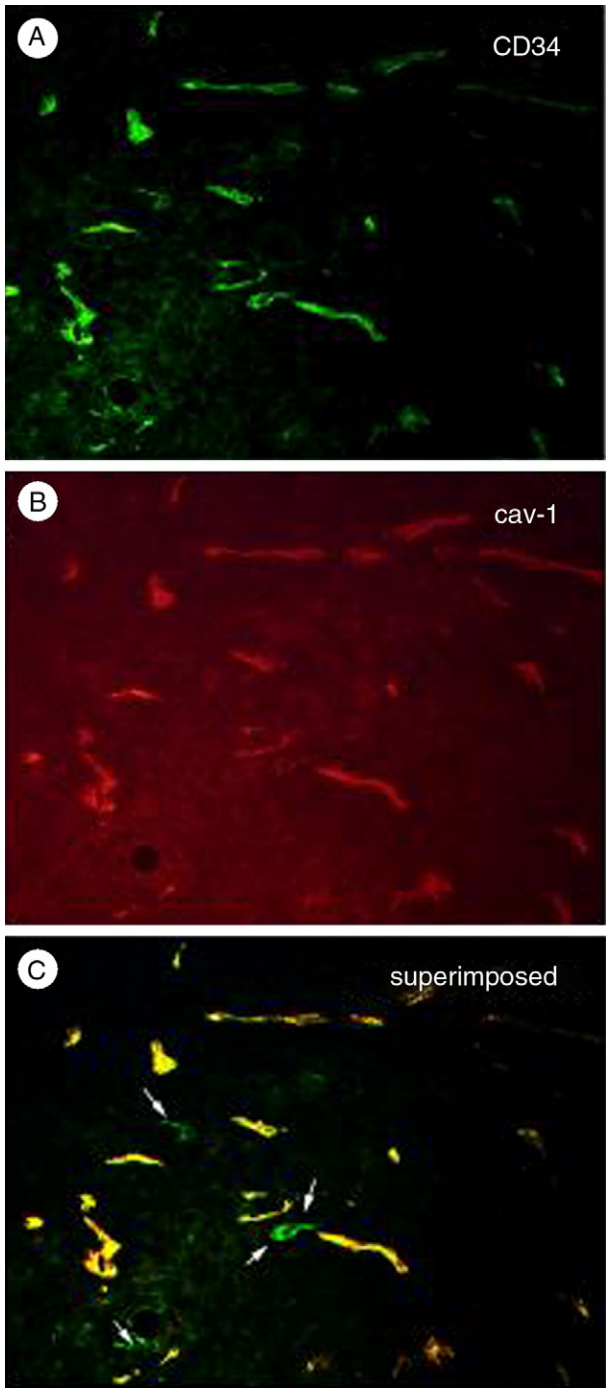

Fig. 1 Analysis of cav-1 positivity in human prostate cancer specimens using cav-1 and CD34 double immunofluorescence labeling. A, $CD34^+$ cells; B, $cav\text{-}1^+$ cells; C, superimposed $CD34^+$ and $cav\text{-}1^+$ cells (arrows indicate cav-1-negative EC).

3.1. Higher MVDs in cav-1-positive tumors

Microvessels labeled with CD34 antibody were quantified within systemically sampled regions of prostate tumor specimens. The MVDs were first assessed according to the cav-1 status of the samples. The MVD value for all cav-1-positive tumors was significantly higher than that for the cav-1-negative tumors (median density, 44 versus 25 microvessels/field; $P = .0140$) (Fig. 2). This difference remained significant ($P = .038$) after adjusting for patients' ages, clinicopathologic tumor stage, and total Gleason score (data not shown).

3.2. Cav-1-positive tumors demonstrate a higher percentage of cav-1-positive microvessels

Most CD34-positive microvessels (>90%) were positively labeled by the cav-1 antibody (Fig. 1A, B); however, a small fraction of the EC aggregates lacked detectable cav-1 protein by immunohistochemistry (Fig. 1C) and tended to form smaller microvessel fragments or to extend via single cell "sprouts" (arrows in Fig. 1C). To calculate the percentage of cav-1-positive microvessels, we used the formula: 100 × (total number of CD34-positive vessels − cav-1-negative, CD-34-positive vessels) / total number of CD34-positive vessels. Thus, the median proportion of cav-1-positive blood vessels in benign prostate specimens was 98.61% (range, 93.19%-100%), compared with 94.41% (range 71.32%-98.76%) in the tumor specimens ($P = .0012$, Fig. 3). After stratification of the samples into cav-1-positive and cav-1-negative groups (n = 25 and 31, respectively), a significantly higher percentage of cav-1-positive microvessels (median, 95.78%; range, 80%-98.76%) was found in cav-1-positive compared with cav-1-negative specimens (median, 92.65%; range71.32%-97.32%) ($P = .0024$; Fig. 4). This difference remained significant ($P = .0280$) after adjustment for patients' ages, clinicopathologic tumor stage, and total Gleason score. Moreover, both the cav-1-negative and the cav-1-positive tumors had a significantly lower percentage of cav-1-positive vessels than the benign prostates specimens ($P = .0004$ or $P = .0148$, respectively) (Fig. 4).

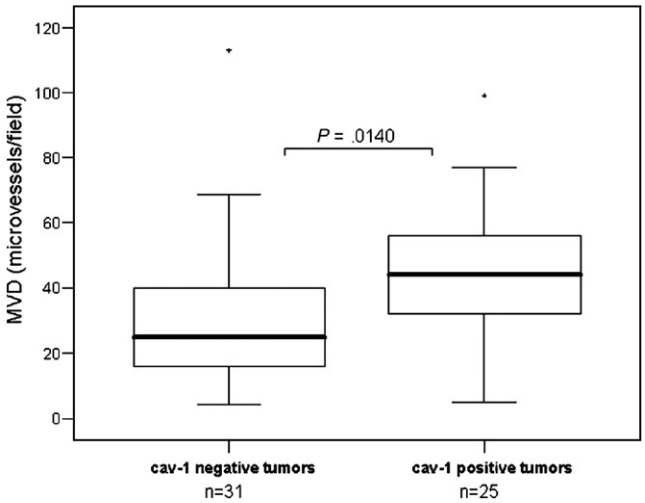

Fig. 2 Comparisons of MVDs between cav-1^+ and cav-1^- tumor specimens as demonstrated by box plots. Top and bottom lines of each box denote 75th and 25 percentile values, whereas the middle line shows the median value. Vertical bars extend to 90th and 10th percentiles, outliers are indicated by crosses.

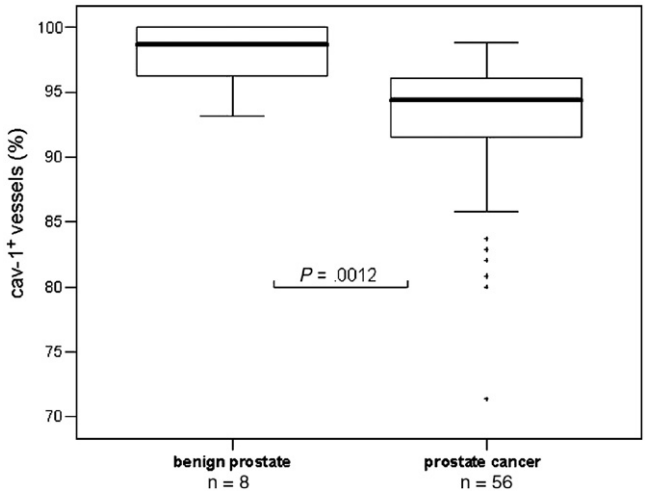

Fig. 3 Cav-1 positivity in vascular EC of benign prostate specimens (n = 8) was compared with that of prostate cancer specimens in box plots. Top and bottom lines of each box denote 75th and 25 percentile values, whereas the middle line shows the median value. Vertical bars extend to 90th and 10th percentiles, outliers are indicated by crosses.

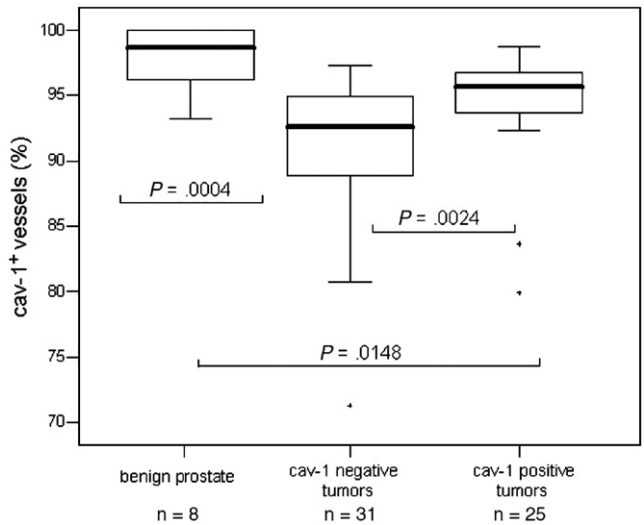

Fig. 4 Comparison of the percentages of cav-1^+ blood vessels between cav-1^+ and cav-1^- tumor specimens as well as benign prostate tissues. In the box plots, top and bottom lines of each box denote 75th and 25 percentile values, whereas the middle line shows the median value. Vertical bars extend to 90th and 10th percentiles, outliers are indicated by crosses.

3.3. Increased percentage of cav-1-positive microvessels surrounding cav-1-positive cancer cells

To further analyze the effect of prostate cancer cell-associated cav-1 expression on angiogenesis, we examined cav-1 positivity in EC within regions of cav-1-positive tumors containing cav-1-positive cancer cells versus that in regions lacking such cells. Results (Fig. 5) showed a higher percentage of cav-1-positive microvessels within cav-1-positive regions (median, 96.30%; range, 79.75%-100%) than in regions comprising cav-1-negative tumor cells (median, 93.55%; range, 72.45%-98.76%) (P = .0102). Further comparison showed that the percentage of cav-1-positive microvessels in tumor regions positive for cav-1 was also significantly higher than in cav-1-negative tumors (P = .0086; Fig. 5).

3.4. Similar proliferative rates in cav-1-positive and cav-1-negative TAEC

The possibility that differences in cav-1 expression in TAEC might be related to cell proliferative rate led us to double-label 12 cav-1-negative tumors with cav-1 and PCNA antibodies and the nuclear dye DAPI to measure proliferative index. The median PCNA labeling index was 0.26 (range, 0.14 -1.27) for cav-1-negative TAEC and 0.40 (range, 0-2.45) for cav-1-positive TAEC (P = .51), suggesting that our cav-1 findings were not significantly influenced by the EC proliferative rate.

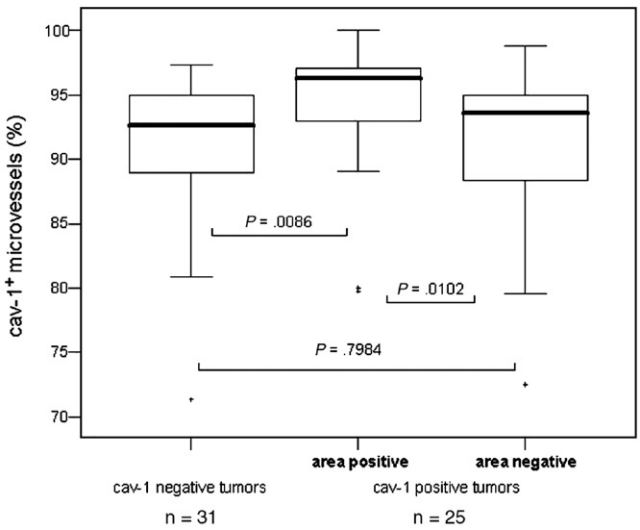

Fig. 5 Comparisons of microvessel cav-1 positivity within cav-1^+ tumor specimens (areas with cav-1^- versus cav-1^+ cancer cells) and between areas with cav-1^- or cav-1^+ cancer cells in cav-1^+ tumor species with cav-1^- cancer specimens. Top and bottom lines of each box denote 75th and 25 percentile values, whereas the middle line shows the median value. Vertical bars extend to 90th and 10th percentiles, outliers are indicated by crosses.

3.5. Higher percentage of VEGFR2-positive microvessels is associated with cav-1-positive tumors

To explore a possible mechanism for the cav-1 effect on angiogenesis, VEGFR2 expression was analyzed on prostate cancer samples double-labeled with VEGFR2 and cav-1 or factor VIII antibodies. We demonstrated that VEGFR2 was present in both prostate cancer cells and some TAEC, and that VEGFR2 tended to be colocalized with cav-1 in TAEC (Fig. 6A). Quantitative analysis indicated that the percentage of microvessels containing VEGFR2-positive TAEC was significantly higher in the cav-1-positive than the cav-1-negative tumors (P = .002, Fig. 6B).

4. Discussion

In a previous study we demonstrated that cav-1 is overexpressed in focal clusters of prostate cancer cells in approximately 30% human prostate cancers, and that the presence of cav-1-positive tumor cells is associated with a poor survival [8]. The relationship of cav-1 overexpression in cancer cells to cancer progression/metastasis has been suggested to involve multiple mechanisms, including the promotion of cancer cells survival [35] and migration [18]. The quantitative immunohistochemical analyses reported here demonstrate a positive correlation of cav-1 expression in prostate cancer cells with MVD, suggesting that cav-1 may play a proangiogenic role in human prostate cancer. In experimental cancer models, cav-1 has been suggested both as an antiangiogenic [36] and as a proangiogenic factor [33], depending on the model system used. Most in vitro studies, however, have shown that cav-1 can exert direct effects on cultured human EC, regulate EC growth and differentiation [28,29], and stimulate capillary tubule formation and EC migration [30,31]. Positive association of cav-1 levels and MVDs has been reported in clear cell renal carcinoma [11]. Consistent with these data, our findings support a proangiogenic role for cav-1 in human prostate cancer. Because increased angiogenesis has been implicated in the development of prostate cancer progression [37], we suggest that the proangiogenic activity of cav-1 may, in part, underlie prostate cancer progression/metastasis.

Our dual labeling technique enabled specific analysis of cav-1 expression in TAEC. By using this technique, we demonstrate that vascular EC in healthy prostate specimens almost invariably express high levels of cav-1 protein. In prostate cancer specimens, however, a small but increased percentage of TAEC does not express cav-1 at a level detectable by immunohistochemical staining. Consequently, the percentage of the cav-1-positive TAEC was significantly lower in malignant as compared with benign prostate specimens. This finding agrees with a recent study

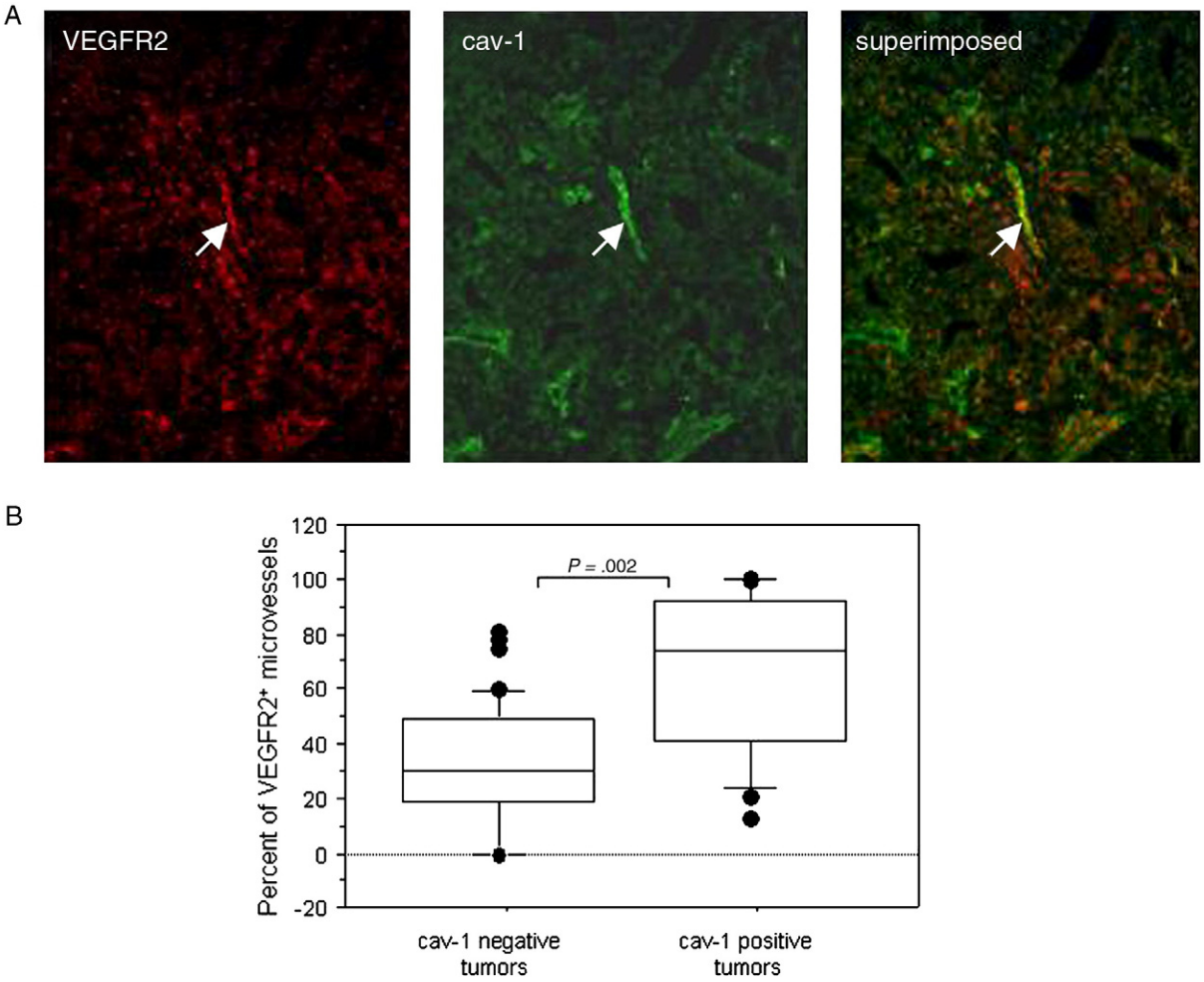

Fig. 6 A, Double immunofluorescence of VEGFR2 and cav-1 expression in a cav-1-positive cancer specimen showed VEGFR2 was present in some EC (indicated by arrows) in addition to cancer cells. The VEGFR2 (red) immunoreactivity was colocalized with cav-1 immunoreactivity (green) in these cells (see merged image). B, Comparisons in the percentages of VEGFR2-positive microvessels between cav-1-positive and cav-1-negative tumor specimens.

demonstrating a tumor-associated cav-1 deficiency in liver EC [38].

Although they account for only a small fraction of the vasculature of a prostate cancer, the cav-1-negative microvessels might represent the most functionally active tumor vasculature. Validation of this hypothesis will require additional studies. However, this concept is supported by the observation that the intratumoral cav-1-negative microvessels often appear as single cell "sprouts," suggesting that these formations are new microvessels. Notably, cav-1 deficiency in some TAEC does not appear to be directly related to EC proliferation, as the proliferative activity of these cells (as indicated by PCNA labeling), was not significantly different from that of cav-1-positive EC. The factors leading to cav-1 reduction in some TAEC remain to be identified. They may involve molecular events associated with EC sprouting/migration in response to certain proangiogenic growth factors (Fig. 7), such as VEGFs, which is known to be produced by prostate cancer cells and has been reported to inhibit cav-1 expression in cultured human EC [32].

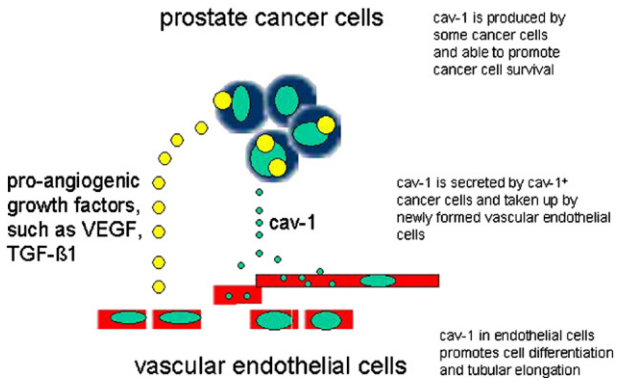

Fig. 7 Schematic layout of the possible mechanisms for cav-1-mediated interaction between cancer cells and adjacent vascular EC. Cav-1 is overexpressed in some prostate cancer cells and may be secreted into their microenvironment. In collaboration with other angiogenic growth factors (such as VEGF, transforming growth factor-β1, etc) also secreted by cancer cells, cav-1 is taken up by newly formed vascular EC that otherwise have very low levels of cav-1. The tumor cells associated cav-1 may thus regulate the formation, differentiation, and extension of the new microvessels.

Another important finding of this study is the association of cav-1 expression in cancer cells with cav-1 positivity in TAEC. In cav-1-positive tumors, there were fewer cav-1-negative TAEC than in the cav-1-negative tumors. Moreover, within the cav-1-positive tumors, TAEC in the regions containing cav-1-positive tumor cells have higher levels of cav-1 than TAEC in regions where cancer cells lacked cav-1 expression. We previously demonstrated that prostate cancer cells can secrete cav-1 and that the secreted protein can promote prostate cancer cell viability and clonal growth under serum-free conditions by inhibiting apoptosis in prostate cancer cells [27]. This activity is similar to that elicited by enforced expression of cav-1 within cells [25,26]. Interestingly, we also detected higher levels of cav-1 in the sera of patients with prostate cancer than in the sera of healthy controls or men with benign prostatic hyperplasia [39], another line of evidence that cancer cells secrete cav-1 into their microenvironment and blood circulation. More recently, we showed that recombinant cav-1 protein is taken up by mouse EC lacking the *cav-1* gene, and that cav-1 protein uptake may enhance the migration of EC (Tahir et al, unpublished results). Thus, the reduction of cav-1-negative TAEC surrounding cav-1-positive cancer cells is likely due, in part, to EC uptake of cav-1 protein secreted by cancer cells into the microenvironment or general circulation (Fig. 7). Thus, cancer cell–derived cav-1 may affect cav-1 levels in TAEC. Through the provision of cav-1 to the small fraction of highly active TAEC that are cav-1 deficient, the cav-1-positive tumors may have an advantage over their cav-1-negative counterparts in facilitating some aspects of tumor associated angiogenesis, and thereby, tumor progression/metastasis.

The molecular mechanism for the cav-1 effect in promoting angiogenesis remains to be investigated. It has been reported that VEGFR2 is a critical mediator of VEGF [40] one of the most potent proangiogenic growth factors in many types of cancer including prostate cancer [41,42]. The stimulation of VEGFR2 by tumor-derived VEGF represents a key event in the initiation of tumor-associated angiogenesis and VEGFR2 is localized in endothelial caveolae and associated with cav-1 [43]. To test for a possible role of VEGFR2 in cav-1-mediated angiogenesis, we analyzed VEGFR2/cav-1 coexpression in prostate cancer specimens by using double antibody labeling techniques. Our data show that VEGFR2 is colocalized with cav-1 protein in TAEC. We further demonstrated that there is a significantly higher percentage of VEGFR2-positive microvessels in the cav-1-positive tumors than in cav-1-negative tumors (Fig. 6). These results suggest that cav-1 may promote angiogenesis via interaction with VEGFR2. It has been reported that cav-1 interacts with VEGFR2 in endothelial caveolae and plays multiple roles in the VEGF-induced signaling cascade [43]. A further study of cav-1 interaction with the VEGF signaling pathway in prostate cancer is warranted.

The findings reported here suggest an important biologic mechanism through which cav-1 promotes prostate cancer progression. The use of our results for clinical application will require additional studies.

References

[1] Thompson TC. Metastasis-related genes in prostate cancer: the role of caveolin-1. Cancer Metastasis Rev 1998;17:439-42.

[2] Williams TM, Lisanti MP. The caveolin genes: from cell biology to medicine. Ann Med 2004;36:584-95.

[3] Galbiati F, Volonte D, Engelman JA, et al. Targeted downregulation of caveolin-1 is sufficient to drive cell transformation and hyperactivate the p42/44 MAP kinase cascade. EMBO J 1998;17:6633-48.

[4] Engelman JA, Zhang XL, Lisanti MP. Genes encoding human caveolin-1 and -2 are co-localized to the D7S522 locus (7q31.1), a known fragile site (FRA7G) that is frequently deleted in human cancers. FEBS Lett 1998;436:403-10.

[5] Yang G, Truong LD, Timme TL, et al. Elevated expression of caveolin is associated with prostate and breast cancer. Clin Cancer Res 1998;4: 1873-80.

[6] Satoh T, Yang G, Egawa S, et al. Caveolin-1 expression is a predictor of recurrence-free survival in pT2N0 prostate carcinoma diagnosed in Japanese patients. Cancer 2003;97:1225-33.

[7] Nasu Y, Timme TL, Yang G, et al. Suppression of caveolin expression induces androgen sensitivity in metastatic androgen-insensitive mouse prostate cancer cells. Nat Med 1998;4:1062-4.

[8] Yang G, Truong LD, Wheeler TM, Thompson TC. Caveolin-1 expression in clinically confined human prostate cancer: a novel prognostic marker. Cancer Res 1999;59:5719-23.

[9] Patlolla JM, Swamy MV, Raju J, Rao CV. Overexpression of caveolin-1 in experimental colon adenocarcinomas and human colon cancer cell lines. Oncol Rep 2004;11:957-63.

[10] Horiguchi A, Asano T, Asakuma J, Asano T, Sumitomo M, Hayakawa M. Impact of caveolin-1 expression on clinicopathological parameters in renal cell carcinoma. J Urol 2004;172:718-22.

[11] Joo HJ, Oh DK, Kim YS, Lee KB, Kim SJ. Increased expression of caveolin-1 and microvessel density correlates with metastasis and poor prognosis in clear cell renal cell carcinoma. BJU Int 2004;93:291-6.

[12] Rajjayabun PH, Garg S, Durkan GC, Charlton R, Robinson MC, Mellon JK. Caveolin-1 expression is associated with high-grade bladder cancer. Urology 2001;58:811-4.

[13] Sanchez-Carbayo M, Socci ND, Charytonowicz E, et al. Molecular profiling of bladder cancer using cDNA microarrays: defining histogenesis and biological phenotypes. Cancer Res 2002;62: 6973-80.

[14] Hung KF, Lin SC, Liu CJ, Chang CS, Chang KW, Kao SY. The biphasic differential expression of the cellular membrane protein, caveolin-1, in oral carcinogenesis. J Oral Pathol Med 2003;32:461-7.

[15] Hu YC, Lam KY, Law S, Wong J, Srivastava G. Profiling of differentially expressed cancer-related genes in esophageal squamous cell carcinoma (ESCC) using human cancer cDNA arrays: over-expression of oncogene MET correlates with tumor differentiation in ESCC. Clin Cancer Res 2001;7:3519-25.

[16] Kato K, Hida Y, Miyamoto M, et al. Overexpression of caveolin-1 in esophageal squamous cell carcinoma correlates with lymph node metastasis and pathologic stage. Cancer 2002;94:929-33.

[17] Ito Y, Yoshida H, Nakano K, et al. Caveolin-1 overexpression is an early event in the progression of papillary carcinoma of the thyroid. Br J Cancer 2002;86:912-6.

[18] Ho CC, Huang PH, Huang HY, Chen YH, Yang PC, Hsu SM. Up-regulated caveolin-1 accentuates the metastasis capability of lung adenocarcinoma by inducing filopodia formation. Am J Pathol 2002;161:1647-56.

[19] Yoo SH, Park YS, Kim HR, et al. Expression of caveolin-1 is associated with poor prognosis of patients with squamous cell carcinoma of the lung. Lung Cancer 2003;42:195-202.

[20] Sunaga N, Miyajima K, Suzuki M, et al. Different roles for caveolin-1 in the development of non-small cell lung cancer versus small cell lung cancer. Cancer Res 2004;64:4277-85.

[21] Suzuoki M, Miyamoto M, Kato K, et al. Impact of caveolin-1 expression on prognosis of pancreatic ductal adenocarcinoma. Br J Cancer 2002;87:1140-4.

[22] Terris B, Blaveri E, Crnogorac-Jurcevic T, et al. Characterization of gene expression profiles in intraductal papillary-mucinous tumors of the pancreas. Am J Pathol 2002;160:1745-54.

[23] Davidson B, Goldberg I, Givant-Horwitz V, et al. Caveolin-1 expression in ovarian carcinoma is MDR1 independent. Am J Clin Pathol 2002;117:225-34.

[24] Van den Eynden GG, Van Laere SJ, Van der Auwera I, et al. Overexpression of caveolin-1 and -2 in cell lines and in human samples of inflammatory breast cancer. Breast Cancer Res Treat 2006;95:219-28 [Epub 2005 Oct 22].

[25] Li L, Ren CH, Tahir SA, Ren C, Thompson TC. Caveolin-1 maintains activated Akt in prostate cancer cells through scaffolding domain binding site interactions with and inhibition of serine/threonine protein phosphatases PP1 and PP2A. Mol Cell Biol 2003;23:9389-404.

[26] Li L, Yang G, Ebara S, et al. Caveolin-1 mediates testosterone-stimulated survival/clonal growth and promotes metastatic activities in prostate cancer cells. Cancer Res 2001;61:4386-92.

[27] Tahir SA, Yang G, Ebara S, et al. Secreted caveolin-1 stimulates cell survival/clonal growth and contributes to metastasis in androgen-insensitive prostate cancer. Cancer Res 2001;61:3882-5.

[28] Carver LA, Schnitzer JE. Caveolae: mining little caves for new cancer targets. Nat Rev Cancer 2003;3:571-81.

[29] Massimino ML, Griffoni C, Spisni E, Toni M, Tomasi V. Involvement of caveolae and caveolae-like domains in signalling, cell survival and angiogenesis. Cell Signal 2002;14:93-8.

[30] Frank PG, Woodman SE, Park DS, Lisanti MP. Caveolin, caveolae, and endothelial cell function. Arterioscler Thromb Vasc Biol 2003;23:1161-8 [Epub 2003 Apr 10].

[31] Sonveaux P, Martinive P, DeWever J, et al. Caveolin-1 expression is critical for vascular endothelial growth factor-induced ischemic hindlimb collateralization and nitric oxide-mediated angiogenesis. Circ Res 2004;95:154-61 [Epub 2004 Jun 17].

[32] Liu J, Razani B, Tang S, Terman BI, Ware JA, Lisanti MP. Angiogenesis activators and inhibitors differentially regulate caveolin-1 expression and caveolae formation in vascular endothelial cells. Angiogenesis inhibitors block vascular endothelial growth factor-induced down-regulation of caveolin-1. J Biol Chem 1999;274:15781-5.

[33] Woodman SE, Ashton AW, Schubert W, et al. Caveolin-1 knockout mice show an impaired angiogenic response to exogenous stimuli. Am J Pathol 2003;162:2059-68.

[34] Vermeulen PB, Gasparini G, Fox SB, et al. Second international consensus on the methodology and criteria of evaluation of angiogenesis quantification in solid human tumours. Eur J Cancer 2002;38:1564-79.

[35] Thompson TC, Timme TL, Li L, Goltsov A. Caveolin-1—a metastasis-related gene that promotes cell survival in prostate cancer. Apoptosis 1999;4:233-7.

[36] Lin MI, Yu J, Murata T, Sessa WC. Caveolin-1-deficient mice have increased tumor microvascular permeability, angiogenesis, and growth. Cancer Res 2007;67:2849-56.

[37] Weidner N, Carroll PR, Flax J, Blumenfeld W, Folkman J. Tumor angiogenesis correlates with metastasis in invasive prostate carcinoma. Am J Pathol 1993;143:401-9.

[38] Yerian LM, Anders RA, Tretiakova M, Hart J. Caveolin and thrombospondin expression during hepatocellular carcinogenesis. Am J Surg Pathol 2004;28:357-64.

[39] Tahir SA, Ren C, Timme TL, et al. Development of an immunoassay for serum caveolin-1: a novel biomarker for prostate cancer. Clin Cancer Res 2003;9:3653-9.

[40] Waltenberger J, Claesson-Welsh L, Siegbahn A, Shibuya M, Heldin CH. Different signal transduction properties of KDR and Flt1, two receptors for vascular endothelial growth factor. J Biol Chem 1994;269:26988-95.

[41] Borre M, Nerstrom B, Overgaard J. Association between immunohistochemical expression of vascular endothelial growth factor (VEGF), VEGF-expressing neuroendocrine-differentiated tumor cells, and outcome in prostate cancer patients subjected to watchful waiting. Clin Cancer Res 2000;6:1882-90.

[42] Ferrer FA, Miller LJ, Andrawis RI, et al. Vascular endothelial growth factor (VEGF) expression in human prostate cancer: in situ and in vitro expression of VEGF by human prostate cancer cells. J Urol 1997;157:2329-33.

[43] Labrecque L, Royal I, Surprenant DS, Patterson C, Gingras D, Beliveau R. Regulation of vascular endothelial growth factor receptor-2 activity by caveolin-1 and plasma membrane cholesterol. Mol Biol Cell 2003;14:334-47.

Tumor Cell–Secreted Caveolin-1 Has Proangiogenic Activities in Prostate Cancer

Salahaldin A. Tahir,[1] Guang Yang,[1] Alexei A. Goltsov,[1] Masami Watanabe,[1] Ken-ichi Tabata,[1] Josephine Addai,[1] El Moataz Abdel Fattah,[1] Dov Kadmon,[1] and Timothy C. Thompson[1,2,3]

[1]Scott Department of Urology, Departments of [2]Molecular and Cellular Biology and [3]Radiology, Baylor College of Medicine, Houston, Texas

Abstract

Caveolin, a major structural component of specialized plasma membrane invaginations (caveolae) that participate in diverse cellular activities, has been implicated in the pathogenesis of several human diseases, including cancer. We showed in earlier studies that caveolin-1 (cav-1) is consistently and strongly overexpressed in metastatic prostate cancer and is secreted in a biologically active form by virulent prostate cancer cells. Using both *in vitro* and *in vivo* model systems, we now present evidence supporting a proangiogenic role for cav-1 in prostate cancer development and progression. Recombinant cav-1 (rcav-1) was taken up by cav-1$^{-/-}$ endothelial cells through either a lipid raft/caveolae- or clathrin-dependent mechanism, leading to specific angiogenic activities (tubule formation, cell migration, and nitric oxide production) that were mediated by rcav-1 stimulation of the PI3K-Akt-eNOS signaling module. Pathologic angiogenesis induced by cav-1 in prostate cancer–bearing mice correlated with an increased frequency, number, and size of lung metastases. We propose that in addition to its antiapoptotic role, cav-1 secreted by prostate cancer cells functions critically as a proangiogenic factor in metastatic progression of this tumor. These new insights into cav-1 function in prostate cancer may provide a base for the design of clinically applicable therapeutic strategies. [Cancer Res 2008;68(3):731–9]

Introduction

As essential components of caveolae, caveolin proteins help to generate and maintain these highly ordered structures at the cell surface. They also mediated endocytosis and transcytosis of molecules attached to the cell surface and organize signaling proteins involved in cell proliferation, adhesion, and migration, among numerous other biological processes (1). This functional versatility has focused increasing attention on the possible role of caveolins in cancer development and progression. Findings to date clearly indicate that caveolin-1 (cav-1), the first of several caveolin family members that differ in structure and tissue distribution, can influence both tumorigenesis and metastatic spread in certain types of cancer (2–6), although the mechanisms of these effects are largely unknown. We showed in earlier studies that cav-1 is consistently and strongly overexpressed in metastatic prostate cancer and is secreted in a biologically active form by virulent prostate cancer cells (2, 3, 7). Interestingly, we detected significantly increased serum cav-1 levels in prostate cancer patients compared with control men or men with benign prostatic hyperplasia, and showed that preoperative serum cav-1 is a potential prognostic marker for recurrence in radical prostatectomy cohort (8, 9). The ability of some prostate cancer cells to secrete biologically active cav-1 (7, 8), and the demonstration that loss of cav-1 function in the TRAMP transgenic mouse prostate cancer model results in highly significant reductions of prostate cancer growth and metastasis (10), led us to suspect that tumor cell–secreted cav-1 may function as a paracrine factor during prostate cancer development, possibly as a regulator of pathologic angiogenesis. The studies described here substantiate this role and suggest a paradigm that may be applicable to other tumors that secrete cav-1.

Materials and Methods

Endothelial cell isolation. Endothelial cells from *cav-1*$^{-/-}$ mice (11) were isolated from mouse aorta according to the primary explant procedure and used throughout the study. Briefly, the aorta was removed from the anaesthetized mice, placed in PBS, and carefully cleaned of periadventitial fat and connective tissue. The vessel was then cut into 1-mm pieces, opened longitudinally, and placed with the intima side down on Matrigel-coated (BD Biosciences) 12-well plates in endothelial cell growth medium (EGM; Cambrex) to generate endothelial outgrowth. The aortic pieces were removed after 4 to 7 days, and the cells were allowed to grow to confluence. After recovery with dispase, the cells were plated on a 12-well plate and then subcultured twice. The confluent monolayers showed the typical cobblestone pattern of endothelial cells stained positively for uptake of Dil-Ac-LDL (Biomedical Technologies).

Western blotting. Protein aliquots from cell lysates were separated by 10% or 12% SDS-PAGE and transferred to nitrocellulose membranes. The membranes were probed with antibodies to cav-1 (Santa Cruz Biotechnology), eNOS, Erk1/2, Akt (BD Biosciences), P-Akt, P-eNOS, or P-Erk1/2 (Cell Signaling Technology).

Recombinant cav-1 and Δrecombinant cav-1 purification. phCav-1V5 and phΔcav-1V5His plasmids were constructed as described previously (8), whereas recombinant cav-1 (rcav-1) and Δrcav-1 were purified by our modified procedure. Briefly, transfected 293PE cells were washed with PBS and lysed with 10 mL of ice-cold buffer A [50 mmol/L phosphate buffer, 300 mmol/L NaCl, 10 mmol/L imidazole, and 5 mmol/L mercaptoethanol (pH.8)] containing 0.5% Triton X-100 and 0.7% octylβ-D-glucopyranoside (OGP). The lysate was centrifuged for 15 min at 4°C, 12,000 × *g*, and the supernatant was mixed and incubated with 1 mL of Ni-NTA agarose slurry for 3 h. The resultant mixture was loaded on to a 10 mL polyprep column (Bio-Rad), and the resin was washed with 10 volumes of buffer A containing 500 mmol/L NaCl, 50 mmol/L imidazole, and 0.2% OGP. The bound cav-1-V5-His was eluted with 3 mL of elution buffer (buffer A containing 300 mmol/L imidazole, 300 mmol/L NaCl, and 0.1% OGP). For Western blot analysis, the crude supernatant as well as unbound and eluted fractions were subjected to SDS-PAGE. FITC labeling of recombinant cav-1 proteins was prepared with the EZ-label FITC

Requests for reprints: Timothy C. Thompson, The University of Texas M. D. Anderson Cancer Center, Department of Genitourinary Medical Oncology, Unit 1374, 1515 Holcombe Boulevard, Houston, TX 77030. Phone: 713-792-9955; Fax: 713-792-9956; E-mail: timthomp@mdanderson.org.

doi:10.1158/0008-5472.CAN-07-2668

protein labeling kit (Pierce Biotechnology, Inc.) according to the manufacturer's instructions.

Tubule formation assay. The *in vitro* tubule formation assay was used as described previously (12). Briefly, endothelial cells were incubated in growth factor–reduced Matrigel-coated 24-well plates in 0.5 mL of endothelial basement medium (EBM; Cambrex) in the presence or absence of rcav-1 or Δrcav-1. Images of tubule structures that formed after 18 to 24 h were captured by phase contrast microscopy, and the length of the endothelial network was quantified by image analysis of five low-power fields using free object quantification software (NucleoTech Corp.).

Wound-healing migration assay. Endothelial cells were cultured in 24-well plates to 70% to 80% confluency in EGM, and a straight longitudinal incision was made on the monolayer. After a wash with EBM and incubation with rcav-1 or Δrcav-1 in EBM containing 0.1% bovine serum albumin (BSA) for 4 h followed by an additional 48 h of incubation in EBM containing 2% of fetal bovine serum (FBS), the cells were stained with the Protocol HEMA3 stain set (Biochemical Sciences, Inc.), and the number of cells migrating into the cleared area were counted with a microscope, using advanced colony counting software (NucleoTech Corp.).

Cell proliferation and [^{3}H]-thymidine incorporation. Endothelial cells were seeded into 12-well plates (5×10^4 cells per well) and incubated overnight. After the medium was removed, the cells were treated with rcav-1 in EBM for 4 h and incubated for an additional 48 h in EBM containing 2% FBS, after which they were trypsinized and counted with a coulter counter. For [^{3}H]-thymidine uptake, the endothelial cells were seeded into 96-well plates (2.5×10^3 cells per well) in EGM then treated with rcav-1 and incubated for 48 h in EGM. [^{3}H]-thymidine (5 μCi/mL) was then added, the cells were incubated for 24 h, and the cell lysate-associated radioactivity was counted.

Nitric oxide determination. The basal and rcav-1 stimulated NO derived from endothelial cells that had accumulated in EBM over a 24-h period was measured with the Nitric Oxide Colorimetric Assay (Roche Diagnostics).

PP1 and PP2A activities. Endothelial cells were treated with rcav-1 and incubated in EBM containing 0.1% BSA for 24 h at 37°C and 5.5% CO_2. The cells were lysed with ice-cold phosphatase lysis buffer, and PP1 and PP2A activities were measured after immunoprecipitation as described previously (13).

Animal models. Orthotopic RM-9 tumors were generated by injecting 5×10^3 cells directly into the dorsolateral prostates of *cav-1*$^{+/+}$ or *cav-1*$^{-/-}$ male mice. The resultant tumors were removed at necroscopy on day 21 postinjection, and their wet weight were determined; all tumors were processed for specific immunostaining protocols (see below).

To generate the LNCaP cav-1 tet-on system, we transfected *cav-1*$^{-/-}$ low passage (LP)-LNCaP cells with pTetOn vector (Clontech), isolated stable G418-resistant clones, and screened them in a transient trasfection reporter assay with pTRE2Luc vector according to the manufacturer's protocol with or without 1 μg/mL doxycycline. Clone LNT36, which had the highest induction level, was chosen for the second cotransfection, in which a pTRECav-1 vector containing full-length human *cav-1* cDNA and the pBabeHygro plasmid were used. Double stable G418- and hygromycin-resistant clones were isolated and tested for cav-1 induction in response to the doxycycline (1.0 μg/mL). Clone LNTB25cav, which showed strong induction of cav-1 after addition of doxycycline to the medium and the lowest endogenous expression in the absence of the drug *in vitro*, was used for further *in vivo* studies.

To establish xenografts, we inoculated male nude mice with LNTB25cav cells that were suspended in Matrigel matrix and injected s.c. Tumors were present 21 days after inoculation, and tumor-bearing mice were divided into two groups that were normalized for tumor size. One group was treated with drinking water containing doxycycline (2 mg/mL) and 5% sucrose, whereas the other (control group) was treated with drinking water containing only 5% sucrose. After 21 days, the animals were sacrificed, and the tumor tissues were harvested and either snap frozen in liquid nitrogen or fixed in 10% neutral formalin.

For the *in vivo* metastasis assay, 1×10^6 LNTB25cav cells were injected into the tail veins of male nude mice to establish experimental metastases. Two months after the initial injection, the mice were divided into two groups: one was treated with drinking water containing doxycycline (2 mg/mL) and 5% sucrose and the other (control group) with drinking water containing only 5% sucrose. After a 42-day treatment, the animals were sacrificed and lung tissue was collected, fixed, and analyzed for tumor foci.

Immunohistochemistry and deconvolution microscopy. Depending on the fluorescent protein treatment, LNCaP, PC-3, and TSU-Pr1 tumor cells or endothelial cells were placed on glass coverslips in 24-well plates and incubated overnight in RPMI 1640 or EGM, respectively. After removal of the medium, the cells were washed twice with PBS buffer, then FITC-rcav-1, FITC-Δrcav-1, Alexa fluor 594–labeled cholera toxin B, and transferrin (Invitrogen) were added to medium that contained 0.1% BSA. The cells were incubated for 5 h, rinsed twice with PBS buffer, and fixed in 4% formaldehyde for 5 min at room temperature.

For immunostaining, fixed cells were permeabilized for 5 min with 0.1% Triton X-100 in PBS buffer and blocked with 3% normal horse or goat serum. They were then incubated with primary antibody followed by biotinylated anti-rabbit IgG (Vector Labs) and rhodamine-conjugated streptavidin or FITC-streptavidin (Jackson Immuno Research). Reactions were evaluated with the Delta Vision Deconvolution Microscopy System (Applied Precision, Inc.), in which a Z-series of optical sections (0.15-μm steps) were digitally imaged and deconvolved with the Delta Vision–constrained iterative algorithm to generate high-resolution images.

Mouse model–derived tumor specimens were stained for CD31 (BD Biosciences) using the avidin-biotin-peroxidase complex technique (ABC kit; Vector Lab) as previously described (14). Quantitative analysis of microvessel density was performed on the stained sections. The vascular "hot region" was first identified by low-power screening (magnification, ×40). Vascular counting was then performed on at least five 200× measuring fields (each with a real area of 0.198 mm^2). For each sample, the highest count per field was used.

Dual-immunofluorescence staining was also performed on these tissues. Briefly, after tissue sections were deparaffinized and rehydrated through graded alcohol, they were heated in 0.01 mol/L citrate buffer at pH 6.0 by microwave for 10 min to enhance antigen retrieval. After a 20-min blocking step with 1.5% normal goat serum, the sections were sequentially incubated with polyclonal cav-1 antibody diluted 1:200 for 90 min, followed by biotinylated anti-rabbit IgG and streptavidin-FITC for 30 min each. The sections were rinsed and reblocked in 1.5% normal horse serum for 20 min and incubated in CD31 rat monoclonal antibody followed by Cy-3–conjugated anti-rat IgG for 30 min. The specificity of immunoreactions was verified by replacing the primary antibodies with PBS or with corresponding normal serum. The labeled specimens were evaluated using a Zeiss fluorescence microscope equipped with a video camera (Hamamatsu). Each section was analyzed systematically, field-by-field (300×400 μm^2), over the area of cancer cells. The percentages of cav-1–positive CD31 microvessels were determined for each field for each fluorophore and on superimposed images of both fluorophores with the aid of OPTIMAS (6.0) software.

Statistical analysis. The Mann-Whitney rank test was used to analyze differences in microvessel density within mouse prostate cancer tissues; comparisons of *in vitro* tubule formation, cell migration, phosphatase activity assay, NO release assay, and RM-9 tumor wet weights relied on the unpaired two-sided *t* test. Fisher's exact test was used for the comparison of the metastasis frequency in LNTB25cav-injected mice. All statistical analyses were performed with Statview software (Version 5.0; SAS Institute).

Results

Cav-1 uptake by prostate cancer cells and endothelial cells. We have shown that prostate cancer cells secrete cav-1 possessing antiapoptotic activity that can be suppressed by cav-1–specific antiserum *in vitro* (7). Such antiserum also suppressed metastasis *in vivo*, raising the possibility that secreted cav-1 is taken up by tumor cells or tumor-associated endothelial cells or both. Thus, we treated cav-1–negative LP-LNCaP tumor cells or primary

endothelial cells, isolated from *cav-1*$^{-/-}$ mouse aorta, with conditioned medium collected from cav-1–transfected LP-LNCaP cells or with rcav-1 alone. Western blot analysis showed that cav-1 contained in conditioned medium was taken up by LP-LNCaP cells in a dose- and time-dependent manner, as indicated by the appearance of cav-1 in cell lysates within 1 h and the achievement of maximal intracellular levels 3 h posttreatment (Fig. 1*A*). Rcav-1 protein was also taken up by the LP-LNCaP cells and *cav-1*$^{-/-}$ endothelial cells in a dose-dependent fashion over a 24-h incubation period (Fig. 1*B* and *C*). Rcav-1 uptake by tumor cells (LP-LNCaP, TSU-Pr1, and PC-3) and endothelial cells [human umbilical vascular endothelial cell (HUVEC), and mouse *cav-1*$^{-/-}$ and *cav-1*$^{+/+}$] was further shown by fluorescence and deconvolution microscopy. FITC-rcav-1 uptake by these cells was temperature dependent, with 5 h of incubation at 0°C, abolishing uptake altogether (data not shown). Internalized FITC-rcav-1 was distributed throughout the cytoplasm (Fig. 1*D*).

Lipid raft/caveolae-dependent and clathrin-dependent endocytic pathways are involved in rcav-1 internalization in endothelial cells. To determine the endocytic pathways responsible for rcav-1 internalization, we pretreated HUVEC and *cav-1*$^{+/+}$ or *cav-1*$^{-/-}$ mouse endothelial cells with methyl-β-cyclodextrin (MCD) or chlorpromazine to disrupt the formation of cholesterol-rich raft microdomains or clathrin-coated pits, respectively. Fluorescence microscopy revealed that MCD effectively inhibited FITC-rcav-1 uptake in both types of endothelial cells, whereas chlorpromazine inhibited FITC-rcav-1 uptake effectively in mouse endothelial cells but only marginally in HUVEC (Fig. 2*A*). Under the same conditions, MCD effectively reduced the uptake of cholera toxin B, whereas chlorpromazine reduced the uptake of transferrin substances known to penetrate cells through cholesterol-rich lipid raft and clathrin endocytic pathways, respectively (Fig. 2*B*). These results indicate that internalization of exogenous rcav-1 proceeds through lipid raft/caveolae and clathrin pathways in both HUVEC and mouse endothelial cells, with the former pathway dominant in HUVEC (Fig. 2*A, left*). To directly show that rcav-1 associates with internalized lipid rafts/caveolae to enter endothelial cells, we incubated HUVEC for 5 h with a mixture of FITC-rcav-1 and cholera toxin B and tested for their cellular colocalization. We found that a majority (76%) of the FITC-rcav-1–positive endosomes also contained cholera toxin B (Fig. 2*C*), indicative of a requirement for caveolae and ganglioside G_{M1} lipid rafts in cav-1 penetration of human endothelial cells.

Internalization of rcav-1 is mediated by cav-1 scaffolding domain. Mutagenesis experiments have identified cav-1 scaffolding domain (CSD) residues 82 to 101 as the region responsible for mediating interactions with a number of signaling proteins including the endothelial form of nitric oxide synthase (eNOS), platelet-activating factor receptors, epidermal growth factor, the kinases Src and Fyn, heterotrimeric G protein,

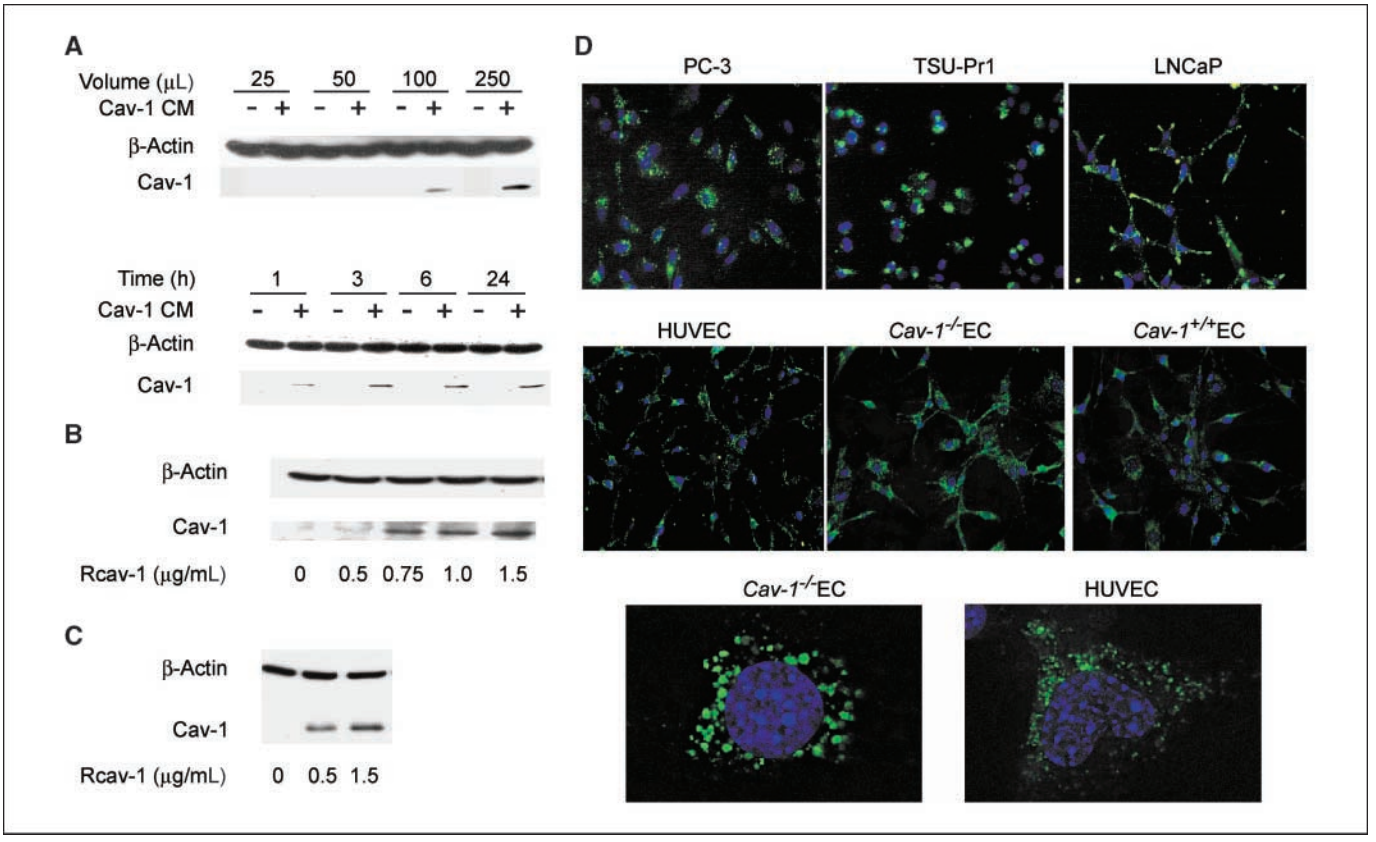

Figure 1. Cav-1 uptake by prostate cancer and bladder cancer cells and endothelial cells. *A,* dose- and time-dependent uptake of cav-1 from *cav-1*–transfected (+) or control-transfected (−) conditioned medium (*CM*) by LP-LNCaP cells. *Top,* detection of cav-1 after a 24-h treatment with conditioned medium over a range of volumes; *bottom,* detection after 1 to 24 h of treatment with 250 μL conditioned medium. *B* and *C,* dose-dependent rcav-1 uptake by LP-LNCaP tumor cells (*B*) and *cav-1*$^{-/-}$ endothelial cells (*EC*; *C*) treated for 24 h. *D,* internalization of FITC-rcav-1 by cancer cells (*top*) and endothelial cells (*middle*) treated with 3.0 μg/mL of FITC-rcav-1 for 5 h. Uptake by endothelial cells (*cav-1*$^{-/-}$ endothelial cells and HUVEC) were imaged by deconvolution microscopy after treatment with FITC-rcav-1 (*bottom*); nuclei were visualized by Hoechst 33342 staining.

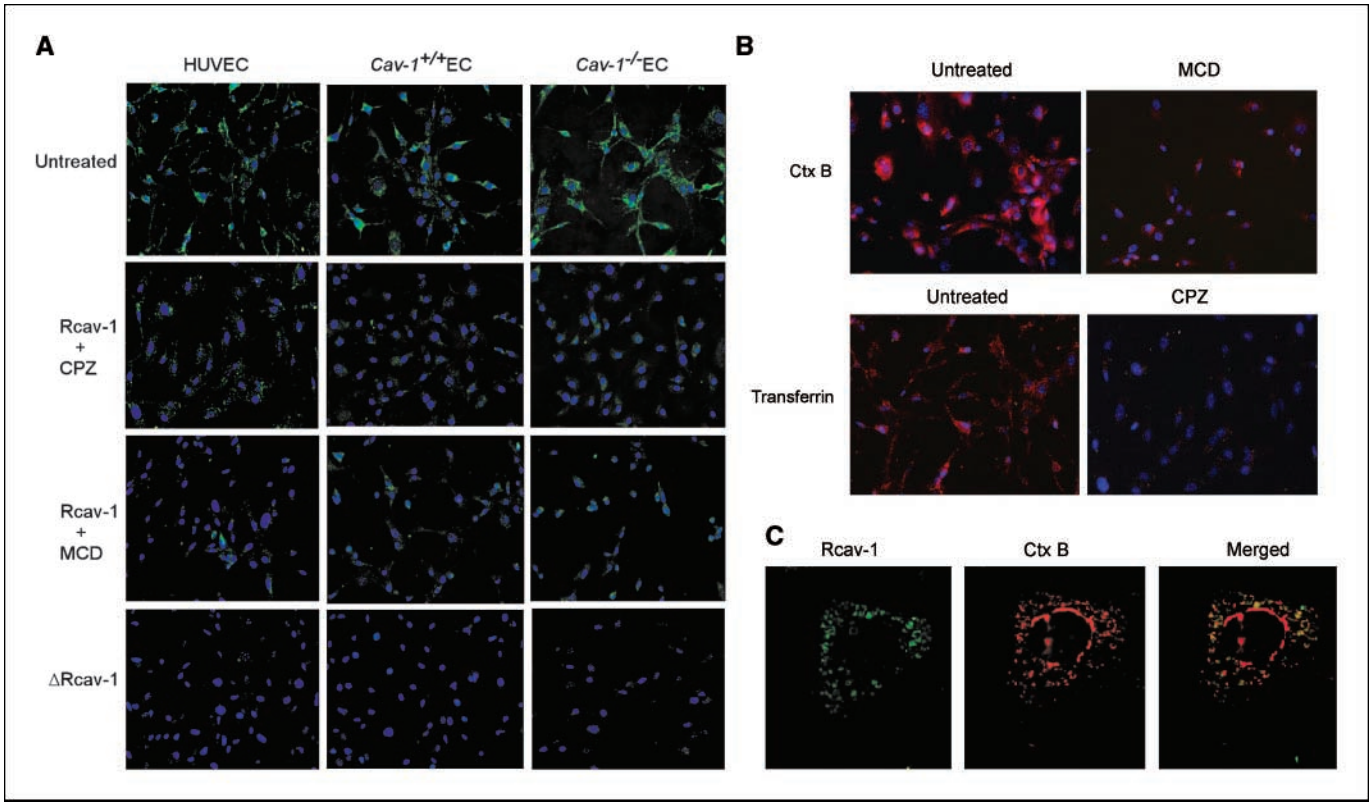

Figure 2. Internalization of rcav-1 by lipid raft/caveolae-dependent and clathrin-dependent endocytic pathways. *A,* cells were incubated with FITC-rcav-1 (3.0 μg/mL) in the presence or absence of 7.5 μg/mL of chlorpromazine (*CPZ*) or 7 mmol/L MCD for 5 h and analyzed by fluorescence microscopy. *B,* cholera toxin B (*Ctx B*) and transferrin internalization are blocked by MCD and chlorpromazine, respectively. HUVEC cells were incubated with Alexa fluor 594–labeled cholera toxin B and transferrin containing the same MCD and chlorpromazine concentrations as in *A* for 5 h and analyzed by fluorescence microscopy. Cholera toxin B internalization was impaired by cholesterol depletion (MCD treatment), whereas transferrin uptake was blocked by disruption of clathrin-coated pits (chlorpromazine treatment). *C,* colocalization of internalized FITC-rcav-1 with cholera toxin B, a ganglioside G_{M1} lipid raft/caveolae marker, as detected by deconvolution microscopy of HUVEC cells after the incubation for 5 h with FITC-rcav-1 and Alexa fluor 594–labeled cholera toxin B; nuclei were visualized by Hoechst 33342 staining.

and cholesterol-binding protein (15). This domain also targets the full-length endogenous cav-1 to lipid rafts/caveolae and cell membranes (16). To determine the role of the CSD in exogenous rcav-1 membrane attachment and cellular uptake, we generated and purified the CSD-deleted rcav-1 protein (Δrcav-1), treated endothelial cells and prostate cancer cells with different concentrations of FITC-Δrcav-1 over 1 to 6 h, and examined the cells for Δrcav-1 uptake using fluorescence microscopy. We did not detect internalized FITC-Δrcav-1 in cells incubated for as long as 6 h at concentrations of the mutant protein ranging to 5.0 μg/mL (Fig. 2*A*). In separate coincubation experiments, we showed uptake of cholera toxin B or transferrin under the same conditions (data not shown). These observations suggest that endocytosis of exogenous rcav-1 protein and its subsequent stimulation of angiogenic activities is mediated, in part, by CSD, which seems critical for cellular internalization of the protein.

Rcav-1 stimulates differentiation and migration of *cav-1*$^{-/-}$ endothelial cells. We initially analyzed the formation of tubules by endothelial cells, isolated from *cav-1*$^{+/+}$ or *cav-1*$^{-/-}$ aorta, on growth factor–reduced Matrigel. Compared with *cav-1*$^{+/+}$ endothelial cells, cells lacking this gene showed significantly reduced tubule formation in the absence of rcav-1 stimulation (Fig. 3*A*; micrographs). However, treatment with rcav-1 stimulated tubule formation in *cav-1*$^{-/-}$ endothelial cells in a dose-dependent manner with a >2-fold increase in tubule length observed with use of 1.5 μg/mL rcav-1 compared with untreated controls (P = 0.021). Importantly, Δrcav-1 at this concentration failed to stimulate tubule formation (Fig. 3*A*). To determine the effects of rcav-1 on *cav-1*$^{-/-}$ endothelial cell migration, we used the *in vitro* wound-healing assay. Rcav-1 treatment stimulated *cav-1*$^{-/-}$ endothelial cell migration in a dose-dependent fashion with a 2-fold increase in the number of migratory cells at a rcav-1 concentration of 1.5 μg/mL (P = 0.019), whereas Δrcav-1 at this concentration failed to increase migration/motility of the endothelial cells (Fig. 3*B*). This enhancement of tubule formation and the number of migratory/motile cells by rcav-1 treatment did not result from increased cell proliferation, as the numbers of cells or levels of thymidine uptake posttreatment were similar to the results for untreated controls (data not shown).

Rcav-1 stimulates the angiogenic activities in *cav-1*$^{-/-}$ endothelial cells through the activation of eNOS. Caveolae and cav-1 play critical roles in ensuring the coupling between vascular endothelial growth factor (VEGF) receptors and downstream mediators of angiogenesis, such as VEGF, which activates Erk and eNOS via the phosphatidylinositol-3-kinase (PI3-K)-Akt signaling pathway (17–19). Thus, to assess the contribution of this signaling module to the angiogenic activities of rcav-1, we tested the effects of inhibitors of PI3 kinase (LY294002), eNOS (L-NAME), and Erk (PD98059) in *cav-1*$^{-/-}$ endothelial cells. Figure 3*C* and *D* shows that both LY294002 and L-NAME, but not PD98059, significantly suppressed rcav-1–stimulated angiogenesis, implicating PI3-K-Akt-eNOS signaling in the pathologic angiogenic effects

of cav-1 in prostate cancer cells. To investigate this possibility further, we measured the levels of accumulated NO (NO_2^- + NO_3^-) at 24 h after rcav-1 treatment of *cav-1*$^{-/-}$ endothelial cells. NO release by these cells was significantly increased by rcav-1 in a dose-dependent manner (P = 0.029 versus untreated control; Fig. 4*A, left*). Analysis of the effects of rcav-1 on the phosphorylation status of Akt and its downstream target protein eNOS in *cav-1*$^{-/-}$ endothelial cells showed a dose-dependent increase in Akt phosphorylation on S473 and T308 with no change in total Akt. Rcav-1 treatment also led to increased eNOS phosphorylation on S1177 but not T495 (Fig. 4*A, right*). The CSD-deleted rcav-1 failed to stimulate eNOS S1177 phosphorylation, as expected (Fig. 4*B, top*). We also tested the effect of LY294002 on the rcav-1–induced phosphorylation of Akt (T308) and eNOS (S1177) in *cav-1*$^{-/-}$ endothelial cells. As expected, LY294002 treatment of the cells diminished the observed Akt phosphorylation induction by rcav-1. Interestingly, the phosphorylation of eNOS (S1177) induced by rcav-1 was reduced but not completely diminished as a result of LY294002 treatment (Fig. 4*B, bottom*).

To further investigate the mechanism(s) that underlies rcav-1–stimulated eNOS activation, we tested the effect of rcav-1 on the activities of serine/threonine protein phosphatases PP1 and PP2A in *cav-1*$^{-/-}$ endothelial cells. These two phosphatases are known to regulate the phosphorylation of multiple protein targets including Akt and eNOS (20, 21) and are inhibited by cav-1 overexpression in prostate cancer cells (13). The activation of eNOS by a number of stimuli including VEGF involves a transient increase in the phosphorylation of S1177 with a decrease in T495 phosphorylation, alternatively, protein kinase C signaling inhibits eNOS activity by phosphorylating T495 and dephosphorylating S1177. Both PP1 and PP2A are associated with eNOS phosphorylation. PP1 is specific for dephosphorylation of T495, whereas PP2A is specific for S1177

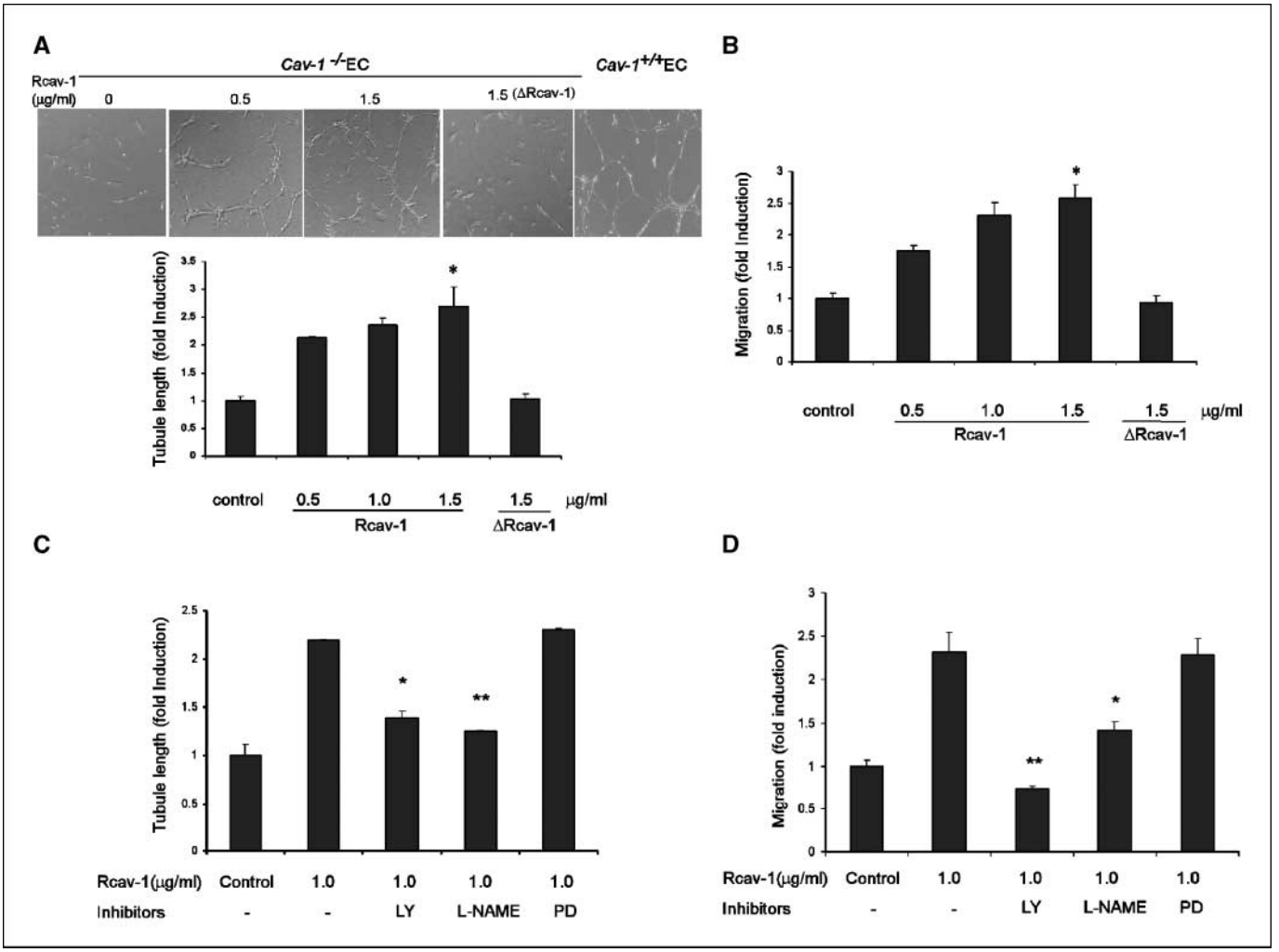

Figure 3. Rcav-1 stimulates tubule formation and cell migration in *cav-1*$^{-/-}$ endothelial cells. *A,* representative micrographs showing newly formed tubules of *cav-1*$^{+/+}$ and *cav-1*$^{-/-}$ endothelial cells cultured on growth factor–reduced Matrigel under basal conditions or after treatment with 0.5 to 1.5 μg/mL of rcav-1 and 1.5 μg/mL Δrcav-1 for 18 h. Bar graph depicts dose-dependent rcav-1 or Δrcav-1 stimulation of tubule formation in *cav-1*$^{-/-}$ endothelial cells. The values are folds of induction relative to untreated control ± SD of three independent experiments. *, P = 0.02 versus untreated control by two-sided t test. *B,* dose-dependent rcav-1 or Δrcav-1 stimulation of *cav-1*$^{-/-}$ endothelial cell migration in a wound-healing assay. The values are folds of induction relative to untreated control ± SD of three independent experiments. *, P = 0.0193 versus untreated control by two-sided t test. *C,* inhibition of rcav-1–stimulated tubule formation by LY294002 (*LY*; 3.0 μmol/L) or L-NAME (1.0 mmol/L) but not by PD98059 (*PD*; 50 μmol/L) in *cav-1*$^{-/-}$ endothelial cells. *, P = 0.008; **, P = 0.003 versus rcav-1 treated only. *D,* inhibition of rcav-1–stimulated wound-healing assay cell migration by LY294002 (3.0 μmol/L) or L-NAME (1.0 mmol/L), but not by PD98059 (50 μmol/L) in *cav-1*$^{-/-}$ endothelial cells. *, P = 0.011; **, P = 0.005 versus rcav-1 treated only, by-two sided t test. Bar graphs in *C* and *D* represent tubule length relative to untreated controls and the number of migratory cells relative to untreated controls, respectively. *Columns,* mean; *bars,* SD.

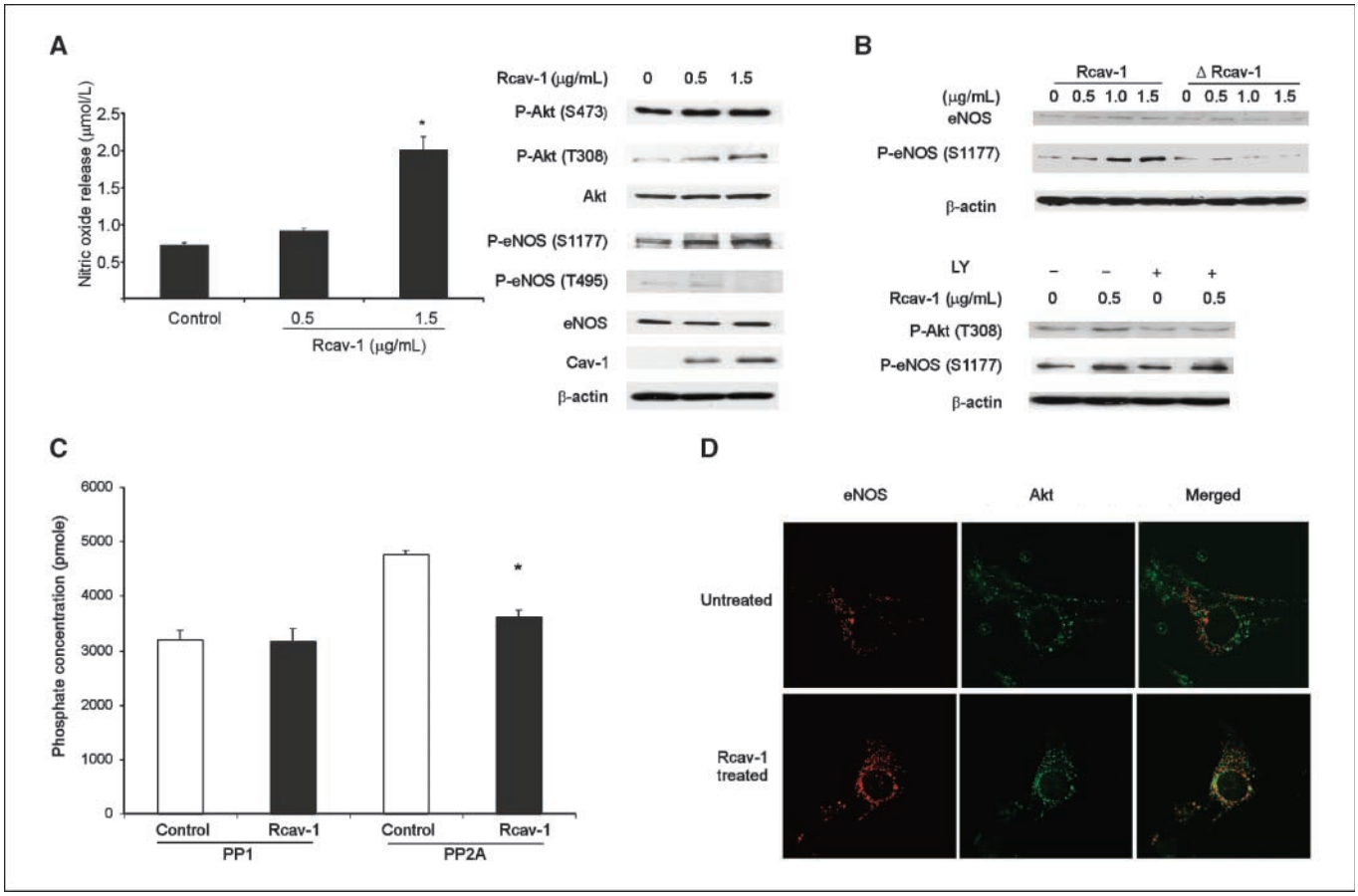

Figure 4. Rcav-1 is involved in PI3-K-Akt-eNOS–mediated stimulation of angiogenic activities in *cav-1*$^{-/-}$ endothelial cells. *A,* dose-dependent NO release by *cav-1*$^{-/-}$ endothelial cells after rcav-1 treatment. *Columns,* mean; *bars,* SD. *, $P = 0.029$ versus untreated control, by two-sided *t* test (*left*). Increased phosphorylation of Akt on S473 and T308, and of eNOS on S1177 by Western blot analysis of *cav-1*$^{-/-}$ endothelial cells lysates treated for 24 h with different concentrations of rcav-1 (*right*). *B,* Δrcav-1 treatment of *cav-1*$^{-/-}$ endothelial cells for 24 h does not affect the phosphorylation status of eNOS on S1177, but rcav-1 increases eNOS phosphorylation on S1177 in a dose-dependent fashion (*top*). Treatment of *cav-1*$^{-/-}$ endothelial cells with LY29400 abolishes the rcav-1–induced Akt phosphorylation on T308 and reduces, but does not completely eliminate, the eNOS phosphorylation on S1177 induced by rcav-1 (*bottom*). *C,* rcav-1 inhibits the activity of PP2A but not PP1 in *cav-1*$^{-/-}$ endothelial cells. PP1-C or PP2A-C immunprecipitation complexes from rcav-1–treated *cav-1*$^{-/-}$ endothelial cells or untreated controls were used to determine phosphatase activities with the serine/threonine protein phosphatase assay. *Columns,* mean; *bars,* SD. *, $P = 0.0002$ by two-sided *t* test. *D*, induction of eNOS/Akt association by rcav-1. *Cav-1*$^{-/-}$ endothelial cells were cultured for 6 h in the presence or absence of rcav-1. After fixation, the cells were double-labeled with anti-eNOS and anti-Akt immunofluorecence. In untreated cells, eNOS (*red*) and Akt (*green*) were localized to separate compartments (*top*), whereas rcav-1 protein treatment of the cells for 6 h induced eNOS (*red*) and Akt (*green*) colocalization in cytoplasmic vesicles (*bottom*), as visualized by deconvolution microscopy.

dephosphorylation (21). The results showed that rcav-1 treatment significantly inhibited the activity of PP2A but had no effect on PP1 activity ($P = 0.0002$ versus control; Fig. 4*C*). These data provide evidence that rcav-1 induces eNOS phosphorylation through Akt activation, and independently of Akt, through inhibition of PP2A, which specifically dephosphorylates eNOS (S1177).

A number of studies have shown that both eNOS and PI3 kinase are colocalized within the caveolar region of the plasma membrane (22, 23); therefore, we investigated the role played by cav-1 in compartmentalization of the PI3-K-Akt-eNOS signaling pathway molecules in *cav-1*$^{-/-}$ endothelial cells. We incubated the cells with or without rcav-1 for 5 h and visualized the cells by deconvolution microscopy for colocalization of Akt with eNOS. We found that Akt was not colocalized with eNOS in untreated cells, whereas significant colocalization of the two molecules was observed in the cells treated with rcav-1 (Fig. 4*D*).

Rcav-1 uptake in tumor-associated endothelial cells and proangiogenic activities in prostate cancer animal models. To investigate the effects of endothelial cells–localized cav-1 on microvessel density and tumor growth *in vivo*, we used an orthotopic RM-9 mouse prostate cancer model (24), in which cav-1 expressing and secreting RM-9 prostate cancer cells are injected directly into the dorsolateral prostate of male *cav-1*$^{+/+}$ or *cav-1*$^{-/-}$ mice. In this model, the mean (1.85 ± 0.167) tumor wet weight was significantly higher in *cav-1*$^{+/+}$ versus *cav-1*$^{-/-}$ mice ($P = 0.045$; Fig. 5*A*). Moreover, immunohistochemical analysis of tumor sections collected from sacrificed mice showed that RM-9 tumors had significantly higher microvessel densities in *cav-1*$^{+/+}$ compared with *cav-1*$^{-/-}$ hosts [median, 21.5 (range, 15.6–36.1) versus 13.3 (range, 8.2–22.8; $P = 0.0078$); Fig. 5*B* and *C*]. Interestingly, >70% of the CD31^{+} microvessels in the *cav-1*$^{-/-}$ mouse tumor sections were positive for cav-1 staining, indicating uptake of RM-9 cell–derived cav-1 by tumor-associated endothelial cells (Fig. 5*D, arrows*).

We examined the association between cav-1 expression and prostate tumor–associated angiogenesis more closely by generating an LNCaP tet-on cav-1 stable cell line (LNTB25cav) in which the expression of cav-1 can be regulated by manipulating doxycycline. In the absence of doxycycline, the level of cav-1 protein in lysate is low, whereas the addition of doxycycline to the culture medium

leads to a rapid induction of cav-1 protein *in vitro* (Fig. 6*A*). LNTB25cav tumors were established as s.c. growing xenografts in adult male nude mice; tumor-bearing mice were then treated with either doxycycline or control sucrose solution added to the drinking water. Tumor volumes in the doxycycline-treated group were significantly greater than those in the control group on days 12, 15, and 18 after treatment ($P = 0.0195$, $P = 0.035$, $P = 0.019$, respectively; Fig. 6*A*). Further immunohistochemical analysis showed increased cav-1 levels in the cytoplasm of tumor cells in doxycycline-treated compared with control mice (Fig. 6*B, top*). Microvessel densities determined by CD31 labeling were greater in cav-1–induced tumors compared with controls ($P = 0.039$; Fig. 6*B, bottom*; Fig. 6*C*). In separate experiments, we injected 1×10^6 LNTB25cav cells into the tail veins of nude mice to establish experimental lung metastases. After 42 days of continuous treatment, the number and frequency of lung metastases in doxycycline-treated animals significantly exceeded results in the control group ($P = 0.008$ and 0.04, respectively; Fig. 6*D*) and their average size was clearly larger in doxycycline-treated mice (data not shown).

Discussion

The establishment of prostate cancer metastases involves the successful negotiation of multiple endogenous physiologic barriers, survival during transit through the blood or lymphatic stream, and colonization at distant sites. The growth and metastasis of prostate cancer and other tumors is dependent on the induction of new blood vessels from preexisting ones through angiogenesis (25, 26). Cav-1 has been implicated in the regulation of endothelial cells proliferation, differentiation, and stabilization (6, 17, 27, 28). In a study using Lewis lung carcinoma cells animal cancer model, cav-1 was found to be antiangiogenic factor (29). In contrast, the results of a number of studies including this report have shown a proangiogenic function for cav-1. In an experimental melanoma model, impairment of pathologic angiogenesis was reported in *cav-1*$^{-/-}$ compared with *cav-1*$^{+/+}$ (30). Increased expression of cav-1 and microvessel density was found to be associated with metastasis and a worse prognosis in human clear cell renal cell carcinoma, suggesting a proangiogenic role for cav-1 (31). We also presented correlative evidence for a proangiogenic role of cav-1 in human prostate cancer (4). Endogenous levels of cav-1 expression in endothelial cells may provide an explanation for this controversy. C*av-1*$^{-/-}$ endothelial cells showed abrogated tubule formation and reduced NO production with or without VEGF treatment. Enforced expression of relatively low levels of cav-1 in cav-1$^{-/-}$ endothelial cells produced increased eNOS phosphorylation (S1177) and NO production in response to VEGF treatment, yet expression of higher levels of cav-1 blocked this process (17).

Apparently, without cav-1, endothelial cells do not undergo proper maturation and maintain a hyperproliferative state. This

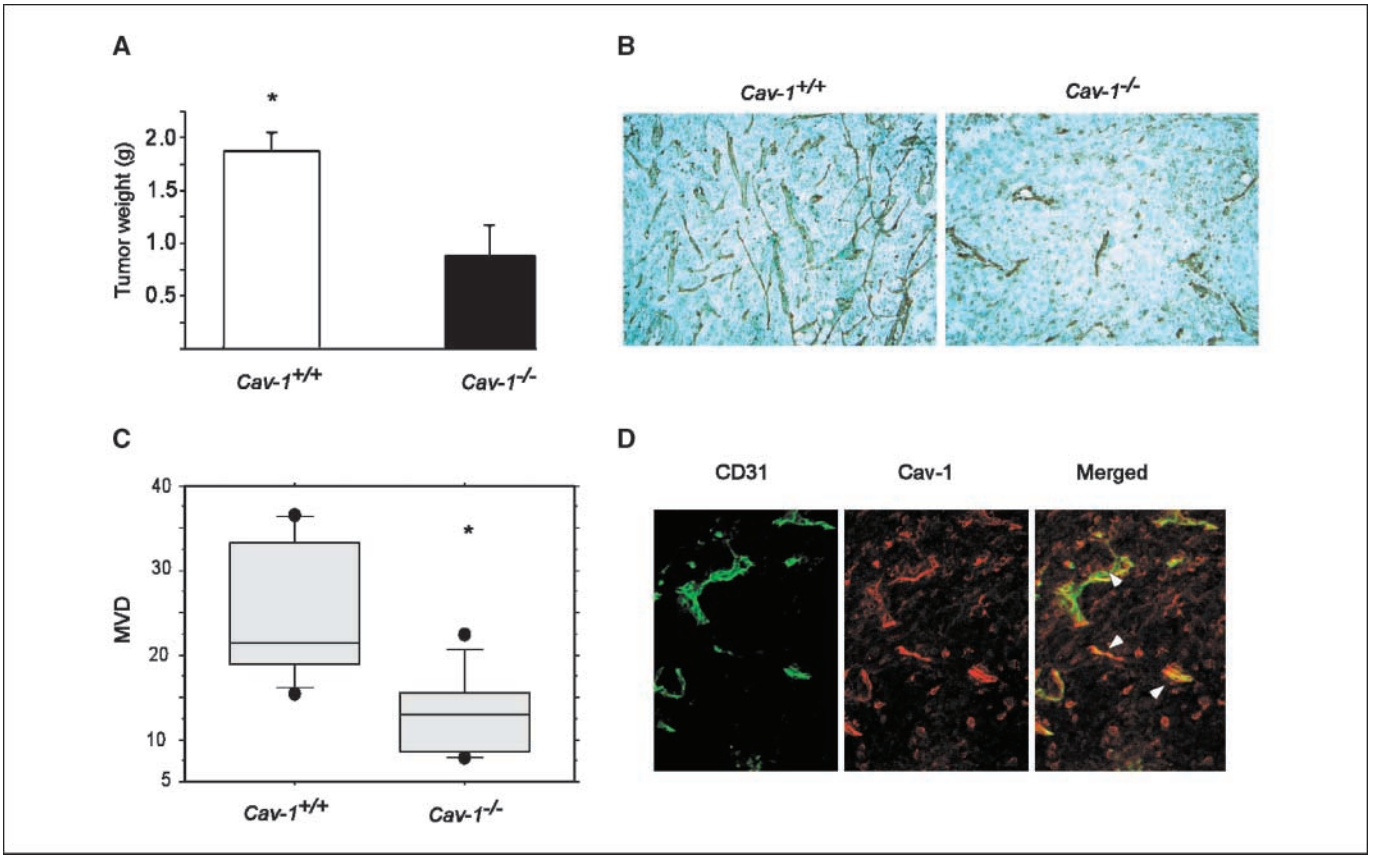

Figure 5. Secreted cav-1 promotes growth and angiogenesis in orthotopic RM-9 mouse prostate cancer model. *A,* increased RM-9 tumor wet weight in *cav-1*$^{+/+}$ hosts ($n = 7$) compared with *cav-1*$^{-/-}$ hosts ($n = 7$). *Columns,* mean; *bars,* SE. *, $P = 0.045$ by two-sided *t* test. *B,* immunohistochemical staining for CD31 in RM-9 tumors shows increased microvessel density in *cav-1*$^{+/+}$ hosts compared with *cav-1*$^{-/-}$ hosts. *C,* quantitative box plot analysis of the microvessel density (*MVD*) in RM-9 tumors from *cav-1*$^{+/+}$ versus *cav-1*$^{-/-}$ hosts. *Top lines,* 10th percentile; *bottom lines,* 90th percentile; *middle lines,* median value. *, $P = 0.0078$ by Mann-Whitney rank test. *D,* images of double immunostaining for CD31 (*green*) and cav-1 (*red*) in a tissue section of an RM-9 tumor from a *cav-1*$^{-/-}$ host. Arrows in the merged image (*yellow*) indicate the uptake by microvessels of cav-1 secreted by RM-9 tumors.

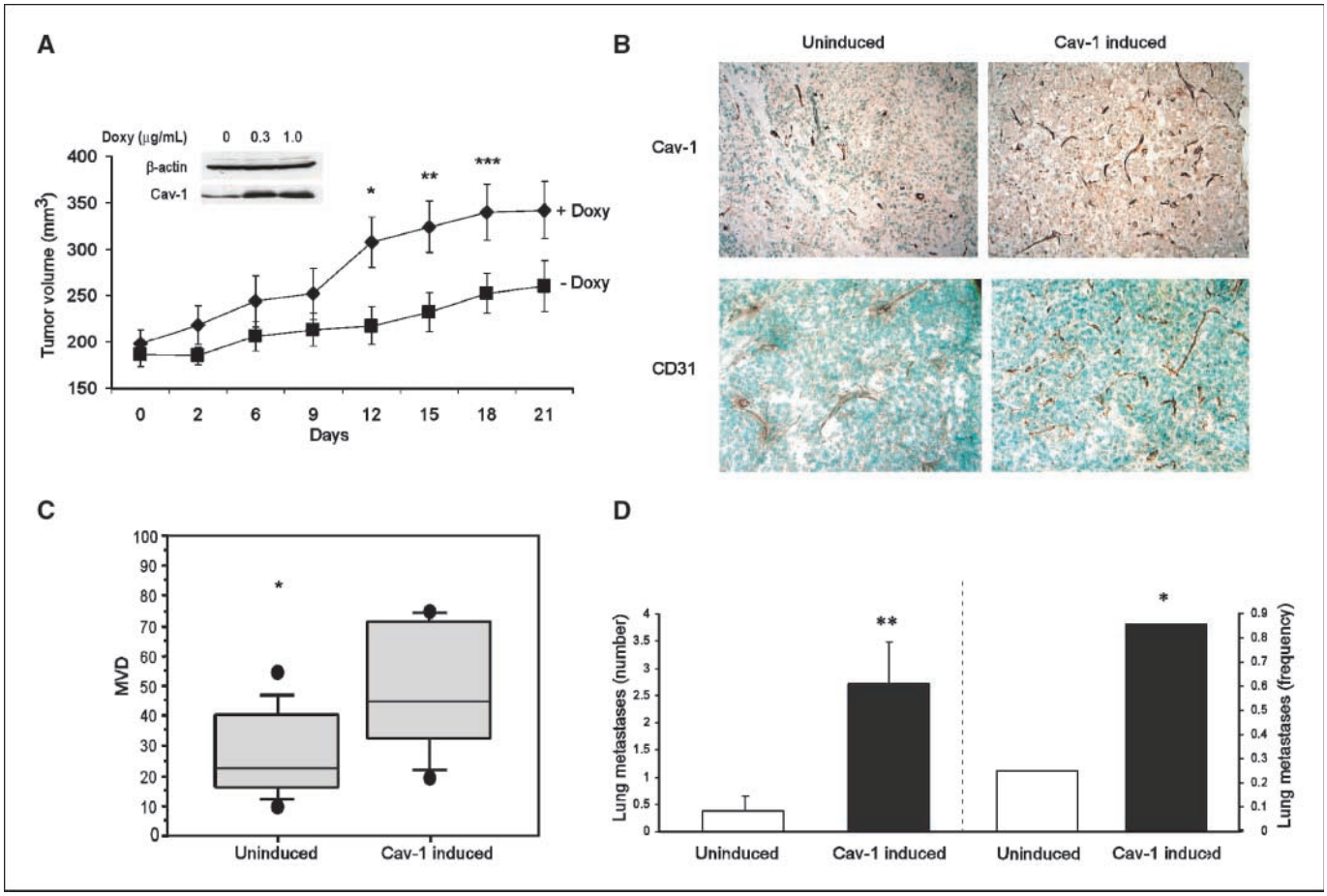

Figure 6. Secreted cav-1 promotes growth and angiogenesis in LNTB25cav tumors. *A,* Cav-1 induction by doxycycline (*Doxy*) leads to increased tumor volume in LNTB25cav s.c xenograft tumors growing s.c. Two groups of mice (n = 8 each) normalized for tumor volume were treated with either doxycycline (2 mg/mL) or control sucrose in drinking water for 21 d. *Points,* mean; *bars,* SE. *, P = 0.0195; **, P = 0.035; ***, P = 0.019 by two-sided t test. *B,* representative immunohistochemical staining for cav-1 and CD31 shows increased cytoplasmic cav-1 in cancer cells (*top*), and increased numbers of microvessels (*bottom*) in cav-1–induced LNTB25cav tumors compared with uninduced LNTB25cav tumors. *C,* quantitative box plot analysis of microvessel density in cav-1–induced (n = 8) and uninduced (n = 11) tumors. *Top lines,* 10th percentile; *bottom lines,* 90th percentiles; *middle lines,* median value. *, P = 0.039 by Mann-Whitney rank test. *D,* increased number and frequency of lung metastases in cav-1–induced compared with uninduced tumors. Lung metastases were established by injecting LNTB25cav cells into the tail veins of nude mice that were subsequently treated with doxycycline (n = 7) or sucrose (n = 8) in drinking water for 42 d. *Columns,* mean; *bars,* SE. *, P = 0.040 by Fisher's exact test; **, P = 0.008 by two-sided t test.

leads to a lack of polarization and a failure to form intercellular junctions (32), which may compromise selective transport mechanisms for specific macromolecules. Similarly, in tumor-associated endothelial cells a certain basal level of cav-1 may be required for minimal functional capacity. We have recently shown that cav-1 low/negative endothelial cells are relevant to prostate cancer. We reported significant reduction in the density of cav-1 positive microvessels in cav-1–negative human prostate cancer tissue compared with benign prostate tissues, clarifying the existence and possible significance of cav-1–negative microvessels in these malignancies (4).

We show that endocytosis of extracellular rcav-1 occurs in cancer cells (TSU-Pr1, DU145, and PC-3) and endothelial cells (HUVEC, *cav-1*$^{-/-}$ endothelial cells, and *cav-1*$^{+/+}$ endothelial cells), and that endothelial cells take up rcav-1 through lipid rafts/caveolae and clathrin-dependent pathways. Our results also show that rcav-1 uptake does not have an absolute cellular requirement for caveolae. The involvement of multiple endocytic pathways is not unique to cav-1 internalization, as these mechanisms have been described for the internalization of a number of proteins such as protein-specific membrane antigen (33), insulin growth factor binding protein-3 (34), transforming growth factor β receptor (35), and decorin (36). A possible explanation for the internalization of cav-1 through multiple pathways is its ability to interact with and bind to a large number of signaling proteins including multiple membrane receptors (15), which places it in proximity to endosome-forming activities of various pathways.

We show that CSD is necessary but may not be sufficient for cav-1 uptake, which leads to tubule formation, cell migration, and NO production in *cav-1*$^{-/-}$ endothelial cells. These data are supported by the results of a study that identified a highly conserved region of the engrailed homeoproteins that bears a high degree of homology with the CSD and are responsible for oligopeptide or oligonucleotide transmembrane, and cellular transport (37). The CSD was also found to have the ability to direct endogeneous cav-1 to cell membranes (16).

We show that cav-1 angiogenic activities involve the PI3-K-Akt-eNOS pathway but not Erk1/2. Indeed, rcav-1 treatment increases phosphorylation of Akt (S473 and T308) and, hence, eNOS phosphorylation (S1177 but not T495), leading to NO production.

Because previous studies show that Akt phosphorylates eNOS on the S1177 site, leading to eNOS activation, our results are consistent with a straight forward molecular pathway through which cav-1 uptake activates Akt, which in turn activates eNOS. However, Akt inhibitor studies indicated that Akt signaling is not the only pathway culminating in eNOS phosphorylation on S1177. That is, rcav-1–stimulated Akt activation was accompanied by inhibition of PP2A, a specific serine/threonine kinase that dephosphorylates S473 and T308 on Akt, and S1177 and T495 on eNOS (13, 21, 38). It is of interest that rcav-1 did not inhibit PP1, a serine/threonine kinase whose substrate specificity is similar to that of PP2A. Because PP1 may have selective activity for the T495 site on eNOS, which unlike the S1177 site leads to inhibition of eNOS activity, the absence of cav-1–mediated inhibition of PP1 could further contribute to eNOS activation (21). This notion is supported by the absence of increased phosphorylation of T495 on eNOS in response to rcav-1 (Fig. 4*A, right*). Because we previously showed that cav-1–stimulated PP1, and PP2A inhibition is mediated through direct interaction between the cav-1 CSD and PP1/PP2A binding sites in prostate cancer cells, (13) it seems reasonable to suggest that this specific interaction also applies to rcav-1–mediated inhibition of PP2A in *cav-1*$^{-/-}$ endothelial cells.

Studies with two complementary animal model systems (i.e., the RM-9-*cav-1*$^{-/-}$ host orthotopic model and the LNTB25cav xenograft model) substantiate our *in vitro* findings that tumor-associated endothelial cells internalize tumor-secreted cav-1, which is associated with tumor growth, and that overexpression of cav-1 in prostate cancer cells promotes angiogenesis and tumor growth.

Overall, our data show that prostate cancer cell–derived and prostate cancer cell–secreted cav-1 has autocrine (tumor cell uptake) and paracrine (tumor-associated endothelial cells uptake) activities that can contribute to angiogenesis, tumor progression, and metastasis. We propose that prostate cancer and potentially other malignancies that overexpress and secrete cav-1, may benefit from anti–cav-1 therapy that could involve cav-1 antibodies or peptide inhibitors of CSD.

Acknowledgments

Received 7/13/2007; revised 9/27/2007; accepted 11/12/2007.

Grant support: NIH grants RO1 CA68814 and Specialized Programs of Research Excellence P50 58204 and DAMD PC051247 from the Department of Defense.

The costs of publication of this article were defrayed in part by the payment of page charges. This article must therefore be hereby marked *advertisement* in accordance with 18 U.S.C. Section 1734 solely to indicate this fact.

References

1. Shaul PW, Anderson RG. Role of plasmalemmal caveolae in signal transduction. Am J Physiol 1998;275: L843–51.

2. Nasu Y, Timme TL, Yang G, et al. Suppression of caveolin expression induces androgen sensitivity in metastatic androgen-insensitive mouse prostate cancer cells. Nat Med 1998;4:1062–4.

3. Yang G, Truong LD, Timme TL, et al. Elevated expression of caveolin is associated with prostate and breast cancer. Clin Cancer Res 1998;4:1873–80.

4. Yang G, Addai J, Ayala G, et al. Correlative evidence that prostate cancer cell-derived caveolin-1 mediated angiogenesis. Hum Pathol 2007;38:1688–95.

5. Williams TM, Lisanti MP. The Caveolin genes: from cell biology to medicine. Ann Med 2004;36:584–95.

6. Carver LA, Schnitzer JE. Caveolae: mining little caves for new cancer targets. Nat Rev Cancer 2003;3: 571–81.

7. Tahir SA, Yang G, Ebara S, et al. Secreted caveolin-1 stimulates cell survival/clonal growth and contributes to metastasis in androgen-insensitive prostate cancer. Cancer Res 2001;61:3882–5.

8. Tahir SA, Ren C, Timme TL, et al. Development of an immunoassay for serum caveolin-1: a novel biomarker for prostate cancer. Clin Cancer Res 2003;9:3653–9.

9. Tahir SA, Frolov A, Hayes TG, et al. Preoperative serum caveolin-1 as a prognostic marker for recurrence in a radical prostatectomy cohort. Clin Cancer Res 2006;12: 4872–5.

10. Williams TM, Hassan GS, Li J, et al. Caveolin-1 promotes tumor progression in an autochthonous mouse model of prostate cancer: genetic ablation of Cav-1 delays advanced prostate tumor development in TRAMP mice. J Biol Chem 2005;10:1074.

11. Cao G, Yang G, Timme TL, et al. Disruption of the caveolin-1 gene impairs renal calcium reabsorption and leads to hypercalciuria and urolithiasis. Am J Pathol 2003;162:1241–8.

12. Brouet A, Sonveaux P, Dessy C, et al. Hsp90 and caveolin are key targets for the proangiogenic nitric oxide-mediated effects of statins. Circ Res 2001;89: 866–73.

13. Li L, Ren CH, Tahir SA, Thompson TC. Caveolin-1 maintains activated Akt in prostate cancer cells through scaffolding domain binding site interactions with and inhibition of serine/threonine protein phosphatases PP1 and PP2A. Mol Cell Biol 2003;23:9389–404.

14. Vermeulen PB, Gasparini G, Fox SB, et al. Second international consensus on the methodology and criteria of evaluation of angiogenesis quantification in solid human tumours. Eur J Cancer 2002;38:1564–79.

15. Smart EJ, Graf GA, McNiven MA, et al. Caveolins, liquid-ordered domains, and signal transduction. Mol Cell Biol 1999;19:7289–304.

16. Schlegel A, Lisanti MP. A molecular dissection of caveolin-1 membrane attachment and oligomerization. Two separate regions of the caveolin-1 C-terminal domain mediate membrane binding and oligomer/oligomer interactions *in vivo*. J Biol Chem 2000;275: 21605–17.

17. Sonveaux P, Martinive P, DeWever J, et al. Caveolin-1 expression is critical for vascular endothelial growth factor-induced ischemic hindlimb collateralization and nitric oxide-mediated angiogenesis. Circ Res 2004;95: 154–61.

18. Labrecque L, Royal I, Surprenant DS, et al. Regulation of vascular endothelial growth factor receptor-2 activity by caveolin-1 and plasma membrane cholesterol. Mol Biol Cell 2003;14:334–47.

19. Liu J, Wang XB, Park DS, Lisanti MP. Caveolin-1 expression enhances endothelial capillary tubule formation. J Biol Chem 2002;277:10661–8.

20. Cohen PT. Protein phosphatase 1-targeted in many directions. J Cell Sci 2002;115:241–56.

21. Michell BJ, Chen Z, Tiganis T, et al. Coordinated control of endothelial nitric-oxide synthase phosphorylation by protein kinase C and the cAMP-dependent protein kinase. J Biol Chem 2001;276:17625–8.

22. Chambliss KL, Shaul PW. Rapid activation of endothelial NO synthase by estrogen: evidence for a steroid receptor fast-action complex (SRFC) in caveolae. Steroids 2002;67:413–9.

23. Stirone C, Boroujerdi A, Duckles SP, Krause DN. Estrogen receptor activation of phosphoinositide-3 kinase, akt, and nitric oxide signaling in cerebral blood vessels: rapid and long-term effects. Mol Pharmacol 2005;67:105–13.

24. Nasu Y, Bangma C, Hull G, et al. Combination gene therapy with adenoviral vector-mediated HSV-tk+GCV and IL-12 in an orthotopic mouse model for prostate cancer. Prostate Cancer Prostatic Diseases 2001;4:44–55.

25. Hanahan D, Folkman J. Patterns and emerging mechanisms of the angiogenic switch during tumorigenesis. Cell 1996;86:353–64.

26. Carmeliet P, Jain RK. Angiogenesis in cancer and other diseases. Nature 2000;407:249–57.

27. Frank PG, Woodman SE, Park DS, Lisanti MP. Caveolin, caveolae, and endothelial cell function. Arterioscler Thromb Vasc Biol 2003;23:1161–8.

28. Massimino ML, Griffoni C, Spisni E, Toni M, Tomasi V. Involvement of caveolae and caveolae-like domains in signalling, cell survival and angiogenesis. Cell Signal 2002;14:93–8.

29. Lin MI, Yu J, Murata T, Sessa WC. Caveolin-1-deficient mice have increased tumor microvascular permeability, angiogenesis, and growth. Cancer Res 2007;67:2849–56.

30. Woodman SE, Ashton AW, Schubert W, et al. Caveolin-1 knockout mice show an impaired angiogenic response to exogenous stimuli. Am J Pathol 2003;162: 2059–68.

31. Joo HJ, Oh DK, Kim YS, Lee KB, Kim SJ. Increased expression of caveolin-1 and microvessel density correlates with metastasis and poor prognosis in clear cell renal cell carcinoma. BJU Int 2004;93:291–6.

32. Razani B, Engelman JA, Wang XB, et al. Caveolin-1 null mice are viable but show evidence of hyperproliferative and vascular abnormalities. J Biol Chem 2001;276:38121–38.

33. Anilkumar G, Barwe SP, Christiansen JJ, et al. Association of prostate-specific membrane antigen with caveolin-1 and its caveolae-dependent internalization in microvascular endothelial cells: implications for targeting to tumor vasculature. Microvasc Res 2006; 72:54–61.

34. Lee KW, Liu B, Ma L, et al. Cellular internalization of insulin-like growth factor binding protein-3: distinct endocytic pathways facilitate re-uptake and nuclear localization. J Biol Chem 2004;279:469–76.

35. Di Guglielmo GM, Le Roy C, Goodfellow AF, Wrana JL. Distinct endocytic pathways regulate TGF-β receptor signalling and turnover. Nat Cell Biol 2003;5:410–21.

36. Feugaing DD, Tammi R, Echtermeyer FG, et al. Endocytosis of the dermatan sulfate proteoglycan decorin utilizes multiple pathways and is modulated by epidermal growth factor receptor signaling. Biochimie 2007;89:637–57.

37. Joliot A, Trembleau A, Raposo G, et al. Association of engrailed homeoproteins with vesicles presenting caveolae-like properties. Development 1997;124: 1865–75.

38. Urbich C, Reissner A, Chavakis E, et al. Dephosphorylation of endothelial nitric oxide synthase contributes to the anti-angiogenic effects of endostatin. FASEB J 2002;16:706–8.

Available online at www.sciencedirect.com
ScienceDirect
Experimental and Molecular Pathology 84 (2008) 131–140
Experimental and Molecular Pathology
www.elsevier.com/locate/yexmp

Mice with *cav-1* gene disruption have benign stromal lesions and compromised epithelial differentiation

Guang Yang [a], Terry L. Timme [a,b], Koji Naruishi [a], Tetsuo Fujita [a], El Moataz Abdel Fattah [a], Guangwen Cao [a], Kartik Rajocopolan [a], Luan D. Troung [c], Timothy C. Thompson [a,b,d,e,*]

[a] *Scott Department of Urology, Baylor College of Medicine, Houston, TX, USA*
[b] *Michael E DeBakey Veterans Affairs Medical Center, Houston, TX, USA*
[c] *Research Institute, The Methodist Hospital, Houston, TX, USA*
[d] *Department of Cellular and Molecular Biology, Baylor College of Medicine, Houston, TX, USA*
[e] *Department of Radiology, Baylor College of Medicine, Houston, TX, USA*

Received 24 July 2007
Available online 31 August 2007

Abstract

Caveolin-1 (cav-1) is a major structural protein of caveolae, small invaginations of the plasma membrane that integrate and regulate signaling pathways involved in cell growth and differentiation. We previously generated a genetically engineered mice that are homozygous for a null mutation in exon 2 of *cav-1* and documented increased incidence of urolithiasis in young male *cav-1*$^{-/-}$ mice. We attributed this, in part, to improper localization of plasma membrane calcium/calmodulin-dependent calcium ATPase in the distal convoluted tubules of the kidney. To document pathologies related to cav-1 function, we maintained *cav-1*$^{-/-}$ and control *cav-1*$^{+/+}$ mice for an extended time period. We report here that *cav-1*$^{-/-}$ mice demonstrate organ-specific growth-related disorders in stromal cells that normally have high levels of cav-1 expression. In many of these organs, epithelial cell growth/differentiation abnormalities were also observed, yet in most of these sites the epithelial cells normally express low to non-detectable levels of cav-1. We propose that loss of cav-1 function in stromal cells of various organs directly leads to a disorganized stromal compartment that, in turn, indirectly promotes abnormal growth and differentiation of adjacent epithelium.

Introduction

Caveolin-1 (cav-1) protein was originally isolated as a structural component of caveolae in endothelial cells (Rothberg et al., 1992) and epithelial cells (Kurzchalia et al., 1992). Subsequently cav-1 expression has been observed in multiple cell types and was shown to play an important role in signal transduction and molecular transport in a cell and context-specific fashion (Fielding and Fielding, 2001; Massimino et al., 2002; Parton, 2003; Shaul and Anderson, 1998; Smart et al., 1999). The role of cav-1 in human disease has been the subject of considerable debate especially with regard to the development and progression of various malignancies. To develop model systems that provide insight into the role of cav-1 in human disease, multiple investigators generated cav-1 gene knockout mice.

There are currently three independent reports of the generation of cav-1 knockout mice (Drab et al., 2001; Razani et al., 2001a; Cao et al., 2003) and one of a cav-2 knockout mouse (Razani et al., 2002). Unexpectedly, *cav-1*$^{-/-}$ mice were viable and apparently healthy despite the absence of cav-1 (Parton, 2001). However, pathologic analysis revealed abnormalities in specific cell types. Pulmonary and cardiac defects were consistently reported for all *cav-1*$^{-/-}$ mice (Drab et al., 2001; Razani et al., 2001a; Cao et al., 2003). We also reported that young *cav-1*$^{-/-}$ male mice demonstrate an increased incidence of urolithiasis that likely results in part from improper localization of plasma membrane calcium/calmodulin-dependent calcium ATPase in the distal convoluted tubules of the kidney (Cao et al., 2003). These studies confirmed a functional role for cav-1 in specific tissues or cell types. Additional studies using *cav-1*$^{-/-}$ mice have focused on the role of cav-1 in

* Corresponding author. 6560 Fannin, Suite 2100, Houston, TX 77030. Fax: +1 713 794 7983.
E-mail address: timothyt@bcm.edu (T.C. Thompson).

0014-4800/$ - see front matter © 2007 Elsevier Inc. All rights reserved.
doi:10.1016/j.yexmp.2007.08.004

malignancy, and early reports suggested that cav-1 was a tumor suppressor. Unambiguous functional evidence for a tumor suppressor gene is the demonstration of tumorigenesis in a knockout mouse model (Hakem and Mak, 2001). The absence of *cav-1* has not been reported to increase the incidence of spontaneous malignancies; however, loss of cav-1 function has been shown to increase the incidence of carcinogen-induced hyperplasia and tumorigenesis following application of dimethylbenzanthracene to the skin (Capozza et al., 2003). The development of epithelial cell hyperplasia but not overt dysplasia in the mammary glands of *cav-1*$^{-/-}$ mice was also reported (Lee et al., 2002). In addition, an increased incidence of dysplastic lesions was observed in *cav-1*$^{-/-}$ mice compared to *cav-1*$^{+/+}$ when the mice were bred with transgenic mice expressing a dominant transforming oncogene, polyoma middle T (PyMT), in breast tissue permissive for MMTV promoter activities (Williams et al., 2003). In older MMTV-PyMT mice, breast cancer lesions appeared sooner and with increased multifocality in female mice in a *cav-1*$^{-/-}$ background than in *cav-1*$^{+/+}$ or *cav-1*$^{+/-}$ mice, and there were more metastatic lesions in the lungs (Williams et al., 2004).

Some reports document down-regulation of cav-1 in various malignancies (Aldred et al., 2003; Bagnoli et al., 2000; Bender et al., 2000; Davidson et al., 2001; Kato et al., 2004; Racine et al., 1999; Sagara et al., 2004; Sunaga et al., 2004; Wiechen et al., 2001; Wikman et al., 2004). However, with regard to prostate cancer, in a recently published study, it was shown that TRAMP (transgenic mouse prostate);*cav-1*$^{-/-}$ mice demonstrate significantly reduced numbers of primary tumors and metastatic lesions compared to TRAMP;*cav-1*$^{+/+}$ mice (Williams et al., 2005). These data are consistent with numerous studies that have clearly documented overexpression of cav-1 is associated with unfavorable clinical prognosis in various adenocarcinomas (reviewed in Bender et al., 2000; Carrion et al., 2003; Davidson et al., 2002; Ho et al., 2002; Horiguchi et al., 2004; Hu et al., 2001; Hung et al., 2003; Ito et al., 2002; Joo et al., 2004; Kato et al., 2002; Mouraviev et al., 2002; Patlolla et al., 2004; Rajjayabun et al., 2001; Sanchez-Carbayo et al., 2002; Satoh et al., 2003; Sunaga et al., 2004; Suzuoki et al., 2002; Terris et al., 2002; Yang et al., 2000, 1998, 1999; Yoo et al., 2003). To provide additional insight into the role of cav-1 in abnormal cellular growth, we further analyzed *cav-1*$^{-/-}$ mice.

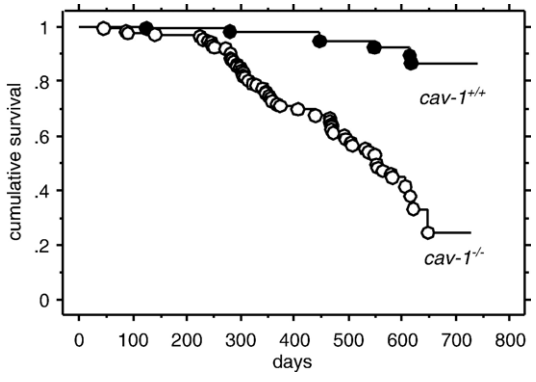

Fig. 1. Kaplan–Meyer survival plot of *cav-1*$^{+/+}$ and *cav-1*$^{-/-}$ mice.

Table 1
Organ wet weight in adult *cav-1*$^{+/+}$ and *cav-1*$^{-/-}$ mice at two time points

	Male				Female			
	cav-1$^{+/+}$		*cav-1*$^{-/-}$		*cav-1*$^{+/+}$		*cav-1*$^{-/-}$	
Age (months)	10	19	10	19	10	19	10	19
N	7	55	15	30	6	37	10	16
Body weight (g)	32.08	31.44	30.38	31.35	23.99	27.71	24.96	27.30
Kidney (mg)	247	302	278	290	187	208	232	206
Spleen (mg)	146	170	445	188	206	176	450	346
Liver (mg)	1506	1700	1710	1657	1179	1501	1586	1533
Lung (mg)	181		385		172		293	
Pancreas (mg)	145		143		165		122	
Prostate (mg)		89		67				

We report here our long-term observations of a cohort of *cav-1*$^{+/+}$ and *cav-1*$^{-/-}$ mice. In agreement with previous observations, *cav-1*$^{-/-}$ have a decreased lifespan (Park et al., 2003). We did not detect any increase in overt cancer development. We document stromal cell growth abnormalities in *cav-1*$^{-/-}$ mice compared to *cav-1*$^{+/+}$ mice. Specifically, these abnormalities were seen in endothelial cells and smooth muscle cells of specific organs that normally express high levels of cav-1. Interestingly, in many of these organs epithelial/parenchymal cells that normally do not express significant levels of cav-1 also demonstrated growth and differentiation abnormalities including glandular malfunction and reduced cytokeratin staining.

Materials and methods

Mice

Using *Lox*P/Cre technology, we generated genetically engineered mice that were homozygous for a deletion of exon 2 of the *cav-1* gene (Cao et al., 2003). The mice were kept in a mixed strain background of C57/BL6 and129/Sv by interbreeding. They had access to food, Harlan TekLab 22/5 Rodent Diet (W), and water *ad libitum*. They were maintained in facilities accredited by the American Association for Accreditation of Laboratory Animal Care and all experiments conducted in accordance with the principles and procedures outlined in the National Institutes of Health's Guide for the Care and Use of Laboratory Animals.

Histopathology and immunohistochemistry

Animals were euthanized and after careful observation for gross changes, selected organs were removed by dissection and weighed. Tissue samples were fresh frozen in OCT (Optimal Cutting Temperature) compound or fixed in 10%

Table 2
Organ confined pathologies in adult (>18 months) *cav-1*$^{+/+}$ and *cav-1*$^{-/-}$ mice

Phenotype	*cav-1*$^{+/+}$	*cav-1*$^{-/-}$
Thickening of alveolar septa in lung	3/44 (7%)	13/23 (56%)
Breast epithelial hyperplasia	2/31 (6%)	6/13 (46%)†
Prostate epithelial cell hyperplasia	3/13 (23%)	2/9 (22%)
Seminal vesicle enlargement	1/12 (8%)	6/9 (67%)‡
Ovarian cysts	1/31 (3%)	3/13 (23%)
Hepatic carcinoma	4/44 (9%)	0/23 (0%)
Lymphoma in spleen	4/44 (9%)	2/23 (9%)
Lymphoma in uterus	2/31 (6%)	0/13 (0%)

$^{\dagger}P=0.0072$ or $^{\ddagger}P=0.0182$; Fisher's exact test.

buffered formalin and embedded in paraffin for sectioning. Sections (4–5 μm) were stained with hematoxylin and eosin (H&E) according to standard protocols and were evaluated histologically. Immunohistochemical (IHC) analysis using standard ABC detection was performed as previously described (Yang et al., 1998). Antibodies used included rabbit polyclonal anti-cav-1 (N-20, Santa Cruz Biotech, Inc., Santa Cruz, CA), goat polyclonal anti-CD31 (M-20, Santa Cruz), rabbit polyclonal anti-cytokeratin (Z0575, Dako, Carpinteria, CA), mouse monoclonal anti-proliferative cell nuclear antigen (PCNA) (PC-10, Dako), mouse monoclonal anti-alpha smooth muscle-specific actin (1A4, Dako), rabbit polyclonal anti-desmin (D8281, Sigma-Aldrich, St. Louis, MO) and goat polyclonal anti-vimentin (V4630, Sigma) and rat monoclonal anti-CD11b (Clone M1/70, Pharmingen, San Diego, CA). The TUNEL technique (Gavrieli et al., 1992) was used to label apoptotic splenocytes as previously described (Yang et al., 1996). IHC quantitation of PCNA-positive and apoptotic splenocytes were conducted on 30 randomly selected measuring fields (0.198 μm^2 each) for each specimen. The number of positively labeled cells per unit spleen area was recorded and the statistical significance of the differences in proliferative and apoptotic activities was evaluated by the Mann–Whitney rank test.

Results

We observed a large cohort of *cav-1*$^{+/+}$ and *cav-1*$^{-/-}$ mice for more than 2 years. The *cav-1*$^{+/+}$ mice had significantly longer overall survival times than their *cav-1*$^{-/-}$ littermates (Fig. 1).

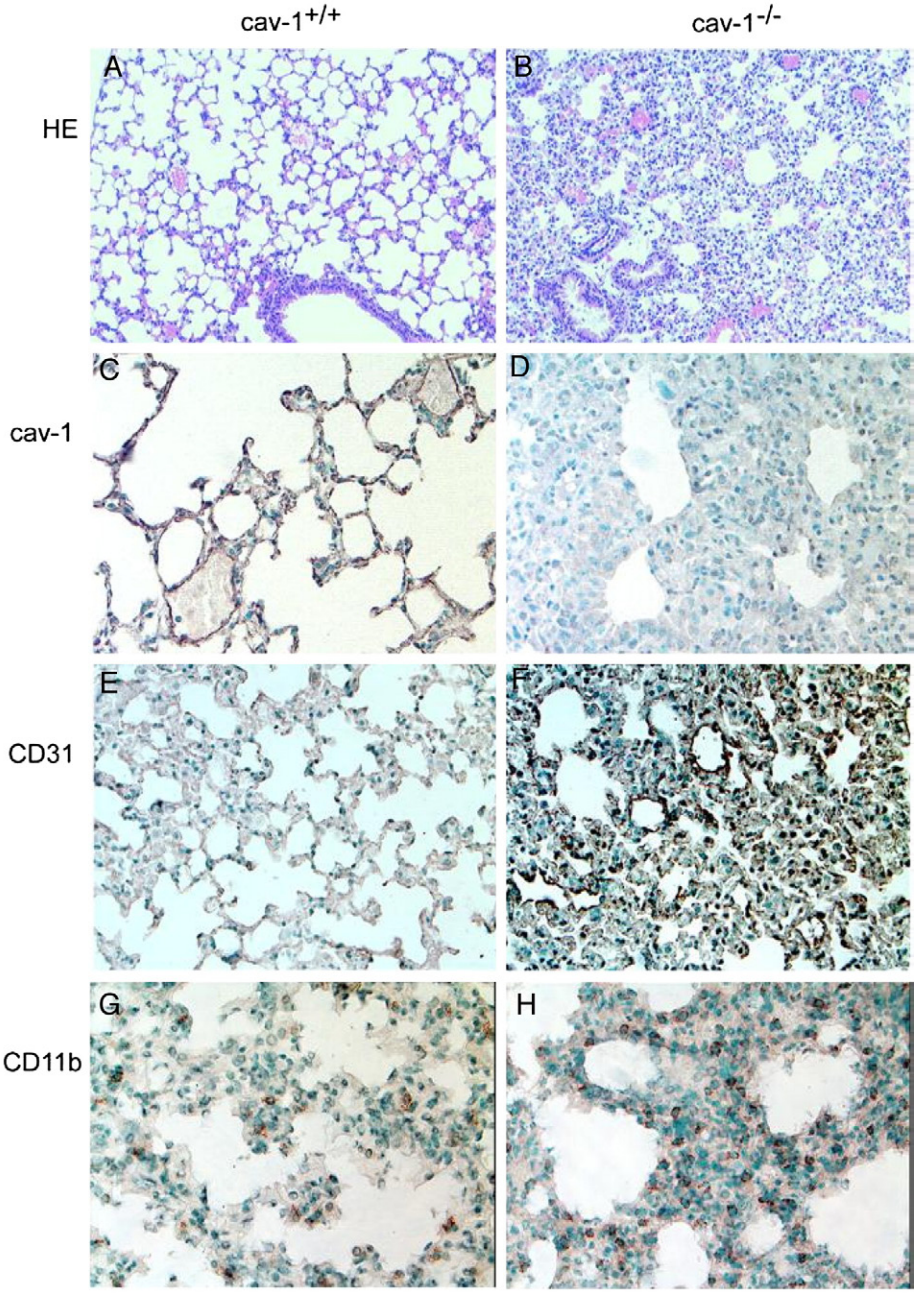

Fig. 2. Histological and IHC characterization of lung tissues from *cav-1*$^{+/+}$ (A, C, E and G) and *cav-1*$^{-/-}$ (B, D, F and H) mice. (A and B) H&E staining; (C and D) cav-1 staining; (E and F) CD31 staining; (G and H) CD11b staining. Original magnification: A and B, 100×; C–F, 200×; G and H, 400×.

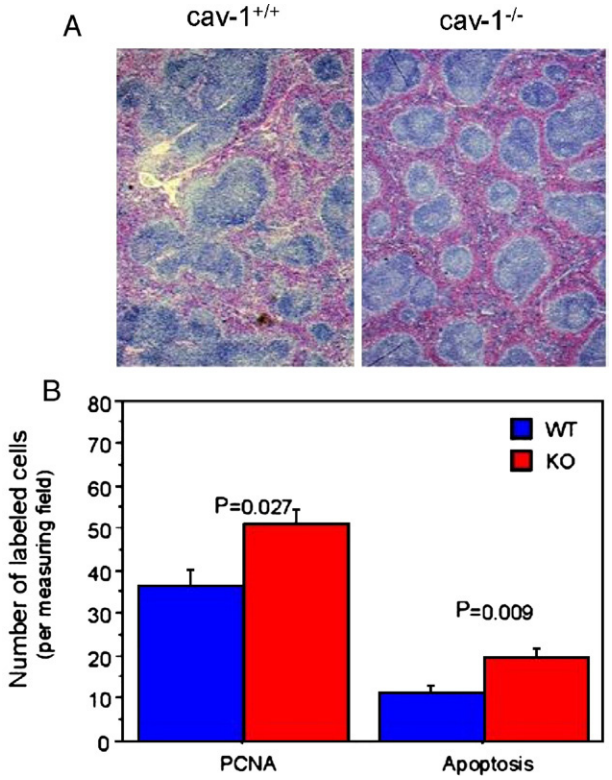

Fig. 3. H&E-stained sections of spleen (A) depicting the morphological difference between 3-month-old *cav-1*$^{+/+}$ and *cav-1*$^{-/-}$ mice. Original magnification: 200×. Quantitation of PCNA and apoptosis labeling (B) in the spleen. The densities of PCNA-positive cells and apoptotic bodies in spleen from *cav-1*$^{-/-}$ mice were significantly higher than in the *cav-1*$^{+/+}$ mice ($P=0.027$ and $P=0.009$, respectively).

The mean survival for the *cav-1*$^{+/+}$ mice was 602±6 days compared with 500±15 days for the *cav-1*$^{-/-}$ mice ($P<0.001$, Mantel-Cox Rank test). A smaller group of heterozygous mice ($n=30$) was also observed to have an intermediate survival time of 537±29 days. There was no difference in survival between male and female mice (data not shown). In most cases no obvious cause of death was apparent. At gross necropsy the most commonly observed abnormalities in older mice were swollen and purulent lymph nodes in the head and neck. One specific abnormality noted in several *cav-1*$^{-/-}$ mice was anal exstrophy.

We sacrificed two cohorts of mice at approximately 10 or 19 months of age and obtained the weight of selected organs (Table 1). The overall body weight was similar for mice of the same sex independent of genotype. However, the wet weights of specific organs including lungs, liver, kidney and spleen were increased in both male and female *cav-1*$^{-/-}$ mice at 10 months compared to *cav-1*$^{+/+}$ of the same sex. These differences achieved statistical significance in the spleen (males $P=0.0026$, females $P=0.0323$) and in the liver of females ($P=0.0164$). In mice evaluated at an age of 19 months these differences largely resolved, except the spleen weight from the *cav-1*$^{-/-}$ females remained significantly increased ($P=0.0404$).

The general gross anatomical and microscopic features based on evaluation of H&E-stained sections from selected organs of both cohorts of the *cav-1*$^{+/+}$ and *cav-1*$^{-/-}$ animals are summarized in Table 2. The penetrance of each abnormal phenotype as well as the incidence of spontaneous tumors in the mice is also compared in Table 2. Hepatocarcinoma and lymphoma were observed in a few animals with no statistical difference in incidence between *cav-1*$^{+/+}$ and *cav-1*$^{-/-}$ mice.

The lungs of *cav-1*$^{-/-}$ mice demonstrated thickened alveolar septa and hypercellularity. The alveolar lumens appeared smaller or constricted, as a result of the hypercellularity as compared to *cav-1*$^{+/+}$ mice (Fig. 2). In *cav-1*$^{-/-}$ mice, immunostaining with CD31 (PECAM) (Fig. 2) demonstrated significantly increased numbers of endothelial cells, whereas vimentin staining failed to show increased fibroblasts in the thickened septa (data not shown). Significantly increased numbers of infiltrating macrophages as demonstrated by CD11b staining were also seen in the thickened alveolar walls of *cav-1*$^{-/-}$ lung (Fig. 2). These lung abnormalities were observed most dramatically in 3- to 4-month-old *cav-1*$^{-/-}$ mice. They persisted in the aged animals with the incidence of the lung abnormalities in *cav-1*$^{-/-}$ significantly higher than that in the *cav-1*$^{+/+}$ mice at 18 months (Table 2).

Tissue sections of the spleen from 3-month-old mice revealed that the red pulp compartment represented a larger percentage of the area in *cav-1*$^{-/-}$ mice compared to *cav-1*$^{+/+}$ mice (Fig. 3A). However, this difference became less dramatic as the mice aged. The proliferative rate of splenocytes as demonstrated by the

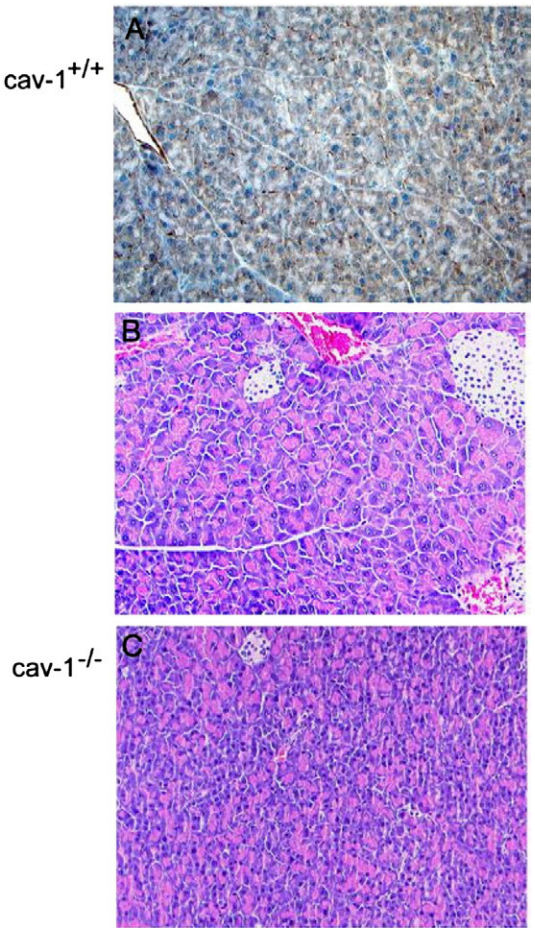

Fig. 4. H&E-stained sections of the pancreas of 3-month-old (A) *cav-1*$^{+/+}$ and (B) *cav-1*$^{-/-}$ mice demonstrating a higher density of exocrine secretory cells in *cav-1*$^{-/-}$ mice versus *cav-1*$^{+/+}$ mice. Original magnification: 200×.

number of PCNA-positive splenocytes per microscopic measuring field was also significantly higher in the *cav-1*$^{-/-}$ mice compared to the *cav-1*$^{+/+}$ mice ($P=0.027$, Mann–Whitney rank test, Fig. 3B). The apoptotic rate of splenocytes was also significantly higher in the *cav-1*$^{-/-}$ mice ($n=12$) compared to the *cav-1*$^{+/+}$ mice ($n=14$, $P=0.009$, Mann–Whitney rank test, Fig. 3B).

In the exocrine pancreas, there was a significant hypercellularity in glandular acini and ductal epithelia in the *cav-1*$^{-/-}$ animals compared to the *cav-1*$^{+/+}$ mice (Fig. 4). In the *cav-1*$^{-/-}$ pancreas, the pyramidal epithelial cells in the acini appeared to have a smaller size than those in the *cav-1*$^{+/+}$ pancreas. These cells tended to form fewer apically oriented zymogen granules and this made the exocrine pancreas appear more basophilic on H&E-stained sections The endocrine pancreas showed no significant difference between *cav-1*$^{+/+}$ and *cav-1*$^{-/-}$ animals.

We previously noted that in mice under 6 months of age soft urinary calculi were seen in the bladders of more than 60% of the *cav-1*$^{-/-}$ male mice and frank stone formation was observed in 13% of *cav-1*$^{-/-}$ males whereas this was not seen in *cav-1*$^{+/+}$ mice (Cao et al., 2003). In the older mice evaluated in the present study soft calculi and calcified deposits were also frequently observed at the juxtaposition of the bladder neck and urethra. Although no hypercellularity was demonstrated in the bladder wall of *cav-1*$^{-/-}$ animals on H&E-stained sections the smooth muscle layer in the bladder wall appeared to be disorganized (Fig. 5). Smooth muscle actin (SMA)-positive staining tended to be less abundant in the bladder wall of *cav-1*$^{-/-}$ mice relative to *cav-1*$^{+/+}$ mice (Fig. 5).

In mice that were over 18 months old, focal epithelial hyperplasia was occasionally seen in the dorsal lobe of prostate (data not shown). The incidence of these lesions did not differ between c*av-1*$^{+/+}$ and *cav-1*$^{-/-}$ mice (Table 2). The cav-1-positive abundant fibromuscular stroma that surrounded the prostatic glandular epithelia appeared slightly thicker in the older mice compared to younger adults (data not shown). No differences in the thickness of the stroma fibromuscular sheath were detected by SMA staining of prostate tissue from *cav-1*$^{-/-}$ and *cav-1*$^{+/+}$ (Figs. 6C and D). Interestingly, in the prostate of *cav-1*$^{-/-}$ mice, there was reduced cytokeratin staining in the glandular epithelia (Figs. 6E and F).

In the urogenital tract, we noted that *cav-1*$^{-/-}$ female mice had profoundly weaker cytokeratin staining in the uterine epithelium (Figs. 6G and H). There was an increase in the

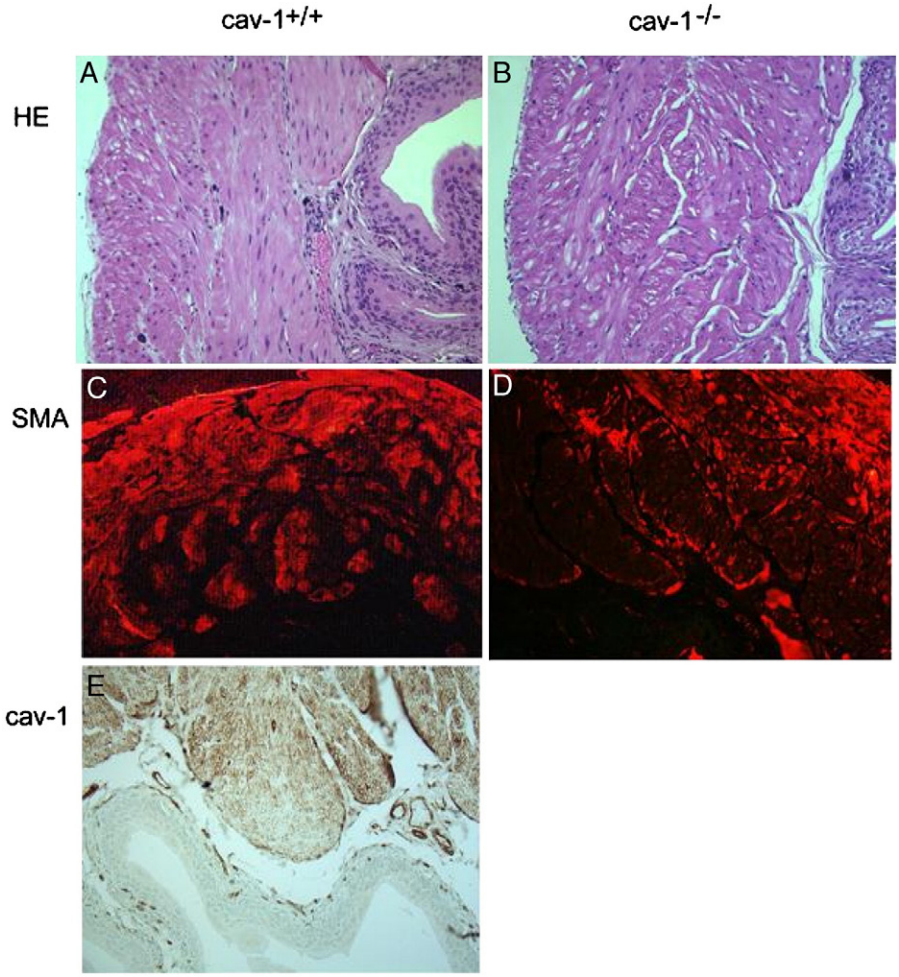

Fig. 5. H&E-stained sections of urinary bladder wall from 10-month-old (A) *cav-1*$^{+/+}$ and (B) *cav-1*$^{-/-}$ mice. SMA staining revealed more intense reactivity in the muscle layer of *cav-1*$^{+/+}$ mice (C) compared to the disorientated appearance in the *cav-1*$^{-/-}$ mice (D). Cav-1 immunostaining in *cav-1*$^{+/+}$ mice is shown in panel E. Original magnification: 200×.

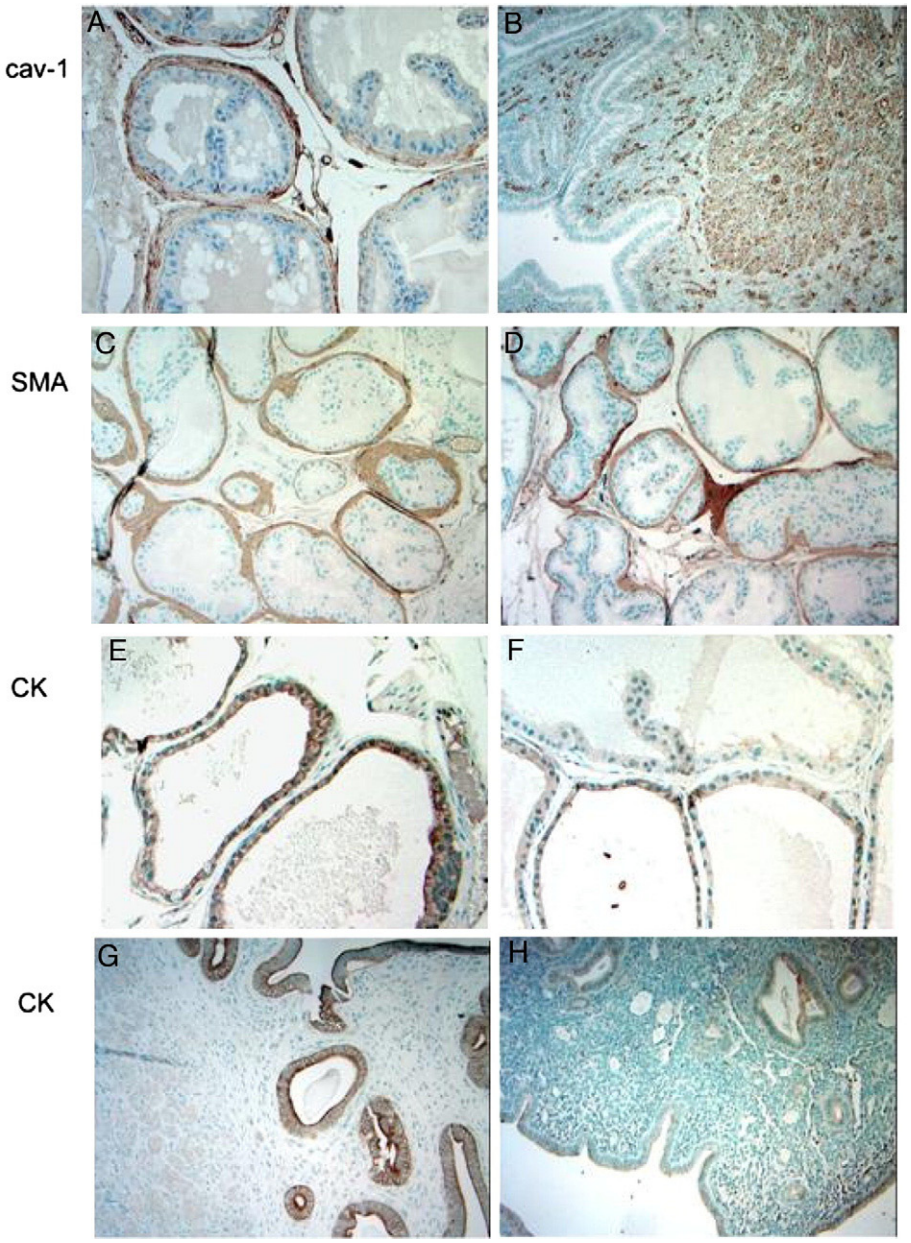

Fig. 6. Prostate and uterus tissues from *cav-1*$^{+/+}$ (A, B, C, E and G) and *cav-1*$^{-/-}$ (D, F and H) mice were stained for cav-1 (A and B), SMA (C and D) or cytokeratin (E–H). Cav-1 was present mainly in smooth muscles and vascular endothelia of the prostate (A) and uterus (B). In the prostates, no differences were evident in the fibromuscular layer surrounding the glandular epithelium between the *cav-1*$^{+/+}$ and *cav-1*$^{-/-}$ mice (C and D, respectively), whereas cytokeratin staining in the glandular epithelium was reduced in *cav-1*$^{-/-}$ (F) as compared with *cav-1*$^{+/+}$ mice (E). In female mice, the uterine epithelia of *cav-1*$^{-/-}$ mice (H) had reduced staining with cytokeratin compared to uterine sections from *cav-1*$^{+/+}$ mice (G). Original magnifications: B: 100×, others: 200×.

number of ovarian cysts observed in *cav-1*$^{-/-}$ mice but this did not achieve statistical significance ($P=0.1297$, χ^2 test, Table 2).

At necropsy, the seminal vesicles from *cav-1*$^{-/-}$ mice appeared to be swollen and enlarged in 67% of animals aged over 18 months ($P=0.0182$, χ^2 test, Table 2). Histological evaluation revealed a marked increase in seminal fluid with epithelial disorientation and a loss of the epithelial chords that normally protrude into the lumen in *cav-1*$^{-/-}$ mice (Figs. 7A and B). SMA staining delineated a thinner seminal vesicle smooth muscle layer in the *cav-1*$^{-/-}$ mice (Figs. 7E and F).

Breast tissues were harvested from *cav-1*$^{+/+}$ and *cav-1*$^{-/-}$ mice at ages ranging from 5 to 21 months. Cav-1 was mainly present in adipocytes, and myoepithelial cells surrounding the glandular epithelia (Fig 8A) in normal *cav-1*$^{+/+}$ breast. Benign epithelial hyperplastic lesions were apparent in H&E-stained sections from 46% of the *cav-1*$^{-/-}$ mice and only 6% of the *cav-1*$^{+/+}$ mice ($P=0.0072$, χ^2 test, Table 2). Features of *cav-1*$^{-/-}$ epithelial hyperplasia included increased numbers of ductal branches and mammary acini, as well as intraductal epithelial cells (Fig. 8). The myoepithelial cell layer that normally surrounds the mammary lining epithelial cells was obscured due to the tangled orientation of the intraductal cells. These morphological hyperplastic changes were also documented through IHC analysis. SMA-positive myoepithelial cells that

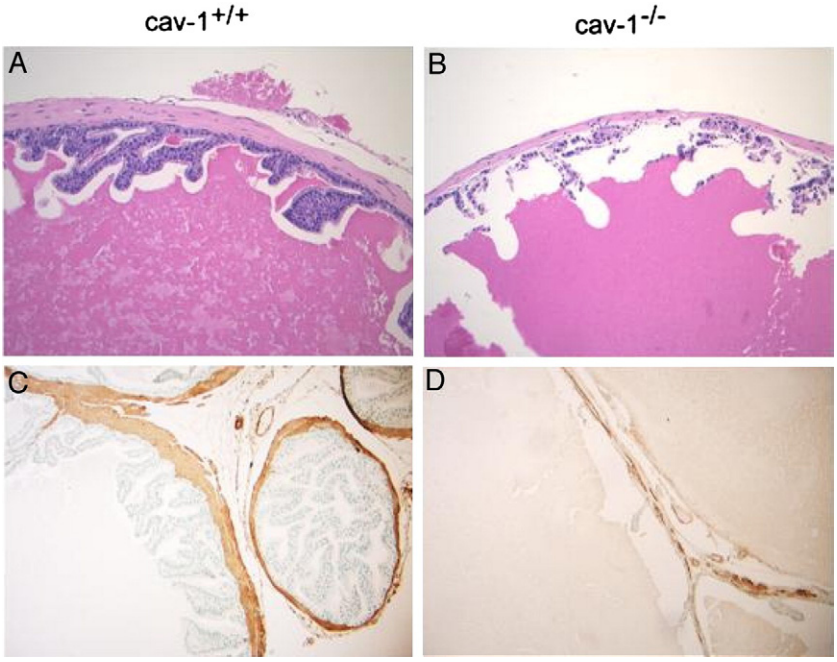

Fig. 7. Sections of seminal vesicle were stained with H&E (A and B) and SMA (C and D). Disorientation of the epithelial layer with a loss of protruding epithelial chords and epithelial detritus was evident in 10 month-old *cav-1*$^{-/-}$ mice (B). SMA staining appeared thinner in *cav-1*$^{-/-}$ mice (D). Original magnifications: 100×.

are normally orientated adjacent to mammary lining cells were admixed with epithelial cells in the *cav-1*$^{-/-}$ breast tissues (Figs. 8C and 8D). Interestingly, in 30% of the hyperplastic *cav-1*$^{-/-}$ breast specimens, SMA antibody strongly labeled intraductal cells (Fig. 8D). However, desmin antibody did not label the hyperplastic cells (data not shown). Vimentin-positive fibroblasts were not observed in the hyperplastic areas but were confined to connective tissue surrounding the hyperplastic epithelia (Fig. 8B). The hyperplastic epithelia in *cav-1*$^{-/-}$ breast sections exhibited attenuated cytokeratin expression compared to the *cav-1*$^{+/+}$ breast epithelia (Figs. 8E and F). Although the mammary hyperplasia-associated morphological and IHC changes were documented, mammary tumors were not observed in any *cav-1*$^{-/-}$ mice.

Discussion

The biological functions of cav-1 in cancer are complex and somewhat controversial (Massimino et al., 2002; Razani et al., 2001b; Thompson et al., 1999, 2001). Cav-1 is involved in multiple pathways that could influence cancer progression such as potocytosis, transcytosis, molecular transport and signal transduction in a cell and context-dependent fashion (Parton, 1996; Shaul and Anderson, 1998). The participation of cav-1 in these critical pathways involves interactions with a relatively large number of molecules in either a scaffolding binding-dependent or -independent manner (Carver and Schnitzer, 2003). The wide spectrum of molecular interactions involving cav-1 is consistent with important, context-dependent roles for cav-1 in signal transduction, molecular transport and other cellular regulatory events.

An association of reduced cav-1 expression in tyrosine kinase oncogene transformed NIH-3T3 cells (Koleske et al., 1995) led to the notion that cav-1 could function as a tumor suppressor gene (Galbiati et al., 1998; Razani et al., 2001b). Subsequent studies clearly demonstrated that overexpression of cav-1 in cells that constitutively express cav-1 (fibroblasts and selected breast cancer cell lines) can suppress growth in vitro (Engelman et al., 1997; Galbiati et al., 2001; Lee et al., 1998). The analysis of clinical specimens has yielded conflicting evidence for the concept of cav-1 as a tumor suppressor. There are several reports that cav-1 expression is down-regulated in cancer including specific types of lung cancer (Kato et al., 2004; Racine et al., 1999; Sunaga et al., 2004; Wikman et al., 2004), colon cancer (Bender et al., 2000), ovarian cancer (Bagnoli et al., 2000; Davidson et al., 2001; Wiechen et al., 2001), breast cancer (Sagara et al., 2004), follicular carcinoma of the thyroid (Aldred et al., 2003) and several types of sarcoma (Wiechen et al., 2001).

Conversely, cav-1 is up-regulated in many human malignancies and is associated with an unfavorable clinical prognosis (reviewed in Mouraviev et al., 2002). In prostate cancer, cav-1 was found to be over-expressed in human metastatic prostate cancer (Yang et al., 1998). Subsequently, positive correlations between cav-1 overexpression and clinical/pathological markers of cancer progression were reported for human prostate cancers (Satoh et al., 2003; Yang et al., 2000, 1999) as well as for other malignancies including metastatic colon cancer (Bender et al., 2000; Patlolla et al., 2004), renal cancer (Campbell et al., 2003; Carrion et al., 2003; Horiguchi et al., 2004; Joo et al., 2004), bladder cancer (Rajjayabun et al., 2001; Sanchez-Carbayo et al., 2002), urothelial carcinoma (Fong et al., 2003), oral squamous cancer (Hung et al., 2003), esophageal

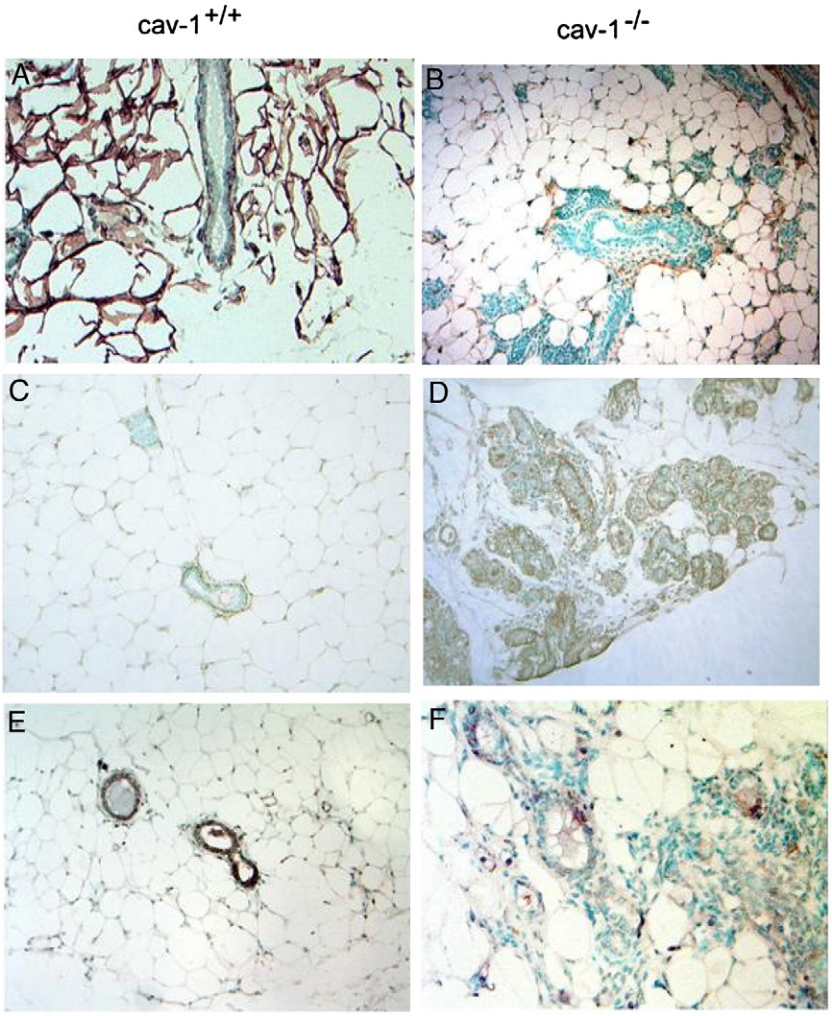

Fig. 8. Immunohistochemistry of mammary glands from 9- to 10-month-old virgin *cav-1*$^{+/+}$ (A, C and E) and *cav-1*$^{-/-}$ (B, D and F) mice as demonstrated by (A) cav-1, (C and D) SMA, (B) vimentin and (E and F) cytokeratin staining. Normal lobular development was apparent in *cav-1*$^{+/+}$ mice (A, C and E) whereas in *cav-1*$^{-/-}$ mammary glands there was pronounced epithelial hyperplasia (B, D and F). Original magnifications: 200×.

squamous cancer (Hu et al., 2001; Kato et al., 2002), papillary carcinoma of the thyroid (Ito et al., 2002), lung cancer (Ho et al., 2002; Sunaga et al., 2004; Yoo et al., 2003), pancreatic cancer (Suzuoki et al., 2002; Terris et al., 2002) and ovarian cancer (Davidson et al., 2002).

In this analysis of *cav-1*$^{-/-}$ and control *cav-1*$^{+/+}$ mice, we observed significantly increased wet weights of specific organs in 10-month-old mice, including kidney, spleen, liver and lung (see Table 1). This result prompted us to further investigate these differences using morphological and IHC analysis. Our studies revealed multiple abnormalities in specific cell types that were directly or indirectly related to growth control. In the lungs of *cav-1*$^{-/-}$ mice, we identified increased numbers of endothelial cells in regions of thickened alveolar septa. Since cav-1 plays an important role in endothelial cell growth, differentiation and maturation (Carver and Schnitzer, 2003) (Smart et al., 1999) this pathology may represent a failure of endothelial cells to properly differentiate, a condition that may contribute to the observed lung pathologies in these mice (Cao et al., 2003; Drab et al., 2001; Razani et al., 2001a; Zhao et al., 2002). In addition, the definitive identification of increased macrophages in these tissues further adds to the etiology of this cav-1-related disorder.

A novel observation of our study is significantly increased spleen size in *cav-1*$^{-/-}$ mice compared to *cav-1*$^{+/+}$ mice (see Table 1). We demonstrated increased splenocyte turnover (see Fig. 4) and suggest that failure of *cav-1*$^{-/-}$ splenocytes to differentiate contribute to the spleen enlargement. In the exocrine pancreas we observed increased numbers of pyramidal epithelial cells of smaller size that demonstrated fewer features of differentiated secretory epithelium in *cav-1*$^{-/-}$ mice. This phenomenon also appeared to be consistent with a failure to differentiate.

Our observations regarding bladder tissue of *cav-1*$^{-/-}$ mice support our previous observations of increased numbers of urinary calculi compared to *cav-1*$^{+/+}$ mice; however, the frequency of frank stone formation was significantly less than we previously observed (Cao et al., 2003). We attribute this to the difference in the age of the mice evaluated in this study (10 months to 1.5 years) compared to those previously evaluated

(3 to 5 months). In the present study, we also observed disorientation of the smooth muscle cell layer in the bladder of *cav-1*$^{-/-}$ mice (see Fig. 6). The intensity of actin staining in these cells was weaker in these cells suggesting that proper differentiation/organization was not achieved. Thickening of the smooth muscle layer in the bladder of *cav-1*$^{-/-}$ mice has been previously reported but the cellular disorganization we observed was not previously described (Woodman et al., 2004). Consistent with this previous study, we also observed a marked increase in the amount of fluid in the seminal vesicles of *cav-1*$^{-/-}$ mice compared to *cav-1*$^{+/+}$ mice with a thinner smooth muscle cell layer and epithelial disorientation accompanying this increased fluid retention.

In contrast with a previous report (Woodman et al., 2004), we did not observe a higher incidence of prostate growth abnormalities in *cav-1*$^{-/-}$ mice. This may be a reflection of differences in strain background.

It is important to note that our studies clarify the growth abnormalities associated with *cav-1*$^{-/-}$ breast that were reported previously (Williams et al., 2003). As in the previous report, we did document complex hyperplasia-related phenomena that involved increased numbers of ductal branches and increased numbers of acini per terminal ductal lobular unit. However, we showed that, at least in some animals, this hyperplastic condition involved myoepithelial cells as confirmed by positive SMA labeling. Since both the epithelial cells and myoepithelial cells may originate from a common progenitor stem cell (Bocker et al., 2002; Boecker and Buerger, 2003), our data suggest that the *cav-1* gene status may affect this differentiation pathway.

Finally, we show that there is markedly reduced cytokeratin expression in glandular epithelia of breast, prostate and uterus in *cav-1*$^{-/-}$ mice compared to *cav-1*$^{+/+}$ mice. It is conceivable that these abnormalities are related to inappropriate stromal differentiation and dysfunctional stromal–epithelial interactions.

The growth abnormalities that we document in this study could be interpreted as conditions that could evolve into a premalignant phenotype or possibly could render the affected cells susceptible to transformation under specific conditions. Indeed a recent study documents increased skin malignancies in *cav-1*$^{-/-}$ mice compared to *cav-1*$^{+/+}$ mice following topical application of a carcinogen (Capozza et al., 2003). However, most of the cell types observed to exhibit hyperplasia in *cav-1*$^{-/-}$ mice were smooth muscle cells that do not commonly undergo spontaneous malignant transformation in either rodents or humans. Furthermore, the hyperplastic pathologies apparent in *cav-1*$^{-/-}$ mice can be interpreted to result from incomplete differentiation that in some cases appeared to resolve to some extent in later years of life rather than progress to malignancy (see Table 2). Notably, we did not observe any increase in malignancies in *cav-1*$^{-/-}$ mice compared to *cav-1*$^{+/+}$ mice in our study. Additional studies will be required to determine the role of cav-1 in the development and progression of malignancy. This study demonstrates that loss of cav-1 function leads to abnormal growth and differentiation of specific cell types including stromal cells. We suggest that in some cases, loss of cav-1 function in stromal cells can lead to disruption of normal stromal–epithelial interactions and dysfunctional organ systems.

Acknowledgments

This work was supported by NIH grants U01-CA84295, P50-CA58204, RO1- CA68814 and a Department of Defence grant W81WH-06-1-116. A portion of these studies were conducted in facilities provided by the Michael E DeBakey VA Medical Center.

References

Aldred, M.A., et al., 2003. Caveolin-1 and caveolin-2, together with three bone morphogenetic protein-related genes, may encode novel tumor suppressors down-regulated in sporadic follicular thyroid carcinogenesis. Cancer Res. 63, 2864–2871.

Bagnoli, M., et al., 2000. Downmodulation of caveolin-1 expression in human ovarian carcinoma is directly related to alpha-folate receptor overexpression. Oncogene 19, 4754–4763.

Bender, F.C., et al., 2000. Caveolin-1 levels are down-regulated in human colon tumors, and ectopic expression of caveolin-1 in colon carcinoma cell lines reduces cell tumorigenicity. Cancer Res. 60, 5870–5878.

Bocker, W., et al., 2002. Common adult stem cells in the human breast give rise to glandular and myoepithelial cell lineages: a new cell biological concept. Lab. Invest. 82, 737–746.

Boecker, W., Buerger, H., 2003. Evidence of progenitor cells of glandular and myoepithelial cell lineages in the human adult female breast epithelium: a new progenitor (adult stem) cell concept. Cell Prolif. 36 (Suppl 1), 73–84.

Campbell, L., et al., 2003. Caveolin-1 overexpression predicts poor disease-free survival of patients with clinically confined renal cell carcinoma. Br. J. Cancer 89, 1909–1913.

Cao, G., et al., 2003. Disruption of the caveolin-1 gene impairs renal calcium reabsorption and leads to hypercalciuria and urolithiasis. Am. J. Pathol. 162, 1241–1248.

Capozza, F., et al., 2003. Absence of caveolin-1 sensitizes mouse skin to carcinogen-induced epidermal hyperplasia and tumor formation. Am. J. Pathol. 162, 2029–2039.

Carrion, R., et al., 2003. Caveolin expression in adult renal tumors. Urol. Oncol. 21, 191–196.

Carver, L.A., Schnitzer, J.E., 2003. Caveolae: mining little caves for new cancer targets. Nat. Rev., Cancer 3, 571–581.

Davidson, B., et al., 2001. Caveolin-1 expression in advanced-stage ovarian carcinoma—a clinicopathologic study. Gynecol. Oncol. 81, 166–171.

Davidson, B., et al., 2002. Caveolin-1 expression in ovarian carcinoma is MDR1 independent. Am. J. Clin. Pathol. 117, 225–234.

Drab, M., et al., 2001. Loss of caveolae, vascular dysfunction, and pulmonary defects in caveolin-1 gene-disrupted mice. Science 293, 2449–2452.

Engelman, J.A., et al., 1997. Recombinant expression of caveolin-1 in oncogenically transformed cells abrogates anchorage-independent growth. J. Biol. Chem. 272, 16374–16381.

Fielding, C.J., Fielding, P.E., 2001. Caveolae and intracellular trafficking of cholesterol. Adv. Drug Deliv. Rev. 49, 251–264.

Fong, A., et al., 2003. Expression of caveolin-1 and caveolin-2 in urothelial carcinoma of the urinary bladder correlates with tumor grade and squamous differentiation. Am. J. Clin. Pathol. 120, 93–100.

Galbiati, F., et al., 1998. Targeted downregulation of caveolin-1 is sufficient to drive cell transformation and hyperactivate the p42/44 MAP kinase cascade. EMBO J. 17, 6633–6648.

Galbiati, F., et al., 2001. Caveolin-1 expression negatively regulates cell cycle progression by inducing G(0)/G(1) arrest via a p53/p21(WAF1/Cip1)-dependent mechanism. Mol. Biol. Cell 12, 2229–2244.

Gavrieli, Y., et al., 1992. Identification of programmed cell death in situ via specific labeling of nuclear DNA fragmentation. J. Cell Biol. 119, 493–4501.

Hakem, R., Mak, T.W., 2001. Animal models of tumor-suppressor genes. Annu. Rev. Genet. 35, 209–241.

Ho, C.C., et al., 2002. Up-regulated caveolin-1 accentuates the metastasis capability of lung adenocarcinoma by inducing filopodia formation. Am. J. Pathol. 161, 1647–1656.

Horiguchi, A., et al., 2004. Impact of caveolin-1 expression on clinicopathological parameters in renal cell carcinoma. J. Urol. 172, 718–722.

Hu, Y.C., et al., 2001. Profiling of differentially expressed cancer-related genes in esophageal squamous cell carcinoma (ESCC) using human cancer cDNA arrays: overexpression of oncogene MET correlates with tumor differentiation in ESCC. Clin. Cancer Res. 7, 3519–3525.

Hung, K.F., et al., 2003. The biphasic differential expression of the cellular membrane protein, caveolin-1, in oral carcinogenesis. J. Oral Pathol. Med. 32, 461–467.

Ito, Y., et al., 2002. Caveolin-1 overexpression is an early event in the progression of papillary carcinoma of the thyroid. Br. J. Cancer 86, 912–916.

Joo, H.J., et al., 2004. Increased expression of caveolin-1 and microvessel density correlates with metastasis and poor prognosis in clear cell renal cell carcinoma. BJU Int. 93, 291–296.

Kato, K., et al., 2002. Overexpression of caveolin-1 in esophageal squamous cell carcinoma correlates with lymph node metastasis and pathologic stage. Cancer 94, 929–933.

Kato, T., et al., 2004. Difference of caveolin-1 expression pattern in human lung neoplastic tissue. Atypical adenomatous hyperplasia, adenocarcinoma and squamous cell carcinoma. Cancer Lett. 214, 121–128.

Koleske, A.J., et al., 1995. Reduction of caveolin and caveolae in oncogenically transformed cells. Proc. Natl. Acad. Sci. U. S. A. 92, 1381–1385.

Kurzchalia, T.V., et al., 1992. VIP21, a 21-kD membrane protein is an integral component of trans-Golgi-network-derived transport vesicles. J. Cell Biol. 118, 1003–1014.

Lee, S.W., et al., 1998. Tumor cell growth inhibition by caveolin re-expression in human breast cancer cells. Oncogene 16, 1391–1397.

Lee, H., et al., 2002. Caveolin-1 mutations (P132L and null) and the pathogenesis of breast cancer: caveolin-1 (P132L) behaves in a dominant-negative manner and caveolin-1 (−/−) null mice show mammary epithelial cell hyperplasia. Am. J. Pathol. 161, 1357–1369.

Massimino, M.L., et al., 2002. Involvement of caveolae and caveolae-like domains in signalling, cell survival and angiogenesis. Cell. Signal. 14, 93–98.

Mouraviev, V., et al., 2002. The role of caveolin-1 in androgen insensitive prostate cancer. J. Urol. 168, 1589–1596.

Park, D.S., et al., 2003. Caveolin-1 null (−/−) mice show dramatic reductions in life span. Biochemistry 42, 15124–15131.

Parton, R.G., 1996. Caveolae and caveolins. Curr. Opin. Cell Biol. 8, 542–548.

Parton, R.G., 2001. Cell biology. Life without caveolae. Science 293, 2404–2405.

Parton, R.G., 2003. Caveolae—from ultrastructure to molecular mechanisms. Nat. Rev., Mol. Cell Biol. 4, 162–167.

Patlolla, J.M., et al., 2004. Overexpression of caveolin-1 in experimental colon adenocarcinomas and human colon cancer cell lines. Oncol. Rep. 11, 957–963.

Racine, C., et al., 1999. Reduction of caveolin 1 gene expression in lung carcinoma cell lines. Biochem. Biophys. Res. Commun. 255, 580–586.

Rajjayabun, P.H., et al., 2001. Caveolin-1 expression is associated with high-grade bladder cancer. Urology 58, 811–814.

Razani, B., et al., 2001a. Caveolin-1 null mice are viable but show evidence of hyperproliferative and vascular abnormalities. J. Biol. Chem. 276, 38121–38138.

Razani, B., et al., 2001b. Caveolin-1, a putative tumour suppressor gene. Biochem. Soc. Trans. 29, 494–499.

Razani, B., et al., 2002. Caveolin-2-deficient mice show evidence of severe pulmonary dysfunction without disruption of caveolae. Mol. Cell Biol. 22, 2329–2344.

Rothberg, K.G., et al., 1992. Caveolin, a protein component of caveolae membrane coats. Cell 68, 673–682.

Sagara, Y., et al., 2004. Clinical significance of caveolin-1, caveolin-2 and HER2/neu mRNA expression in human breast cancer. Br. J. Cancer 91, 959–965.

Sanchez-Carbayo, M., et al., 2002. Molecular profiling of bladder cancer using cDNA microarrays: defining histogenesis and biological phenotypes. Cancer Res. 62, 6973–6980.

Satoh, T., et al., 2003. Caveolin-1 expression is a predictor of recurrence-free survival in pT2N0 prostate carcinoma diagnosed in Japanese patients. Cancer 97, 1225–1233.

Shaul, P.W., Anderson, R.G., 1998. Role of plasmalemmal caveolae in signal transduction. Am. J. Physiol. 275, L843–L851.

Smart, E.J., et al., 1999. Caveolins, liquid-ordered domains, and signal transduction. Mol. Cell Biol. 19, 7289–7304.

Sunaga, N., et al., 2004. Different roles for caveolin-1 in the development of non-small cell lung cancer versus small cell lung cancer. Cancer Res. 64, 4277–4285.

Suzuoki, M., et al., 2002. Impact of caveolin-1 expression on prognosis of pancreatic ductal adenocarcinoma. Br. J. Cancer 87, 1140–1144.

Terris, B., et al., 2002. Characterization of gene expression profiles in intraductal papillary—mucinous tumors of the pancreas. Am. J. Pathol. 160, 1745–1754.

Thompson, T., et al., 1999. Caveolin-1: a complex and provocative therapeutic target in prostate cancer and potentially other malignancies. Emerg. Ther. Targets 3, 337–346.

Thompson, T.C., et al., 2001. Molecular pathways that underlie prostate cancer progression: the role of caveolin-1. In: Chung, L. (Ed.), Prostate Cancer in the 21st Century. Humana Press.

Wiechen, K., et al., 2001. Down-regulation of caveolin-1, a candidate tumor suppressor gene, in sarcomas. Am. J. Pathol. 158, 833–839.

Wikman, H., et al., 2004. Caveolins as tumour markers in lung cancer detected by combined use of cDNA and tissue microarrays. J. Pathol. 203, 584–593.

Williams, T.M., et al., 2003. Loss of caveolin-1 gene expression accelerates the development of dysplastic mammary lesions in tumor-prone transgenic mice. Mol. Biol. Cell 14, 1027–1042.

Williams, T.M., et al., 2004. Caveolin-1 gene disruption promotes mammary tumorigenesis and dramatically enhances lung metastasis in vivo. Role of Cav-1 in cell invasiveness and matrix metalloproteinase (MMP-2/9) secretion. J. Biol. Chem. 279, 51630–51646.

Williams, T.M., et al., 2005. Caveolin-1 promotes tumor progression in an autochthonous mouse model of prostate cancer: genetic ablation of Cav-1 delays advanced prostate tumor development in TRAMP mice. J. Biol. Chem. 10, 1074.

Woodman, S.E., et al., 2004. Urogenital alterations in aged male caveolin-1 knockout mice. J. Urol. 171, 950–957.

Yang, G., et al., 1996. Perineural invasion of prostate carcinoma cells is associated with reduced apoptotic index. Cancer 78, 1267–1271.

Yang, G., et al., 1998. Elevated expression of caveolin is associated with prostate and breast cancer. Clin. Cancer Res. 4, 1873–1880.

Yang, G., et al., 1999. Caveolin-1 expression in clinically confined human prostate cancer: a novel prognostic marker. Cancer Res. 59, 5719–5723.

Yang, G., et al., 2000. Elevated caveolin-1 levels in African-American versus White-American prostate cancer. Clin. Cancer Res. 6, 3430–3433.

Yoo, S.H., et al., 2003. Expression of caveolin-1 is associated with poor prognosis of patients with squamous cell carcinoma of the lung. Lung Cancer 42, 195–202.

Zhao, Y.Y., et al., 2002. Defects in caveolin-1 cause dilated cardiomyopathy and pulmonary hypertension in knockout mice. Proc. Natl. Acad. Sci. U. S. A. 99, 11375–11380.

RESEARCH PAPER

Cancer Biology & Therapy 8:23, 78-88; December 1, 2009; © 2009 Landes Bioscience

Caveolin-1 regulates VEGF-stimulated angiogenic activities in prostate cancer and endothelial cells

Salahaldin A. Tahir, Sanghee Park and Timothy C. Thompson*

Department of Genitourinary Medical Oncology Research; The University of Texas M.D. Anderson Cancer Center; Houston, TX USA

Key words: caveolin-1, VEGFR2, PLCγ1, caveolin-1 scaffolding domain, angiogenesis

Abbreviations: Cav-1, caveolin-1; VEGF, vascular endothelial growth factor; VEGFR2, vascular endothelial growth factor receptor 2; LP-LNCaP, low passage-LNCaP; HUVEC, human umbilical vein endothelial cell; CSD, caveolin-1 scaffolding domain; FITC, fluorescein isothiocyanate conjugated; TRITC, tetramethyl rhodamine isothiocyanate conjugated; EGM-2, endothelial growth medium-2; EBM-2, endothelial basal medium-2

Caveolin-1 (cav-1) is a multifunctional protein and major component of caveolae membranes serving important functions related to signal transduction, endocytosis, transcytosis, and molecular transport. We previously showed that cav-1 is overexpressed and secreted by metastatic prostate cancer cells. We now report that cav-1 gene transduction (Adcav-1) or recombinant cav-1 (rcav-1) protein treatment of cav-1-negative prostate cancer cell line LP-LNCaP or *cav-1*$^{-/-}$ endothelial cells potentiated VEGF-stimulated angiogenic signaling.

Downregulation of cav-1 in prostate cancer cell line PC-3 or human umbilical vein endothelial cells (HUVECs) through cav-1 siRNA significantly reduced basal and VEGF-stimulated phosphorylation of VEGFR2 (Y951), PLCγ1 (Y783) and/or Akt (S473 & T308) relative to those in control siRNA treated cells. Additionally rcav-1 stimulation of cav-1 siRNA treated HUVECs restored this signaling pathway. Confocal microscopy and immunoprecipitation analysis revealed association and colocalization of VEGFR2 and PLCγ1 with cav-1 following VEGF stimulation in HUVECs. Interestingly, treatment of HUVECs with cav-1 scaffolding domain (CSD) caused significant reduction in the VEGF-stimulated phosphorylation of VEGFR2, PLCγ1 and Akt suggesting that CSD inhibits cav-1-mediated angiogenic signaling. VEGF stimulation of HUVECs significantly increased tubule length and cell migration, but this stimulatory effect was significantly reduced by cav-1 siRNA and/or CSD treatment.

The present study demonstrates that cav-1 regulates VEGF-stimulated VEGFR2 autophosphorylation and activation of downstream angiogenic signaling, possibly through compartmentalization of specific signaling molecules. Our results provide mechanistic insight into the role of cav-1 in prostate cancer and suggest the use of CSD as a therapeutic tool to suppress angiogenic signaling in prostate cancer.

Introduction

Caveolin-1 (cav-1) is a multifunctional protein and major component of caveolae membranes, serving important regulatory functions for signal transduction, endocytosis, transcytosis and molecular transport.[1,2] Specific proteins such as receptor tyrosine kinases, Ser/Thr kinases, phospholipases, G-protein-coupled receptors, and Src family kinases, are localized in lipid rafts and caveolar membranes, where they interact with cav-1 through the cav-1 scaffolding domain (CSD). CSD domain-mediated activities result in the generation of platforms for compartmentalization of discrete signaling events.[3] We showed previously that cav-1 is overexpressed in metastatic prostate cancer, and demonstrated that virulent prostate cancer cells secrete biologically active cav-1 that is taken up by cav-1 negative tumor cells and/or endothelial cells (ECs), leading to stimulation of specific angiogenic activities through PI3K-Akt-eNOS signaling module.[4-8] Thus, secreted cav-1 has both proangiogenic and anti-apoptotic roles in the metastatic progression of prostate cancer.

Angiogenesis is a vital function for the growth of normal tissues during embryogenesis, and for the malignant growth of solid tumors. This EC-focused process involves several distinct and sequential steps, including degradation of basement membrane by proteolytic enzymes, migration, proliferation, formation of vascular loops, maturation of neovessels and neosynthesis of basement membrane constituents. However, abnormal angiogenesis often occurs in pathological conditions such as a malignant tumor, rheumatoid arthritis, diabetic retinopathy, and other chronic inflammatory diseases.[9] A key angiogenic factor, vascular endothelial growth factor (VEGF), promotes the survival, permeability, migration and proliferation in ECs during neovascularization. At the surface of ECs, the VEGF receptor 2 (VEGFR2; also known as KDR or Flk1) receptor

*Correspondence to: Timothy C. Thompson; Email: timthomp@mdanderson.org
Submitted: 08/05/09; Revised: 09/15/09; Accepted: 09/19/09
Previously published online: www.landesbioscience.com/journals/cbt/article/10138

tyrosine kinase, has been identified as the major mediator of VEGF-dependent signaling and physiological and pathological angiogenic activities.[10] Binding of the dimeric VEGF to the extracellular domains of two monomeric VEGFR2 receptors induces dimerization and activation of the tyrosine kinase and phosphorylation of multiple tyrosine residues (e.g., Y951, Y1175, Y1214, Y1054 and Y1059) which, in turn, stimulate binding, phosphorylation and activation of multiple downstream molecules involved in different signaling pathways such as PLCγ1, PKC and PI3K-Akt.[11-14] The Y951 phosphorylation site binds T-cell-specific adapter and subsequently forms a complex with Src that leads to the regulation of cell migration.[15] VEGFR2 (Y1175) autophosphorylation site in human is another site that serves as a docking site for PLCγ1, which indirectly mediates activation of the mitogen-activated protein (MAP) kinase pathway and thus regulates cell proliferation.[13] VEGFR2 (Y1175) is also a binding site for Src homology 2 and thereby activates PI3K and promotes cell migration.[14] Another VEGFR2 phosphorylation site is Y1214, which is involved in the activation of Cdc42 and p38 MAP kinase pathway that regulates cell motility.[16] VEGFR2 is localized in endothelial caveolae through association with cav-1 which seems to play an important role in its activation and downstream signal transduction.

Dissociation of VEGFR2 from caveolae has been shown to be essential for its autophosphorylation and activation of downstream signaling events.[17] Furthermore, reports have shown that upon VEGF stimulation, phosphorylation of both VEGFR2 and cav-1 (Y14) occur simultaneously, triggering their release from caveolae/lipid rafts and colocalization at focal complexes, at the edge of lamellipodia. Thus, phospho-cav-1 appears to function as a scaffolding protein for VEGF-mediated signaling by serving as a docking site for phospho-tyrosine-binding molecules at focal adhesion complexes.[18,19] However, despite the importance of VEGFR2 in the orchestration of angiogenic response, the molecular mechanisms critical for the regulation of its signaling and biological activities are not well defined, and little is known about the role of cav-1 in VEGF-mediated angiogenesis.

We demonstrate here that induction of cav-1 expression or recombinant cav-1 (rcav-1) treatment of cav-1 negative LP-LNCaP prostate cancer cells or *cav-1*$^{-/-}$ ECs led to induction of VEGF/VEGFR2 mediated angiogenic signaling. In contrast, cav-1 knockdown in PC-3 prostate cancer cells or human umbilical vein endothelial cells (HUVECs) impaired VEGF/VEGFR2-induced signaling. In HUVECs cav-1 knockdown also reduced differentiation/tubule formation and cellular migration but these activities were restored in response to rcav-1 treatment. We further show increased physical association and colocalization of cav-1 with VEGFR2 or PLCγ1 in HUVECs following VEGF stimulation. Interestingly, CSD significantly reduced VEGF-stimulated phosphorylation of VEGFR2 and downstream signaling molecules and suppressed tubule formation and cell migration in HUVEC. Our results demonstrate that cav-1 plays a pivotal role in VEGF/VEGFR2-stimulated angiogenesis signaling and associated angiogenic biological activities, and suggest a potential therapeutic use of CSD to suppress angiogenic signaling in prostate cancer.

Results

Cav-1 regulates VEGF-stimulated angiogenesis signaling in prostate cancer cells and Cav-1$^{-/-}$ ECs. We previously demonstrated that cav-1 stimulates angiogenic responses in prostate cancer cells and ECs through a mechanism that involves the PI3K-Akt-eNOS pathway.[7] To determine the role played by cav-1 in VEGF-stimulated VEGFR2 autophosphorylation and its downstream effects, we infected cav-1 negative LP-LNCaP cells with Adcav-1 or control AdRSV, and then treated the cells with VEGF. Cav-1 overexpression significantly increased the phosphorylation of VEGFR2 (Y951) (**Fig. 1A**). Increased phosphorylation of PLCγ1 (Y783), Akt (S473) and Akt (T308) was also demonstrated with no change in total protein in response to cav-1 overexpression and/or VEGF treatment. The observed significant increase in the phosphorylation of VEGFR2 and PLCγ1 in response to cav-1 could be due to the effect of cav-1-mediated increased expression and secretion of growth factors including VEGF in these cells.[20] On the other hand treatment of the cells with VEGF had little or no effect on the phosphorylation in the control AdRSV infected cells at all time points (0, 5 and 15 min). These results indicate that in the absence of cav-1, VEGF stimulation of VEGFR2 autophosphorylation and its downstream effects is minimal, and that cav-1 is required for optimal VEGF-stimulated signaling (**Fig. 1A**).

To further investigate the role of cav-1 in VEGF-stimulated angiogenic activities in ECs, we introduced cav-1 into *cav-1*$^{-/-}$ ECs either by Adcav-1 infection to the MOI 200, or by rcav-1 treatment, followed by analysis of the phosphorylation status of VEGF/VEGFR2 signaling pathway associated proteins. Increased phosphorylation of VEGFR2 (Y951), PLCγ1 (Y783), Akt (S473) and Akt (T308) was observed after overexpression of cav-1 by Adcav-1, and a further increase in the phosphorylation status of these proteins as well as PLCγ1 (Y783) was observed after VEGF treatment (**Fig. 1B**). VEGF treatment of cells infected with control AdRSV showed a slight increase in the phosphorylation of VEGFR2 (Y951), Akt (S473) and Akt (T308) only at the 15-min time point with no increase in PLCγ1 (Y783), which indicates a low or limited response to VEGF stimulation in the absence of cav-1. These observations suggest that cav-1 plays an important role in both basal and VEGF-stimulated VEGFR2-mediated signaling.

We also tested the effect of rcav-1 on basal and VEGF-stimulated VEGFR2-mediated angiogenic signaling in *cav-1*$^{-/-}$ ECs. Rcav-1-treated ECs showed a significant increase in the basal phosphorylation of VEGFR2 (Y951), PLCγ1 (Y783), Akt (S473) and Akt (T308) and VEGF stimulation led to significantly increased phosphorylation of VEGFR2 (Y951), PLCγ1 (Y783), Akt (S473) and Akt (T308) in rcav-1-treated cells, compared to cells that were not treated with rcav-1 (**Fig. 1C**).

Cav-1 knockdown in PC-3 and HUVECs impairs VEGF-stimulated angiogenesis signaling. We investigated cav-1 regulation of basal and VEGF-stimulated VEGFR2-mediated angiogenic signaling in PC-3 cells and human ECs. We transfected PC-3 cells with cav-1-specific siRNA or siRNA of irrelevant target specificity as a non-specific control (NC), to downregulate

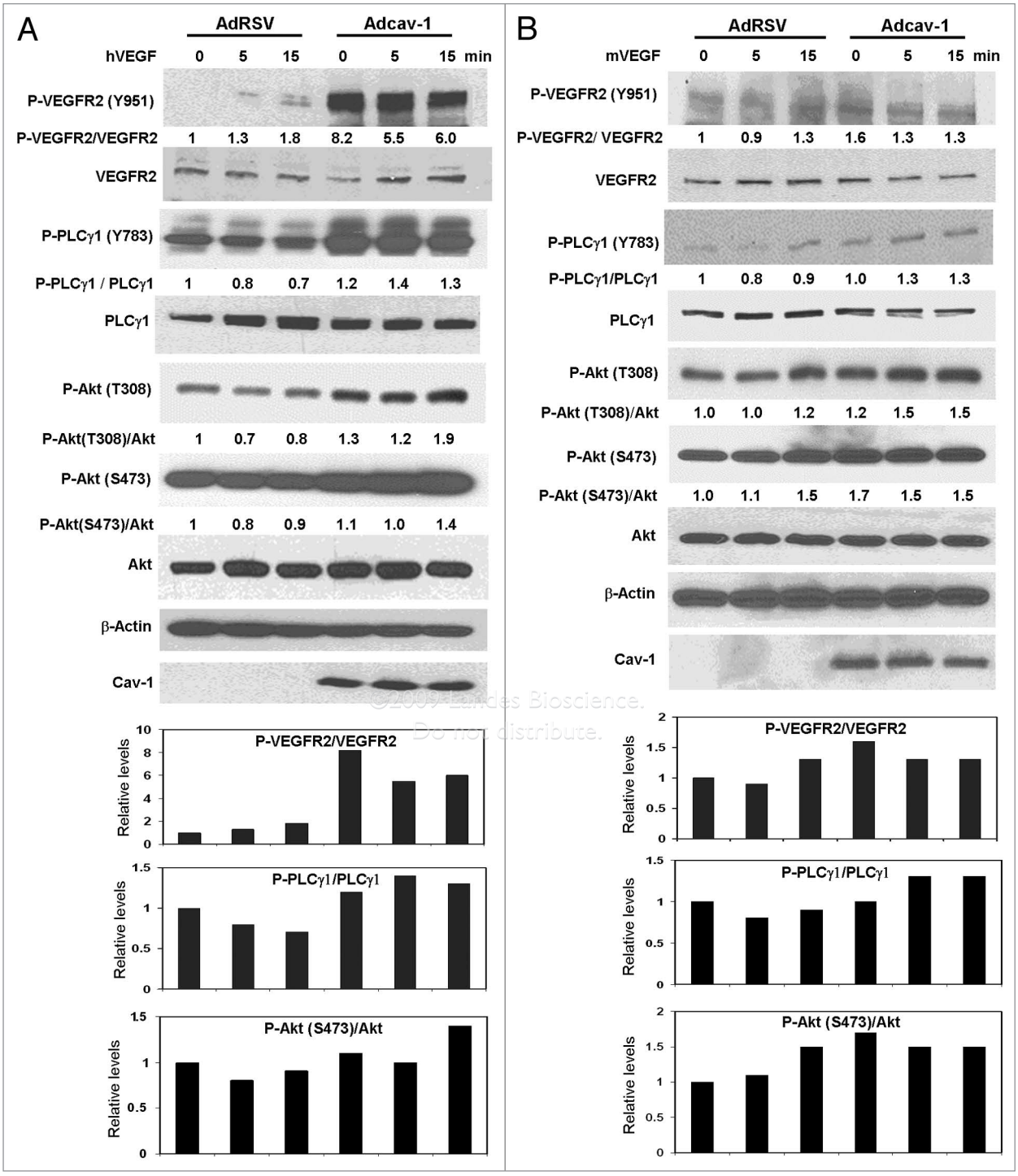

Figure 1A and B. Cav-1 stimulates the VEGF/VEGFR2 induced angiogenesis signaling pathway. (A) LP-LNCaP cells were infected with Adcav-1 or control AdRSV at an MOI of 10. Cells were incubated with SFM for 8 h, treated with hVEGF (25 ng/ml) for 0–15 min, lysed and analyzed by western blotting (B), *cav-1*$^{-/-}$ ECs were infected with Adcav-1 or control AdRSV at an MOI of 200. Cells were incubated in EBM-2 medium for 8 h, treated with mVEGF (50 ng/ml) for 0–15 min and lysed.

cav-1 expression. In unstimulated cells the phosphorylation status of VEGFR2 (Y951), PLCγ1 (Y783) and Akt (S473 & T308) was not changed significantly after downregulation of cav-1. However, downregulation of cav-1 reduced the response to VEGF stimulation as shown in reduced phosphorylation of VEGFR2 (Y951), PLCγ1 (Y783) and Akt (S473 & T308) at two time points (5 and 15 min) as compared with that of the NC. Interestingly, cav-1 phosphorylation (Y14) increased significantly in response to VEGF at both 5 and 15 min and in both NC and cav-1 siRNA (**Fig. 2A**).

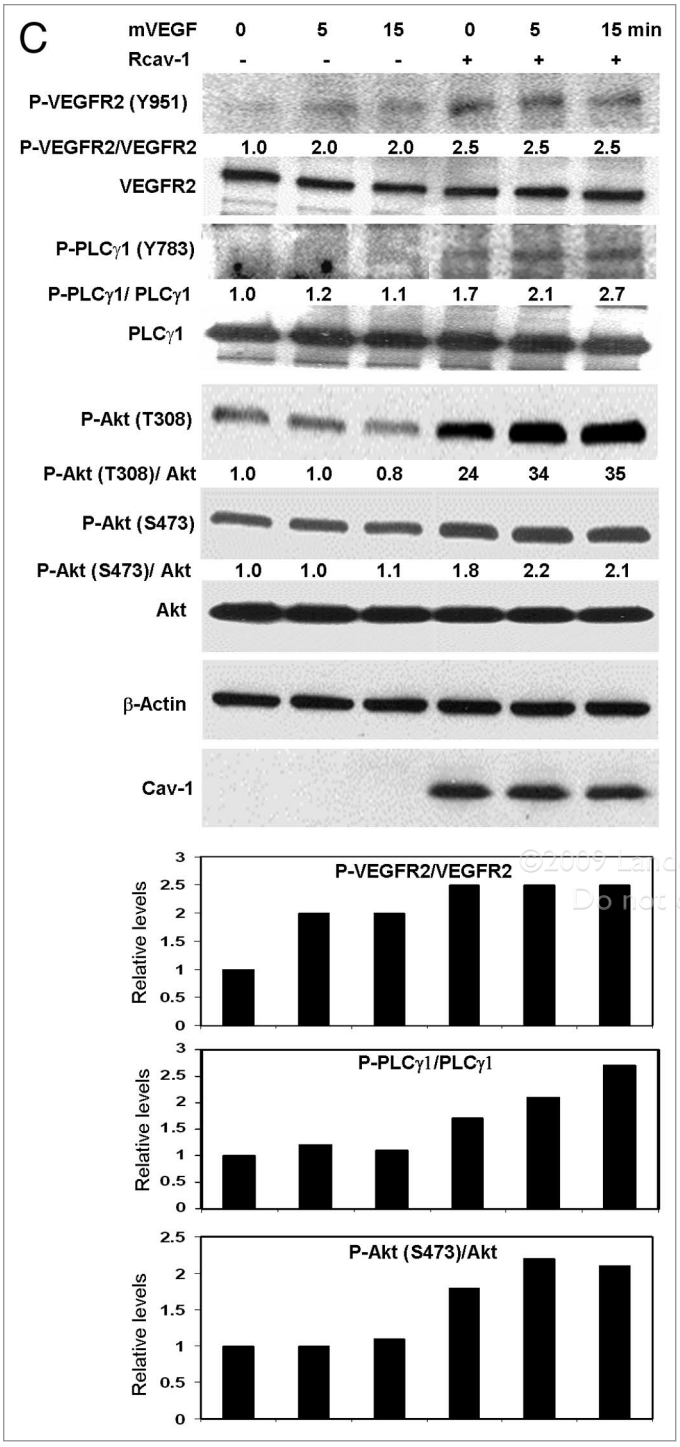

Figure 1C. Cav-1 stimulates the VEGF/VEGFR2 induced angiogenesis signaling pathway. (C) *cav-1*$^{-/-}$ ECs were plated overnight and incubated with 3.0 μg/ml of rcav-1 in EBM-2 for 8 h. The cells were then treated with mVEGF (50 ng/ml) for 0–15 min and lysed. In (A–C) introducing cav-1 to the cells significantly increased the phosphorylation of VEGFR2, PLCγ1 and Akt and it further stimulated their response to VEGF treatment. Blots shown (A-C) are representative of three independent experiments. Bar graphs represent densitometric data of ratio units of selected phosphorylated protein bands per total protein bands relative to that in the untreated and unstimulated controls.

We also investigated the effect of cav-1 on VEGF/VEGFR2 signaling in HUVECs through downregulation of cav-1 using cav-1 siRNA transfection, and through rcav-1 treatment followed by stimulation with VEGF in HUVECs that had been previously treated with cav-1 siRNA. Using a double transfection protocol, the cav-1 levels were reduced significantly after specific cav-1 siRNA treatment (**Fig. 2B**). Downregulation of cav-1 in HUVECs significantly reduced basal and VEGF-stimulated phosphorylation of VEGFR2 (Y951), PLCγ1 (Y783) and Akt (S473 & T308) compared to those treated with the NC. Interestingly, rcav-1 treatment of these cells restored the basal phosphorylation status of these signaling molecules and partially restored the response to VEGF stimulation, i.e., P-VEGFR2, PLCγ1 and P-Akt (**Fig. 2B**). These results demonstrate that cav-1 is an important regulator of basal and VEGF-stimulated angiogenesis signaling in prostate cancer cells and HUVECs. Importantly, rcav-1 restored VEGF-stimulated angiogenic signaling in cav-1 siRNA treated HUVECs, further demonstrating a potential role for secreted cav-1 in vivo.[7]

Cav-1 regulation of VEGF-stimulated angiogenesis signaling is associated with Cav-1 binding to VEGFR2 and PLCγ1. We investigated whether VEGF stimulation of angiogenesis signaling involves cav-1-VEGFR2 and/or cav-1-PLCγ1 interaction and direct binding that may sequester these molecules to specific cellular compartments. Amino acid sequence analysis revealed one potential cav-1-binding motif at the VEGFR2 C terminus, ^{1089}WSFGVLLWEIF^{1099}, and the PLCγ1 molecule revealed two potential cav-1-binding consensus sequence, one at the N terminus, ^{293}FFLDEFVTF^{301}, and the other at the C terminus, ^{1154}FAFLRFVVY^{1162}. We performed reversed coimmunoprecipitation using HUVEC lysates under high stringency in the presence of NP-40. VEGFR2 immunoprecipitation complexes contained cav-1, and cav-1 levels were increased (70%) following VEGF treatment (**Fig. 3A**). Similar results were obtained in the reversed coimmunoprecipitation complexes, in which cav-1 immunoprecipitation complexes contained VEGFR2, and VEGFR2 levels were increased (50%) following VEGF treatment (**Fig. 3A**). Interestingly, cav-1, and VEGFR2 colocalization was demonstrated using confocal microscopy. In unstimulated cells cav-1 and VEGFR2 were primarily colocalized in the plasma membrane, and after treatment with VEGF for 5 min both VEGFR2 and cav-1 were internalized to the cytoplasm as seen by intracellular punctuate staining (**Fig. 3B**). Cav-1 and PLCγ1 immunoprecipitation experiments also revealed PLCγ1 in the cav-1 coimmunoprecipitation complexes, and PLCγ1 levels were increased (60%) following VEGF treatment. Conversely, PLCγ1 immunoprecipitation complexes contained cav-1, and cav-1 levels were increased (60%) following VEGF treatment (**Fig. 3C**). Confocal microscopy also showed a similar pattern of PLCγ1 and cav-1 colocalization to those of VEGFR2 and cav-1 in unstimulated and VEGF-stimulated cells (**Fig. 3D**).

These results demonstrate that VEGFR2 and PLCγ1 exist partially bound to cav-1 in HUVECs and that VEGF treatment initially increases the degree of association, colocalization and internalization, suggesting that cav-1 participates mechanistically in VEGF-stimulated angiogenic responses in this system.

CSD inhibits VEGF-stimulated angiogenesis signaling. We previously showed that rcav-1 lacking CSD failed to stimulate angiogenic activities in *cav1*$^{-/-}$ ECs, including tubule formation, migration and stimulation of eNOS phosphorylation (S1177).[7] These results showed that endocytosis of exogenous rcav-1 and stimulation of angiogenic activities is mediated in part by CSD, which is critical for cellular internalization of the protein. CSD was also shown by others to inhibit VEGF-induced vascular leakage through the inhibition of eNOS.[21] We first tested whether the CSD peptide can penetrate and become internalized in HUVECs without requiring a peptide carrier. Biotin-conjugated peptide and scrambled (s) control peptide were incubated with HUVECs in serum free culture medium. Both the CSD and the control sCSD became internalized in HUVECs and distributed throughout the cytoplasm (**Fig. 4A**), demonstrating that CSD readily penetrates and is internalized without requiring the antennapedia (AP) internalization sequence.[21]

To test the effect of CSD on VEGF-stimulated angiogenesis signaling, we treated HUVECs with CSD peptide in serum free medium followed by treatment with VEGF. CSD treatment of HUVECs significantly reduced VEGF-stimulated phosphorylation of VEGFR2 (Y951), PLCγ1 (Y783) and Akt (S473 &T308) as compared to those treated with control sCSD (**Fig. 4B**). Modest reductions in basal phosphorylation levels of Akt were observed in CSD-treated compared to sCSD-treated HUVECs (**Fig. 4B**). These data demonstrate that CSD inhibits VEGF-stimulated angiogenesis signaling through inhibition of endogenous cav-1 function.

VEGF-stimulated tubule formation and cell migration is mediated by Cav-1 and inhibited by CSD. EC migration and differentiation are important events for angiogenesis which involve new capillary formation from preexisting vessels. To further demonstrate the role of cav-1 in VEGF-stimulated angiogenesis in vitro, we used two biological assays, tubule formation and wound healing migration, in which HUVECs were transfected with cav-1 siRNA or NC and then treated with VEGF or left untreated. VEGF treatment of HUVECs increased the tubule length and cell migration in NC transfected cells compared to their untreated counterparts, but this stimulatory effect of VEGF was significantly impaired when cav-1 was downregulated (**Fig. 5A–D**). Downregulation of cav-1 by transfection with specific siRNA in unstimulated and VEGF-stimulated HUVECs caused a significant reduction in tubule length ($p < 0.05$, and $p < 0.01$, respectively; **Fig. 5B**) and the number of migrated cells compared with that of NC ($p < 0.01$, and $p < 0.01$, respectively; **Fig. 5D**). An interesting finding was that CSD treatment of unstimulated and VEGF-stimulated HUVECs reduced the tubule length in NC-transfected cells ($p < 0.05$, and $p < 0.01$, respectively; **Fig. 5B**), but not in cav-1 siRNA transfected cells (**Fig. 5B**) compared to treatment with sCSD. Additionally, CSD treatment of unstimulated and VEGF-stimulated HUVECs significantly reduced cell migration in NC-transfected cells ($p < 0.05$, and $p < 0.01$, respectively; **Fig. 5D**), and in cav-1 siRNA transfected cells ($p < 0.05$, and $p < 0.05$, respectively; **Fig. 5D**) compared to treatment with sCSD. These results show that downregulation of cav-1 through cav-1 siRNA or CSD treatment alone led to significant reductions of angiogenic activities in HUVECs, and that combining the two treatments yields additive or synergistic effects.

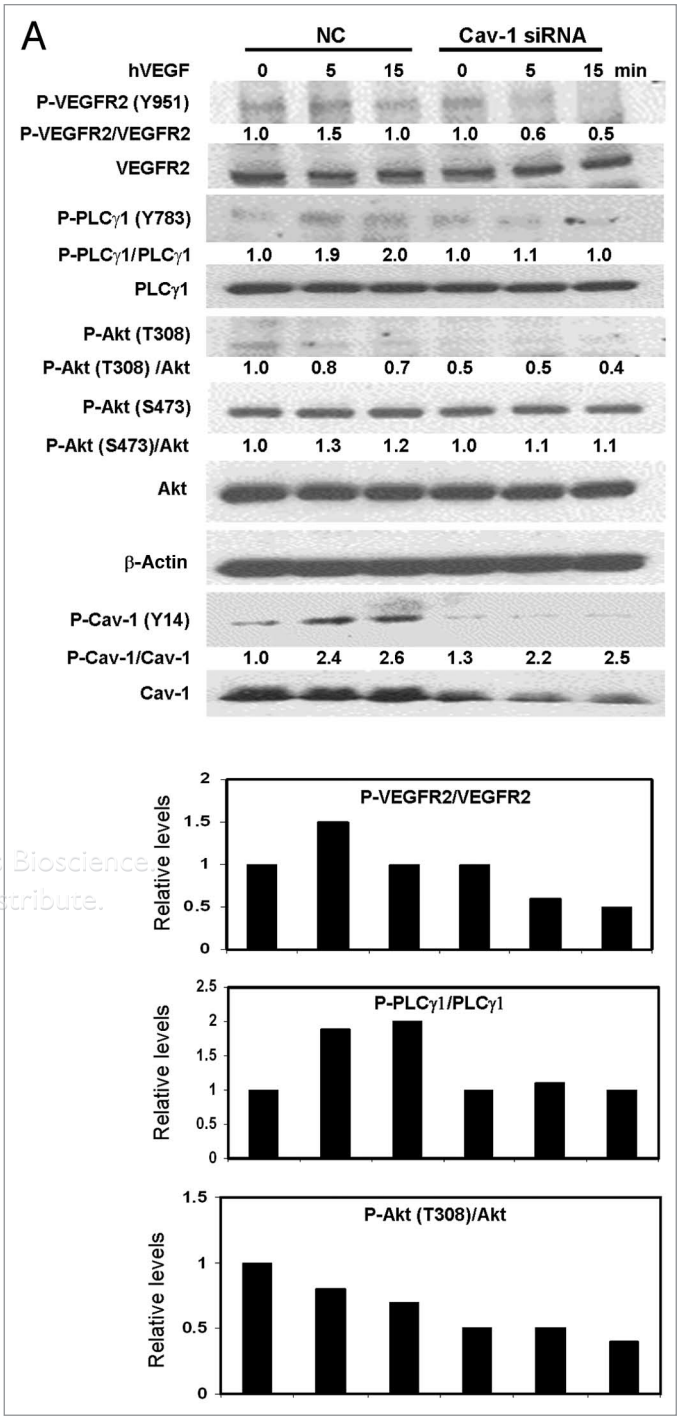

Figure 2A. Downregulation of cav-1 in PC-3 cells and HUVECs by cav-1 siRNA impaired the VEGF/VEGFR2 angiogenesis signaling pathway. (A) PC-3 cells were transfected with specific cav-1 siRNA or a control siRNA, followed by incubation with SFM for 8 h prior to hVEGF (25 ng/ml) treatment for 0–15 min.

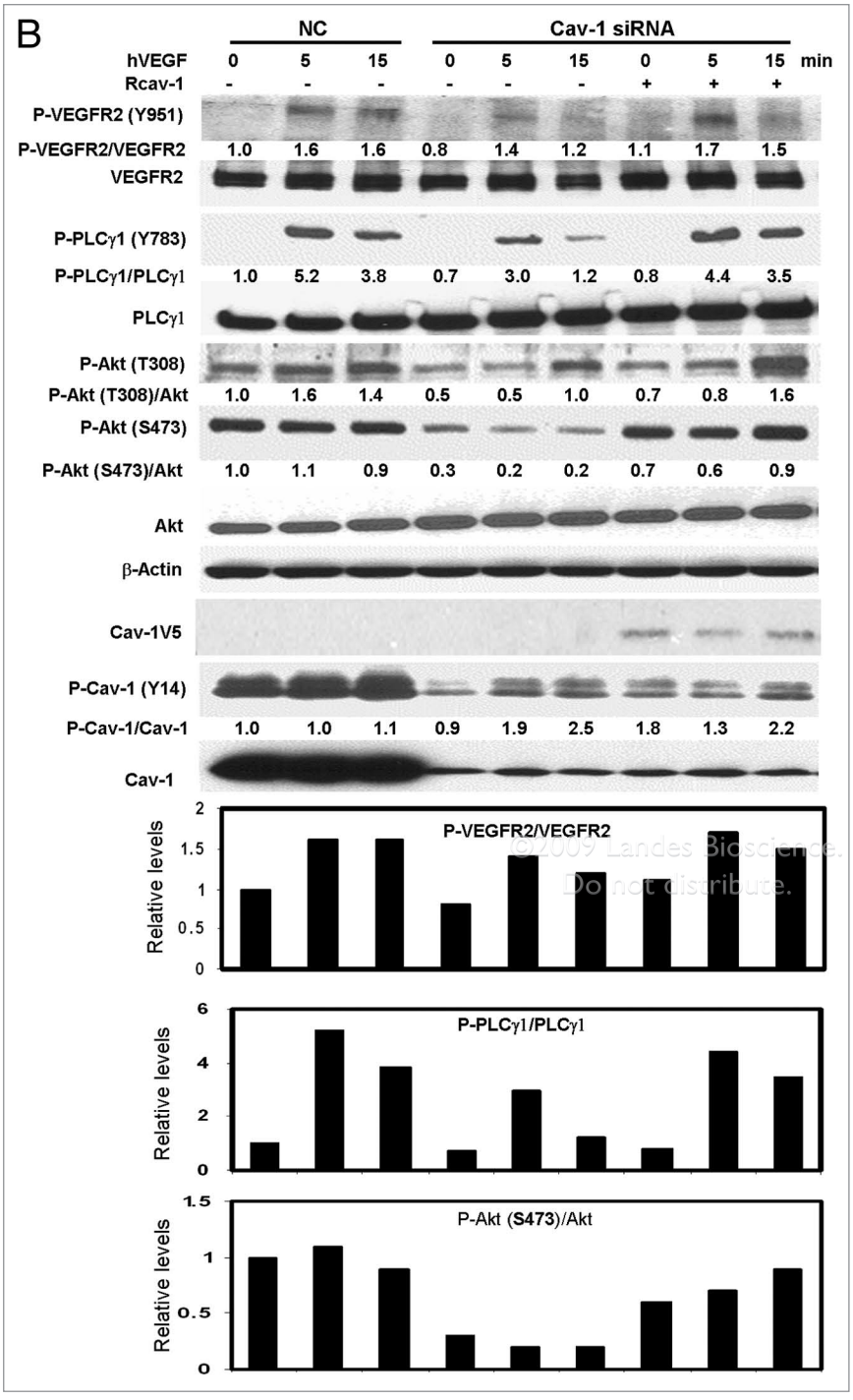

Figure 2B. Downregulation of cav-1 in PC-3 cells and HUVECs by cav-1 siRNA impaired the VEGF/VEGFR2 angiogenesis signaling pathway. (B) HUVECs were transfected on two consecutive days and incubated with rcav-1 in EBM-2 for 8 prior to treatment with hVEGF (25 ng/ml) for 0–15 min. Cav-1 downregulation not only reduced the phosphorylation status of VEGFR2, PLCγ1 and Akt significantly but also reduced the VEGF stimulated specific phosphorylation sites of these proteins. Rcav-1 (3 μg/ml) treatment of the transfected HUVECs restored the phosphorylation and the VEGF stimulated phosphorylation levels of VEGFR2, PLCγ1 and Akt. Blots shown (A and B) are representative of three independent experiments. Bar graphs represent densitometric data of ratio units of selected phosphorylated protein bands per total protein bands relative to that in the untreated and unstimulated controls.

Discussion

The molecular mechanisms involved in VEGFR2-mediated signaling of VEGF stimulated angiogenic responses in cancer cells and ECs are still poorly understood. The present study demonstrated that cav-1 plays a critical role in VEGF-stimulated VEGFR2 autophosphorylation and activation of downstream signaling in prostate cancer cells and ECs, possibly through compartmentalization of the signaling molecules. Despite a number of reports on the involvement of cav-1 in VEGF-stimulated angiogenesis, whether cav-1 is a stimulator or an inhibitor of angiogenesis is still controversial. Cav-1 was shown to play an important role in VEGF-stimulated angiogenic activities by acting both as a negative regulator of VEGFR-2 activity under resting conditions and as a substrate that is tyrosine-phosphorylated under activating conditions.[17] In addition, cav-1 overexpression was reported to enhance endothelial capillary tubule formation.[22] We and others found that production of nitric oxide and tubule formation in *cav-1*$^{-/-}$ ECs were significantly reduced compared with those in *cav-1*$^{+/+}$ with or without VEGF treatment.[7,23] Localization of VEGFR2 within caveolae was found to be essential in coupling VEGF-stimulated VEGFR2 phosphorylation and downstream angiogenic signaling, and it was also demonstrated that phosphorylated VEGFR2 dissociates rapidly from caveolae following stimulation.[17] Recently, Ikeda et al. reported that VEGF stimulation of ECs results in the phosphorylation of both VEGFR2 and cav-1 (Y14) and that the two molecules remain associated following their release from caveolae/lipid raft.[19] These reports emphasize the multiple and complex functions of cav-1 in VEGF-stimulated angiogenic responses. They further reveal that the mechanisms through which these responses are mediated are still incompletely understood.

In this study we demonstrated that introduction of cav-1 through adenoviral vector-mediated gene transduction or rcav-1 treatment caused a significant increase in VEGFR2 phosphorylation and its downstream signaling effectors in the cav-1-deficient prostate cancer cell line LP-LNCaP and in *cav-1*$^{-/-}$ ECs, in both the presence and absence of exogenously added VEGF. We previously found that treating *cav-1*$^{-/-}$ ECs with rcav-1 led to cellular internalization of rcav-1 followed by stimulation of angiogenic activities through the

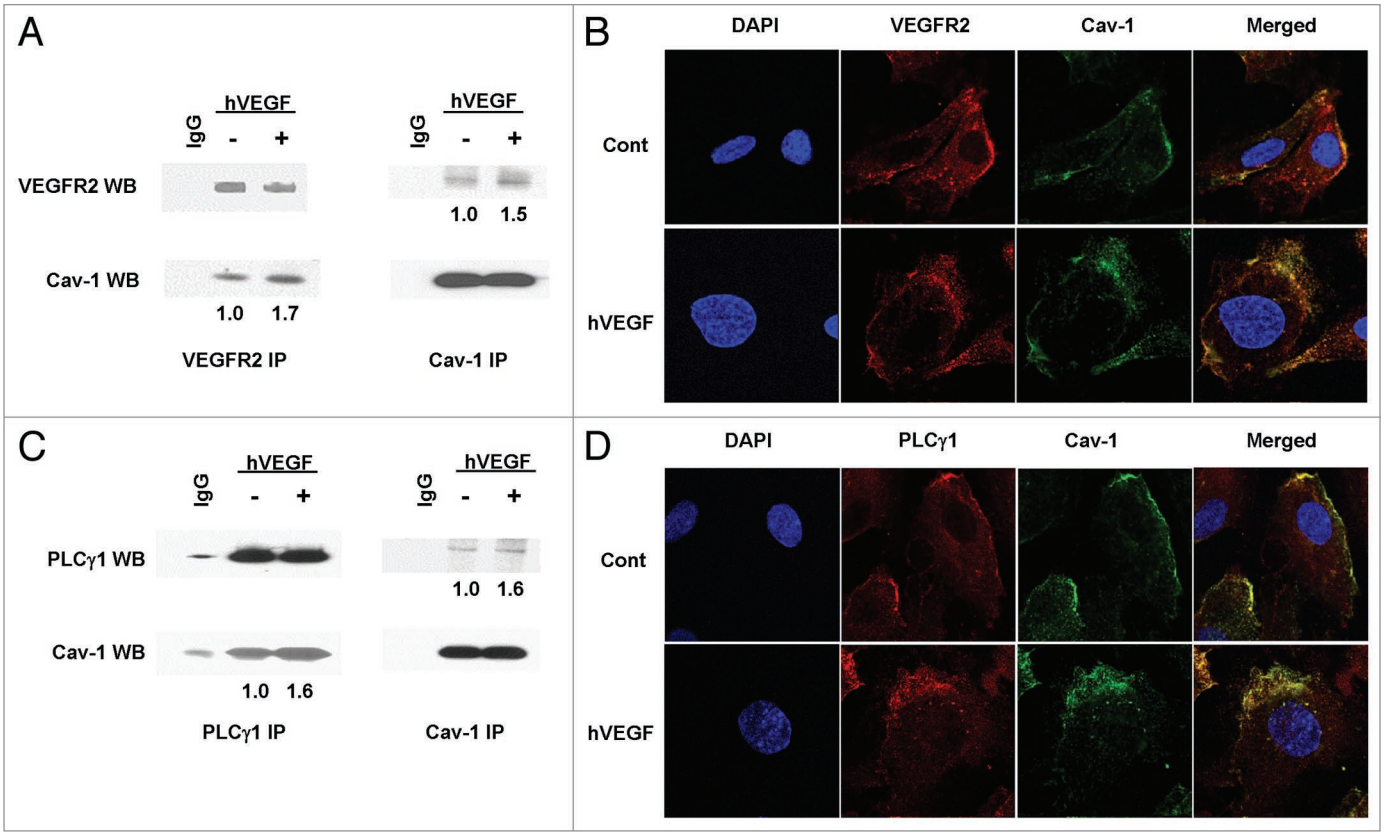

Figure 3. Cav-1 interacts with VEGFR2 and PLCγI in HUVEC. The cells were incubated with EBM-2 medium for 8 h and stimulated with 25 ng/ml of VEGF for 5 min. (A) Cell lysates were immunoprecipitated (IP) with either anti-cav-1 or anti-VEGFR2 rabbit pAb, and mock immunoprecipitates with IgG and Protein A/G Plus were also included. The coimmunoprecipitates were analyzed by western blotting (WB) with anti-cav-1 or anti-VEGFR2 mouse mAb. (B and D) HUVECs were incubated with EBM-2 for 8 h and treated with hVEGF (25 ng/ml) for 5 min. The cells were fixed, permeabilized and incubated with anti-cav-1 rabbit pAb, anti-VEGFR2 mouse mAb in (B), and anti-PLCγI mouse mAb in (D). The cells were dually stained with FITC anti-rabbit IgG, and TRITC anti-mouse IgG. Nuclei were visualized by Hoechst 33342 staining. (C) Cell lysates were immunoprecipitated with either anti-cav-1 or anti-PLCγI rabbit pAb, and analyzed by western blotting with anti-cav-1 or anti-PLCγI mouse mAb. Equal amounts of cell lysates were used to perform immunoprecipitation. Blots shown in (A and C) are representative of three independent experiments. Quatifitication by denisometry of the coimmunoprecipitated protein bands in (A and C) represent the ratio units of bound protein in VEGF treated preparations with respect to that in untreated controls.

PI3K-Akt-eNOS pathway.[7] Importantly, we further showed that rcav-1 internalization and stimulation of angiogenic responses were mediated by CSD. We demonstrated here that cav-1 is critical for ECs to maintain maximal angiogenic signaling, and that VEGF stimulation of angiogenesis is impaired without moderate levels of intracellular cav-1. These data are supported by the demonstration of angiogenic responses in *cav-1*$^{-/-}$ ECs when relatively low levels of cav-1 were introduced by transfection of cav-1 cDNA into these cells.[23] By using immunoprecipitation and immunostaining we showed that cav-1 interacts directly with VEGFR2 or PLCγ1 and that this interaction increases in cells treated with VEGF (25 ng/ml) for 5 min. Cav-1 was reported to interact with VEGFR2 in the resting state but to dissociate from VEGFR2 when cells are treated with VEGF, which also leads to the phosphorylation of both molecules.[17] Another group reported that cav-1 is associated with VEGFR2 within

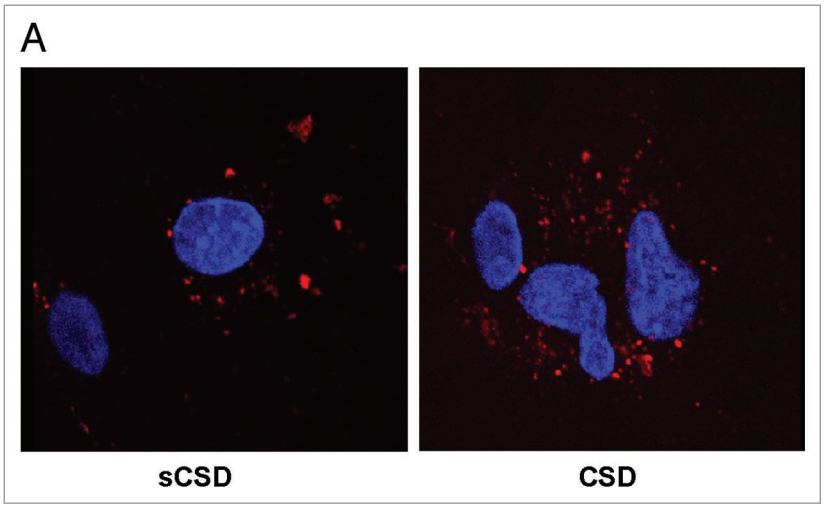

Figure 4A. CSD inhibits VEGF and cav-1 mediated angiogenesis signaling. (A) HUVECs were treated with biotin conjugated CSD or sCSD (5.0 μM) in EBM-2 for 8 h and were then washed, fixed, permeabilized and stained with TRITC-Streptavidin. The internalization of CSD and sCSD was detected on confocal microscopy and nuclei were visualized by using Hoechst 33342 staining.

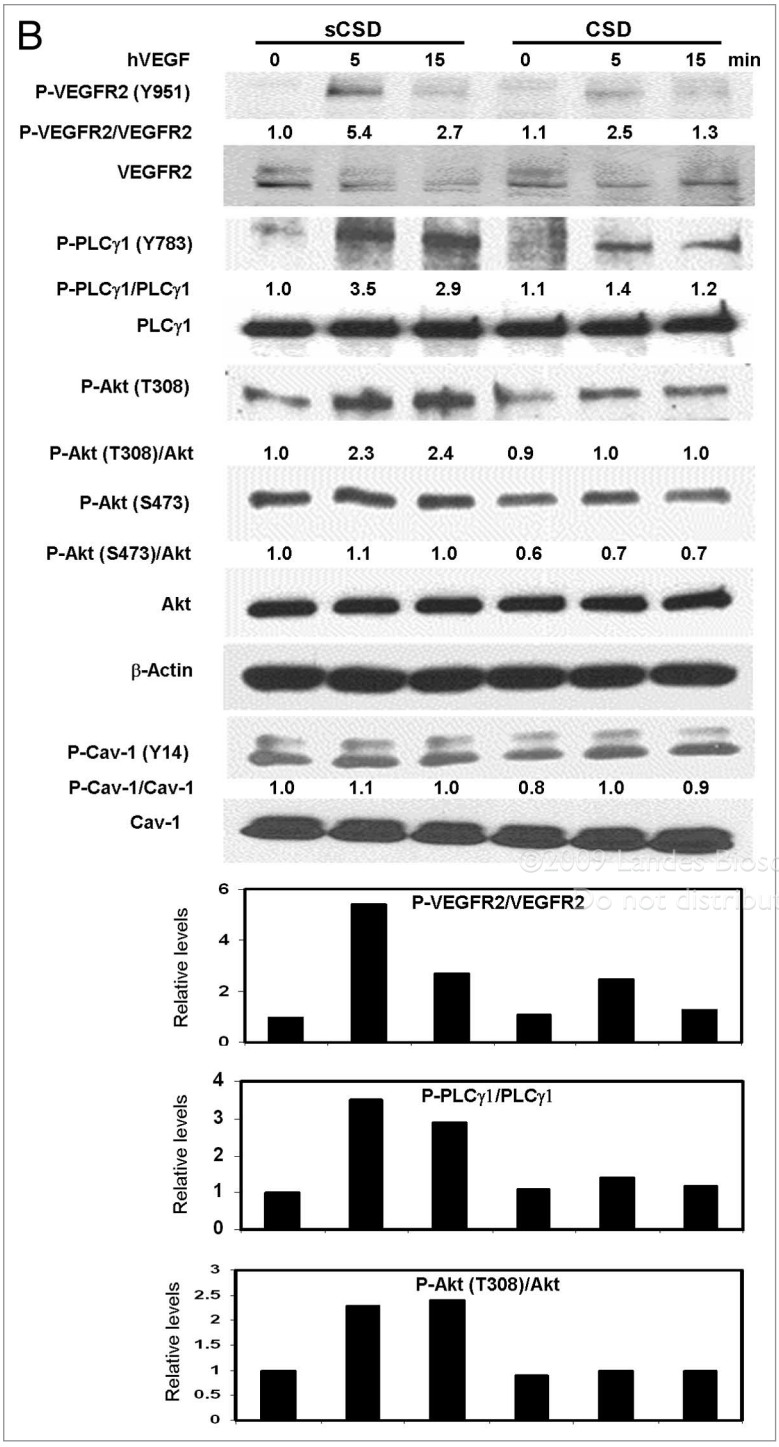

Figure 4B. CSD inhibits VEGF and cav-1 mediated angiogenesis signaling. (B) HUVECs were plated overnight and treated with CSD or sCSD (5.0 μM) in EBM-2 for 8 h. The cells were then treated with hVEGF (25 ng/ml) for 0–15 min, lysed and western blotted. CSD treatment of HUVEC reduced the VEGF stimulated phosphorylation of VEGFR2, PLCγI and Akt compared with that obtained with sCSD treatment. Blots shown are representative of three independent experiments. Bar graphs represent densitometric data of ratio units of phophorylated protein bands per total protein bands relative to that in the untreated and unstimulated controls.

caveolae and that VEGF treatment leads to phosphorylation of both molecules and their release from the caveolae as a complex.[19] The differences between the results of these studies may be explained by variations in VEGF concentration and treatment times or by the methods used in the analysis.

In the past decade, the list of proteins localized to the caveolae or bound to cav-1 has grown and includes G-protein-coupled receptors, growth factors receptors, tyrosine kinases, Ser/Thr kinases, enzymes, cellular proteins/adaptors, nuclear proteins, and structural proteins.[24] Most of the reports that point to VEGFR2 or PLCγ1 colocalization within caveolae or binding to cav-1 have been based on immunofluorescence, or density-gradient centrifugation, often in combination with extraction of membrane fractions with cold Triton X-100 to isolate detergent-resistant, cav-1-rich, low buoyancy membranes. Co-fractionation of a protein with these detergent-resistant membranes might indicate caveolar localization. However, such fractionation leads to the isolation of low-buoyant-density fractions and has the disadvantage that the isolated fractions contain both caveolae and non-caveolar lipid rafts. Thus additional studies that utilize coimmunoprecipitation combined with immunofluorescence or electron microscopy are necessary to confirm the caveolar localization or direct binding of a given protein to cav-1.

In primary ECs VEGFR2 is localized to both the plasma membrane and endosomes. VEGF binding stimulates VEGFR2 autophosphorylation, internalization and the subsequent ubiquitination necessary for endosomal sorting events that lead to lysosomal degradation.[25] Our results showing direct cav-1 binding to VEGFR2 before and after VEGF stimulation suggest an important role for cav-1 in stabilizing VEGFR2 after ligand binding. These data are supported by cav-1-VEGFR2 colocalization and internalization 5 min after VEGFR2 stimulation (**Fig. 3**). Additional studies that address the kinetics and compartmentalization of cav-1 following VEGF stimulation will further clarify this role. It is also of interest that cav-1 binds to PLCγ1 and that cav-1-PLCγ1 colocalization and internalization follow a pattern that is similar to cav-1 and VEGFR2 following VEGF stimulation in HUVECs (**Fig. 3**). These data imply that cav-1 is involved in the organization and compartmentalization of multiple signaling molecules during VEGF-stimulated angiogenic signaling.

It is noteworthy that exogenously added rcav-1 functioned similarly to endogenously expressed cav-1 in *cav-1*$^{-/-}$ ECs and HUVECs (**Figs. 1 and 2**). Although, in general, the signaling responses to rcav-1 were less than those elicited by cav-1 gene transduction, rcav-1 stimulation of VEGFR2 signaling was clear. It is particularly interesting that rcav-1 treatment significantly increased VEGFR2 and Akt phosphorylation in *cav-1*$^{-/-}$ ECs and HUVECs (**Figs. 1C and 2B**). This result extends our previous analysis of

the effects of rcav-1 on angiogenic signaling that showed virulent prostate cancer cells secrete biologically active cav-1.[6] Rcav-1 is taken up by cav-1 negative tumor cells and/or ECs leading to stimulation of specific angiogenic activities through the PI3K-Akt-eNOS signaling module.[7] Activation of VEGFR2 signaling in prostate cancer cells and prostate cancer associated ECs by prostate cancer-derived, secreted cav-1 presents an interesting paradigm for understanding the engagement of the tumor microenvironment by cav-1. Additional studies in this area are warranted.

In this paper we also report that CSD treatment can inhibit VEGF-stimulated angiogenic signaling, tubule formation and cell migration. To date, the available data on the effect of CSD in angiogenesis are controversial, with no consensus yet reached on a clearly defined mechanism of action. One group used CSD conjugated to the C terminus of the AP and found that treatment of ECs with CSD led to enhanced capillary tubule formation.[22] On the other hand, the same peptide, cavtratin, was reported to inhibit eNOS-dependent vascular leakage in established tumors by enhancing apoptosis, and decreasing tumor angiogenesis.[21] Both of those reports suggested that the mechanism of cavtratin's action is similar to that of molecular cav-1, in that the peptide functions as an enhancer of capillary tubule formation[22] and as a negative regulator of eNOS;[21] in other words, the CSD acts as a surrogate of cav-1.

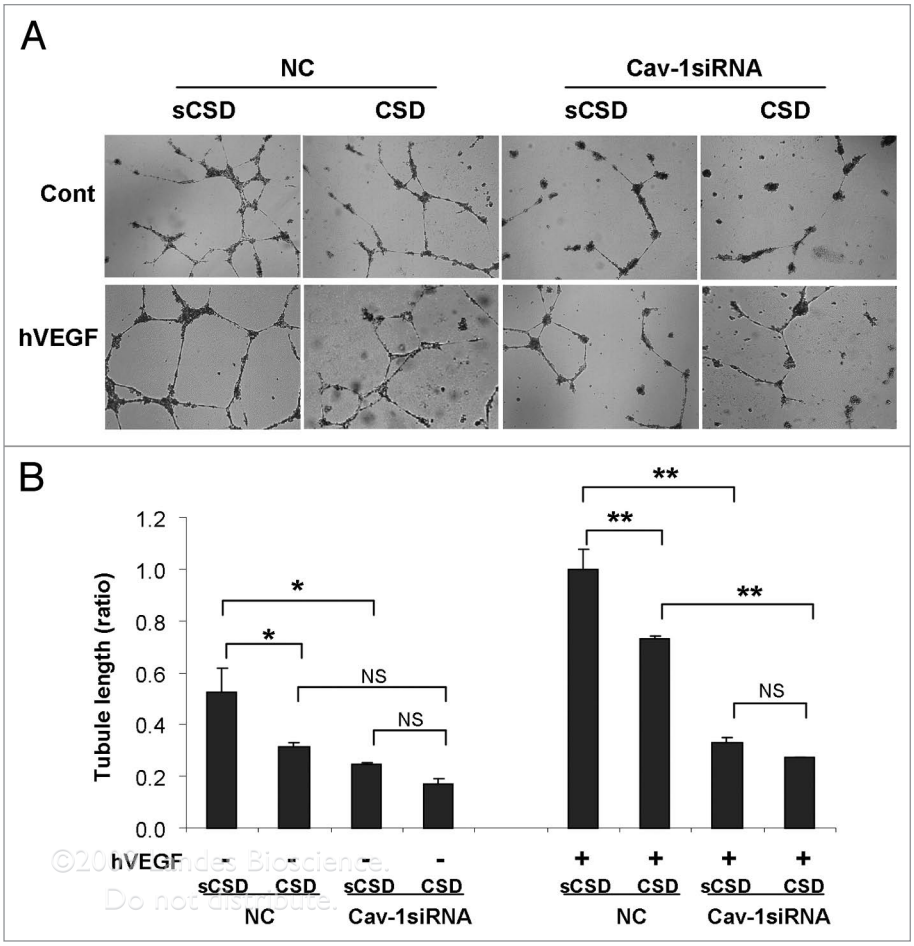

Figure 5A and B. VEGF-stimulated tubule formation and cell migration is mediated by cav-1 and inhibited by CSD. (A) Representative micrograph shows newly formed tubules of HUVECs transfected with cav-1 siRNA or NC and cultured on Matrigel matrix for 18 h in the presences and absence of hVEGF (25 ng/ml), and treated with sCSD or CSD (5 μM). (B) Bar graph represents the relative tubule lengths of HUVECs incubated as in (A).

We show in this paper that CSD treatment led to a reduction in the VEGF-stimulated phosphorylation of VEGFR2, PLCγ1 and Akt (**Fig. 4**). We further show that CSD inhibition of angiogenesis signaling is associated with inhibition of two critical biological activities in angiogenesis, i.e., EC tubule formation and migration (**Fig. 5**). Our results are not in conflict with those of the previous study that showed CSD-mediated inhibition of angiogenesis.[21] However, our results, in aggregate, are consistent with a mechanism of CSD inhibition of cav-1-mediated, VEGF-stimulated angiogenesis, rather than a mechanism through which CSD acts as a "cav-1 surrogate" for angiogenesis stimulation[22] or inhibition.[21]

Overall, our results show that endogenously expressed or exogenously added cav-1 plays an important role in VEGFR2 autophosphorylation, VEGF mediated signaling, and EC tubule formation and migration in prostate cancer cells and ECs. These activities are associated with cav-1 binding to and compartmentalization with VEGFR2 and PLCγ1. Finally, our data present a novel mechanism for potential therapeutic use of CSD to suppress angiogenic signaling in prostate cancer.

Materials and Methods

Cells, antibodies and reagents. ECs from *cav-1*$^{-/-}$ mouse aortas were isolated and prepared and grown in endothelium growth medium (EGM) as described previously.[7] HUVECs (Lonza, Inc., Walkersville, MD) were cultured at 37°C in 5% CO_2 in EGM-2 Bullet kit medium (Lonza). Cells from passages 4 to 7 were used for these studies. LNCaP and PC-3 cells were obtained from ATCC and maintained at 37°C in 5% CO_2 in complete RPMI1640 medium supplemented with 10% fetal bovine serum (Atlanta Biologicals, Lawrenceville, GA). Anti-cav-1 and anti-VEGFR2 were purchased from Santa Cruz Biotechnology (Santa Cruz, CA). Anti-PLCγ1, anti-phospho PLCγ1 (Y783), anti-phospho-Akt (T308), and anti-phospho Akt (S473) were purchased from Cell Signaling Technology (Danvers, MA) and anti-Phospho-cav-1, anti-PLCγ1 (mAb), and Akt were purchased

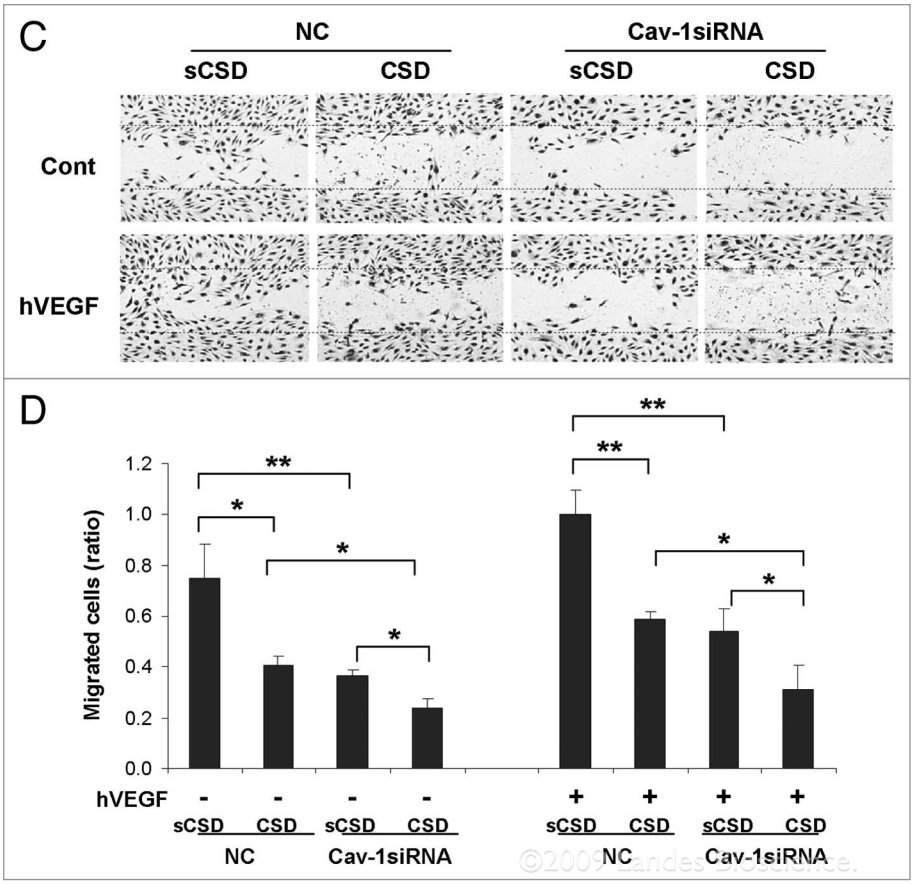

Figure 5C and D. VEGF-stimulated tubule formation and cell migration is mediated by cav-1 and inhibited by CSD. (C) Representative micrograph shows wound healing migration of HUVECs transfected with siRNA or NC and treated with or without VEGF (25 ng/ml) and with sCSD or CSD (5μM). (D) Bar graph represents the relative numbers of HUVECs transfected with cav-1 siRNA or NC that migrated into the cleared area after wounding of the culture. Cells were treated with sCSD or CSD and hVEGF for 24 h and the number of migrated cells were counted. The ratios in (B and D) represent tubule lengths and numbers of migrated cells relative to those in cells transfected with NC and treated with sCSD and hVEGF condition ± SD of three independent experiments. p values in (B and D) were determined by two-sided t test. *statistically significant difference (*$p < 0.05$, **$p < 0.01$), NS Columns, mean data; error bars, SD.

from BD Biosciences (San Jose, CA). Anti-phospho-VEGFR2 (Y 951) and recombinant human and mouse VEGF were purchased from Invitrogen (Carlsbad, CA). Rcav-1 was purified by the modified procedure described previously.[7] The CSD (DGI WKA SFT TFT VTK YWF YR) peptide and its control scrambled CSD (WGI DKA FFT TST VTY KWF RY) conjugated to biotin through its N terminal were purchased from Biosynthesis, Inc., (Lewisville, TX).

Small interfering RNA. PC-3 cells or HUVECs were transfected with cav-1 specific small interfering RNA (siRNA) and negative control siRNA constructs (Ambion, Inc., Austin, TX) using siPORT™ Amine transfection reagent according to the manufacturer's instruction (Ambion). Briefly, cells were transfected with 20 nM cav-1 siRNA (on two consecutive days for HUVECs), and after 48 h, cells were incubated with endothelium basal medium-2 (EBM-2) (Lonza, Inc.,) or serum free medium (SFM, for PC-3 cells) for 8 h followed by recombinant human (rh) VEGF (Invitrogen) treatment for 0–15 min. The cells were lysed in RIPA buffer containing protease inhibitor cocktail (Roche Applied Science, Indianapolis, IN), and phosphatase inhibitor cocktails I and II (Sigma, Inc., St. Louis, MO).

Overexpression of Cav-1 in low passage LNCaP and Cav-1$^{-/-}$ EC. Recombinant adenoviral vectors containing human cav-1 cDNA (Adcav-1) or control AdRSV without a cDNA were used to infect low passage LNCaP (LP-LNCaP) cells at a multiplicity of infection (MOI) of 10 or *cav-1*$^{-/-}$ ECs at MOI of 200. Cells were infected in SFM for 3 h, after which the medium was replaced with complete medium and incubated for 48 h. The medium was then removed and cells were incubated in SFM (LP-LNCaP cells) or EBM-2 (*cav-1*$^{-/-}$ ECs) for 8 h. Recombinant human or mouse VEGF were added to the cells, incubated for 0 to 15 min, and then cells were lysed with RIPA lysis buffer containing the protease and phosphatase inhibitor cocktails.

Immunoprecipitation and western blotting. For immunoprecipitation, cells were solubilized with lysis buffer containing 1% NP-40, 50 mM Tris-HCl (pH 7.5), 150 mM NaCl, 10% glycerol, 1 mM EGTA, protease inhibitor cocktail, and phosphatase inhibitor cocktails I and II. Soluble proteins (0.5 mg) were precleared and incubated with primary antibody (2 μg) overnight at 4°C with shaking. Protein A/G Plus Agarose (Santa Cruz Biotechnology) was added and incubated for 1 h, after which the bound proteins were washed three times with lysis buffer, boiled in SDS sample buffer and analyzed by western blotting.

The proteins were transferred onto nitrocellulose membrane, and blotted with specific antibody and antibody detection was performed by using a chemiluminescence-based detection system (Pierce Biotechnology, Rockford, IL). Quantification was carried out using Nikon's NIS-Elements AR 3.0 imaging and quantification software; data expressed as the ratio units of phosphorylated protein per total protein relative to that in the untreated and unstimulated controls.

Immunofluoresence microscopy. Fixed cells were permeabilized and immunostained using the following primary antibodies: Rabbit polyclonal anti-cav-1 antibody (pAb), mouse monoclonal (mAb) anti-VEGFR2 (Santa Cruz Biotechnology) and anti-PLCγ1 mAb (BD Biosciences) as described previously.[7] Cav-1 was detected with anti-rabbit fluorescein isothiocyanate conjugated (FITC) (Jackson Immuno Research, West Grove, PA), and VEGFR2 and PLCγ1 were detected with anti-mouse tetramethyl rhodamine isothiocyanate conjugated (TRITC)

(Invitrogen). Nuclei were visualized using Hoecgst 33342 staining. Immunostaining was analyzed using an Olympus IX71 FV500 laser-scanning confocal microscope with photomultiplier tubes (PMTs). Images were visualized using an Olympus 60x PlanApo oil immersion objective and captured using FluoView v5.0 software and the PMTs. All images were captured using the same PMT voltages, which were determined by the brightest experimental conditions.

Tubule formation assays. The tubule formation assay was performed as described previously.[7] Briefly, Cells were trypsinized counted and plated on Matrigel™ Matrix (growth factor-reduced matrigel; BD Biosciences) coated 24 well-plates in EGM-2 (Lonza, Inc.,) medium containing 1% fetal calf serum. After 16–20 h of incubation at 37°C in 5% CO_2, images of the tubules formed were captured by phase contrast microscopy. The tubule lengths in each well were measured in 5 low-power fields using Nikon's NIS-Elements AR 3.0 imaging and quantification software.

Wound-healing migration assay. The wound-healing migration assay was also performed as described previously.[7] Briefly, HUVECs in EGM-2 medium were incubated for 16 h in 24-well plates to 70–80% confluence. A straight longitudinal incision was made on the monolayer using a pipette tip, and the cells were washed with EGM-2. The cells were then reincubated for 24 h in EGM-2 and stained using the HEMA3 stain set (Biochemical Sciences Inc., Swedesboro, NJ) according to the manufacturer's instructions. The cells that had migrated into the cleared area were counted using Nikon's NIS-Elements AR 3.0 colony count software.

Statistical analysis. Differences in tubule length and the number of migrated cell were determined by unpaired two-sided t test, using StatView software (Version 5.0; SAS Institute).

Acknowledgement

This work was supported in part by NIH RO1 CA68814 and Department of Defense grant DAMD PC051247.

References

1. Parton RG, Simons K. The multiple faces of caveolae. Nat Rev Mol Cell Biol 2007; 8:185-94.
2. Shaul PW, Anderson RG. Role of plasmalemmal caveolae in signal transduction. Am J Physiol 1998; 275:L843-51.
3. Shatz M, Liscovitch M. Caveolin-1: a tumor-promoting role in human cancer. Int J Radiat Biol 2008; 84:177-89.
4. Nasu Y, Timme TL, Yang G, Bangma CH, Li L, Ren C, et al. Suppression of caveolin expression induces androgen sensitivity in metastatic androgen-insensitive mouse prostate cancer cells. Nat Med 1998; 4:1062-4.
5. Yang G, Truong LD, Timme TL, Ren C, Wheeler TM, Park SH, et al. Elevated expression of caveolin is associated with prostate and breast cancer. Clin Cancer Res 1998; 4:1873-80.
6. Tahir SA, Yang G, Ebara S, Timme TL, Satoh T, Li L, et al. Secreted caveolin-1 stimulates cell survival/clonal growth and contributes to metastasis in androgen-insensitive prostate cancer. Cancer Res 2001; 61:3882-5.
7. Tahir SA, Yang G, Goltsov AA, Watanabe M, Tabata K, Addai J, et al. Tumor cell-secreted caveolin-1 has proangiogenic activities in prostate cancer. Cancer Res 2008; 68:731-9.
8. Yang G, Addai J, Wheeler TM, Frolov A, Miles BJ, Kadmon D, et al. Correlative evidence that prostate cancer cell-derived caveolin-1 mediates angiogenesis. Hum Pathol 2007; 38:1688-95.
9. Carmeliet P. Angiogenesis in health and disease. Nat Med 2003; 9:653-60.
10. Ferrara N, Gerber HP, LeCouter J. The biology of VEGF and its receptors. Nat Med 2003; 9:669-76.
11. Dougher M, Terman BI. Autophosphorylation of KDR in the kinase domain is required for maximal VEGF-stimulated kinase activity and receptor internalization. Oncogene 1999; 18:1619-27.
12. Kendall RL, Rutledge RZ, Mao X, Tebben AJ, Hungate RW, Thomas KA. Vascular endothelial growth factor receptor KDR tyrosine kinase activity is increased by autophosphorylation of two activation loop tyrosine residues. J Biol Chem 1999; 274:6453-60.
13. Takahashi T, Yamaguchi S, Chida K, Shibuya M. A single autophosphorylation site on KDR/Flk-1 is essential for VEGF-A-dependent activation of PLC-gamma and DNA synthesis in vascular endothelial cells. EMBO J 2001; 20:2768-78.
14. Holmqvist K, Cross MJ, Rolny C, Hagerkvist R, Rahimi N, Matsumoto T, et al. The adaptor protein shb binds to tyrosine 1175 in vascular endothelial growth factor (VEGF) receptor-2 and regulates VEGF-dependent cellular migration. J Biol Chem 2004; 279:22267-75.
15. Matsumoto T, Bohman S, Dixelius J, Berge T, Dimberg A, Magnusson P, et al. VEGF receptor-2 Y951 signaling and a role for the adapter molecule TSAd in tumor angiogenesis. EMBO J 2005; 24:2342-53.
16. Lamalice L, Houle F, Jourdan G, Huot J. Phosphorylation of tyrosine 1214 on VEGFR2 is required for VEGF-induced activation of Cdc42 upstream of SAPK2/p38. Oncogene 2004; 23:434-45.
17. Labrecque L, Royal I, Surprenant DS, Patterson C, Gingras D, Beliveau R. Regulation of vascular endothelial growth factor receptor-2 activity by caveolin-1 and plasma membrane cholesterol. Mol Biol Cell 2003; 14:334-47.
18. Kaverina I, Krylyshkina O, Small JV. Regulation of substrate adhesion dynamics during cell motility. Int J Biochem Cell Biol 2002; 34:746-61.
19. Ikeda S, Ushio-Fukai M, Zuo L, Tojo T, Dikalov S, Patrushev NA, et al. Novel role of ARF6 in vascular endothelial growth factor-induced signaling and angiogenesis. Circ Res 2005; 96:467-75.
20. Li L, Ren C, Yang G, Goltsov AA, Tabata K, Thompson TC. Caveolin-1 promotes autoregulatory, Akt-mediated induction of cancer-promoting growth factors in prostate cancer cells. Mol Cancer Res 2009; 7:1781-91.
21. Gratton JP, Lin MI, Yu J, Weiss ED, Jiang ZL, Fairchild TA, et al. Selective inhibition of tumor microvascular permeability by cavtratin blocks tumor progression in mice. Cancer Cell 2003; 4:31-9.
22. Liu J, Wang XB, Park DS, Lisanti MP. Caveolin-1 expression enhances endothelial capillary tubule formation. J Biol Chem 2002; 277:10661-8.
23. Sonveaux P, Martinive P, DeWever J, Batova Z, Daneau G, Pelat M, et al. Caveolin-1 expression is critical for vascular endothelial growth factor-induced ischemic hindlimb collateralization and nitric oxide-mediated angiogenesis. Circ Res 2004; 95:154-61.
24. Razani B, Woodman SE, Lisanti MP. Caveolae: from cell biology to animal physiology. Pharmacol Rev 2002; 54:431-67.
25. Ewan LC, Jopling HM, Jia H, Mittar S, Bagherzadeh A, Howell GJ, et al. Intrinsic tyrosine kinase activity is required for vascular endothelial growth factor receptor 2 ubiquitination, sorting and degradation in endothelial cells. Traffic 2006; 7:1270-82.

Functional Analysis of Secreted Caveolin-1 in Mouse Models of Prostate Cancer Progression

Masami Watanabe,[1] Guang Yang,[3] Guangwen Cao,[1] Salahaldin A. Tahir,[3] Koji Naruishi,[1] Ken-ichi Tabata,[1] Elmoataz Abdel Fattah,[1] Kartik Rajagopalan,[1] Terry L. Timme,[1] Sanghee Park,[3] Shinji Kurosaka,[3] Kohei Edamura,[3] Ryuta Tanimoto,[3] Francesco J. Demayo,[2] Alexei A. Goltsov,[3] and Timothy C. Thompson[3]

[1]Scott Department of Urology and [2]Department of Molecular and Cellular Biology, Baylor College of Medicine, and [3]Department of Genitourinary Medical Oncology-Research, The University of Texas M.D. Anderson Cancer Center, Houston, Texas

Abstract

Previously, we reported that caveolin-1 (cav-1) is overexpressed in metastatic prostate cancer and that virulent prostate cancer cells secrete biologically active cav-1. We also showed that cav-1 expression leads to prosurvival activities through maintenance of activated Akt and that cav-1 is taken up by other cav-1–negative tumor cells and/or endothelial cells, leading to stimulation of angiogenic activities through PI-3-K-Akt-eNOS signaling. To analyze the functional consequences of cav-1 overexpression on the development and progression of prostate cancer *in vivo*, we generated PBcav-1 transgenic mice. Adult male PBcav-1 mice showed significantly increased prostatic wet weight and higher incidence of epithelial hyperplasia compared with nontransgenic littermates. Increased immunostaining for cav-1, proliferative cell nuclear antigen, P-Akt, and reduced nuclear $p27^{Kip1}$ staining occurred in PBcav-1 hyperplastic prostatic lesions. PBcav-1 mice showed increased resistance to castration-induced prostatic regression and elevated serum cav-1 levels compared with nontransgenic littermates. Intraprostatic injection of androgen-sensitive, cav-1–secreting RM-9 mouse prostate cancer cells resulted in tumors that were larger in PBcav-1 mice than in nontransgenic littermates ($P = 0.04$). Tail vein inoculation of RM-9 cells produced significantly more experimental lung metastases in PBcav-1 males than in nontransgenic male littermates ($P = 0.001$), and in *cav-1*$^{+/+}$ mice than in *cav-1*$^{-/-}$ mice ($P = 0.041$). Combination treatment with surgical castration and systemic cav-1 antibody dramatically reduced the number of experimental metastases. These experimental data suggest a causal association of secreted cav-1 and prostate cancer growth and progression. (Mol Cancer Res 2009;7(9):1446–55)

Introduction

Caveolin-1 (cav-1) is a major structural component of caveolae, which are specialized plasma membrane invaginations that are involved in multiple cellular processes such as molecular transport, cell adhesion, and signal transduction (1, 2). Although under some conditions cav-1 may suppress tumorigenesis (3), cav-1 is associated with and contributes to malignant progression through various mechanisms (4-8). A high level of expression of intracellular cav-1 is associated with metastatic progression of human prostate cancer (9, 10) and other malignancies, including lung (11), renal (12), and esophageal squamous cell cancers (13).

It has been shown that virulent prostate cancer cell lines secrete biologically active cav-1 protein *in vitro*, and cav-1 promotes prostate cancer cell viability and clonal growth (14-16). The cancer-promoting effects of secreted cav-1 include antiapoptotic activities similar to those observed following enforced expression of cav-1 within the cells (14, 17). In addition to demonstrating cav-1–mediated autocrine activities, we recently showed that recombinant cav-1 protein is taken up by prostate cancer cells and endothelial cells *in vitro* and that recombinant cav-1 increases angiogenic activities *in vitro* and *in vivo* by activating Akt- and/or NOS-mediated signaling (18). We also documented significantly higher serum cav-1 levels in men with prostate cancer than in men with benign prostatic hyperplasia (18) and also in patients with elevated risk of cancer recurrence after radical prostatectomy (19).

Expression and secretion of cav-1 by prostate cancer cells is a unique concept in malignant progression. The autocrine and paracrine activities of cav-1 mediated through activation of Akt and/or NOS signaling may lead to pervasive engagement of the local tumor microenvironment, involving but not limited to the proangiogenic activities we previously showed.

One of the goals of this project was to identify specific phenotypic alterations that result from cav-1 overexpression in prostate cancer; to do that, we generated transgenic mice with targeted overexpression of cav-1 in the prostate using the short rat probasin (PB) promoter, yielding PBcav-1 mice.

Received 2/24/09; revised 5/14/09; accepted 6/18/09; published OnlineFirst 9/8/09.
Grant support: National Institutes of Health grants R01 CA68814 and 5U01 CA084296 and Department of Defense grant W81-WH-06-1-0116.
The costs of publication of this article were defrayed in part by the payment of page charges. This article must therefore be hereby marked *advertisement* in accordance with 18 U.S.C. Section 1734 solely to indicate this fact.
Note: Supplementary data for this article are available at Molecular Cancer Research Online (http://mcr.aacrjournals.org/).
Requests for reprints: Timothy C. Thompson, Department of Genitourinary Medical Oncology-Research, Unit 1374, The University of Texas M.D. Anderson Cancer Center, 1515 Holcombe Boulevard, Houston, TX 77030. Phone: 713-792-9955; Fax: 713-792-9956. E-mail: timthomp@mdanderson.org

doi:10.1158/1541-7786.MCR-09-0071

Immunostaining analysis showed that cav-1 overexpression resulted in prostatic epithelial hyperplasia accompanied by increased levels of P-Akt. PBcav-1 prostatic tissues showed reduced androgen sensitivity under castration-induced regression but not to exogenous testosterone stimulation *in vivo*. We found not only those prostatic epithelial cells derived from PBcav-1 mouse possessed the capacity to secrete cav-1 but also that serum cav-1 levels in PBcav-1 male mice were higher than the nontransgenic littermates. Lastly, cav-1-expressing, androgen-sensitive mouse prostate cancer cell line, RM-9, was injected intraprostatically to PBcav-1 mice and their nontransgenic littermates to establish orthotopic tumors, or i.v. to PBcav-1, their nontransgenic littermate, *cav-1*$^{-/-}$ and *cav-1*$^{+/+}$, male mice to establish experimental metastases. The results of these studies showed that locally secreted cav-1 was associated with increased RM-9 orthotopic tumor growth and that serum cav-1 levels were positively associated with increased RM-9 metastatic activities. Furthermore, the data suggest combined androgen deprivation with cav-1 antibody (Ab) treatment, or cav-1 Ab alone, is potential therapy for metastatic prostate cancer.

Results

Cav-1 Expression in PBcav-1 Transgenic Mice

To generate transgenic mice with prostate-specific expression of cav-1, we constructed a vector expressing mouse cav-1 cDNA under the transcriptional regulation of the androgen-responsive short PB promoter (Fig. 1A) that restricts transgene expression to the mouse prostate (20, 21). Transgenic mice were generated by pronuclear injection of linearized vector DNA, and three independent founder lines (#8489, #8041, and #8647) were identified by PCR using transgene-specific primers. Preliminary comparative expression analysis of those three transgenic mouse lines using reverse transcription-PCR showed that all three expressed the transgene in the prostate at various levels of specificity (data not shown). Because the PBcav-1 transgenic mouse line #8489 showed the most robust prostate-specific expression of transgene, it was chosen for analysis in the experiments described here.

To analyze the specificity of transgene expression, RNA was isolated from the ventral, dorsolateral, and anterior prostate lobes as well as from multiple mouse tissues and subjected to RT-PCR analysis with the transgene-specific primers P1 and P2 (Supplementary S1A; Fig. 1A). Quantitative reverse transcription-PCR analysis of cav-1 RNA revealed higher cav-1 RNA expression in the ventral and dorsolateral prostatic lobes of PBcav-1 mice (2.0- and 1.5-fold, respectively) than in the nontransgenic mice (Fig. 1B) but relatively low to no detectable levels of cav-1 transgene expressions in the testes, seminal vesicles, spleen, kidney, and liver (Supplementary Fig. S1A).

Cav-1 protein levels in prostatic tissues were analyzed by Western blotting. Cav-1 protein was detected in all lobes of the prostates with the dorsolateral lobe having the highest and anterior lobe the lowest cav-1 levels in the nontransgenic animals. Invariably, the cav-1 level in each lobe was significantly higher in the transgenic mice than that in the nontransgenic littermates, although the largest transgenic induction of cav-1 was seen in the ventral lobe (Fig. 1C). The levels of total cav-1 protein in other organs of the PBcav-1 male mice were comparable with those in their nontransgenic counterparts (Supplementary Fig. S1B), confirming the prostate-specific expression of the cav-1 transgene.

Cav-1 Overexpression in Prostatic Tissue Induces Prostatic Hyperplasia

To study the effect of cav-1 overexpression on mouse prostate development, histopathologic and immunohistochemical analysis was done on samples obtained at necropsy from the group of 11- to 13-month-old PBcav-1 transgenic ($n = 28$) and the nontransgenic littermates (wild-type; $n = 29$). The wet weight of the whole prostate glands from PBcav-1 transgenic mice was significantly greater than that of their nontransgenic littermates (Fig. 2A). The prostate glands of the transgenic mice also displayed a higher incidence of epithelial hyperplasia than the nontransgenic littermates did (43% versus 6.8%). More strikingly, 18% of the PBcav-1 transgenic mouse prostates were characterized by the presence of focal dysplastic glandular epithelium with disorganized multicellular layers, intraepithelial space formation, and nuclear atypia (Fig. 1D) in addition to the hyperplasia. Focal stromal hyperplasia was also seen in 7% of the transgenic mouse prostates (Fig. 1D). Interestingly, these lesions were focal and restricted to the ventral and dorsolateral lobes and they were not observed in the anterior lobe of the transgenic prostates. The epithelial lesions in the PBcav-1 mice showed strongly positive cytoplasmic staining for both cav-1 and P-Akt proteins (Fig. 1E). In the lesion-free regions of the transgenic mouse prostates and in the nontransgenic mouse prostate tissues, the glandular epithelium was negative or minimally positive for cav-1 and P-Akt staining (data not shown; Fig. 1E). Cav-1 was expressed abundantly in the stromal cells of all prostate tissues. However, in the PBcav-1 prostate tissues, some stromal cells that surround the epithelial lesions tended to have reduced cav-1 expression. The prostatic epithelium also showed increased proliferating cell nuclear antigen (PCNA) staining (Fig. 2B) and reduced nuclear p27^{Kip1} staining in PBcav-1 mice with hyperplastic lesions compared with the normal epithelium of prostate tissues in the nontransgenic mice (Fig. 2C and D), although no significant difference was found in immunostaining between the lesion-free PBcav-1 mouse prostates and that in the nontransgenic mouse prostates (data not shown).

Reduced Androgen Sensitivity in PBcav-1 Prostatic Tissues

PBcav-1 adult male mice and their nontransgenic littermates were subjected to surgical castration, surgical castration plus testosterone pellet implantation, or sham operations. Twenty-one days following these procedures, animals were euthanized, and the whole prostatic tissues were evaluated. Analysis of whole prostatic wet weights showed resistance to castration-induced regression in PBcav-1 mouse prostate tissues, compared with that in the nontransgenic littermates ($P = 0.04$; Fig. 3A). However, PBcav-1 prostatic tissues showed no significant increase in responsiveness to testosterone stimulation, compared with those from the nontransgenic littermates ($P = 0.58$; Fig. 3B).

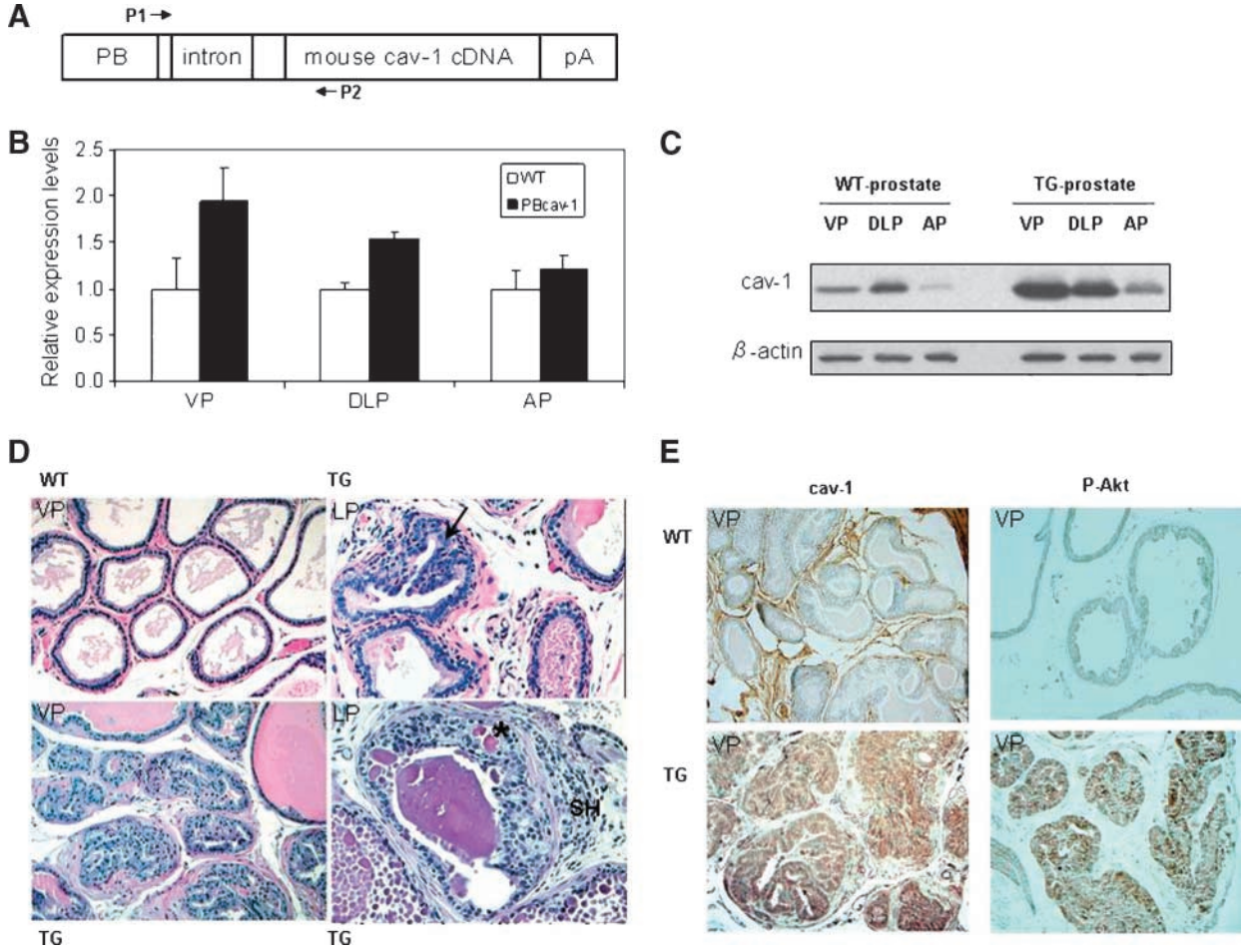

FIGURE 1. Generation and expression analysis of PBcav-1 transgenic mice with prostate specific cav-1 expression. **A.** Schematic representation of PBcav-1 transgene construct. **B.** Relative levels of total cav-1 mRNA or Cav-1 protein (**C**) in ventral prostate (*VP*), dorsolateral prostate (*DLP*), and anterior prostate (*AP*) for nontransgenic (*WT*) and PBcav-1 transgenic (*TG*) male mice was determined by quantitative real-time PCR and Western blotting, respectively. **D.** Histologic analysis of the ventral lobe mouse prostate (H&E). Compared with the benign prostatic tissue of nontransgenic (*top left*), the PBcav-1 transgenic prostates developed hyperplastic glandular epithelia (*bottom left*) and dysplasic epithelial lesions (*right*) characterized by multiple layers of cells, nuclear irregularity (*arrow in top right* indicates an enlarged nucleus) and intraepithelial space formation (*star in bottom right*), and focal stromal hyperplasia (*SH, bottom right*). **E.** Immunohistochemical analysis of cav-1 and P-Akt expression in the ventral lobe of nontransgenic and PBcav-1 mouse prostate.

Serum Cav-1 Levels and Prostate Secretion Levels in PBcav-1 Mice Were Higher

It has been reported that human and mouse prostate cancer cells overexpress and secrete cav-1 protein (14-16) and that patients with prostate cancer show relatively high levels of serum cav-1 (18). To test the secretory potential of the mouse prostate gland, we performed 24-hour organ cultures of prostates collected from PBcav-1 mice and nontransgenic littermates. Western blotting analysis of the organ-culture medium from PBcav-1 mice prostates revealed considerably higher cav-1 protein secretion compared with those of nontransgenic mice prostates (Fig. 4A). We further measured serum cav-1 in PBcav-1 mice, in their nontransgenic littermates, and in *cav-1*$^{-/-}$ and *cav-1*$^{+/+}$ (22) adult male mice. Serum cav-1 levels were significantly higher in PBcav-1 transgenic male mice than in the nontransgenic mice, and as expected, serum cav-1 levels were lower in *cav-1*$^{-/-}$ adult male mice than they were in genetically matched *cav-1*$^{+/+}$ adult male mice (Fig. 4B).

Greater RM-9 Experimental Metastasis and Orthotopic Prostate Tumor Growth in PBcav-1 Mice

To test the effect of secreted cav-1 on prostate cancer cell growth and metastasis formation *in vivo*, the androgen-sensitive, cav-1–secreting RM-9 mouse prostate cancer cells (23, 24) were injected into adult male PBcav-1 mice and their nontransgenic littermates through two different routes: intraprostatically (dorsolateral prostate) and i.v. (tail vein). Direct dorsolateral prostate injection of RM-9 cells formed significantly larger orthotopic prostate tumors in PBcav-1 mice than in their nontransgenic littermates after 21 days (Fig. 5A and B). The result is consistent with those from our previous study that showed RM-9 cells formed significantly larger orthotopic tumors in *cav-1*$^{+/+}$ than in *cav-1*$^{-/-}$ male mice (18).

For experimental metastasis model, RM-9 cells were injected into the tail vein of PBcav-1 mice and their nontransgenic littermates. After 21 days, the mice were euthanized, and the lung tumor nodules on the lung surface were

counted, and also the sizes of the tumor nodules were measured to evaluate the lung tumor burden. Both the numbers and sizes of the tumor nodules in the PBcav-1 mice were significantly greater than they were in the nontransgenic hosts (Fig. 5A, C, and D). Representative pictures of the lung tumor nodules from both PBcav-1 and their nontransgenic littermates are shown in Fig. 5C. PCNA and terminal deoxynucleotidyl transferase-mediated dUTP nick end labeling (TUNEL) immunostaining on the lung tumor nodules from PBcav-1 mice, and their nontransgenic littermates were done to compare the proliferative and apoptotic activities. Although PCNA immunostaining was relatively higher in the RM-9 metastatic nodules from PBcav-1 mice, the difference from that in nontransgenic littermates was not statistically significant (data not shown). However, positivity of TUNEL immunostaining was significantly less in the RM-9 lung tumor nodules from PBcav-1 mice than that in the nontransgenic littermates (Fig. 5E).

Up-Regulation of Cav-1, P-Akt, and Vascular Endothelial Growth Factor in PBcav-1 Lung Tumor Nodules

To study molecular pathways associated with reduced apoptosis in lung tumor nodules from PBcav-1 mice, we analyzed the expression of cav-1 and its downstream protein target P-Akt, which is involved in cell proliferation and apoptosis (25-27), and that of the Akt-regulated vascular endothelial growth factor (VEGF; refs. 28-30) using Western blotting. Both normal lung tissue taken from lungs that harbored RM-9 lung tumor nodules and RM-9 lung tumor nodules from PBcav-1 mice and their nontransgenic littermates were microdissected, lysed, and analyzed by immunoblotting.

There were no significant differences between the levels of cav-1, P-Akt, total Akt, and VEGF immunostaining in the PBcav-1 mice and those in their nontransgenic littermates for the normal lung tissues (Fig. 6A and C). However, in the lung tumor nodules isolated from PBcav-1 mice, the expression levels of cav-1, P-Akt, and VEGF were significantly up-regulated relative to the tumor lung nodules from nontransgenic littermates (Fig. 6B and C). We also analyzed serum VEGF levels in metastasis-bearing PBcav-1 mice and their nontransgenic littermates. Serum levels of VEGF in PBcav-1 mice bearing RM-9 lung metastases were significantly higher than in the tumor-bearing nontransgenic littermates or in nontumor bearing PBcav-1 mice. However, no difference was found between the nontumor bearing mice of both types (Fig. 6D).

To detect any association between relatively high-serum VEGF levels and the number of lung metastases in PBcav-1 mice and their nontransgenic littermates, we performed regression analysis. A significant correlation between serum VEGF level and the number of experimental lung metastases was observed in PBcav-1 mice (correlation coefficient, 0.639; $P = 0.0268$) but not in the control mice (data not shown). These data suggest that high serum level of VEGF is not due exclusively to the host associated effect but rather reflects an interaction between the host and the presence of metastatic lung tumor nodules.

Suppression of Experimental Metastasis by Combined Androgen Deprivation and Cav-1 Ab Treatment

To analyze the effects of testicular androgens and/or serum cav-1 on experimental metastatic activities, surgical castration and i.p. cav-1 Ab were administered to cohorts of four different genotypes of adult male mice-PBcav-1, nontransgenic littermates, *cav-1*$^{-/-}$, and *cav-1*$^{+/+}$ (20). These four cohorts, which showed various serum cav-1 levels (Fig. 4B), were injected with RM-9 prostate cancer cells via tail vein. Two days after the tumor cell injections, the mice were randomized and treated with either sham + HBSS, castration + HBSS, rabbit IgG, cav-1 Ab, or castration + cav-1 Ab (Fig. 7A). The treatments were given i.p. every other day for 21 days. At the end of the time course, the number of lung tumor nodules were scored and compared among the treatment groups for each mouse genotype. Control rabbit IgG treatment produced similar results as the control sham + HBSS treatment ($P = 0.31–0.68$) in all four

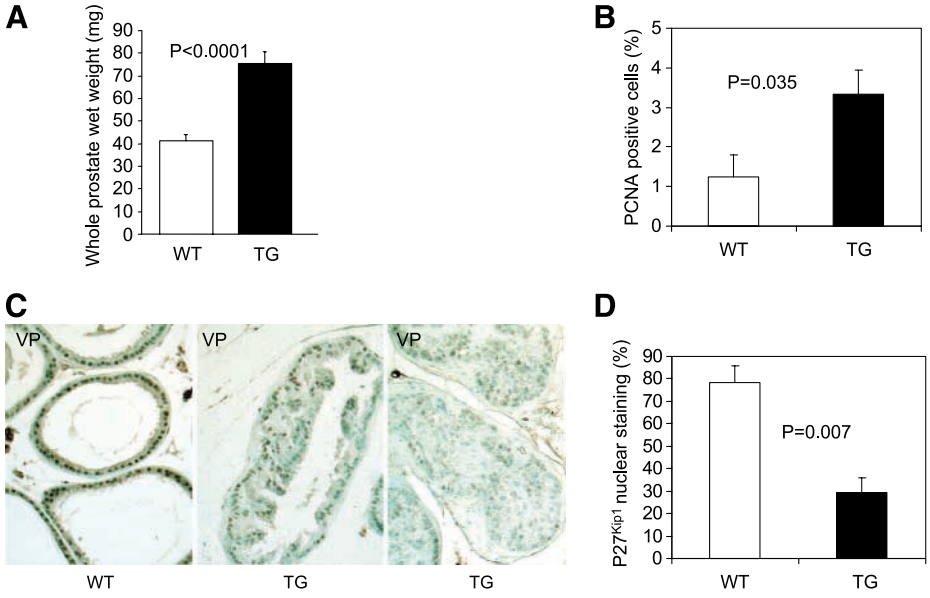

FIGURE 2. Prostatic epithelial hyperplasia in PBcav-1 male mice. **A.** Increased prostate wet weight in PBcav-1 mice (*TG*). **B.** Higher number of PCNA positive cells (%). **C.** Reduced nuclear p27 ^{Kip1} staining compared with that in nontransgenic littermates (*WT*). **D.** Quantitative (%) representation of nuclear p27^{Kip1} staining in mouse prostate tissues.

mouse genotypes. Compared with sham + HBSS treatment, surgical castration resulted in significant suppression in the number of lung tumor nodules in all four mouse genotypes ($P = 0.0002$). Interestingly, the cohort of *cav-1*$^{-/-}$ mice showed the greatest reduction in the lung tumor nodules by castration treatment (85% reduction from sham + HBSS) among the four genotypes. As expected, the highest numbers of lung tumor nodules were found in PBcav-1 mice (five times more than *cav-1*$^{-/-}$ mice), and this group benefited most from cav-1 Ab treatment (83% reduction in sham + HBSS). Although, extensive lung tumor nodule formation occurred in the PBcav-1 sham+ HBSS control treatment group [number of lung tumor nodules (n) = 20.3], the PBcav-1 cav-1 Ab treatment group showed a significantly reduced number of lung tumor nodules (n = 3.4), almost to the level found in *cav-1*$^{-/-}$ Ab treatment group (n = 2.2). Generally, suppression of lung metastases by cav-1 Ab treatment was much more extensive ($P < 0.0001$) than suppression by castration treatment in all the genotypes of the mice except in the cohort of *cav-1*$^{-/-}$ mice (Fig. 7B). However, the difference in actual number of tumor lung nodules between castration and cav-1 Ab treatment for *cav-1*$^{-/-}$ mice is marginal and not statistically significant (n = 0.6 versus 2.2; $P = 0.06$). The combination of androgen deprivation by castration and cav-1 Ab treatment resulted in suppression of experimental metastasis similar to the suppression produced by cav-1 Ab treatment alone in all four genotype cohorts.

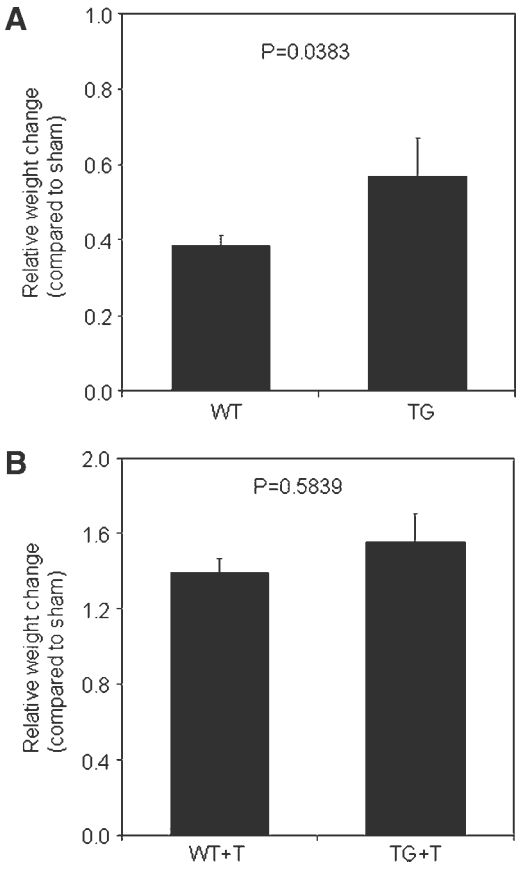

FIGURE 3. Androgenic manipulation of PBcav-1 and nontransgenic adult male mice. **A.** Resistance to castration induced prostatic regression in PBcav-1 (*TG*) male mice compared with nontransgenic littermates (*WT*) and (**B**) androgen-stimulated prostatic growth in PBcav-1 male mice was comparable with nontransgenic littermates. The wet weight of whole mouse prostate was measured 21 d after castration. Testosterone pellets (*T*) were implanted same day of the surgical castration. The data represent relative wet weight change compared with the sham-treated group for PBcav-1 and nontransgenic cohorts.

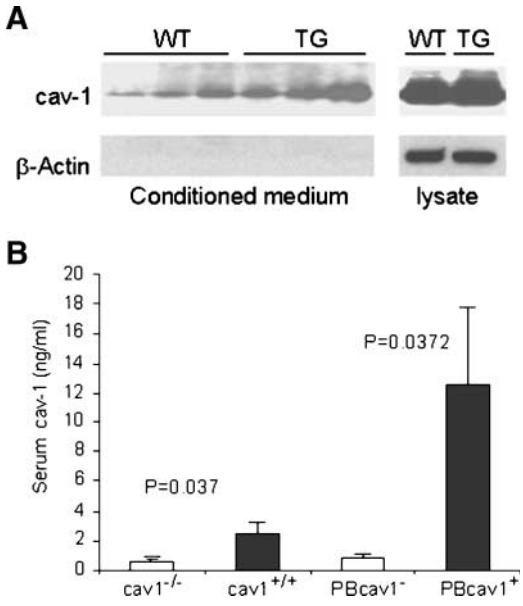

FIGURE 4. Prostatic cav-1 secretion and serum cav-1 level comparisons. **A.** Western blotting analysis of the conditioned medium collected from *in vitro* 24-h organ culture of prostates from three nontransgenic (*WT*) and three PBcav-1 (*TG*) mice (*left*). Cav-1 levels in prostate tissue lysates served as positive controls (*right*). **B.** Serum cav-1 levels of *cav-1*$^{-/-}$, *cav-1*$^{+/+}$, PBcav-1^{-} (nontransgenic), and PBcav-1^{+} (transgenic) male mice determined by ELISA.

Discussion

Here, we report generation and characterization of PBcav-1 transgenic mice, which express prostate-specific cav-1 under the transcriptional regulation of the short PB promoter. The transgenic mice expressed relatively high levels of cav-1 in prostatic tissues, which was associated with the development of prostatic epithelial hyperplasia. Overexpression of cav-1 led to stabilization of P-Akt, reduced nuclear p27^{Kip1} staining, and increased PCNA staining in the hyperplastic prostatic epithelia of male PBcav-1 animals (Figs. 1 and 2). This up-regulation of P-Akt and reduction in nuclear p27^{Kip1} is consistent with our previous data demonstrating a novel mechanism of Akt stabilization mediated through cav-1 binding to and inhibition of protein phosphatase 2A (17, 31). It is of interest to note that these cav-1–mediated activities are associated with epithelial hyperplasia and epithelial atypia but not with prostate cancer and thus the data suggest additional oncogenic pathways are required for the transformation of prostatic epithelium.

We further characterized the responses of the prostatic tissues to androgen deprivation and stimulation through the use of surgical castration and exogenous testosterone stimulation *in vivo*. The results indicated that prostatic

tissues of PBcav-1 transgenic mice were refractory to castration-induced regression but were not overly sensitive to the stimulatory effects of exogenous testosterone relative to those in their nontransgenic littermates (Fig. 2). Although these data are consistent with increased levels of P-Akt, further studies are necessary to test whether stabilization of P-Akt by cav-1 underlies these aberrant responses to hormonal manipulation.

Recently, we reported that secreted cav-1 protein is taken up by prostate cancer cells and cancer-associated endothelial cells and through this process stimulates Akt-mediated angiogenic activities (18). To better understand the biological and potential clinical significance of prostate cancer cell–derived secreted cav-1, we tested the capacity of PBcav-1 mouse prostatic tissues to secrete cav-1 and to produce relatively high serum cav-1 levels. What we found was that PBcav-1 transgenic mice prostate indeed secreted more cav-1 and had higher serum cav-1 levels than their nontransgenic littermates (Fig. 4). These data led us to reason that the relatively high serum cav-1 level derived from PBcav-1 mouse prostatic tissues could stimulate the growth of local prostate tumors and the development of distant prostate cancer metastases.

As postulated, PBcav-1 mice produced significantly larger tumors from direct dorsolateral prostate injection of RM-9 mouse prostate cancer cells compared with their nontransgenic littermates after 21 days. Given the prosurvival and proangiogenic activities of cav-1 within the context of prostate cancer and other malignancies (4-8), it is interesting to speculate whether cav-1 secretion from premalignant cells contributes to a "field effect." Further studies may reveal a role for cav-1 expression in the development of hyperplastic and/or premalignant prostatic lesions, including the establishment of a tumor-promoting environment.

The results of our experimental metastasis analyses using RM-9 cells also showed that host-associated factors promoted the growth of experimental lung metastases in PBcav-1 mice compared with that in the nontransgenic littermates (Fig. 5). Lower apoptotic activity and higher P-Akt levels in the PBcav-1 mice compared with those in the nontransgenic littermates (Fig. 5E and 6E–C) are consistent with the uptake of serum cav-1 and with cav-1–mediated stabilization of P-Akt levels in metastatic cells. Although a statistically significant increase in tumor-associated angiogenesis was not documented in metastases in the PBcav-1 mice compared with those in the nontransgenic littermates, we did observe greater VEGF expression in the metastases and greater serum VEGF levels in the tumor-bearing PBcav-1 mice than in the tumor-bearing nontransgenic littermates or in the mice of the both types that were not exposed to tumor (Fig. 6D).

It is well-established that various tumor growth factors are expressed and secreted under the regulation of intracellular PI3-K-Akt signaling (25-27, 32, 33). In cancer cells, activated

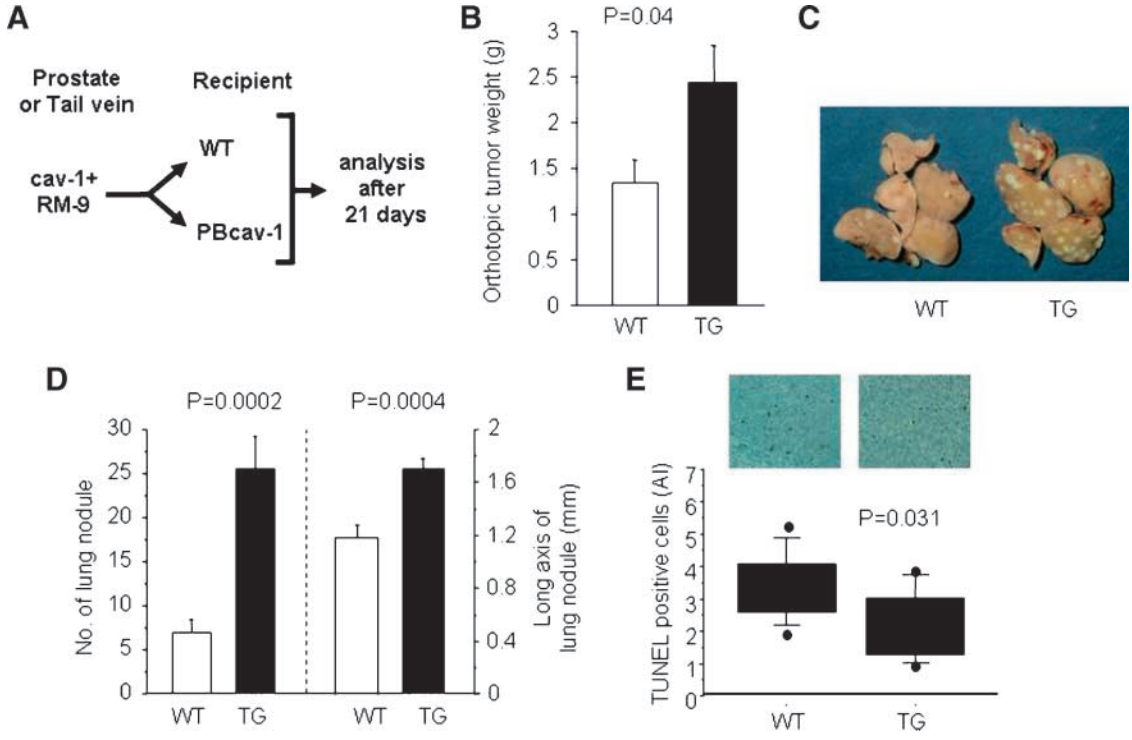

FIGURE 5. Elevated levels of cav-1 in prostate and serum stimulate prostate cancer progression in PBcav-1 mice. **A.** Diagram of orthotopic prostate or experimental metastasis experiment (tail vein injection) using mouse prostate cancer cell line RM-9 in PBcav-1 and nontransgenic littermates male mice. **B.** Increased orthotopic RM-9 prostate tumor weight in PBcav-1 mice (*TG*) compared with nontransgenic littermates (*WT*). **C.** Representative micrographs of RM-9 lung metastases in nontransgenic littermates and PBcav-1 mice. **D.** Increased number and size of RM-9 metastatic lung nodules in PBcav-1 mice compared with nontransgenic littermates. **E.** Histologic analysis of experimental lung metastatic lesions in nontransgenic and PBcav-1 mice. Top, representative example of TUNEL staining. TUNEL-positive staining (*AI*, apoptotic index) is reduced in metastases of PBcav-1 mice compared with the metastases in nontransgenic animals. Differences in PCNA or CD31 (MVD)-positive staining were not significant between these two groups of mice (data not shown).

Akt has been reported to be a positive regulator of tumor angiogenesis factors such as VEGF (28-30). It is important to note that higher than normal expression of VEGF may have clinical significance in prostate cancer (34). We hypothesize that cav-1–mediated increases in the level of intracellular P-Akt trigger enhanced expression of this angiogenic factor. Increased levels of intracellular cav-1 in the metastatic RM-9 nodules that developed in PBcav-1 mice may be due to increased uptake of circulating serum cav-1 compared with RM-9 nodules that develop in nontransgenic littermates. Further studies may reveal important associations between cav-1 overexpression, stabilization of P-Akt, and VEGF overexpression and secretion.

In our previous analysis of serum cav-1 levels, we found significantly higher serum cav-1 levels in men with prostate cancer than in normal men and men with benign hyperplasia (18, 19), raising the possibility that serum cav-1 may also affect the metastatic potential of human prostate cancer. Together with the possibility of a field effect mediated by secretion of cav-1 in hyperplastic and/or premalignant prostatic tissues, the presence of substantial levels of serum cav-1 in the absence of malignancy may be considered a possible risk factor for the development and progression of prostate cancer, and further studies in this area are warranted.

The results of our experimental metastasis analyses specifically showed that the secretion of cav-1 into the circulation promoted the growth of experimental lung metastases in PBcav-1 mice (Fig. 7). Although RM-9 cells are cav-1–secreting cells, our results clearly show that host-derived serum cav-1 contributes to metastatic activities once the cells are established at an attached site in the experimental metastasis model system. The PBcav-1 cohort generated two to five times more lung metastases than the other three genotype cohorts, but after the systemic cav-1 Ab treatments, the number of the lung nodules was brought down close to the *cav-1*$^{-/-}$ cohort level. Surgical castration treatment also resulted in significant reduction in the number of tumor lung nodules in all genotype cohorts. However, the data showed that in general, cav-1 Ab treatment was more effective than surgical castration in suppression of experimental metastasis (Fig. 7). Combination treatment with surgical castration plus cav-1 Ab was remarkably effective in suppressing metastasis, but the suppression achieved was not statistically different than the effects of cav-1 Ab treatment alone (P = 0.69–0.89 except in case of *cav-1*$^{-/-}$). But because actual number of metastasis was very low in both treatment cases, it is conceivable that further studies using additional models would reveal potential therapeutic advantages associated with this

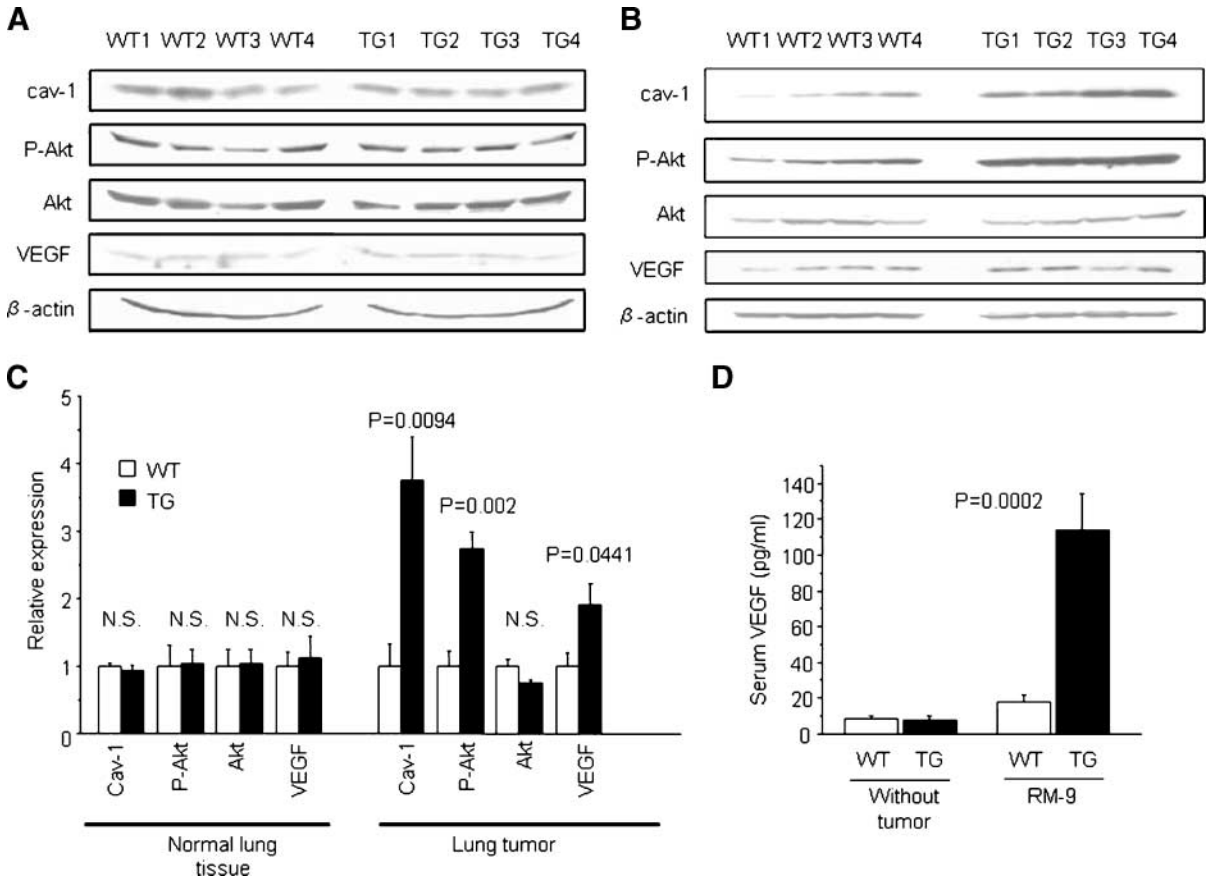

FIGURE 6. Western blot analysis of normal lung tissues and lung tumor nodules from metastasis-bearing nontransgenic and transgenic mice. **A.** Expression analysis (Western blot) of cav-1, P-Akt, Akt, and VEGF of normal lung tissues taken from lungs that harbored RM-9 lung tumor nodules and **B.** RM-9 metastatic lesions from nontransgenic (*WT*) and PBcav-1 (*TG*) mice. Each lane represents tissues from an individual mouse. **C.** Relative expressions of Western blotting (**A** and **B**) were measured by densitometry. **D.** Increased serum VEGF levels in nontumor-bearing nontransgenic littermates and PBcav-1 male mice (*left*) and metastases-bearing mice nontransgenic littermates and PBcav-1 male mice (*right*). N.S. = not statistically significant.

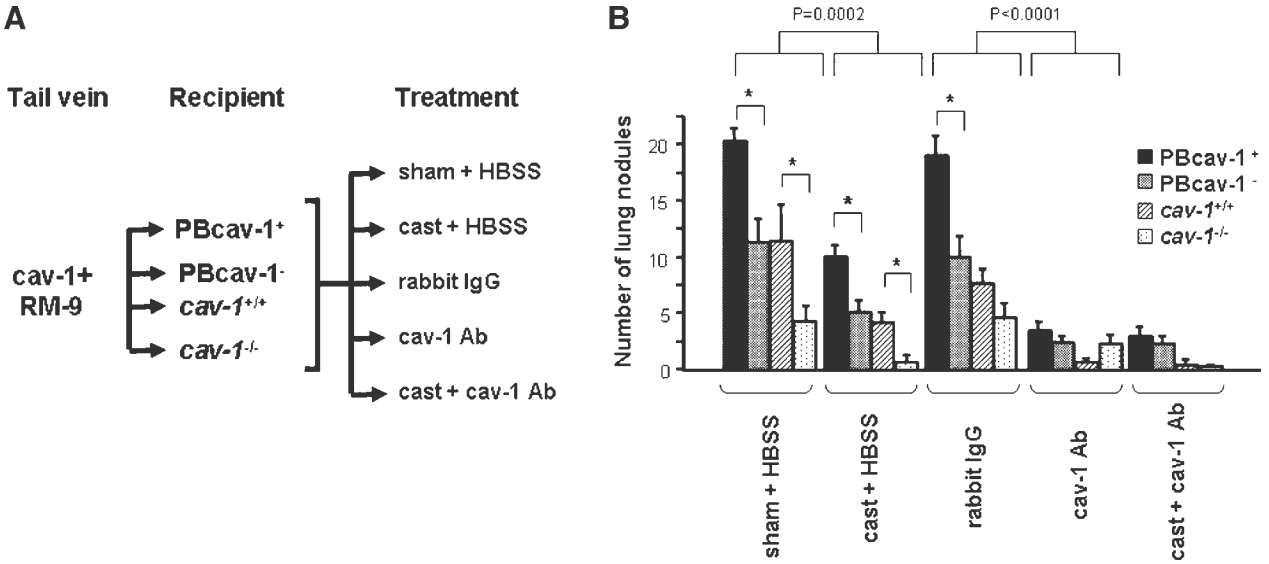

FIGURE 7. Suppression of experimental RM-9 metastasis by androgen deprivation and cav-1 Ab treatment in four genetic cohorts of mice with different endogenous serum cav-1 levels. **A.** Schematic diagram of experimental metastasis intervention experiment. Cohorts of PBcav-1$^+$, PBcav-1$^-$ (nontransgenic) littermates, *cav-1* $^{-/-}$, and *cav-1*$^{+/+}$ male mice received a tail vein injection of RM-9 mouse prostate cancer cells and each cohort was divided into five treatment groups: sham + HBSS, castration (*cast + HBSS*), control rabbit IgG, cav-1 Ab, or castration + cav-1 Ab. **B.** Number of experimental lung metastases scored for each treatment within each genotype cohort 21 d after RM-9 injection. *, $P < 0.05$ between the bracketed groups.

combination approach. Overall, these data suggest the possible convergence of cav-1 expression and secretion, and androgen-receptor signaling. This notion is consistent with our initial report regarding cav-1 expression in prostate cancer (35), which defined an important relationship between cav-1 expression, androgen receptor expression, and androgen sensitivity in prostate cancer cells.

In summary, we have generated a novel transgenic mouse, PBcav-1, and showed that cav-1 overexpression leads to epithelial prostatic hyperplasia accompanied by increased levels of P-Akt, reduced nuclear $p27^{Kip1}$, and increased serum cav-1 levels. We exploited the induction of secreted cav-1 without the complications of active malignancy to test the effects of localized cav-1 secretion and serum cav-1 on orthotopic prostate cancer growth and experimental metastasis, respectively. We showed that RM-9 cells formed significantly larger orthotopic prostate tumors in PBcav-1 mice than in their nontransgenic littermates. Using this model of androgen-sensitive metastatic prostate cancer, we also tested the effects of surgical castration and/or cav-1 Ab treatment on the development of experimental lung metastases. The data showed that host-derived cav-1 is causally associated with experimental metastasis and validated systemic cav-1 Ab treatment as a potential therapy for prostate cancer. Further experiments should test the feasibility of targeting systemic cav-1 protein as well as combination treatment of cav-1 Ab and antiandrogens as novel therapeutic strategies.

Materials and Methods

Generation and Genotyping of Cav-1–Expressing Transgenic Mice

Plasmid carrying PBcav-1 transgene was generated using our previously constructed MMTVcav-1 plasmid containing mouse mammary tumor virus promoter, rabbit β-globin splice sequences (part of exon I, intron I, and exon II) 687-bp mouse cav-1 cDNA (35), and bGH-polyadenylation sequence (36). The mouse mammary tumor virus promoter was excised by BamHI and replaced by a short rat PB promoter fragment (−426/+28) that was lifted from SK-PB/SV40Tag plasmid by SalI digestion (20). To make the vector and promoter DNA compatible for ligation, GA and TC base fill-ins were done on BamHI and SalI fragments, respectively. Recombinant PBcav-1 plasmid DNA was purified, and the integrity of the PBcav-1 transgene was confirmed by sequencing. The resulting PBcav-1 plasmid was linearized by KpnI and NotI, and the 2.2-kb PBcav-1 transgene fragment, devoid of vector sequences, was microinjected into fertilized C57B6 mouse embryos.

Purified transgene DNA was injected into the pronucleus of a fertilized C57BL6/J embryo according to the standard technique used in the Transgenic Core facility at Baylor College of Medicine.

The founder transgenic mice were screened for transgene presence and transmission by using PCR with forward 5′-CCATGTTCATGCCTTCTTCT-3′ and reverse 5′-ATCGTAGACAACAAGCGGTA-3′ primers using the following conditions: 95°C × 2 min, 94°C × 30 s, 55°C × 30 s, and 72°C × 30 s, for 35 cycles.

Mice were housed under specific pathogen-free conditions in facilities accredited by the American Association for Accreditation of Laboratory Animal Care. Three to 13-mo-old mice were used throughout this study unless otherwise indicated in the text. All experiments were conducted in accordance with the principles and procedures outlined in the NIH 's Guide for the Care and Use of Laboratory Animals.

RNA Isolation and Analysis

Total RNA was isolated from microdissected mouse tissues by using a RiboPure RNA purification kit from Ambion. The

cDNA was generated using 1.6 μg of total RNA, and RT reactions were carried out using a High Capacity cDNA Archive kit (Applied Biosystems) according to the manufacturer's protocol. Reverse transcription-PCR was done as previously described (37) using PBcav-1 transgene–specific primers P1:5′-CCTTGTCAGTGAGGTCCAGATA-3′ and P2: 5′-CGTCGTCGTTGAG-ATGCTT-3′. Quantitative real-time PCR analysis of cav-1 expression was done using the Universal PCR Master Mix and TaqMan Gene expression assay for mouse cav-1 Mm_00483057 (Applied Biosystems).

Analysis of Androgen Sensitivity in PBcav-1 Prostatic Tissues

PBcav-1 adult male mice and their nontransgenic littermates were subjected to surgical castration, surgical castration plus implantation of testosterone propionate in silastic tubing pellets, or sham operations as previously described (35). Three weeks following these procedures, animals were euthanized, and whole prostatic tissues were evaluated. Wet weights of the whole prostates from PBcav-1 mice and their nontransgenic littermates were compared for each experimental condition.

Animal Models

Orthotopic Prostate Tumors. Subconfluent mouse RM-9 prostate cancer cells were prepared and injected to PBcav-1 and nontransgenic mice as described preciously (22). Cells (5×10^3) were injected directly into dorsolateral prostates of the mice, and after 21 d, the tumors were excised and weighted.

Experimental Metastasis. Cells (5×10^3) of RM-9 were injected via tail vein as described previously (22). After 21 d, mice were euthanized, and serum and tumor lung nodules were collected. The number and size on the long axis of lung tumor nodules were measured with help of dissecting microscope. Lung tumor nodules that were 2 to 3 mm long on the longest axis and normal lung tissues were microdissected and snap frozen in liquid nitrogen and stored at −80°C. For histologic examinations, the lung tissues of interest were snap frozen for cryostat sectioning or were fixed in 10% phosphate-buffered formalin before being embedded in paraffin. Selected samples of the fixed lung metastases were photographed with the use of a Nikon Coolpix 4500 camera.

Suppression of Experimental Metastasis

Four different genotypes of adult male mice-PBcav-1, nontransgenic littermates, *cav-1*$^{-/-}$, and *cav-1*$^{+/+}$ (20) were injected with RM-9 prostate cancer cells via tail vein as described above. Each cohort of four genotypically different mice were randomly divided into five treatment groups: sham + HBSS, castration + HBSS, rabbit IgG, cav-1 Ab, and castration + cav-1 Ab. Mice that were included in the castration treatment groups underwent surgical castration 1 wk before the tumor cell injection. Mice that were included in the Ab treatment groups were treated as appropriate with 100 μL of HBSS (control), 10 μg/100 μL rabbit IgG (Santa Cruz Biotechnology), or 10 μg/100 μL cav-1 Ab (Santa Cruz Biotechnology) every other day for 21 d as previously described (13). At the end of the time course mice were euthanized, and the number of lung tumor nodules were counted with the aid of a dissecting microscope as described previously (13).

Mouse Cav-1 and VEGF Levels in Serum Samples

Serum samples were assayed for mouse cav-1 by ELISA, as previously described (18, 19). For the serum VEGF assay, a mouse VEGF ELISA kit was purchased from R&D Systems. The serum samples were diluted (1:2 in the specific diluent) and tested according to the manufacturer's instructions. The kit recognizes both 164- and 120-amino acid isoforms of mouse VEGF. The minimum detectable concentration is <3 pg/mL.

Preparation of Tissue Extracts and Conditioned Medium

Tissues were homogenized in ice-cold lysis buffer [20 mmol/L Tris (pH 7.5) containing 150 mmol/L NaCl, 1 mmol/L Na_2EDTA, 1 mmol/L EGTA, 1% NP40, 1% sodium deoxycholate, 2.5 mmol/L sodium pyrophosphate, 1 mmol/L β-glycerophosphate, 1 mmol/L Na_3VO_4, and 1 μg/mL of leupeptin]. The lysates were centrifuged for 10 min at 20,000 × *g* and 4°C to remove any debris and insoluble material. The resulting samples were stored at −80°C, and protein concentrations were determined using a protein assay kit (Bio-Rad).

For preparation of prostate organ culture–conditioned medium, the prostate tissues from individual mice were collected and cut into ~1-mm pieces and washed thrice with ice-cold PBS. After the organ pieces were incubated in 0.5 mL of serum-free medium for 24 h at 37°C, the medium was collected and centrifuged at 1,000 × *g* and then at 100,000 × *g* to minimize debris contamination. The protein in the medium was precipitated by application of trichloroacetic acid and then the precipitate was washed with acetone and redissolved in 30 μL of lysis buffer.

Western Blot Analysis

Protein extract from mouse tissues (50 μg) or 15 μL of the prepared conditioned medium was mixed with 6× loading buffer and separated on 12% SDS-PAGE. The separated proteins were transferred to nitrocellulose membranes and were blotted with specific Ab for 12 to 18 h at 4°C. Horseradish peroxidase–conjugated secondary antibodies and an enhanced chemiluminescence substrate kit (Pierce Biotechnology) were used for detection of specific proteins. Densitometry of the bands was done with the NIH IMAGE software program. For quantitative analyses, the intensity of protein bands was normalized to the intensity of β-actin in the same sample.

Rabbit polyclonal antibodies against cav-1 (sc-894) and VEGF (sc-507) were obtained from Santa Cruz Biotechnology. Monoclonal Ab against PKBα/Akt (clone 55) was purchased from BD Biosciences, and rabbit polyclonal Ab against phospho-Akt (Ser473) was from Cell Signaling Technology. Monoclonal anti–β-actin (clone AC-15) was from Sigma-Aldrich.

Histologic and Immunohistochemical Procedures

Prostate tissues from PBcav-1 transgenic mice and their nontransgenic littermates or from lung metastases these mice developed were fixed in 10% formalin and processed for routine paraffin embedding and sectioning. Histologic features of the tissues were evaluated on H&E-stained sections. Apoptotic and proliferative activities in the tissues were investigated using the TUNEL technique and PCNA immunostaining, respectively, following the procedure previously developed (38). The tissues were also immunostained with antibodies to cav-1 (Santa Cruz Biotechnology), P-Akt

(Ser473; Cell Signaling), and $p27^{Kip1}$ (a generous gift from Dr. Xin Lu, Ludwig Institute for Cancer Research, Oxford Branch, Oxford, United Kingdom) using the avidin-biotin-peroxidase complex procedure and an ABC kit (Vector Laboratories). Immunolabeling was assessed quantitatively via computer-assisted image analysis of 20 to 30 randomly selected microscopic fields at ×200 magnification. The data were recorded as apoptotic index, which is the number of apoptotic bodies per 1,000 epithelial cells or the nuclear labeling rate for $p27^{Kip1}$ or PCNA staining.

Statistical Analyses

All values are expressed as means ± SEM. Statistical analyses were carried out using the two-tailed Student's unpaired *t* test and, for more than two groups, by using ANOVA followed by Fisher's protected least significant difference analysis.

The correlation between serum VEGF level and the number of experimental lung metastases was evaluated with the simple regression analysis. Differences were considered statistically significant when the P value is <0.05. All analyses were done using Statview 5.0 software (SAS Institute).

Disclosure of Potential Conflicts of Interest

No potential conflicts of interest were disclosed.

Acknowledgments

We are grateful for M.D. Anderson Cancer Center DNA Analysis Facility which is funded by National Cancer Institute grant CA16672 for mouse genotyping.

References

1. Shaul PW, Anderson RG. Role of plasmalemmal caveolae in signal transduction. Am J Physiol 1998;275:L843–51.

2. Sternberg PW, Schmid SL. Caveolin, cholesterol and Ras signalling. Nat Cell Biol 1999;1:E35–7.

3. Williams TM, Lisanti MP. Caveolin-1 in oncogenic transformation, cancer, and metastasis. Am J Physiol 2005;288:C494–506.

4. Cavallo-Medved D, Mai J, Dosescu J, Sameni M, Sloane BF. Caveolin-1 mediates the expression and localization of cathepsin B, pro-urokinase plasminogen activator and their cell-surface receptors in human colorectal carcinoma cells. J Cell Sci 2005;118:1493–503.

5. Li L, Yang G, Ebara S, et al. Caveolin-1 mediates testosterone-stimulated survival/clonal growth and promotes metastatic activities in prostate cancer cells. Cancer Res 2001;61:4386–92.

6. Tahir SA, Yang G, Goltsov AA, et al. Tumor cell-secreted caveolin-1 has proangiogenic activities in prostate cancer. Cancer Res 2008;68:731–9.

7. Williams TM, Hassan GS, Li J, et al. Caveolin-1 promotes tumor progression in an autochthonous mouse model of prostate cancer: genetic ablation of Cav-1 delays advanced prostate tumor development in tramp mice. J Biol Chem 2005; 280:25134–45.

8. Woodman SE, Ashton AW, Schubert W, et al. Caveolin-1 knockout mice show an impaired angiogenic response to exogenous stimuli. Am J Pathol 2003;162: 2059–68.

9. Yang G, Truong LD, Timme TL, et al. Elevated expression of caveolin is associated with prostate and breast cancer. Clin Cancer Res 1998;4:1873–80.

10. Yang G, Truong LD, Wheeler TM, Thompson TC. Caveolin-1 expression in clinically confined human prostate cancer: a novel prognostic marker. Cancer Res 1999;59:5719–23.

11. Ho CC, Huang PH, Huang HY, Chen YH, Yang PC, Hsu SM. Up-regulated caveolin-1 accentuates the metastasis capability of lung adenocarcinoma by inducing filopodia formation. Am J Pathol 2002;161:1647–56.

12. Joo HJ, Oh DK, Kim YS, Lee KB, Kim SJ. Increased expression of caveolin-1 and microvessel density correlates with metastasis and poor prognosis in clear cell renal cell carcinoma. BJU Int 2004;93:291–6.

13. Kato K, Hida Y, Miyamoto M, et al. Overexpression of caveolin-1 in esophageal squamous cell carcinoma correlates with lymph node metastasis and pathologic stage. Cancer 2002;94:929–33.

14. Tahir SA, Yang G, Ebara S, et al. Secreted caveolin-1 stimulates cell survival/clonal growth and contributes to metastasis in androgen-insensitive prostate cancer. Cancer Res 2001;61:3882–5.

15. Wu D, Foreman TL, Gregory CW, et al. Protein kinase cε has the potential to advance the recurrence of human prostate cancer. Cancer Res 2002;62:2423–9.

16. Bartz R, Zhou J, Hsieh JT, Ying Y, Li W, Liu P. Caveolin-1 secreting LNCaP cells induce tumor growth of caveolin-1 negative LNCaP cells *in vivo*. Int J Cancer 2008;122:520–5.

17. Li L, Ren CH, Tahir SA, Ren C, Thompson TC. Caveolin-1 maintains activated Akt in prostate cancer cells through scaffolding domain binding site interactions with and inhibition of serine/threonine protein phosphatases PP1 and PP2A. Mol Cell Biol 2003;23:9389–404.

18. Tahir SA, Ren C, Timme TL, et al. Development of an immunoassay for serum caveolin-1: a novel biomarker for prostate cancer. Clin Cancer Res 2003;9:3653–9.

19. Tahir SA, Frolov A, Hayes TG, et al. Preoperative serum caveolin-1 as a prognostic marker for recurrence in a radical prostatectomy cohort. Clin Cancer Res 2006;12:4872–5.

20. Greenberg NM, DeMayo F, Finegold MJ, et al. Prostate cancer in a transgenic mouse. Proc Natl Acad Sci U S A 1995;92:3439–43.

21. Greenberg NM, DeMayo FJ, Sheppard PC, et al. The rat probasin gene promoter directs hormonally and developmentally regulated expression of a heterologous gene specifically to the prostate in transgenic mice. Mol Endocrinol 1994; 8:230–9.

22. Cao G, Yang G, Timme TL, et al. Disruption of the caveolin-1 gene impairs renal calcium reabsorption and leads to hypercalciuria and urolithiasis. Am J Pathol 2003;162:1241–8.

23. Baley PA, Yoshida K, Qian W, Sehgal I, Thompson TC. Progression to androgen insensitivity in a novel *in vitro* mouse model for prostate cancer. J Steroid Biochem Mol Biol 1995;52:403–13.

24. Nasu Y, Bangma CH, Hull GW, et al. Adenovirus-mediated interleukin-12 gene therapy for prostate cancer: suppression of orthotopic tumor growth and pre-established lung metastases in an orthotopic model. Gene Ther 1999;6: 338–49.

25. Testa JR, Bellacosa A. AKT plays a central role in tumorigenesis. Proc Natl Acad Sci U S A 2001;98:10983–5.

26. Nicholson KM, Anderson NG. The protein kinase B/Akt signalling pathway in human malignancy. Cell Signal 2002;14:381–95.

27. Vivanco I, Sawyers CL. The phosphatidylinositol 3-Kinase AKT pathway in human cancer. Nat Rev 2002;2:489–501.

28. Laughner E, Taghavi P, Chiles K, Mahon PC, Semenza GL. HER2 (neu) signaling increases the rate of hypoxia-inducible factor 1α (HIF-1α) synthesis: novel mechanism for HIF-1-mediated vascular endothelial growth factor expression. Mol Cell Biol 2001;21:3995–4004.

29. Tan C, Cruet-Hennequart S, Troussard A, et al. Regulation of tumor angiogenesis by integrin-linked kinase (ILK). Cancer Cell 2004;5:79–90.

30. Stanley G, Harvey K, Slivova V, Jiang J, Sliva D. Ganoderma lucidum suppresses angiogenesis through the inhibition of secretion of VEGF and TGF-β1 from prostate cancer cells. Biochem Biophysic Res Commun 2005; 330:46–52.

31. Li L, Ittmann MM, Ayala G, et al. The emerging role of the PI3-K-Akt pathway in prostate cancer progression. Prostate Cancer Prostatic Dis 2005;8: 108–18.

32. Blume-Jensen P, Hunter T. Oncogenic kinase signalling. Nature 2001;411: 355–65.

33. Brazil DP, Hemmings BA. Ten years of protein kinase B signalling: a hard Akt to follow. Trends Biochem Sci 2001;26:657–64.

34. Ferrer FA, Miller LJ, Andrawis RI, et al. Vascular endothelial growth factor (VEGF) expression in human prostate cancer: *in situ* and *in vitro* expression of VEGF by human prostate cancer cells. J Urol 1997;157:2329–33.

35. Nasu Y, Timme TL, Yang G, et al. Suppression of caveolin expression induces androgen sensitivity in metastatic androgen-insensitive mouse prostate cancer cells. Nat Med 1998;4:1062–4.

36. Ma ZQ, Chua SS, DeMayo FJ, Tsai SY. Induction of mammary gland hyperplasia in transgenic mice over-expressing human Cdc25B. Oncogene 1999;18: 4564–76.

37. Li L, Abdel Fattah E, Cao G, et al. Glioma pathogenesis-related protein 1 exerts tumor suppressor activities through proapoptotic reactive oxygen species-c-Jun-NH2 kinase signaling. Cancer Res 2008;68:434–43.

38. Yang G, Timme TL, Park SH, Wu X, Wyllie MG, Thompson TC. Transforming growth factor β 1 transduced mouse prostate reconstitutions: II. Induction of apoptosis by doxazosin. Prostate 1997;33:157–63.

Caveolin-1 Promotes Autoregulatory, Akt-Mediated Induction of Cancer-Promoting Growth Factors in Prostate Cancer Cells

Likun Li, Chengzhen Ren, Guang Yang, Alexei A. Goltsov, Ken-ichi Tabata, and Timothy C. Thompson

Department of Genitourinary Medical Oncology, The University of Texas M. D. Anderson Cancer Center, Houston, Texas

Abstract

Caveolin-1 (cav-1) and the cancer-promoting growth factors vascular endothelial growth factor (VEGF), transforming growth factor β1 (TGF-β1), and fibroblast growth factor 2 (FGF2) are often found to be upregulated in advanced prostate cancer and other malignancies. However, the relationship between cav-1 overexpression and growth factor upregulation remains unclear. This report presents, to our knowledge, the first evidence that in prostate cancer cells, a positive autoregulatory feedback loop is established in which VEGF, TGF-β1, and FGF2 upregulate cav-1, and cav-1 expression, in turn, leads to increased levels of VEGF, TGF-β1, and FGF2 mRNA and protein, resulting in enhanced invasive activities of prostate cancer cells, i.e., migration and motility. Our results further show that cav-1–enhanced mRNA stability is a major mechanism underlying the upregulation of these cancer-promoting growth factors, and that PI3-K-Akt signaling is required for forming this positive autoregulatory feedback loop. (Mol Cancer Res 2009;7(11): 1781–91)

Introduction

Prostate cancer is one of the most common types of cancers and the second leading cause of cancer-related death in American men (1). In most cases, death from prostate cancer results from metastatic disease. Understanding the mechanisms underlying the progression of prostate cancer will facilitate the development of biomarkers and novel therapeutic strategies to control this devastating malignancy.

Caveolin-1 (cav-1) is a major structural component of caveolae, specialized plasma membrane invaginations that are involved in molecular transport, endocytosis, cell adhesion, and signal transduction (2, 3). The role of cav-1 in cancer is complex and remains somewhat controversial (reviewed in refs. 4-7). We previously found that elevated expression of cav-1 is associated with human prostate cancer, correlated with tumor angiogenesis, and may function as a valuable prognostic marker (8-12). In alignment with a growing body of clinical data that showed upregulation of cav-1 expression in various types of malignancies and multidrug-resistant tumor cells (reviewed in refs. 4, 6, 7), experimental results showed that suppression of cav-1 expression reverses androgen insensitivity in metastatic androgen-insensitive mouse prostate cancer cells (13) and that genetic ablation of cav-1 attenuates the development and progression of prostate tumors in TRAMP mice (14). We previously showed that cav-1 was secreted by mouse and human prostate cancer cell lines and that secreted cav-1 promoted cancer cell survival and clonal growth *in vitro* (15-17). We further showed that tumor cell–secreted cav-1 promotes proangiogenic activities in prostate cancer through the PI3-K-Akt-eNOS signaling module (18). With regard to the underlying mechanism(s) responsible for cav-1–mediated oncogenic activities, we showed that cav-1 maintains activated Akt in prostate cancer cells through binding to and inhibition of the serine/threonine protein phosphatases PP1 and PP2A (15).

Of note, multiple growth factors (GF) with tumor-promoting activities, including vascular endothelial GF (VEGF), transforming GF β1 (TGF-β1), and fibroblast GFs (FGF), are also upregulated in advanced cancer (19-22). VEGF is one of the key mediators of angiogenesis that is produced at high levels in many types of tumors; it promotes proliferation, survival, and migration of endothelial cells and is essential to blood vessel formation and neovascularization (23, 24). TGF-β1 is a potent regulator of cell proliferation and extracellular matrix remodeling, with tumor-suppressor functions in the normal prostate gland and tumor-promoter functions in malignant and metastatic prostate cancer (25, 26). FGF2 is expressed at increased levels in human prostate, bladder, renal, and testicular cancers and play an important role in the neovascularization process that occurs in inflammation, angioproliferative diseases, and tumor growth (27, 28). The intricate balance of these GFs is crucial to the regulation of normal cell growth. Disruption of normal GF homeostasis in malignancy is often associated with apoptotic evasion, uncontrolled proliferation, and increased invasive potential. Various mechanisms are reported to be involved in deregulation of these GFs in cancer cells, including transcriptional regulation (29-31) and alteration of mRNA stability (32-35). The potential association of cav-1

Received 6/10/09; revised 9/16/09; accepted 9/24/09; published OnlineFirst 11/10/09.

Grant support: Grant R01-50588 from the National Cancer Institute and by grant PC051247 from the Department of Defense.

The costs of publication of this article were defrayed in part by the payment of page charges. This article must therefore be hereby marked *advertisement* in accordance with 18 U.S.C. Section 1734 solely to indicate this fact.

Note: Supplementary data for this article are available at Molecular Cancer Research Online (http://mcr.aacrjournals.org/).

L. Li and C. Ren contributed equally to this work.

Requests for reprints: Timothy C. Thompson, Department of Genitourinary Medical Oncology, Unit 1374-Rsch, The University of Texas M. D. Anderson Cancer Center, 1515 Holcombe Boulevard, Houston, TX 77030-4009. Phone: 713-792-9955; Fax: 713-792-9956. E-mail: timthomp@mdanderson.org

doi:10.1158/1541-7786.MCR-09-0255

and cancer-promoting GFs in malignant progression prompted us to investigate whether cav-1 and expression of specific cancer-promoting GFs are functionally and mechanistically linked in prostate cancer progression. In this study, we found that multiple GFs stimulate cav-1 expression in prostate cancer cells and that cav-1 expression leads to increased levels of VEGF, TGF-β1, and FGF2 and enhances cancer cell migration and motility in an Akt-dependent manner. Furthermore, we found that cav-1–enhanced mRNA stability is a major mechanism for the upregulation of these cancer-promoting GFs.

Results

Induction of Cav-1 Expression and Secretion by GFs

Because overexpression of specific cancer-promoting GFs occurs in parallel with cav-1 overexpression in many types of malignancies, including prostate cancer, we sought to determine whether there was any potential correlation between cav-1 and these GFs. We first examined the ability of selected GFs to stimulate cav-1 expression. Since our early observations suggested that GF treatment does not stimulate cav-1 expression in early passage (cav-1 negative) LNCaP cells, a cav-1–expressing LNCaP variant, LNCaP (c^+), which expresses low-moderate levels of cav-1, and DU145 and PC-3, which express high levels of cav-1, were used for this part of the study (see Fig. 1A and the insert in Fig. 1B for the relative cav-1 levels in these three cell lines). Treatment with multiple GFs, including platelet-derived GF (PDGF), nerve GF (NGF), FGF1, FGF2, epidermal GF (EGF), TGF-β1, and VEGF, led to significantly increased cav-1 protein levels in LNCaP (c^+) cells (1.5- to 3-fold) and slightly increased cav-1 protein levels in DU145 and PC-3 cells (Fig. 1A and B). Similar to the low–cav-1 LNCaP (c^+), a cav-1 antisense stable mouse prostate cancer cell clone ABAC3 (13) also showed induction of cav-1 expression and secretion by GFs (Supplementary Fig. S1).

We previously found that tumor cell–secreted cav-1 stimulates cell survival and clonal growth and contributes to angiogenesis and metastasis (17, 18), so it was also of interest to determine whether these GFs can also increase cav-1 secretion. As shown in Fig. 1C and D, with the exception of NGF, treatment with the GFs also led to increased levels of secreted cav-1 in LNCaP (c^+) cells (1.5- to 2.0-fold). Although the GFs had only minor effects on the cav-1 expression in high–cav-1 prostate cancer cells DU145 and PC-3, they significantly increased cav-1 secretion from these two cell lines (1.5 to 3.2-fold; Fig. 1C and D).

Cav-1 Expression Stimulates Expression of VEGF, TGF-β1, and FGF2

Because multiple GFs are capable of inducing cav-1 expression and cav-1 upregulation occurs in focal areas of prostate

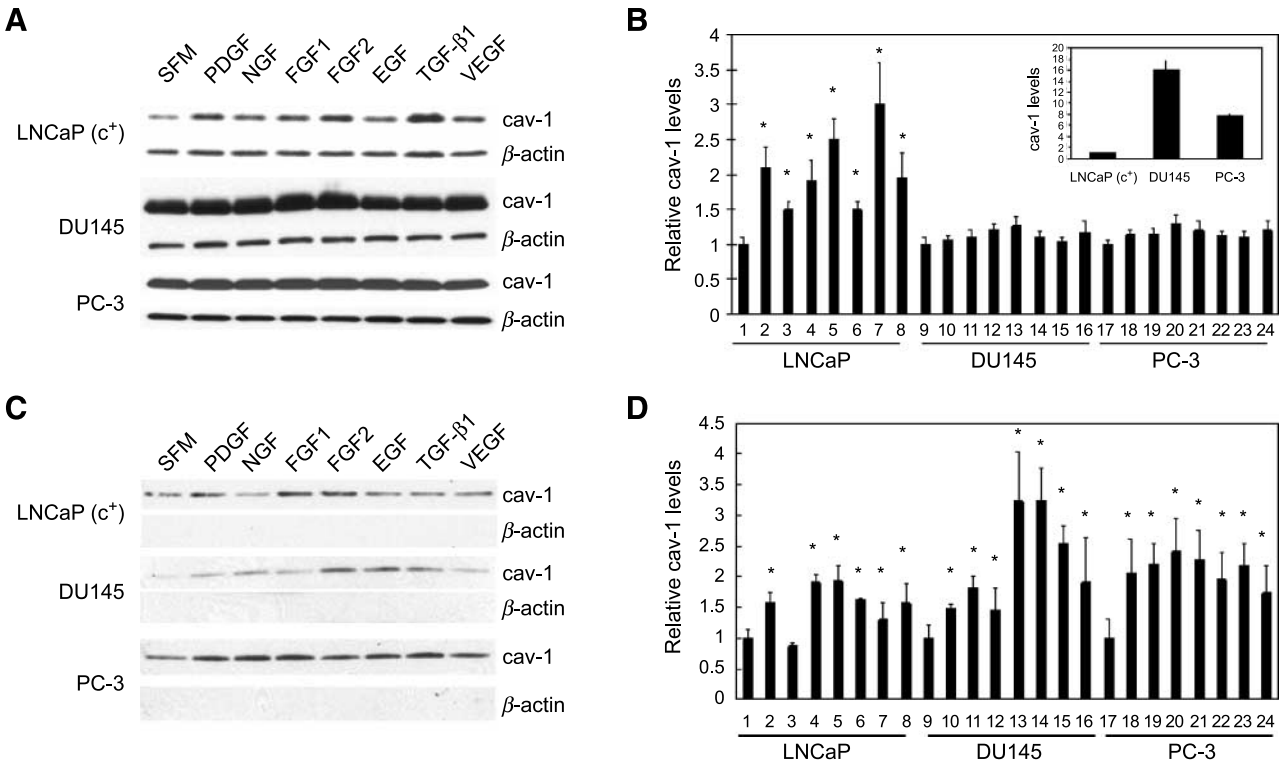

FIGURE 1. Induction of cav-1 expression and secretion by GFs. **A.** Representative Western blot showing cellular levels of cav-1 in LNCaP (c^+), DU145, and PC-3 cells after incubation of cells in SFM with and without the indicated GFs for 48 h. **B.** Quantitative analysis of cellular levels of cav-1 in GF-treated LNCaP (c^+), DU145, and PC-3 cells. Insert (**B**), relative cav-1 levels in these three cell lines. **C.** Representative Western blot showing secreted cav-1 in conditioned medium after incubation of LNCaP (c^+), DU145, and PC-3 cells in SFM with and without indicated GFs for 24 h. The equivalents of conditioned medium produced from 5.0×10^5 cells were loaded on gel for the determination of secreted cav-1 levels. **D.** Quantitative analysis of levels of secreted cav-1 in conditioned medium derived from GF-treated LNCaP (c^+), DU145, and PC-3 cells. Columns, mean of three independent experiments (**B** and **D**); bars, SD; *, statistically significant $P < 0.05$. Lanes 1, 9, and 17, SFM; lanes 2,10, and 18, PDGF; lanes 3, 11, and 19, NGF; lanes 4, 12, and 20, FGF1; lanes 5, 13, and 21, FGF2; lanes 6, 14, and 22, EGF; lanes 7, 15, and 23, TGF-β1; lanes 8, 16, and 24, VEGF.

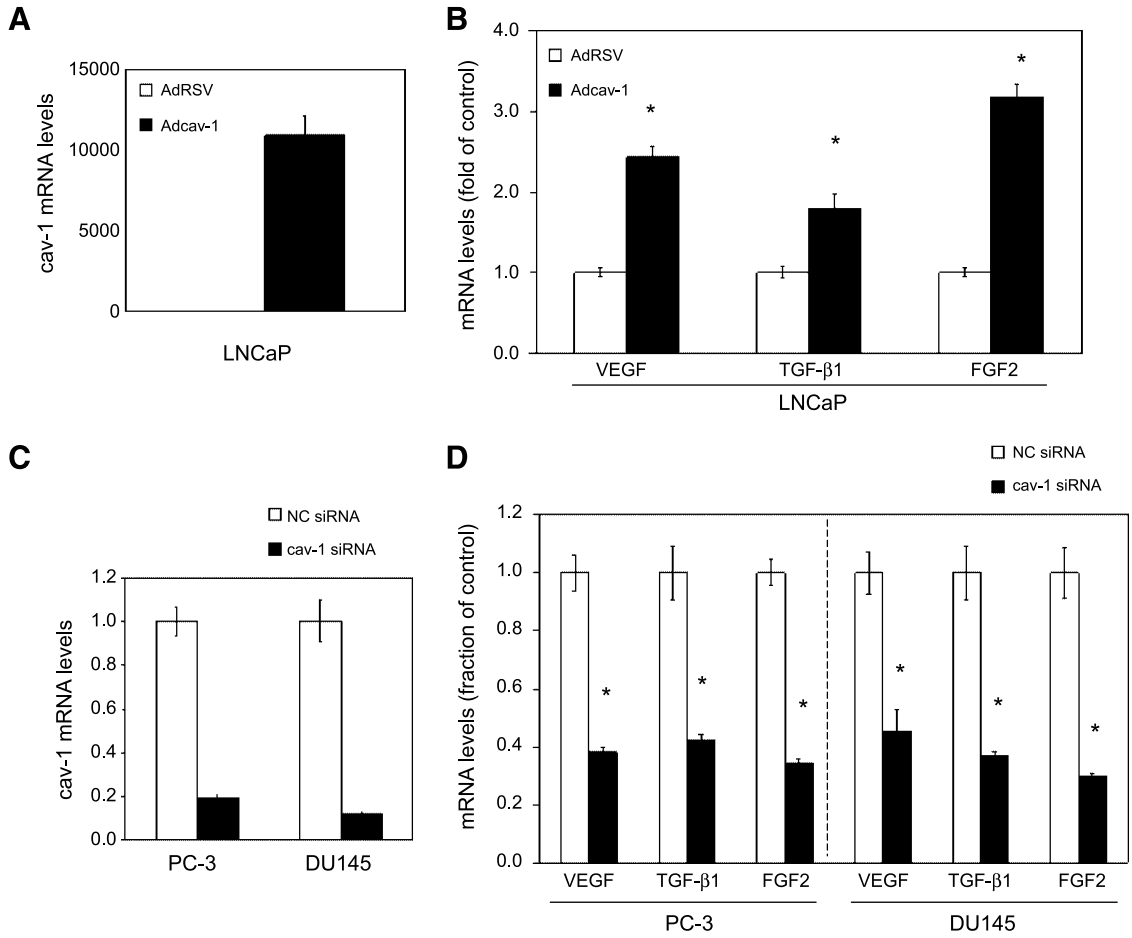

FIGURE 2. Cav-1 upregulates mRNA levels of VEGF, TGF-β1, and FGF2. Quantitative reverse transcription-PCR analysis for mRNA levels of cav-1, VEGF, TGF-β1, and FGF2 in cav-1–manipulated prostate cancer cells. Columns, mean; bars, SD. *, statistically significant, $P < 0.05$. **A.** mRNA levels of cav-1 in Adcav-1– and AdRSV-infected LNCaP cells. **B.** mRNA levels of VEGF, TGF-β1, and FGF2 in Adcav-1– and AdRSV-infected LNCaP cells. **C.** mRNA levels of cav-1 in cav-1 siRNA– or NC siRNA–transfected PC-3 and DU145 cells. **D.** mRNA levels of VEGF, TGF-β1, and FGF2 in cav-1 siRNA– or NC siRNA-transfected PC-3 and DU145 cells.

cancer (10), we considered the possibility that cav-1 generates a positive-feedback, autoregulatory loop involving cav-1–stimulated GFs. We selected VEGF, TGF-β1, and FGF2 from the panel of GFs that stimulate cav-1 expression on the basis of their previously established importance in prostate cancer progression and focused on these specific GFs in subsequent experiments. As shown in Fig. 2, overexpression of cav-1 in cav-1–negative, low-passage LNCaP prostate cancer cells using adenoviral vector–mediated gene transduction (Fig. 2A) led to significantly increased levels of VEGF, TGF-β1, and FGF2 mRNA (Fig. 2B) and protein (Fig. 3A). In contrast, when endogenous cav-1 in high–cav-1 PC-3 and DU145 prostate cancer cell lines was knocked down by cav-1 small interfering RNA (siRNA; Fig. 2C), FGF2, TGF-β1, and VEGF mRNA (Fig. 2D) and protein levels (Fig. 3B) were remarkably reduced. In addition to its stimulatory effect on the cellular levels of VEGF, TGF-β1, and FGF2, cav-1 promoted the secretion of these GFs into the medium (Fig. 3C), indicating that cav-1 and these cav-1–stimulated GFs can generate a positive autocrine loop.

To confirm the relationship between cav-1 and the expression of these cancer-promoting GFs *in vivo*, we used an LNCaP tet-on stable clone (LNTB25cav) to establish LNTB25cav subcutaneous xenografts as previously described (18). Immunochemical analysis of tumor tissues from the doxycycline + sucrose– and sucrose only–treated mice showed that the induction of cav-1 in the LNTB25cav xenografts resulted in increased expression of VEGF and TGF-β1 (Fig. 3D). Thus, our *in vivo* data validated our *in vitro* results that show increased VEGF and TGF-β1 levels in cav-1–overexpressing cancer cells. We did not include FGF2 immunochemical analysis of tumor tissues owing to low FGF2 protein level in the LNTB25cav tumors.

Akt Activation Is Involved in Cav-1–Mediated Upregulation of VEGF, TGF-β1, and FGF2

We reported previously that overexpression of cav-1 in cav-1–negative LNCaP cells through adenoviral vector–mediated gene transduction led to significantly increased levels of phosphorylated Akt, which in turn led to enhanced cancer

cell survival (15). We wondered whether cav-1–mediated Akt activities are also associated with the expression of cancer-promoting GFs in prostate cancer cells. As we reported previously, overexpression of cav-1 in cav-1–negative LNCaP cells resulted in significantly increased levels of phosphorylated Akt, whereas the phosphorylation status of the c-Jun-NH_2-kinase (JNK), p44/p42, and p38 pathways remained relatively unchanged (Fig. 4A). In contrast, suppression of endogenous cav1 using cav-1–specific siRNA in the high–cav-1 prostate cancer cell lines PC-3 and DU145 reduced the levels of phosphorylated Akt, whereas the activities of JNK, p44/42, and p38 were still relatively unchanged (Fig. 4B). To address whether Akt is involved in cav-1–mediated upregulation of VEGF, TGF-β1, and FGF2, we suppressed Akt activities in LNCaP cells using the PI3-K inhibitor LY294002 (LY) 3 hours after the cells were transduced with cav-1–expressing adenoviral vector. The results showed that the treatment with LY effectively inhibited cav-1–mediated Akt activation and largely if not completely eliminated cav-1–mediated upregulation of VEGF, TGF-β1, and FGF2 (Fig. 4B). Note that LY also suppressed activity of endogenous Akt, leading to lower levels of VEGF, TGF-β1, and FGF2 (Fig. 4B, compare *AdRSV+LY* to *AdRSV*).

Cav-1 Enhances Cancer Cell Motility in an Akt-Dependent Manner

Cell survival and invasion are two important components of cancer progression. Previously, we reported that endogenously expressed and/or secreted cav-1 enhances prostate cancer cell survival and promotes angiogenic activities of endothelial cells (15-18). In this study, we tested the effects of cav-1 on cancer cell motility. Using a wound-healing assay, we showed that Adcav-1–mediated overexpression of cav-1 in cav-1–negative LNCaP cells increased the number of cells ~60% that migrated into the cleared area compared with the number of AdRSV-infected LNCaP cells (Fig. 5A and B). Conversely, suppression of endogenous cav-1 with cav-1 siRNA in high–cav-1 DU145 and PC-3 prostate cancer cells reduced cell migration 30% to 40% compared with that in corresponding control cells that were transfected with NC siRNA (Fig. 5A and B). Treatment with LY effectively blocked cancer cell migration in Adcav-1–transduced LNCaP cells (Fig. 5A and B), demonstrating that the PI3-K-Akt pathway plays an important role in cav-1–mediated cancer cell migration (potentially through VEGF, TGF-β1, and FGF2).

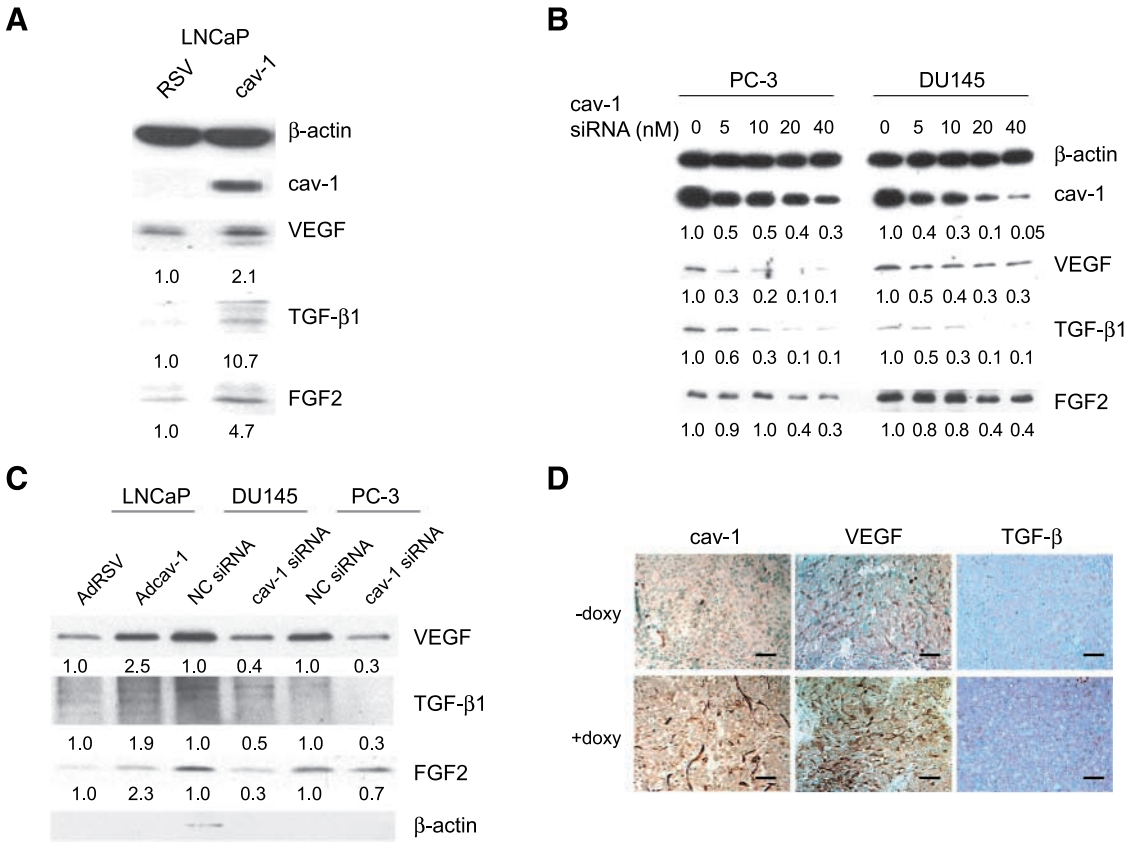

FIGURE 3. Cav-1 upregulates protein levels of VEGF, TGF-β1, and FGF2. **A** to **C.** Western blot analysis for protein levels of cav-1, VEGF, TGF-β1, and FGF2 in cav-1–manipulated prostate cancer cells. The numbers below protein bands are relative protein levels compared with corresponding controls. **A.** Adcav-1– or AdRSV-infected LNCaP cells. **B.** PC-3 and DU145 cells transfected with various concentrations of cav-1 siRNA or NC siRNA. **C.** Secreted VEGF, TGF-β1, and FGF2 in the conditioned medium of Adcav-1– and AdRSV-infected LNCaP cells and in that of cav-1 siRNA– and NC siRNA–transfected PC-3 and DU145 cells. The equivalents of conditioned medium produced from 5.0×10^5 cells were loaded onto the gel. **D.** Immunochemical analysis for cav-1, VEGF, and TGF-β1 levels in doxycycline-induced (+*doxy*) or doxycycline-uninduced (–*doxy*) LNTB25cav tumors. Scale bars, 40 μm.

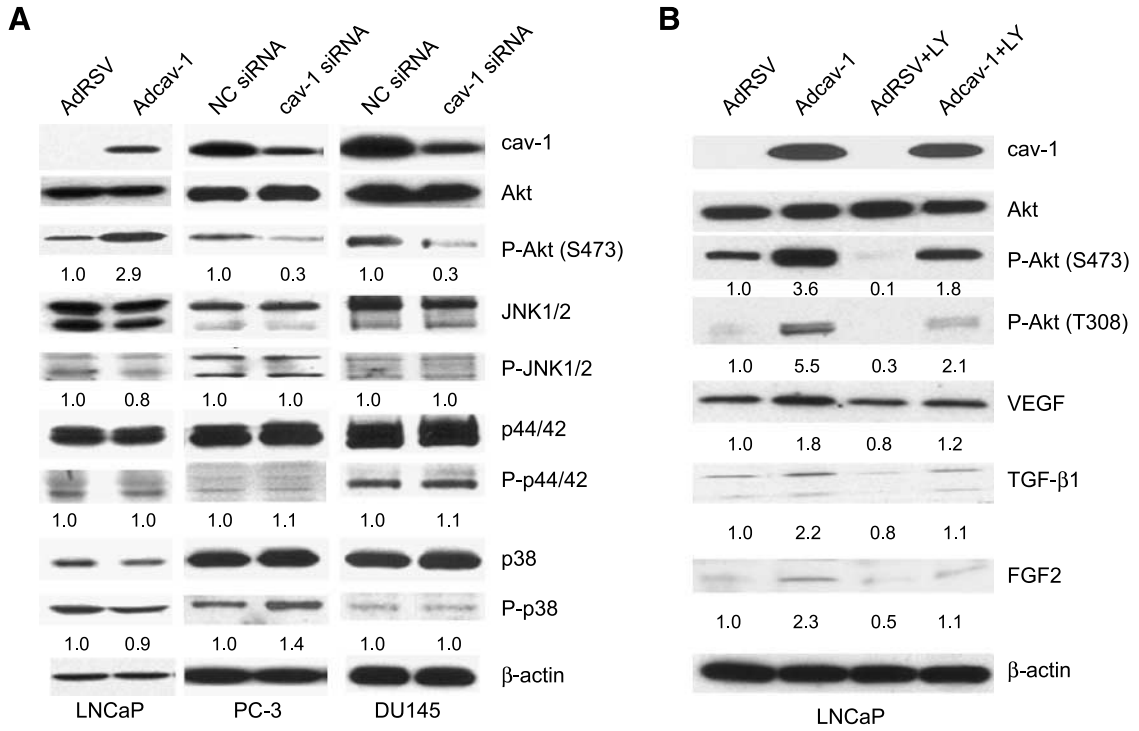

FIGURE 4. Akt is required for the cav-1–induced upregulation of VEGF, TGF-β1, and FGF2. **A.** Western blot analysis showing the increase of Akt phosphorylation in Adcav-1–infected LNCaP cells and the decrease of Akt phosphorylation in cav-1 siRNA–transfected PC-3 and DU145 cells. Note that JNK, p44/42, and p38 phosphorylation were relatively unchanged. **B.** PI3-K inhibitor LY effectively blocked Akt activation and upregulation of VEGF, TGF-β1, and FGF2 in Adcav-1–infected LNCaP cells. The numbers below protein bands are relative protein levels compared with corresponding controls.

To extend our results on the role of cav-1 in prostate cancer cell migration, we performed Transwell chamber assays. The results showed that enforced expression of cav-1 in cav-1–negative LNCaP cells nearly doubled cancer cell migration through the chamber membrane relative to that of the empty-vector control cells (Fig. 5C and D). In contrast, suppression of endogenous cav-1 in DU145 and PC-3 cells using cav-1 siRNA reduced cancer cell migration through the chamber membrane approximately 40% to 50% relative to that of the NC siRNA control cells (Fig. 5C and D). As it did in the wound-healing assay, treatment with LY effectively blocked cancer cell migration through the chamber membranes (Fig. 5C and D).

Cav-1 Upregulates VEGF, TGF-β1, and FGF2 through Akt-Mediated Maintenance of mRNA Stability

Regulation of GF expression is complex because it is controlled by steroid hormones, oncogenes, extracellular stresses, transcriptional factors, and GFs themselves. Mechanistically, GF regulation may occur at the transcriptional or posttranscriptional level. To gain insight into cav-1 stimulation of tumor-promoting GFs, we first examined the effect of cav-1 expression on VEGF, TGF-β1, and FGF2 promoter activities in cav-1–manipulated prostate cancer cells using a dual luciferase reporter assay system. We found, unexpectedly, that cav-1 did not alter the promoter activities of VEGF, TGF-β1, and FGF2, either in LNTB25cav cells when cav-1 expression was induced by doxycycline (Fig. 6A) or in high–cav-1 DU145 (Fig. 6B) and PC-3 (Fig. 6C) cells when cav-1 was suppressed by cav-1 siRNA. Given these results, we considered the possibility of cav-1 effects on mRNA stability of these GFs. A time course study following the incubation of cells with the transcriptional inhibitor actinomycin revealed that induction of cav-1 expression in LNTB25cav cells significantly increased mRNA stabilities of VEGF and TGF-β1 and showed a clear trend of increased mRNA stability of FGF2 (Fig. 7A, *top*). In contrast, suppression of cav-1 expression in high–cav-1 DU145 and PC-3 prostate cancer cells using cav-1 siRNA significantly reduced mRNA stability of VEGF, TGF-β1, and FGF2 (Fig. 7A, *middle* and *bottom*). Thus, our data show that cav-1–mediated, enhanced mRNA stability is a major mechanism for the upregulation of these cancer-promoting GFs. Importantly, our results also indicate that PI3-K-Akt signaling is required for cav-1–mediated, enhanced VEGF, TGF-β1, and FGF2 mRNA stability, because the PI3-K inhibitor LY abolished these cav-1–induced, or sustained, activities in LNTB25cav cells (Fig. 7A, *top*) or in high cav-1 DU145 and PC-3 (Fig. 7A, *middle* and *bottom*), respectively.

Together, our *in vitro* and *in vivo* data provide the first evidence to our knowledge that cav-1 increases levels of cancer-promoting GFs and enhances cancer progression through PI3-K-Akt–mediated maintenance of mRNA stability.

Discussion

Overexpression of cav-1 and cancer-promoting GFs is frequently observed in advanced prostate cancer and many other types of malignancies (4, 6, 23, 25, 28, 36, 37). In addition, increased levels of tissue and serum cav-1 and specific GFs

have prognostic potential for prostate cancer progression (10, 22, 38-40). Previous studies suggested that cav-1 and cancer-promoting GFs may collaborate in the progression of prostate cancer, although evidence is lacking (12). We showed in this study that multiple GFs, including VEGF, TGF-β1, and FGF2, can upregulate cav-1 expression and secretion in prostate cancer cells, and cav-1 expression can, in turn, increase cellular levels and secretion of VEGF, TGF-β1, and FGF2. Our *in vitro* data together with LNTB25cav xenograft data support those of our previous *in vivo* studies, in which we found that cav-1–expressing tumors had significantly higher tumor weight and significantly increased microvessel density (18). In addition, our results using two complementary assays showed that cav-1 overexpression leads to enhanced prostate cancer cell migration. This new information, together with our previous data (15-18), shows that upregulated cav-1 expression can promote cancer cell survival, angiogenesis, and invasion, all critical factors for cancer progression.

We noted that there were some apparently inconsistent observations regarding the effect of GFs on cav-1 expression in the literature. For example, earlier reports showed that VEGF and basic FGF reduced cav-1 expression in ECV304, a human umbilical vein endothelial cell line (41), and that chronic EGF treatment resulted in transcriptional downregulation of cav-1 in A431, a human epidermoid carcinoma cell line (42). The causes for such diverse observations remain unclear at this stage; however, context-dependent GF effects on cav-1 expression, including origin of cells, endogenous cav-1 levels, and concentrations of GFs used, could be a possible explanation.

We showed, mechanistically, that cav-1 mediates upregulation of VEGF, TGF-β1, and FGF2 and promotes cancer cell migration through Akt signaling. Furthermore, we showed that cav-1 upregulates VEGF, TGF-β1, and FGF2 through Akt-dependent increased mRNA stability. We believe that these results provide the first evidence, to our knowledge, that cav-1 and specific cancer-promoting GFs form a positive autoregulatory

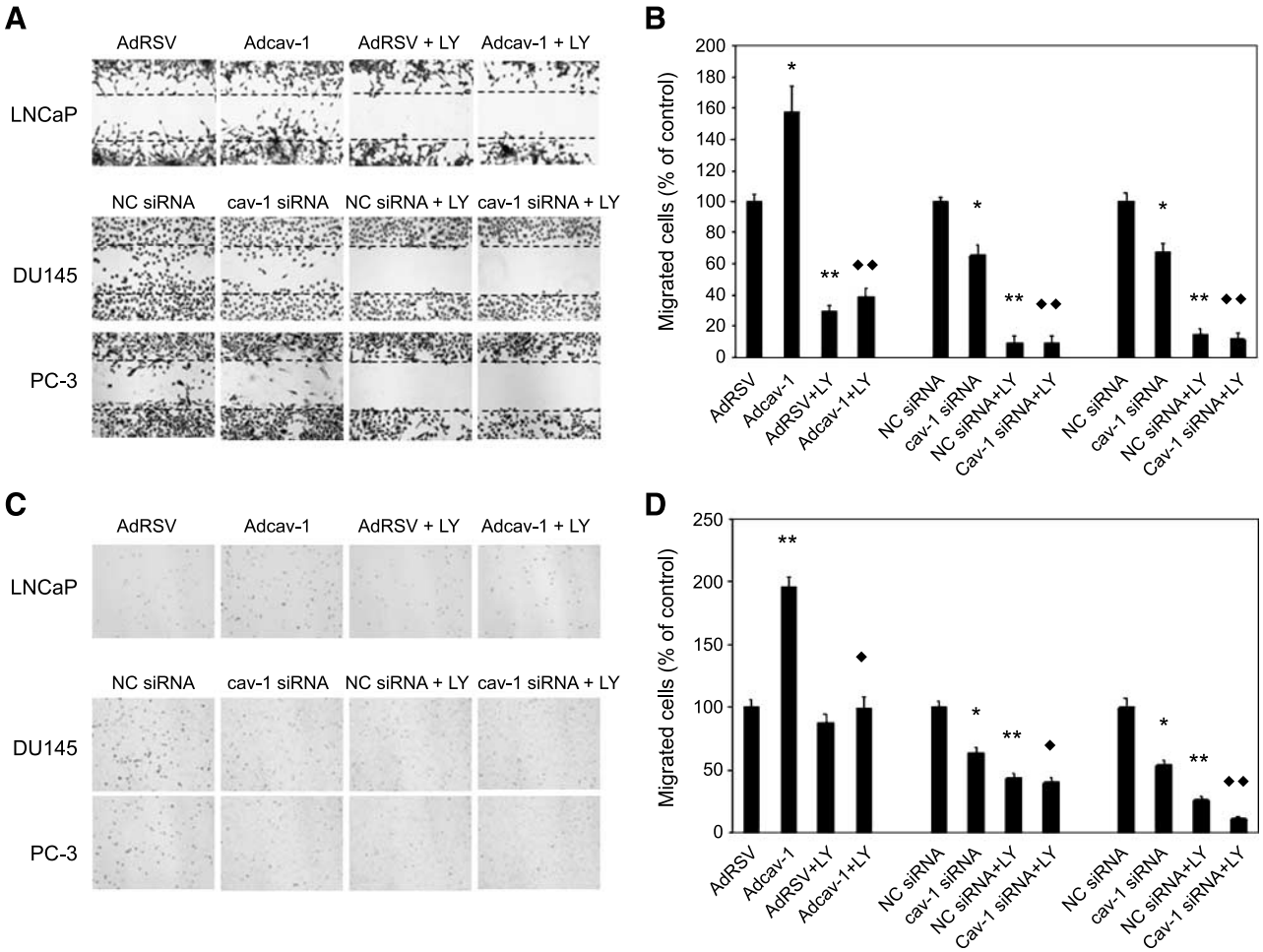

FIGURE 5. Cav-1 promotes cancer cell migration/motility. **A** and **B.** Wound healing assay. **A.** Representative images showing increased cell migration to the wounded area (*clear area, defined by dashed lines*) in Adcav-1–infected LNCaP cells and decreased cell migration to the wounded area in cav-1 siRNA–transfected DU145 and PC-3 cells. PI3-K-Akt inhibitor LY effectively blocked cancer cell migration. **B.** Quantitative analysis of triplicate wound healing assay experiments. **C** and **D.** Transwell chamber assays. **C.** Representative images showing increased transwell cell migration in Adcav-1–infected LNCaP cells and decreased migration in cav-1 siRNA–transfected DU145 and PC-3 cells. LY significantly reduced transwell cell migration. **D.** Quantitative analysis of triplicate Transwell migration assay experiments. Columns, mean (**B** and **D**); bars, SD, *, for the comparison to control AdRSV or NC siRNA; ♦, for the comparison of Adcav-1 + LY with Adcav-1. * or ♦, statistically significant ($P < 0.05$); ** or ♦♦, statistically very significant ($P < 0.0001$).

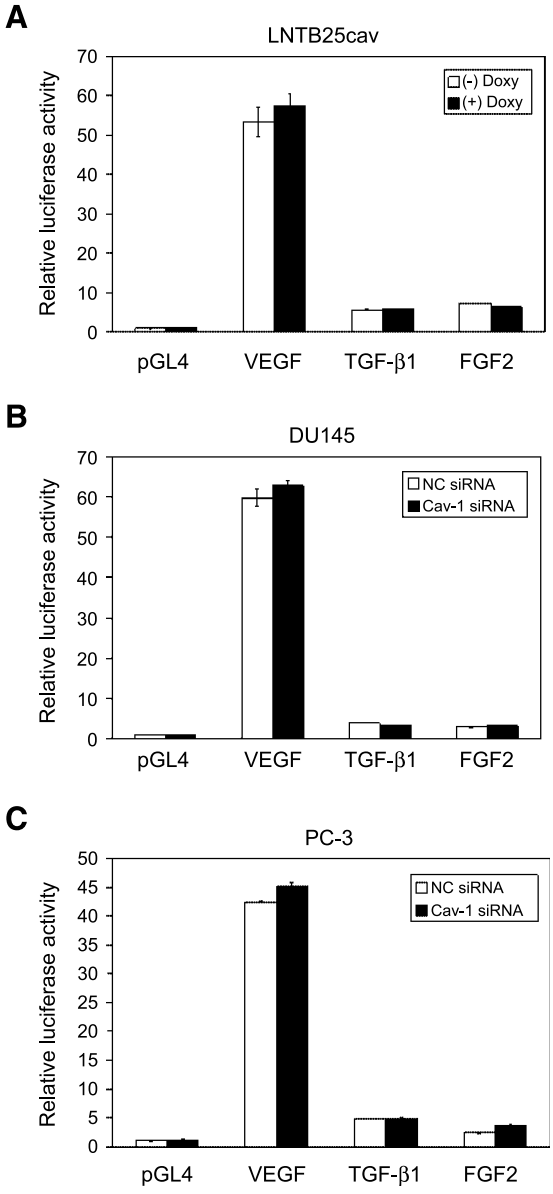

FIGURE 6. Luciferase reporter assays for VEGF, TGF-β1, and FGF2 promoter activities. The GF-luc readings were normalized with Renilla luciferase readings generated from a cotransfected vector (pGL4.73) and expressed as fold of control (pGLA4, *–doxy*). **A.** LNTB25cav. **B.** DU145. **C.** PC-3. Columns, mean; bars, SD.

feedback loop in which GFs upregulate cav-1 expression, and cav-1 expression, in turn, leads to increased mRNA stability of the same GFs, leading to the enhanced survival and invasive activities of prostate cancer cells.

The role of cav-1 in cancer is complex and continues to be somewhat controversial (4-7). However, a growing body of evidence indicates that cav-1 is upregulated in many types of human cancer and in several multidrug-resistant and metastatic cancer cell lines. In many of these studies, cav-1 was shown to correlate with aggressive disease (reviewed in refs. 4, 6, 7). Besides that gained from clinically based studies, substantial insight into the biological functions of cav-1 in prostate cancer progression has been attained from studies of genetically engineered mice. Genetic ablation of *cav-1* impedes prostate tumor progression in TRAMP mice (14). Mice with *cav-1* gene disruption have benign stromal lesions and compromised epithelial differentiation (43). Mouse and human prostate cancer cell–secreted cav-1 has proangiogenic activities (17, 18, 44). These findings clearly show an oncogenic role for cav-1 in prostate cancer.

We previously showed that cav-1 maintains activated Akt in prostate cancer cells through interaction with and inhibition of the serine/threonine protein phosphatases PP1 and PP2A (15). We also reported recently that tumor cell–secreted cav-1 can promote tumor angiogenesis through a PI3-K-Akt-eNOS–mediated mechanism (18). In this study, we found that PI3-K-Akt signaling is required for cav-1–mediated upregulation of VEGF, TGF-β1, and FGF2 and for cav-1–enhanced prostate cancer cell migration *in vitro*. Although we did not show that cav-1 inhibition of PP1 and/or PP2A underlies Akt activation in these experiments, this mechanism seems likely. The results of this current study extend the role of cav-1–mediated Akt activation as a contributing mechanistic pathway to prostate cancer.

The regulation of GFs is complex. In normal cells, the intricate balance of these GFs is controlled by coordinated regulation of hormones, transcriptional factors, and GFs themselves. In cancer and other malignant cells, however, this homeostasis is disrupted through various mechanisms. Inactivation or mutation of tumor suppressor genes (32, 45), activation of oncogenes (33), or overexpression of certain GFs (34) can impair the mRNA decay machinery, leading to aberrant GF mRNA accumulation. Akt, interestingly, may also stabilize AU-rich element–containing transcripts by phosphorylation of butyrate response factor 1, preventing it from binding to those AU-rich element–containing transcripts to facilitate deadenylation and rapid degradation of these transcripts (46, 47). We previously reported that cav-1 maintains activated Akt in prostate cancer cells (15). In this current study, we found that cav-1 promotes mRNA stability of VEGF, TGF-β1, and FGF2 and invasive activities of prostate cancer cells in an Akt-dependent manner. Taken together, the results of these studies suggest a cav-1 ⇒ Akt ⇒ GF signaling pathway. It's conceivable that Akt-mediated butyrate response factor 1 activities are also involved in cav-1–induced VEGF, TGF-β1, and FGF2 mRNA stability.

We also found that PI3-K-Akt inhibitor LY could not only eliminate cav-1–mediated Akt activation and GF upregulation, leading to the inhibition of cancer cell migration, but also suppress endogenous Akt in AdRSV-transduced LNCaP cells (AdRSV+LY) and cav-1-uninduced LNTB25cav, impairing cancer cell migration and reducing GF mRNA stability. In high–cav-1 DU145 and PC-3 cells, LY further reduced cancer cell migration and GF mRNA stability in cav-1 siRNA–transfected cells. Together, these data suggest that (*a*) Akt is required for cav-1–mediated maintenance of GF mRNA stability and cav-1–enhanced cancer cell motility; and (*b*) Akt works downstream of cav-1 and therefore can facilitate maintenance of GF mRNA stability and enhance cancer cell motility through other molecular signaling events that activate Akt.

Importantly, the results of this study define a positive autoregulatory feedback mechanism (Fig. 7B) that could lead to sustained cav-1, VEGF, TGF-β1, and FGF2 expression and secretion in prostate cancer cells. Since we previously showed

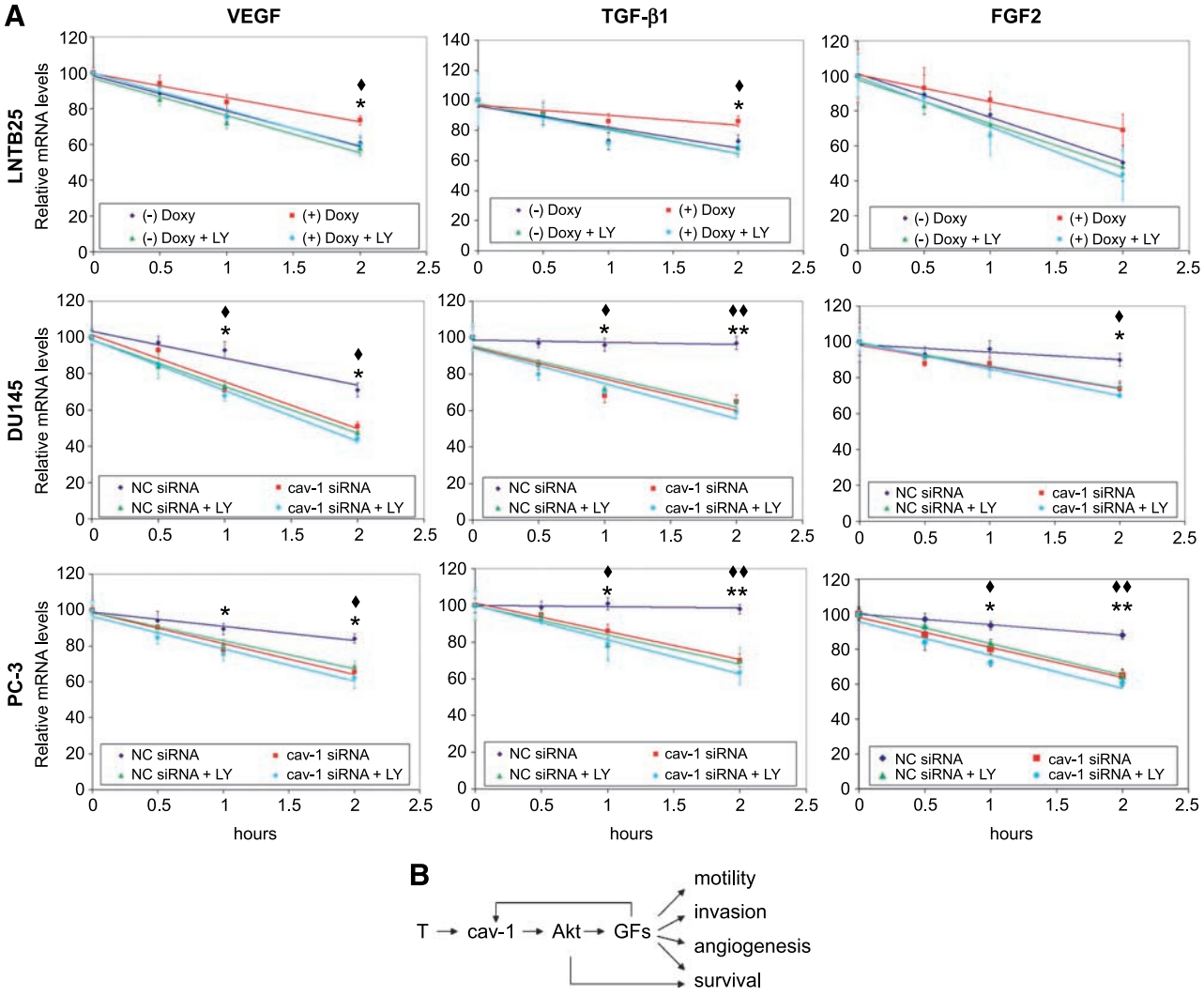

FIGURE 7. Cav-1 enhances mRNA stabilities of VEGF, TGF-β1, and FGF2. **A.** cav-1–manipulated LNTB25cav, DU145, and PC-3 cells were treated with 10 μg/mL of actinomycin in the presence and absence of LY for the indicated times, followed by quantitative reverse transcription-PCR analysis for mRNA levels of VEGF, TGF-β1, and FGF2. Points, mean; bars, SD. The data were fitted with linear trend lines, and the data from actinomycin treatment for 1 and 2 h were subjected to statistical analysis. *, the comparison to control (–) doxycycline (*doxy*) or NC siRNA; ♦, the comparison of (+) doxy + LY with (+) doxy or NC siRNA+LY with NC siRNA. * or ♦, statistically significant ($P < 0.05$); ** or ♦♦, statistically very significant ($P < 0.0001$). **B.** diagram summarizes cav-1-GF autoregulatory loop. T, testosterone.

that prostate cancer cell–derived, secreted cav-1 can stimulate angiogenic activities *in vitro* and *in vivo* (18), it seems reasonable to assume that induction of VEGF, TGF-β1, and FGF2, which are potent angiogenic factors, would contribute to cav-1–mediated angiogenesis in prostate cancer. Together with cav-1–stimulated prostate cancer cell migration, these cav-1–induced growth and invasive activities likely have a profound effect on the malignant properties of prostate cancer cells. In addition, this cav-1-GF positive feedback loop has implications for identification of aggressive, virulent prostate cancer among a considerable fraction of prostate cancers that will not progress to clinical significance (48). Further, the autonomous nature of this positive feedback loop provides insight into the inexorable nature of prostate cancer progression.

In light of this new information, it becomes important to consider the events that lead to the cav-1-GF positive feedback loop in prostate cancer. Since we previously showed that cav-1 is induced by testosterone in prostate cancer cells (16), it is conceivable that cav-1 expression is initially upregulated by testosterone. However, this possibility raises important questions, such as "at what point in the development of prostate cancer does this occur?" and "what molecular events facilitate testosterone-mediated cav-1 expression?" It is also possible that GF expression initiates cav-1 expression. In our early studies of cav-1, we showed that androgen-insensitive cav-1–positive prostate cancer can arise in the presence of physiologic levels of testosterone in mouse models of prostate cancer (9, 13). These results are consistent with a model that implicates testosterone as the initial stimulatory event, with subsequent cav-1–stimulated GF expression sustaining cav-1 expression (Fig. 7B). The eventual development of the cav-1-GF positive feedback loop suggests a plausible pathway for the development of

androgen-insensitive prostate cancer. Since cav-1 expression is very low to undetectable in normal prostate epithelial cells, it seems likely that initiating oncogenic events are required to facilitate cav-1 expression.

Overall, the results of this study show that the cav-1–induced PI3-K-Akt–mediated increased mRNA stability of VEGF, TGF-β1, and FGF2 is a novel and important molecular mechanism by which cav-1 promotes cancer progression. Our results further define a cav-1-GF positive regulatory loop that could sustain many malignant properties in prostate cancer cells. Further studies are necessary to understand the biological and clinical implications of this cav-1–mediated oncogenic pathway in prostate cancer.

Materials and Methods

Cell Lines and Cell Culture Conditions

Human prostate cancer cell lines LNCaP, PC-3, DU145 and LNCaP (c^+), a cav-1–expressing LNCaP variant that was obtained during propagation of LNCaP, were grown in RPMI 1640 with 10% fetal bovine serum. LNTB25cav, a cav-1–inducible clone generated from LNCaP, was grown in RPMI 1640 with 9% tet system–approved fetal bovine serum.

Induction of Cav-1 Expression and Secretion by GFs

LNCaP (c^+), DU145, and PC-3 cells were seeded in complete culture medium and grown overnight. After being rinsed once with serum-free medium (SFM), cells were incubated in SFM with or without a specific GF at the following concentrations: human GFs: PDGF-AB, 10 ng/mL (Invitrogen); NGF, 10 ng/mL (Prospec); FGF1, 5 ng/mL (Invitrogen); FGF2, 2 ng/mL (Invitrogen); EGF, 5 ng/mL (Invitrogen); TGF-β1, 1 ng/mL (Invitrogen), and VEGF, 10 ng/mL (Upstate). Mouse GFs: PDGF–BB, 10 ng/mL (Invitrogen); NGF, 10 ng/mL (Invitrogen); FGF1, 5 ng/mL (R & D Systems); FGF2, 2 ng/mL (Invitrogen); EGF, 5 ng/mL (Invitrogen); and VEGF, 10 ng/mL (Invitrogen).

For determining cav-1 expression, cell lysates were prepared 48 h after treatment with the GFs. For determining secreted cav-1 levels, conditioned media were collected 24 h after treatment with the GFs. The conditioned media were then centrifuged once at 130 × *g* for 5 min to remove floating cells and once at 10,000 × *g* for 20 min to removed remaining insoluble materials. The resulting supernatants were concentrated 50- to 100-fold using Amicon Ultra-4 with 10- kDa cutoff. The equivalents of conditioned media produced from 5.0×10^5 cells were loaded on gel for the determination of secreted cav-1 levels.

Analysis of mRNA Expression

Total RNA from human prostate cancer cell lines was extracted with TRI Reagent Solution (Ambion). Reverse transcription was carried out with the High Capacity cDNA Archive kit (Applied Biosystems). PCRs were done using the following Taqman probes and primers (Applied Biosystems): Hs00184697_m1 for cav-1, Hs99999905_m1 for glyceraldehyde-3-phosphate dehydrogenase, Hs00173626_m1 for VEGF, Hs00171257_m1 for TGF-β1, and Hs00266645-m1 for FGF2. Real-time PCR was done using the ABI Prism 7000 Sequence Detection System (Applied Biosystems). The relative quantity of a specific mRNA was determined by the $\Delta\Delta C_T$ method and normalized to glyceraldehyde-3-phosphate dehydrogenase or actin RNA in the same cDNA preparation.

Western Blot Analysis

Proteins in the samples were separated by 4% to 15% gradient SDS-PAGE and Western blotting was done according to standard procedures. Primary antibodies were as follows: rabbit polyclonal antibodies against cav-1, VEGF, TGF-β1, and FGF2 (Santa Cruz); monoclonal antibody to PKBα/Akt (clone 55; BD Biosciences); rabbit polyclonal antibodies against phospho-Akt (Ser473), phospho-Akt (Thr308), p42/44, phosphor-p42/44, JNK, phospho-JNK, p38, and phosphor-p38 (Cell Signaling); and monoclonal antibody to β-actin (Sigma). Quantitative analysis were done by measuring the density of each protein bands using a computer-assisted software (Nikon, NIS-Elements AR3.0) and by making calculations according to the following methods: for cell lysates, the protein bands of interest were first normalized by corresponding β-actin and each normalized value was then compared with control (control as 1); for conditioned medium, the protein bands of interest were compared with control (SFM).

siRNA Transfection and Viral Infection

Cells were seeded at a density of 1.0×10^5 cells per well in 12-well plates or at equivalent cell density in other culture dish formats 1 d before transfection. Transfection was done using siPORTAmine (Ambion) and cav-1–specific siRNA or negative control (NC) siRNA (Ambion). Adenovirus-mediated gene transduction was carried out as described previously (16).

Preparation of Conditioned Media for Analysis of Secreted GFs

The conditioned media for analysis of secreted GFs were prepared and concentrated as described for the preparation of secreted cav-1.

Wound Healing Assay

Twenty-four hours after gene transduction with adenoviral vectors (LNCaP) or transfection with siRNA (PC-3 or DU145), a straight longitudinal scratch was made on the monolayer of cells using a pipette tip. After removal of the existing medium, fresh RPMI 1640 complete medium with or without 20 μmol/L PI3-K inhibitor LY (CalBiochem) was added, and the cells were incubated for 16 h (PC-3 and DU145) or 48 h (LNCaP). Cells were then stained with HEMA3 (Biochemical Sciences), and the numbers of cells migrating into the clear area were counted and imaged with a microscope using NIS-Elements AR2.30 software (Nikon).

Transwell Chamber Assay

Twenty-four hours after gene transduction with adenoviral vectors (LNCaP) or transfection with siRNA (PC-3 or DU145), the cells were trypsinized and single-cell suspensions were prepared. Five thousand cells were seeded into each Falcon cell culture insert (8.0 μm pore size, 24-well format; Becton Dickinson Labware) with 300 μL of serum-free RPMI 1640 with or without 20 μmol/L LY and with 700 μL RPMI 1640 complete medium in the outer well. After 16- to 24-h incubation, the medium and cells inside the insert were carefully removed, and the cells that had migrated onto the outer

membrane of the insert were stained, counted, and imaged as just described for the wound healing assay.

Generation of LNTB25cav Xenograft and Processing of Tumor Tissue

LNTB25cav xenograft was established as described previously (18), with 10 of the mice given 2 mg/mL of doxycycline in their drinking water containing 5% sucrose and 11 animals given drinking water containing only 5% sucrose as controls. After 21 d, the animals were euthanized, and the tumor tissues were harvested and fixed in 10% neutral formalin. The tissues were then processed for making 5-μm paraffin-embedded sections.

Immunohistochemistry

Immunostaining of paraffinized sections was conducted using polyclonal antibodies to cav-1, TGF-β1, or VEGF and an ABC kit (Vector Laboratories). The specificity of the immunoreactions was verified by using PBS to replace the specific primary antibodies.

Luciferase Reporter Assay

A 1.5-kb VEGF promoter containing Sp1 sites and an HIF-1α site was obtained from genomic DNA by PCR using forward primer 5′ GGAGAAGTAGCCAAGGGAT 3′ and reverse primer 5′ CCTGTCGCTTTCGCTGCT 3′. The PCR fragment was digested with SacI and inserted into the SacI site of the pGL4 luciferase reporter vector (Promega). A 1,077-bp TGF-β1 promoter (CHR19_M0615_R1) and a 1,012-bp FGF2 promoter (CHR4-P0576-R1) were purchased from SwitchGear Genomics. LNTB25cav cells were seeded (2.5×10^5 cells per well, 12-well plate) and grown in the medium with or without 0.2 μg/mL doxycycline overnight and then were cotransfected with a specific GF-luc reporter vector or control vector pGL4 and a Renilla luciferase reporter vector (pGL4.73, Promega) using FuGENE HD transfection reagent (Roche). DU145 and PC-3 cells were seeded (1.0×10^5 cells per well, 12-well plate) and grown in the complete medium overnight and then were transfected with 50 nmol/L cav-1 siRNA or NC siRNA using siPORT Amine. Three hours after siRNA transfection, cells were cotransfected with a specific GF-luc reporter vector or control vector pGL4 and the normalizer reporter vector as described above. Twenty-four hours after the reporter transfection, luciferase activity was determined using a dual-luciferase reporter assay system (Promega) and a Synergy 2 multimode microplate reader (BioTek). The GF-luc readings were normalized with Renilla luciferase readings and expressed relative to the control (pGLA4, doxycycline).

mRNA Stability Assay

Cav-1 expression in LNTB25cav cells was induced with doxycycline, and DU145 or PC-3 cells were transfected with cav-1 siRNA or NC siRNA as described for the luciferase reporter assay. Twenty-four hours after induction with doxycycline or transfection of siRNA, cells were treated with 10 μg/mL of actinomycin in the presence or absence of the PI3-K inhibitor LY (20 μmol/L) for 0, 0.5, 1, or 2 h. RNAs were prepared, and mRNA levels of cav-1 and each GF were determined by quantitative reverse transcription-PCR as described earlier.

Statistical Analysis

The unpaired *t* test was used in the experiments in which probability levels were determined. A *P* value of <0.05 (*) was considered statistically significant, and one <0.0001 (**) was considered statistically very significant.

Disclosure of Potential Conflicts of Interest

No potential conflicts of interest were disclosed.

Acknowledgments

We thank Karen Phillip and Park Sanghee for editorial assistance.

References

1. Jemal A, Siegel R, Ward E, et al. Cancer statistics, 2008. CA Cancer J Clin 2008;58:71–96.

2. Liu P, Rudick M, Anderson RG. Multiple functions of caveolin-1. J Biol Chem 2002;277:41295–8.

3. Parton RG, Simons K. The multiple faces of caveolae. Nat Rev Mol Cell Biol 2007;8:185–94.

4. Mouraviev V, Li L, Tahir SA, et al. The role of caveolin-1 in androgen insensitive prostate cancer. J Urol 2002;168:1589–96.

5. Williams TM, Lisanti MP. Caveolin-1 in oncogenic transformation, cancer, and metastasis. Am J Physiol Cell Physiol 2005;288:C494–506.

6. Shatz M, Liscovitch M. Caveolin-1: a tumor-promoting role in human cancer. Int J Radiat Biol 2008;84:177–89.

7. Goetz JG, Lajoie P, Wiseman SM, Nabi IR. Caveolin-1 in tumor progression: the good, the bad and the ugly. Cancer Metastasis Rev 2008;27:715–35.

8. Yang G, Timme TL, Frolov A, Wheeler TM, Thompson TC. Combined c-Myc and caveolin-1 expression in human prostate carcinoma predicts prostate carcinoma progression. Cancer 2005;103:1186–94.

9. Yang G, Truong LD, Timme TL, et al. Elevated expression of caveolin is associated with prostate and breast cancer. Clin Cancer Res 1998;4:1873–80.

10. Yang G, Truong LD, Wheeler TM, Thompson TC. Caveolin-1 expression in clinically confined human prostate cancer: a novel prognostic marker. Cancer Res 1999;59:5719–23.

11. Satoh T, Yang G, Egawa S, et al. Caveolin-1 expression is a predictor of recurrence-free survival in pT2N0 prostate carcinoma diagnosed in Japanese patients. Cancer 2003;97:1225–33.

12. Yang G, Addai J, Wheeler TM, et al. Correlative evidence that prostate cancer cell-derived caveolin-1 mediates angiogenesis. Hum Pathol 2007;38:1688–95.

13. Nasu Y, Timme TL, Yang G, et al. Suppression of caveolin expression induces androgen sensitivity in metastatic androgen-insensitive mouse prostate cancer cells. Nat Med 1998;4:1062–4.

14. Williams TM, Hassan GS, Li J, et al. Caveolin-1 promotes tumor progression in an autochthonous mouse model of prostate cancer: genetic ablation of Cav-1 delays advanced prostate tumor development in tramp mice. J Biol Chem 2005;280:25134–45.

15. Li L, Ren CH, Tahir SA, Ren C, Thompson TC. Caveolin-1 maintains activated Akt in prostate cancer cells through scaffolding domain binding site interactions with and inhibition of serine/threonine protein phosphatases PP1 and PP2A. Mol Cell Biol 2003;23:9389–404.

16. Li L, Yang G, Ebara S, et al. Caveolin-1 mediates testosterone-stimulated survival/clonal growth and promotes metastatic activities in prostate cancer cells. Cancer Res 2001;61:4386–92.

17. Tahir SA, Yang G, Ebara S, et al. Secreted caveolin-1 stimulates cell survival/clonal growth and contributes to metastasis in androgen-insensitive prostate cancer. Cancer Res 2001;61:3882–5.

18. Tahir SA, Yang G, Goltsov AA, et al. Tumor cell-secreted caveolin-1 has proangiogenic activities in prostate cancer. Cancer Res 2008;68:731–9.

19. Linderholm B, Grankvist K, Wilking N, Johansson M, Tavelin B, Henriksson R. Correlation of vascular endothelial growth factor content with recurrences, survival, and first relapse site in primary node-positive breast carcinoma after adjuvant treatment. J Clin Oncol 2000;18:1423–31.

20. Landriscina M, Cassano A, Ratto C, et al. Quantitative analysis of basic fibroblast growth factor and vascular endothelial growth factor in human colorectal cancer. Br J Cancer 1998;78:765–70.

21. Ito N, Kawata S, Tamura S, et al. Elevated levels of transforming growth

factor β messenger RNA and its polypeptide in human hepatocellular carcinoma. Cancer Res 1991;51:4080–3.

22. Poon RT, Fan ST, Wong J. Clinical implications of circulating angiogenic factors in cancer patients. J Clin Oncol 2001;19:1207–25.

23. Ferrara N. VEGF and the quest for tumour angiogenesis factors. Nat Rev Cancer 2002;2:795–803.

24. Breen EC. VEGF in biological control. J Cell Biochem 2007;102:1358–67.

25. Danielpour D. Functions and regulation of transforming growth factor-β (TGF-β) in the prostate. Eur J Cancer 2005;41:846–57.

26. Barrack ER. TGF β in prostate cancer: a growth inhibitor that can enhance tumorigenicity. Prostate 1997;31:61–70.

27. Cronauer MV, Schulz WA, Seifert HH, Ackermann R, Burchardt M. Fibroblast growth factors and their receptors in urological cancers: basic research and clinical implications. Eur Urol 2003;43:309–19.

28. Kwabi-Addo B, Ozen M, Ittmann M. The role of fibroblast growth factors and their receptors in prostate cancer. Endocr Relat Cancer 2004;11:709–24.

29. Josko J, Mazurek M. Transcription factors having impact on vascular endothelial growth factor (VEGF) gene expression in angiogenesis. Med Sci Monit 2004;10:RA89–98.

30. Koos RD, Kazi AA, Roberson MS, Jones JM. New insight into the transcriptional regulation of vascular endothelial growth factor expression in the endometrium by estrogen and relaxin. Ann N Y Acad Sci 2005;1041:233–47.

31. Buck MB, Knabbe C. TGF-β signaling in breast cancer. Ann N Y Acad Sci 2006;1089:119–26.

32. Cash J, Korchnak A, Gorman J, Tandon Y, Fraizer G. VEGF transcription and mRNA stability are altered by WT1 not DDS(R384W) expression in LNCaP cells. Oncol Rep 2007;17:1413–9.

33. Kanies CL, Smith JJ, Kis C, et al. Oncogenic Ras and transforming growth factor-β synergistically regulate AU-rich element-containing mRNAs during epithelial to mesenchymal transition. Mol Cancer Res 2008;6:1124–36.

34. Song QH, Klepeis VE, Nugent MA, Trinkaus-Randall V. TGF-β1 regulates TGF-β1 and FGF-2 mRNA expression during fibroblast wound healing. Mol Pathol 2002;55:164–76.

35. Touriol C, Morillon A, Gensac MC, Prats H, Prats AC. Expression of human fibroblast growth factor 2 mRNA is post-transcriptionally controlled by a unique destabilizing element present in the 3′-untranslated region between alternative polyadenylation sites. J Biol Chem 1999;274:21402–8.

36. Juhasz M, Chen J, Tulassay Z, Malfertheiner P, Ebert MP. Expression of caveolin-1 in gastrointestinal and extraintestinal cancers. J Cancer Res Clin Oncol 2003;129:493–7.

37. Podar K, Anderson KC. Caveolin-1 as a potential new therapeutic target in multiple myeloma. Cancer Lett 2006;233:10–5.

38. El-Gohary YM, Silverman JF, Olson PR, et al. Endoglin (CD105) and vascular endothelial growth factor as prognostic markers in prostatic adenocarcinoma. Am J Clin Pathol 2007;127:572–9.

39. Gravdal K, Halvorsen OJ, Haukaas SA, Akslen LA. Expression of bFGF/FGFR-1 and vascular proliferation related to clinicopathologic features and tumor progress in localized prostate cancer. Virchows Arch 2006;448:68–74.

40. Tahir SA, Frolov A, Hayes TG, et al. Preoperative serum caveolin-1 as a prognostic marker for recurrence in a radical prostatectomy cohort. Clin Cancer Res 2006;12:4872–5.

41. Liu J, Razani B, Tang S, Terman BI, Ware JA, Lisanti MP. Angiogenesis activators and inhibitors differentially regulate caveolin-1 expression and caveolae formation in vascular endothelial cells. Angiogenesis inhibitors block vascular endothelial growth factor-induced down-regulation of caveolin-1. J Biol Chem 1999;274:15781–5.

42. Lu Z, Ghosh S, Wang Z, Hunter T. Downregulation of caveolin-1 function by EGF leads to the loss of E-cadherin, increased transcriptional activity of β-catenin, and enhanced tumor cell invasion. Cancer Cell 2003;4:499–515.

43. Yang G, Timme TL, Naruishi K, et al. Mice with cav-1 gene disruption have benign stromal lesions and compromised epithelial differentiation. Exp Mol Pathol 2008;84:131–40.

44. Bartz R, Zhou J, Hsieh JT, Ying Y, Li W, Liu P. Caveolin-1 secreting LNCaP cells induce tumor growth of caveolin-1 negative LNCaP cells *in vivo*. Int J Cancer 2007.

45. Datta K, Mondal S, Sinha S, et al. Role of elongin-binding domain of von Hippel Lindau gene product on HuR-mediated VPF/VEGF mRNA stability in renal cell carcinoma. Oncogene 2005;24:7850–8.

46. Benjamin D, Schmidlin M, Min L, Gross B, Moroni C. BRF1 protein turnover and mRNA decay activity are regulated by protein kinase B at the same phosphorylation sites. Mol Cell Biol 2006;26:9497–507.

47. Schmidlin M, Lu M, Leuenberger SA, et al. The ARE-dependent mRNA-destabilizing activity of BRF1 is regulated by protein kinase B. Embo J 2004; 23:4760–9.

48. Dall'Era MA, Cooperberg MR, Chan JM, et al. Active surveillance for early-stage prostate cancer: review of the current literature. Cancer 2008;112: 1650–9.

PCAN Open

Prostate Cancer and Prostatic Diseases (2009), 1–6

1365-7852/09 $32.00
www.nature.com/pcan

REVIEW

The role of caveolin-1 in prostate cancer: clinical implications

TC Thompson[1], SA Tahir[1], L Li[1], M Watanabe[2], K Naruishi[3], G Yang[1], D Kadmon[4], CJ Logothetis[1], P Troncoso[1], C Ren[1], A Goltsov[1] and S Park[1]

[1]*Department of Genitourinary Medical Oncology—Research, The University of Texas MD Anderson Cancer Center, Houston, TX, USA;* [2]*Department of Urology, Okayama University Graduate School of Medicine, Dentistry and Pharmaceutical Sciences, Okayama, Japan;* [3]*Department of Pathophysiology–Periodontal Science, Okayama University Graduate School of Medicine, Dentistry and Pharmaceutical Sciences, Okayama, Japan and* [4]*Scott Department of Urology, Baylor College of Medicine, Houston, TX, USA*

Caveolin-1 (cav-1) is reportedly overexpressed in prostate cancer cells and is associated with disease progression. Specific oncogenic activities of cav-1 associated with Akt activation also occur in prostate cancer. A membrane-associated protein, cav-1, is nonetheless secreted by prostate cancer cells; results of recent studies showed that secreted cav-1 can stimulate cell survival and angiogenic activities, defining a role for cav-1 in the prostate cancer microenvironment. Serum cav-1 levels were also higher in prostate cancer patients than in control men without prostate cancer, and the preoperative serum cav-1 concentration had prognostic potential in men undergoing radical prostatectomy. Secreted cav-1 is therefore a potential biomarker and therapeutic target for prostate cancer.
Prostate Cancer and Prostatic Diseases advance online publication, 7 July 2009; doi:10.1038/pcan.2009.29

Keywords: caveolin-1; progression; angiogenesis; biomarkers

Introduction

Caveolin-1 (cav-1) is a major structural component of caveolae, which are specialized plasma membrane invaginations involved in multiple cellular processes such as molecular transport, cell adhesion and signal transduction.[1,2] Although under some conditions cav-1 may suppress tumorigenesis,[3] cav-1 is associated with and contributes to malignant progression through various mechanisms.[4–8] Specific proteins such as receptor tyrosine kinases, serine/threonine kinases, phospholipases, G protein-coupled receptors and Src family kinases are localized in lipid rafts and caveolar membranes, where they interact with cav-1 through the cav-1 scaffolding domain; the activities mediated by this domain result in the generation of platforms for compartmentalization of discrete signaling events.[9] A high level of intracellular cav-1 expression is associated with metastatic progression of human prostate cancer[10,11] and other malignancies, including lung,[12] renal[13] and esophageal squamous cell cancers.[14]

Virulent prostate cancer cell lines reportedly secrete biologically active cav-1 protein *in vitro*, and cav-1 promotes prostate cancer cell viability and clonal growth.[15–17] The cancer-promoting effects of secreted cav-1 include antiapoptotic activities similar to those observed following enforced expression of cav-1 within the cells.[15,18] In addition to showing cav-1-mediated autocrine activities, a recent study showed that recombinant cav-1 protein is taken up by prostate cancer cells and endothelial cells *in vitro* and that recombinant cav-1 increases angiogenic activities both *in vitro* and *in vivo* by activating Akt- and/or nitric oxide synthase-mediated signaling.[6] Moreover, significantly higher serum cav-1 levels have been documented in men with prostate cancer than in men with benign prostatic hyperplasia[19] and also in patients with elevated risk of cancer recurrence after radical prostatectomy.[20]

The concept of expression and secretion of cav-1 by prostate cancer cells in malignant progression is unique. The autocrine and paracrine activities of cav-1 mediated through the activation of Akt and/or nitric oxide synthase signaling may lead to pervasive engagement of the local tumor microenvironment, involving but not limited to the proangiogenic activities previously documented.

In this review, we discuss the unique functional properties of cav-1 in prostate cancer, especially on secreted cav-1 and its capacity to engage the prostate cancer microenvironment. We also discuss the potential for development of serum cav-1 as a biomarker for prostate cancer, with particular reference to the preoperative cav-1 serum level as a prognostic tool. Finally, we discuss the possibility of biologically targeting cav-1 as the foundation for the development of novel effective therapies for prostate cancer.

Correspondence: Dr TC Thompson, Department of Genitourinary Medical Oncology—Research, Unit 1374, The University of Texas MD Anderson Cancer Center, 1515 Holcombe Boulevard, Houston, TX 77030, USA.
E-mail: timthomp@mdanderson.org
Received 27 April 2009; accepted 4 June 2009

Cav-1 upregulation in prostate cancer

We previously reported increased cav-1 immunostaining in prostate cancer relative to that in the normal adjacent prostatic epithelial cells, which express low-to-nondetectable levels of cav-1.[10,11] An important finding was that increased cav-1 immunostaining had independent prognostic potential in men undergoing radical prostatectomy.[11] These results were supported by those in two subsequent independent reports of studies that also evaluated prostate cancer tissue using immunohistochemical analysis and yielded similar conclusions.[21,22] An important common observation from the cases examined in these studies is that cav-1 immunostaining in localized prostate cancer is focal and expressed only in a relatively small percentage of prostate cancer cells. These results also showed that cav-1 was positively correlated with Gleason grade, an important suggestion that even though it is focally expressed, cav-1 is a biomarker for clinically aggressive disease.

The molecular basis for the initiation of cav-1 expression in prostate cancer and other malignancies is not clear. The *cav-1* and *cav-2* genes are co-localized to 7q31.1, a highly conserved region that encompasses a known fragile site that is deleted, associated with loss of heterozygosity, or amplified in a variety of human cancers, including prostate cancer.[3,23–25] Although some investigators have used these data to support a case for both loss and gain of cav-1 expression, no convincing data specifically correlate genetic alterations at this site with changes in cav-1 expression for prostate cancer.[26,27] The *cav-1* gene promoter has multiple CpG sites, and alterations in gene methylation have been shown in prostate cancer.[28] However, patterns of *cav-1* gene methylation have not, thus far, provided a convincing argument for the upregulation of cav-1 in prostate cancer. It is interesting that a recent article suggests that the loss of function for a tumor suppressor miRNA (miR-205) may lead to upregulation of cav-1 in prostate cancer.[29]

As many genetic alterations that occur in primary prostate cancer have also been documented in premalignant disease, such as high-grade prostatic intraepithelial neoplasia, it would be interesting to analyze cav-1 in those premalignant lesions. Although it is focally expressed in primary prostate cancer, it is important to note that cav-1 is expressed in most metastatic cells.[15] This focal expression in primary prostate cancer and significantly increased cav-1 expression in associated metastases fit well with the notion that cav-1 is more aligned with the criteria of a progression-related protein than with those of a protein that significantly affects localized tumor growth.[30] The idea of association of cav-1 with clinically significant prostate cancer is novel, and the prospect that cav-1 expression may segregate clinically significant prostate cancer from clinically insignificant prostate cancer is exciting.[31]

Although the association between cav-1 overexpression in prostate cancer and aggressive, clinically significant disease has been found consistently in multiple studies, the relationship between cav-1 overexpression and androgen sensitivity is less clear. Early studies showed that cav-1 overexpression was inversely associated with androgen sensitivity and positively associated with tumor growth in mouse models of prostate cancer.[32] The *cav-1* gene is transcriptionally upregulated in androgen-sensitive prostate cancer cells, although the level of induction was modest.[5] In general, cav-1 has been associated with the stimulatory effects of steroid receptors, including the androgen receptor, suggesting a point of convergence for further mechanistic studies.[33,34] Overall, the available information on cav-1 expression fits the hypothesis that prostate cancer progression, even in the presence of normal levels of circulating testosterone, is coincidental with the development of androgen insensitivity. Certainly, the development of castrate-resistant prostate cancer involves selection for unique malignant properties that allow prostate cancer cells to metastasize in the presence of castrate levels of androgens. However, the emergence of castrate-resistant prostate cancer does not preclude co-selection of metastatic and androgen-insensitive prostate cancer in men who have not undergone hormone therapy.

Mechanisms of cav-1-mediated oncogenic activities in prostate cancer

Overexpression of cav-1 was reported in various malignancies, including cancer of the colon,[35] kidney,[13] bladder,[36] lung,[12] pancreas[37] and ovary,[38] and in some types of breast cancer.[39] The level of cav-1 expression may depend on the tumor type and stage; for example, high cav-1 levels were reported in late or advanced squamous cell carcinoma[40] and in metastatic prostate cancer.[15,32] These results have led many investigators to attempt to identify cav-1-related oncogenic pathways for various malignancies. Although cav-1 activities impinge on various oncogenic pathways and can inhibit or activate these pathways, depending on the cell type and context,[3] the results of multiple studies now indicate that Akt activation has an important role in cav-1-mediated oncogenic functions in prostate cancer. The first demonstration of a direct association between cav-1 expression and Akt indicated that the overexpression of cav-1 increased binding to and inhibited the serine/threonine phosphatases, PP1 and PP2A, in human prostate cancer cells. These interactions, which were likely mediated through cav-1 binding to a cav-1 scaffolding domain-binding site on PP1 and PP2A and inhibition of their activities, led to significantly increased levels of phospho-Akt and sustained activation of downstream oncogenic Akt targets.[18] Findings from a recent independent study supported this mechanism and further showed that the putative oncogene inhibitor of differentiation-1 induced Akt activation by promoting the binding activity of cav-1 and PP-2A.[41] It is important to consider that the activation of Akt has been previously associated with prostate cancer and is clearly one of the most important oncogenic activities that underlie prostate cancer progression.[42] It is worthwhile to consider the idea that activated Akt contributes to the expression and secretion of multiple growth factors (GFs) that have important roles in the growth, survival and progression of prostate cancer cells through autocrine and paracrine activities[42] (Figure 1). The molecular mechanisms that may connect cav-1 upregulation to GF expression and secretion through the activation of Akt are worthy of future investigation.

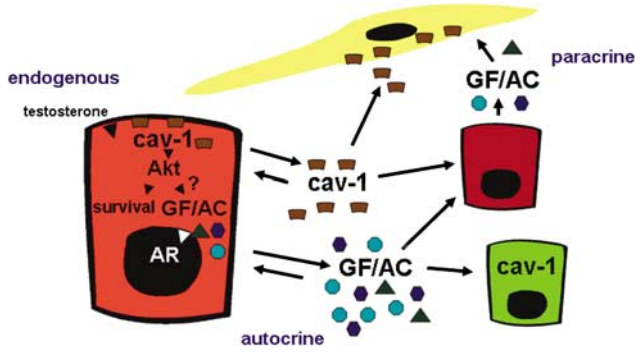

Figure 1 Caveolin-1 (cav-1) upregulation in prostate cancer promotes cell survival through Akt-mediated activities. Prostate cancer-derived, secreted cav-1, which is taken up by prostate cancer cells and tumor-associated endothelial cells, stimulates angiogenesis. The unique autocrine and paracrine activities associated with cav-1 in prostate cancer present a novel paradigm for the development of biomarkers and therapeutic approaches for prostate cancer. GFs, growth factors; ACs, angiogenic cytokines; AR, androgen receptor.

Recent studies further showed that alterations in Akt activities regulate the expression of fatty acid synthase, a putative metabolic oncogene, and its co-localization with cav-1 in lipid rafts in prostate cancer cells.[43] The same article reported that Src, an oncogenic tyrosine kinase, has an important role in this process. It is important to note that cav-1 was initially identified as a v-Src substrate, P-Y14cav-1.[44] Overall, these recent articles suggest that an interactive and interdependent network of oncogenic proteins, including cav-1, Akt, fatty acid synthase and Src, has an important role in prostate cancer. Although initiation and maintenance of this oncogenic protein network appear to be a critical mechanism through which cav-1 promotes malignant activities in prostate cancer, there are certainly others. Results of a recent study showed that cellular levels of P-Y14cav-1 are critically associated with Rho/ROCK- and Src-dependent regulation of tumor cell motility and invasion.[45]

Prostate cancer cells secrete cav-1

Cav-1, which is secreted by mouse and human prostate cancer cell lines, promotes cancer cell survival *in vitro*.[15] These results were validated in independent studies and were extended to include perineural cells in the prostate cancer microenvironment.[17,46] At the time these results were reported, a previous study had shown that cav-1 was secreted by normal pancreatic acinar cells *in vitro*,[47] but to our knowledge, there were no previous reports of cav-1 secretion by malignant cells. These results raised the question of the mechanism responsible for cav-1 secretion from cancer cells and whether this mechanism was specific to prostate cancer cells or the prostate cancer microenvironment. An intriguing article reported that cav-1 was found in 'prostasomes,' which are vesicular organelles enriched with raft components, of PC-3 cells, suggesting that cav-1 is secreted by prostate cancer cells through a unique mechanism.[48] The results of a more recent study supported the concept that cav-1 is secreted by prostate cancer cells through a unique exosome–prostasome-mediated pathway.[49] Additional studies are warranted to further characterize the specificity and mechanism(s) involved in cav-1 secretion by prostate cancer cells and potentially by specific stromal cells within the prostate cancer microenvironment.

Prostate cancer-derived, secreted cav-1 alters the tumor microenvironment through proangiogenic activities

Prostate cancer is unique in its capacity to influence and become dependent on stromal cells that reside in the tumor microenvironment. GFs derived from prostate cancer cells, including vascular endothelial growth factor, transforming GF-β1 and multiple fibroblast GFs, are known to significantly affect, through autocrine and paracrine activities, the capacity of prostate cancer cells to grow and metastasize.[50–53] Various mechanisms are reportedly involved in the deregulation of these GFs in cancer cells, including transcriptional regulation[54] and alteration of mRNA stability.[55–58]

We recently found, unexpectedly, that prostate cancer-derived secreted cav-1 is also capable of significantly altering the tumor microenvironment by stimulating angiogenesis. Specifically, cav-1 is taken up by cav-1-negative tumor cells and/or endothelial cells, leading to stimulation of specific angiogenic activities through the PI3K–Akt–eNOS signaling module.[6] This study followed a previous study which had shown greater angiogenesis in cav-1-positive prostate cancer than in cav-1-negative prostate cancer and that also showed co-localization of cav-1 with vascular endothelial growth factor receptor-2 in tumor-associated endothelial cells.[59] The combined action of prostate cancer-derived, secreted cell-derived GFs and/or angiogenic cytokines and cav-1 could have a profound effect on prostate cancer microenvironment (Figure 1). The combined effect could potentially result in structural modification of the pre-existing signaling pathways through the interaction of cav-1 with specific signaling molecules. As many of the molecules involved in angiogenic signaling pathways possess cav-1 scaffolding domain-binding sites, for example, vascular endothelial growth factor receptor-2 and Src,[9] these interactions are likely mediated in part through the cav-1 scaffolding domain–scaffolding domain-binding site interface. It is interesting to note that an abnormal augmentation of these signaling pathways could further potentiate the downstream autocrine and/or paracrine activities of GFs and/or angiogenic cytokines secreted by prostate cancer cells, representing unique co-stimulatory activities with profound potential to alter the tumor microenvironment toward a progressively increasing malignant state.

Secreted cav-1 as a biomarker and therapeutic target

The expression and secretion of cav-1 by prostate cancer cells presents an opportunity for the development of cav-1-based biomarkers for prostate cancer. We previously developed an immunoassay for measuring serum cav-1

levels and showed that the median serum cav-1 level in men with clinically localized prostate cancer was significantly higher than that in healthy control men (that is, in those with normal findings on digital rectal examination and serum prostate-specific antigen levels of $\leqslant 1.5\,ng\,ml^{-1}$ over a period of 2 years) and in men with clinical benign prostatic hyperplasia.[19] Further, in a larger population study in men with a serum prostate-specific antigen of $>10\,ng\,ml^{-1}$, high pretreatment levels of cav-1 in the serum were associated with a shorter time to biochemical recurrence (defined as a serum prostate-specific antigen level of $\geqslant 0.2\,ng\,ml^{-1}$ on two consecutive measurements).[20] High pretreatment serum cav-1 levels were established using a cutoff determined by using the minimum *P*-value method.

These initial clinical and basic laboratory study results, together with those of pathology-based tissue analysis, show the potential of serum cav-1 as a prognostic biomarker for the identification of men with clinically aggressive prostate cancer. Specifically, the pretreatment serum cav-1 concentration may be used to identify men with clinically significant prostate cancer who are likely to experience a rapid recurrence of the cancer following radical prostatectomy. Although further studies are necessary to validate these results, it is conceivable that serum cav-1 analysis would contribute to the identification of the subset of the men undergoing localized therapy for presumed localized disease who would benefit from neoadjuvant or adjuvant therapy, for example, local radiotherapy, localized biologic therapy, androgen-deprivation therapy and/or targeted systemic therapy.[60–63]

We have considered, in addition to the potential use of serum cav-1 analysis as a prognostic biomarker for clinically aggressive prostate cancer, the possibility that secreted cav-1 is a therapeutic target for prostate cancer. Our recent studies revealed that systemic treatment of mice with cav-1 antisera significantly reduced the development and growth of primary site tumors and metastases in both orthotopic and experimental metastasis mouse models of prostate cancer.[15,64] These studies further showed that metastatic prostate cancer cells may survive and grow partly through the uptake of secreted cav-1. As targeted systemic antibody therapy has been used successfully to treat specific malignancies,[65,66] the development of cav-1-targeted antibody therapy should be further pursued as a potential therapy for prostate cancer.

Summary

The initial observations that prostate cancer cells overexpress cav-1 and that cav-1 is associated with clinically significant prostate cancer have led to extensive basic laboratory and clinical studies of the role of cav-1 in prostate cancer and other malignancies. Although the molecular and cellular biology of cav-1 is complex, these studies thus far have shown that the overexpression and secretion of cav-1 leads to the amplification of the tumor-promoting effects of cav-1 through the activation of endogenous oncogenic pathways and engagement of tumor microenvironment. The association between cav-1 and clinically significant prostate cancer is unique, and the prospect that cav-1 expression may segregate clinically significant prostate cancer from clinically insignificant prostate cancer is exciting. By virtue of the capacity of prostate cancer cells to secrete cav-1, specific cav-1-based biomarker and therapeutic strategies have been proposed and tested. The initial results are promising and indicate that further studies may lead to clinically useful prognostic and therapeutic tools for prostate cancer.

Conflict of interest

The data included in this paper are relevant to intellectual property that has been licensed by Baylor College of Medicine to Progression Therapeutics Inc., a private biotechnology start-up. The association to the start-up is indirect and does not in any way constitute a conflict of interest.

Acknowledgements

This work was supported in part by NIH R01 CA68814 and Department of Defense Grant DAMD PC051247.

References

1 Shaul PW, Anderson RG. Role of plasmalemmal caveolae in signal transduction. *Am J Physiol* 1998; **275**: L843–L851.
2 Sternberg PW, Schmid SL. Caveolin, cholesterol and Ras signalling. *Nat Cell Biol* 1999; **1**: E35–E37.
3 Williams TM, Lisanti MP. Caveolin-1 in oncogenic transformation, cancer, and metastasis. *Am J Physiol* 2005; **288**: C494–C506.
4 Cavallo-Medved D, Mai J, Dosescu J, Sameni M, Sloane BF. Caveolin-1 mediates the expression and localization of cathepsin B, pro-urokinase plasminogen activator and their cell-surface receptors in human colorectal carcinoma cells. *J Cell Sci* 2005; **118**: 1493–1503.
5 Li L, Yang G, Ebara S, Satoh T, Nasu Y, Timme TL *et al*. Caveolin-1 mediates testosterone-stimulated survival/clonal growth and promotes metastatic activities in prostate cancer cells. *Cancer Res* 2001; **61**: 4386–4392.
6 Tahir SA, Yang G, Goltsov AA, Watanabe M, Tabata K, Addai J *et al*. Tumor cell-secreted caveolin-1 has proangiogenic activities in prostate cancer. *Cancer Res* 2008; **68**: 731–739.
7 Williams TM, Hassan GS, Li J, Cohen AW, Medina FA, Philippe GF *et al*. Caveolin-1 promotes tumor progression in an autochthonous mouse model of prostate cancer: genetic ablation of Cav-1 delays advanced prostate tumor development in TRAMP mice. *J Biol Chem* 2005; **10**: 1074.
8 Woodman SE, Ashton AW, Schubert W, Lee H, Williams TM, Medina FA *et al*. Caveolin-1 knockout mice show an impaired angiogenic response to exogenous stimuli. *Am J Pathol* 2003; **162**: 2059–2068.
9 Shatz M, Liscovitch M. Caveolin-1: a tumor-promoting role in human cancer. *Int J Radiat Biol* 2008; **84**: 177–189.
10 Yang G, Truong LD, Timme TL, Ren C, Wheeler TM, Park SH *et al*. Elevated expression of caveolin is associated with prostate and breast cancer. *Clin Cancer Res* 1998; **4**: 1873–1880.
11 Yang G, Truong LD, Wheeler TM, Thompson TC. Caveolin-1 expression in clinically confined human prostate cancer: a novel prognostic marker. *Cancer Res* 1999; **59**: 5719–5723.
12 Ho CC, Huang PH, Huang HY, Chen YH, Yang PC, Hsu SM. Up-regulated caveolin-1 accentuates the metastasis capability of lung adenocarcinoma by inducing filopodia formation. *Am J Pathol* 2002; **161**: 1647–1656.

13 Joo HJ, Oh DK, Kim YS, Lee KB, Kim SJ. Increased expression of caveolin-1 and microvessel density correlates with metastasis and poor prognosis in clear cell renal cell carcinoma. *BJU Int* 2004; **93**: 291–296.
14 Kato K, Hida Y, Miyamoto M, Hashida H, Shinohara T, Itoh T *et al*. Overexpression of caveolin-1 in esophageal squamous cell carcinoma correlates with lymph node metastasis and pathologic stage. *Cancer* 2002; **94**: 929–933.
15 Tahir SA, Yang G, Ebara S, Timme TL, Satoh T, Li L *et al*. Secreted caveolin-1 stimulates cell survival/clonal growth and contributes to metastasis in androgen-insensitive prostate cancer. *Cancer Res* 2001; **61**: 3882–3885.
16 Wu D, Foreman TL, Gregory CW, McJilton MA, Wescot GG, Ford OH *et al*. Protein kinase cepsilon has the potential to advance the recurrence of human prostate cancer. *Cancer Res* 2002; **62**: 2423–2429.
17 Bartz R, Zhou J, Hsieh JT, Ying Y, Li W, Liu P. Caveolin-1 secreting LNCaP cells induce tumor growth of caveolin-1 negative LNCaP cells *in vivo*. *Int J Cancer* 2008; **122**: 520–525.
18 Li L, Ren CH, Tahir SA, Ren C, Thompson TC. Caveolin-1 maintains activated Akt in prostate cancer cells through scaffolding domain binding site interactions with and inhibition of serine/threonine protein phosphatases PP1 and PP2A. *Mol Cell Biol* 2003; **23**: 9389–9404.
19 Tahir SA, Ren C, Timme TL, Gdor Y, Hoogeveen R, Morrisett JD *et al*. Development of an immunoassay for serum caveolin-1: a novel biomarker for prostate cancer. *Clin Cancer Res* 2003; **9**: 3653–3659.
20 Tahir SA, Frolov A, Hayes TG, Mims MP, Miles BJ, Lerner SP *et al*. Preoperative serum caveolin-1 as a prognostic marker for recurrence in a radical prostatectomy cohort. *Clin Cancer Res* 2006; **12**: 4872–4875.
21 Goto T, Nguyen BP, Nakano M, Ehara H, Yamamoto N, Deguchi T. Utility of Bcl-2, P53, Ki-67, and caveolin-1 immunostaining in the prediction of biochemical failure after radical prostatectomy in a Japanese population. *Urology* 2008; **72**: 167–171.
22 Karam JA, Lotan Y, Roehrborn CG, Ashfaq R, Karakiewicz PI, Shariat SF. Caveolin-1 overexpression is associated with aggressive prostate cancer recurrence. *Prostate* 2007; **67**: 614–622.
23 Cohen AW, Hnasko R, Schubert W, Lisanti MP. Role of caveolae and caveolins in health and disease. *Physiol Rev* 2004; **84**: 1341–1379.
24 Engelman JA, Zhang XL, Lisanti MP. Genes encoding human caveolin-1 and -2 are co-localized to the D7S522 locus (7q31.1), a known fragile site (FRA7G) that is frequently deleted in human cancers. *FEBS Lett* 1998; **436**: 403–410.
25 Nupponen NN, Kakkola L, Koivisto P, Visakorpi T. Genetic alterations in hormone-refractory recurrent prostate carcinomas. *Am J Pathol* 1998; **153**: 141–148.
26 Bachmann N, Haeusler J, Luedeke M, Kuefer R, Perner S, Assun G *et al*. Expression changes of CAV1 and EZH2, located on 7q31 approximately q36, are rarely related to genomic alterations in primary prostate carcinoma. *Cancer Genet Cytogenet* 2008; **182**: 103–110.
27 Hurlstone AF, Reid G, Reeves JR, Fraser J, Strathdee G, Rahilly M *et al*. Analysis of the CAVEOLIN-1 gene at human chromosome 7q31.1 in primary tumours and tumour-derived cell lines. *Oncogene* 1999; **18**: 1881–1890.
28 Cui J, Rohr LR, Swanson G, Speights VO, Maxwell T, Brothman AR. Hypermethylation of the caveolin-1 gene promoter in prostate cancer. *Prostate* 2001; **46**: 249–256.
29 Gandellini P, Folini M, Longoni N, Pennati M, Binda M, Colecchia M *et al*. miR-205 exerts tumor-suppressive functions in human prostate through down-regulation of protein kinase Cepsilon. *Cancer Res* 2009; **69**: 2287–2295.
30 Thompson TC, Park SH, Timme TL, Ren C, Eastham JA, Donehower LA *et al*. Loss of p53 function leads to metastasis in ras+myc-initiated mouse prostate cancer. *Oncogene* 1995; **10**: 869–879.
31 Dall'era MA, Cooperberg MR, Chang JM, Davies BJ, Albertsen PC, Klotz LH *et al*. Active surveillance for early-stage prostate cancer: review of the current literature. *Cancer* 2008; **112**: 1650–1659.
32 Nasu Y, Timme TL, Yang G, Bangma CH, Li L, Ren C *et al*. Suppression of caveolin expression induces androgen sensitivity in metastatic androgen-insensitive mouse prostate cancer cells [see comments]. *Nat Med* 1998; **4**: 1062–1064.
33 Lu ML, Schneider MC, Zheng Y, Zhang X, Richie JP. Caveolin-1 interacts with androgen receptor. A positive modulator of androgen receptor mediated transactivation. *J Biol Chem* 2001; **276**: 13442–13451.
34 Razandi M, Alton G, Pedram A, Ghonshani S, Webb P, Levin ER. Identification of a structural determinant necessary for the localization and function of estrogen receptor alpha at the plasma membrane. *Mol Cell Biol* 2003; **23**: 1633–1646.
35 Patlolla JM, Swamy MV, Raju J, Rao CV. Overexpression of caveolin-1 in experimental colon adenocarcinomas and human colon cancer cell lines. *Oncol Rep* 2004; **11**: 957–963.
36 Rajjayabun PH, Garg S, Durkan GC, Charlton R, Robinson MC, Mellon JK. Caveolin-1 expression is associated with high-grade bladder cancer. *Urology* 2001; **58**: 811–814.
37 Suzuoki M, Miyamoto M, Kato K, Hiraoka K, Oshikiri T, Nakakubo Y *et al*. Impact of caveolin-1 expression on prognosis of pancreatic ductal adenocarcinoma. *Br J Cancer* 2002; **87**: 1140–1144.
38 Davidson B, Goldberg I, Givant-Horwitz V, Nesland JM, Berner A, Bryne M *et al*. Caveolin-1 expression in ovarian carcinoma is MDR1 independent. *Am J Clin Pathol* 2002; **117**: 225–234.
39 Van den Eynden GG, Van Laere SJ, Van der Auwera I, Merajver SD, Van Marck EA, Van Dam P *et al*. Overexpression of caveolin-1 and -2 in cell lines and in human samples of inflammatory breast cancer. *Breast Cancer Res Treat* 2006; **95**: 219–228.
40 Yoo SH, Park YS, Kim HR, Sung SW, Kim JH, Shim YS *et al*. Expression of caveolin-1 is associated with poor prognosis of patients with squamous cell carcinoma of the lung. *Lung Cancer* 2003; **42**: 195–202.
41 Zhang X, Ling MT, Wang Q, Lau CK, Leung SC, Lee TK *et al*. Identification of a novel inhibitor of differentiation-1 (ID-1) binding partner, caveolin-1, and its role in epithelial-mesenchymal transition and resistance to apoptosis in prostate cancer cells. *J Biol Chem* 2007; **282**: 33284–33294.
42 Li L, Ittmann MM, Ayala G, Tsai MJ, Amato RJ, Wheeler TM *et al*. The emerging role of the PI3-K-Akt pathway in prostate cancer progression. *Prostate Cancer Prostatic Dis* 2005; **8**: 108–118.
43 Di Vizio D, Adam RM, Kim J, Kim R, Sotgia F, Williams T *et al*. Caveolin-1 interacts with a lipid raft-associated population of fatty acid synthase. *Cell Cycle* 2008; **7**: 2257–2267.
44 Glenney Jr JR, Zokas L. Novel tyrosine kinase substrates from Rous sarcoma virus-transformed cells are present in the membrane skeleton. *J Cell Biol* 1989; **108**: 2401–2408.
45 Joshi B, Strugnell SS, Goetz JG, Kojic LD, Cox ME, Griffith OL *et al*. Phosphorylated caveolin-1 regulates Rho/ROCK-dependent focal adhesion dynamics and tumor cell migration and invasion. *Cancer Res* 2008; **68**: 8210–8220.
46 Ayala GE, Dai H, Tahir SA, Li R, Timme T, Ittmann M *et al*. Stromal antiapoptotic paracrine loop in perineural invasion of prostatic carcinoma. *Cancer Res* 2006; **66**: 5159–5164.
47 Liu P, Li WP, Machleidt T, Anderson RG. Identification of caveolin-1 in lipoprotein particles secreted by exocrine cells. *Nat Cell Biol* 1999; **1**: 369–375.
48 Llorente A, de Marco MC, Alonso MA. Caveolin-1 and MAL are located on prostasomes secreted by the prostate cancer PC-3 cell line. *J Cell Sci* 2004; **117**: 5343–5351.
49 Lu Q, Zhang J, Allison R, Gay H, Yang WX, Bhowmick NA *et al*. Identification of extracellular delta-catenin accumulation for prostate cancer detection. *Prostate* 2009; **69**: 411–418.
50 Chung LW, Huang WC, Sung SY, Wu D, Odero-Marah V, Nomura T *et al*. Stromal-epithelial interaction in prostate cancer progression. *Clin Genitourin Cancer* 2006; **5**: 162–170.
51 Kwabi-Addo B, Ozen M, Ittmann M. The role of fibroblast growth factors and their receptors in prostate cancer. *Endocr Relat Cancer* 2004; **11**: 709–724.
52 Morrissey C, Vessella RL. The role of tumor microenvironment in prostate cancer bone metastasis. *J Cell Biochem* 2007; **101**: 873–886.

53 Reynolds AR, Kyprianou N. Growth factor signalling in prostatic growth: significance in tumour development and therapeutic targeting. *Br J Pharmacol* 2006; **147** (Suppl 2): S144–S152.
54 Josko J, Mazurek M. Transcription factors having impact on vascular endothelial growth factor (VEGF) gene expression in angiogenesis. *Med Sci Monit* 2004; **10**: RA89–RA98.
55 Cash J, Korchnak A, Gorman J, Tandon Y, Fraizer G. VEGF transcription and mRNA stability are altered by WT1 not DDS(R384W) expression in LNCaP cells. *Oncol Rep* 2007; **17**: 1413–1419.
56 Kanies CL, Smith JJ, Kis C, Schmidt C, Levy S, Khabar KS *et al*. Oncogenic Ras and transforming growth factor-beta synergistically regulate AU-rich element-containing mRNAs during epithelial to mesenchymal transition. *Mol Cancer Res* 2008; **6**: 1124–1136.
57 Song QH, Klepeis VE, Nugent MA, Trinkaus-Randall V. TGF-beta1 regulates TGF-beta1 and FGF-2 mRNA expression during fibroblast wound healing. *Mol Pathol* 2002; **55**: 164–176.
58 Touriol C, Morillon A, Gensac MC, Prats H, Prats AC. Expression of human fibroblast growth factor 2 mRNA is post-transcriptionally controlled by a unique destabilizing element present in the 3′-untranslated region between alternative polyadenylation sites. *J Biol Chem* 1999; **274**: 21402–21408.
59 Yang G, Addai J, Wheeler TM, Frolov A, Miles BJ, Kadmon D *et al*. Correlative evidence that prostate cancer cell-derived caveolin-1 mediates angiogenesis. *Hum Pathol* 2007; **38**: 1688–1695.
60 Ayala G, Satoh T, Li R, Shalev M, Gdor Y, Aguilar-Cordova E *et al*. Biological response determinants in HSV-tk + ganciclovir gene therapy for prostate cancer. *Mol Ther* 2006; **13**: 716–728.
61 Efstathiou E, Troncoso P, Wen S, Do KA, Pettaway CA, Pisters LL *et al*. Initial modulation of the tumor microenvironment accounts for thalidomide activity in prostate cancer. *Clin Cancer Res* 2007; **13**: 1224–1231.
62 Pisters LL, Pettaway CA, Troncoso P, McDonnell TJ, Stephens LC, Wood CG *et al*. Evidence that transfer of functional p53 protein results in increased apoptosis in prostate cancer. *Clin Cancer Res* 2004; **10**: 2587–2593.
63 Sonpavde G, Chi KN, Powles T, Sweeney CJ, Hahn N, Hutson TE *et al*. Neoadjuvant therapy followed by prostatectomy for clinically localized prostate cancer. *Cancer* 2007; **110**: 2628–2639.
64 Watanabe M, Yang G, Cao G, Tahir SA, Naruishi K, Tabata K *et al*. Functional analysis of secreted caveolin-1 in mouse models of prostate cancer progression. *Mol Can Res* 2009 (in press).
65 Ma WW, Adjei AA. Novel agents on the horizon for cancer therapy. *CA Cancer J Clin* 2009; **59**: 111–137.
66 Weiner GJ. Monoclonal antibody mechanisms of action in cancer. *Immunol Res* 2007; **39**: 271–278.